

**THE cJUN NH₂-TERMINAL KINASE PATHWAY IN MAMMARY GLAND
BIOLOGY AND CARCINOGENESIS**

A Dissertation Presented

By

Nomeda Aleksandra Girnius

Submitted to the Faculty of the

University of Massachusetts Graduate School of Biomedical Sciences, Worcester

In partial fulfillment of the requirements for the degree of

DOCTOR OF PHILOSOPHY

March 8th, 2018

CANCER BIOLOGY

THE cJUN NH₂-TERMINAL KINASE PATHWAY IN MAMMARY GLAND
BIOLOGY AND CARCINOGENESIS

A Dissertation Presented by
Nomedra Aleksandra Girnius

This work was undertaken in the Graduate School of Biomedical Sciences,
Program of Cancer Biology

Under the mentorship of

Roger J. Davis, Ph.D., Thesis Advisor

Sharon B. Cantor, Ph.D, Member of Committee

Craig J. Ceol, Ph.D., Member of Committee

Brian C. Lewis, Ph.D., Member of Committee

Senthil K. Muthuswamy, Ph.D., External Member of Committee

The signature of the Chair of the Committee signifies that the written dissertation
meets the requirements of the Dissertation Committee

Leslie M. Shaw, Ph.D., Chair of the Committee

The signature of the Dean of the Graduate School of Biomedical Sciences
signifies that the student has met all graduation requirements of the School.

Mary Ellen Lane, Ph.D.,
Dean of the Graduate School of Biomedical Sciences

March 8th, 2018

DEDICATION

To my family: my parents, my husband, and my children. Your sacrifices have made these pages possible.

ACKNOWLEDGEMENTS

I would like to thank my mentor, Dr. Roger J. Davis, for the opportunity to work in his lab. He has provided scientific guidance, while allowing me to explore projects that I initiated. Because of his vigilance and encouragement, I have been able to participate in many collaborations that have resulted in a number of publications. He has also given me opportunities to cultivate leadership and mentoring skills during my time as a graduate student. For all this, I am extremely grateful.

I have been fortunate to receive technical assistance from Julie Cavanagh-Kyros, Armanda Roy, Tammy Barret, and Vicky Benoit. Kathy Gemme provided administrative assistance and support. I am grateful to Dr. Yvonne Edwards for her assistance analyzing RNA sequencing data and to Dr. Garlick for pathology insight and impromptu lessons. The work of former rotation students Seda Barutcu, Mona Motwani, and Lola Yu provided valuable insight into project directions. I am also grateful to former and current lab members, in particular Dr. Santiago Vernia, Dr. Kasmir Ramo, Zeynep Itah, and Dr. Cristina Cellurale for scientific discussions, collaborations, and assistance.

I would like to thank my committee members Drs. Leslie M. Shaw, Sharon B. Cantor, Craig J. Ceol, and Brian C. Lewis for their insight, guidance and encouragement throughout my graduate career. I am also grateful to Dr. Senthil

K. Muthuswamy for serving as my external examiner. Their efforts to hold my exam on its scheduled day in spite of Mother Nature's best efforts will be long-remembered and appreciated.

I also thank Dr. Gabriel Cunningham for his assistance editing this thesis and for his willingness to write time-saving scripts. I appreciate his patience every time I have asked for help with statistics, or for extra time in the lab. Together with my parents, he has provided moral support and help throughout my graduate career.

Abstract

The cJUN NH₂-terminal kinase (JNK) pathway responds to environmental stresses and participates in many cellular processes, including cell death, survival, proliferation, migration, and genome maintenance. Importantly, genes that encode components of the JNK signaling pathway are frequently mutated in human breast cancer, but the functional consequence of these mutations in mammary carcinogenesis is unclear.

Anoikis – suspension-induced apoptosis – has been implicated in oncogenic transformation and tumor cell metastasis. Anoikis also contributes to lumen formation during mammary gland development and epithelial cell clearance during post-lactational involution. JNK is known to contribute to certain forms of cell death, but the role of JNK during anoikis was unclear. I examined the requirement of JNK in anoikis and discovered that JNK promotes cell death by transcriptional and post-translational regulation of pro-apoptotic BH3-only proteins. This conclusion suggested that JNK signaling may contribute to mammary gland remodeling during involution. Indeed, JNK deficiency in mammary epithelial cells disrupted the remodeling program of gene expression and delayed involution. Finally, I sought to understand the importance of JNK in mammary carcinogenesis. I found that JNK loss in the mammary epithelium was sufficient for genomic instability and tumor formation. Moreover, JNK loss in a model of breast cancer resulted in significantly accelerated tumor development. Collectively, these studies advance our understanding of the JNK pathway and

breast biology, and provide insight that informs the design of therapeutic approaches that target the JNK signal transduction pathway.

TABLE OF CONTENTS

TITLE	i
SIGNATURE PAGE	ii
DEDICATION	iii
ACKNOWLEDGEMENTS	iv
ABSTRACT	vi
TABLE OF CONTENTS	viii
LIST OF FIGURES	xi
LIST OF ABBREVIATIONS	xv
PREFACE	xviii
PUBLICATIONS	xix
CHAPTER I: INTRODUCTION	1
CHAPTER II: JNK PROMOTES EPITHELIAL CELL ANOIKIS BY TRANSCRIPTIONAL AND POST-TRANSLATIONAL REGULATION OF BH3-ONLY PROTEINS	
Abstract	44
Introduction	45
Results	48
Discussion	79
Materials and Methods	85

CHAPTER III: THE JNK PATHWAY CONTRIBUTES TO MOUSE MAMMARY GLAND REMODELING DURING INVOLUTION

Abstract	94
Introduction	95
Results	99
Discussion	126
Materials and Methods	131

CHAPTER IV: DISRUPTION OF JNK SIGNALING PROMOTES THE DEVELOPMENT OF BREAST CANCER

Abstract	140
Introduction	141
Results	145
Discussion	176
Materials and Methods	181

CHAPTER V: DISCUSSION AND FUTURE DIRECTIONS

Discussion	194
Future Directions	204

APPENDIX A: JNK IS DISPENSABLE FOR EPITHELIAL CELL MIGRATION

Abstract	218
Introduction	219
Results	222
Discussion	238
Materials and Methods	241

APPENDIX B:	BREAST CANCER CELL SENSITIVITY TO GENOTOXIC DRUGS IN THE CONTEXT OF JNK INACTIVATION	
	Abstract	248
	Introduction	249
	Results and Discussion	252
	Conclusions	263
	Materials and Methods	264
REFERENCES		267

LIST OF FIGURES

Chapter I

Figure I.1. The JNK signaling pathway.

Figure I.2. The mammary gland is a dynamic organ capable of multiple cycles of expansion and contraction in adulthood.

Figure I.3. Processes occurring during the normal stages of mammary gland development are also involved in carcinogenesis.

Figure I.4. Mammary gland structure during pubertal development into adulthood.

Figure I.5. Mammary gland structure during pregnancy and lactation.

Chapter II

Figure II.1. JNK promotes anoikis of human mammary epithelial cells.

Figure II.2. JNK promotes anoikis of murine epithelial cells.

Figure II.3. MLK2 and 3 proteins are not essential for epithelial cell anoikis.

Figure II.4. Autophagy induction is comparable in Control and JNK^{KO} cells.

Figure II.5. BAK and BAX are required for JNK-promoted anoikis.

Figure II.6. BCL2 family gene expression in suspended epithelial cells.

Figure II.7. Anoikis causes JNK-independent decreased expression of MCL-1.

Figure II.8. Anoikis causes JNK-dependent increased expression of BH3-only genes.

Figure II.9. BH3-only gene expression by suspended epithelial cells.

Figure II.10. BIM and BMF contribute to JNK-promoted anoikis.

Figure II.11. Constitutively activated JNK1 causes increased expression of the BH3-only genes *Hrk* and *Pmaip1*.

Figure II.12. BIM and BMF contribute to normal mammary gland development.

Figure II.13. BIM/BMF^{KO} compound mutant mice exhibit impaired mammary gland development.

Figure II.14. Basal and luminal cells occlude ducts of BIM/BMF^{KO} mammary glands.

Figure II.15. Phosphorylation of BMF, but not BIM, contributes to JNK-promoted anoikis.

Figure II.16. Mammary gland development in mice with defects in JNK-mediated BIM and BMF phosphorylation.

Chapter III

Figure III.1. *Mapk8* and *Mapk9* gene disruption in luminal mammary epithelial cells.

Figure III.2. JNK is required for efficient mammary gland involution.

Figure III.3. JNK is required for mammary gland involution.

Figure III.4. Epithelial cell populations in mammary glands after involution.

Figure III.5. JNK-deficiency suppresses cell death during involution.

Figure III.6. Caspase 3 activation in mammary glands after 7 days of involution.

Figure III.7. STAT3 signaling is not disrupted in JNK^{KO} glands.

Figure III.8. JNK deficiency does not alter STAT5 or SMAD2/3 activation during involution.

Figure III.9. JNK-deficiency suppresses the increase in AP1-related transcription factor expression during involution.

Figure III.10. JNK promotes involution-associated gene expression.

Figure III.11. Summary of RNA sequencing analysis.

Figure III.12. Enrichment of AP1 binding sites with genes that exhibit JNK-dependent expression during involution.

Figure III.13. Mammary gland expression of *Mmp* and *Timp* genes.

Figure III.14. Mammary gland expression of cathepsin.

Figure III.15. JNK-deficiency suppresses the expression of pro-apoptotic BH3-only genes.

Figure III.16. Mammary gland expression of BH3-only genes.

Chapter IV

Figure IV.1. JNK deficiency in mammary epithelial cells is sufficient for tumor formation and genomic instability.

Figure IV.2. Expression of estrogen and progesterone receptors in breast tumors caused by JNK deficiency in the mammary epithelium.

Figure IV.3. Summary of exome sequence data.

Figure IV.4. JNK deficiency is sufficient to promote tumor-associated gene expression.

Figure IV.5. JNK deficiency accelerates tumor formation in a mouse model of breast cancer.

Figure IV.6. Tumors in JNK^{KO} mice are primarily adenocarcinomas and display a spectrum of hormone receptor expression patterns.

Figure IV.7. Tumor latency in JNK^{WT} and JNK^{KO} mice is not influenced by parity or litter sizes.

Figure IV.8. Exome sequencing of Control and JNK deficient tumor cells.

Figure IV.9. Gene expression analysis of control and JNK deficient tumor cells.

Figure IV.10. RNA-seq analysis demonstrates that a sub-set of tumor-associated gene expression requires JNK.

Figure IV.11. Comparison of signaling pathways in control and JNK deficient tumor cells.

Figure IV.12. Stem cell populations are comparable in JNK^{WT} and JNK^{KO} tumor cells.

Figure IV.13. JNK-deficient tumor cells do not exhibit enhanced tumor stem cell activity.

Figure IV.14. JNK^{WT} and JNK^{KO} tumor cells exhibit similar phenotypes.

Figure IV.15. JNK deficiency promotes early disease lesions.

Chapter V

Figure V.1. JNK participates in several aspects of mammary gland biology.

Figure V.2. JNK promotes anoikis through transcriptional regulation of BIM and phosphorylation of BMF.

Appendix A

- A.1. JNK-deficient cells proliferate comparably to Control cells.**
- A.2 Paxillin is phosphorylated at serine 178 in cells despite JNK pathway inactivation.**
- A.3. Compound JNK-deficiency does not inhibit migration of kidney epithelial cells.**
- A.4. Motility of Control cells is not repressed by JNK inhibitor treatment.**
- A.5. Treatment of kidney epithelial cells with NMPP1 decreases wound healing, regardless of genotype.**
- A.6. Loss of JNK1 promotes wound healing.**
- A.7. Cell migration in response to conditioned media.**

Appendix B

- Figure B.1. JNK pathway inhibition in MDA-MB-231 by JNK-IN-8.**
- Figure B.2. JNK-IN-8 treatment does not sensitize MDA-MB-231 cells to cisplatin, doxorubicin, etoposide, or methyl methanesulfonate.**
- Figure B.3. Titration of cisplatin and doxorubicin concentrations results in similar growth of MDA-MB-231 cells, regardless of JNK-IN-8 treatment.**
- Figure B.4. Proliferation of tumor cells is similar regardless of JNK status.**
- Figure B.5. Murine tumor-derived cells respond variably to drug treatments.**

LIST OF ABBREVIATIONS

7AAD	7-aminoactinomycin D
ANOVA	Analysis of variance
AKT	Protein kinase B
AP	Activator protein
ASK	Apoptosis signal-regulating kinase
ATF	Activating transcription factor
ATM	Ataxia-telangiectasia
ATR	ATM and Rad3 related
<i>Axin2</i>	Axis inhibition protein
BAD	BCL2-associated agonist of cell death
BAK	BCL2 homologous antagonist killer
BAX	BCL2-associated X protein
<i>Bbc3</i>	BCL2 binding component 3, encodes PUMA
BCL2	B-cell CLL/lymphoma 2
<i>Bcl2l11</i>	BCL2-like 11, gene encoding BIM
BCLXL	B cell lymphoma extra long
BID	BH3-interacting domain death agonist
BIM	BCL2-interacting mediator of cell death, encoded by <i>Bcl2l11</i>
BMF	BCL2-modifying factor
<i>Bmi</i>	B lymphoma Mo-MLV insertion region
BMP	Bone morphogenetic protein
BNIP	BCL2 interacting protein
BOK	BCL2 ovarian killer
Bp	Base pairs
BRCA1/2	Breast Cancer 1/2
BrdU	Bromodeoxyuridine
CASP8	Caspase 8
c-C3	Cleaved caspase 3
CCND	Cyclin D
CDH1	Cadherin I, also E-cadherin
CHEK	Checkpoint kinase
CK	Keratin
CNV	Copy number variation
DAPI	2-(4-amidinophenyl)-1H -indole-6-carboxamide
DCIS	Ductal carcinoma <i>in situ</i>
DLK	Dual leucine zipper kinase
DII	Delta-like
DMEM	Dulbecco's modified Eagle's medium
DMEM/F12	Dulbecco's modified Eagle's medium: nutrient mixture F12
DMSO	Dimethyl sulfoxide

DPP	Decapentaplegic
DSB	Double-strand break
EGF	Epidermal growth factor
EGFR	Epidermal growth factor receptor
ER	Estrogen receptor
ERBB2	Epidermal growth factor receptor B2
ERK	Extracellular regulated kinases
FBS	Fetal bovine serum
FGF	Fibroblast growth factor
FPKM	Fragments per kilobase of exon per million fragments mapped
GFP	Green fluorescent protein
GSEA	Gene set enrichment analysis
GSK	Glycogen synthase kinase
H&E	Hematoxylin and eosin
HCC	Hepatocellular carcinoma
HER	Human epidermal growth factor receptor
HR	Homologous recombination
HRK	Harakiri
IL	Interleukin
Indel	Insertions/deletions
IPA	Ingenuity Pathway Analysis
JAK	Janus kinase
JNK	cJUN NH ₂ -terminal kinase
JNK ^{CA}	MKK7 β 2-Jnk1 α 1
JUN ^{AA}	cJUN Ser ^{63,73} to Ala mutant
KEGG	Kyoto Encyclopedia of Genes and Genomes
LC3	Microtubule-associated protein light change 3
LIF	Leukemia inducible factor
LZK	Leucine zipper-bearing kinase
MAPK	Mitogen-activated protein kinase
MAP2K	Mitogen-activated protein kinase kinase
MAP3K	Mitogen-activated protein kinase kinase kinase
MCL	Myeloid cell leukemia
MDCK	Madin-Darby canine kidney cell line
MEC	Mammary epithelial cells
MEF	Mouse embryonic fibroblasts
MEKK	MAPK/extracellular signal-regulated kinase kinase
MIN	Mammary intraepithelial neoplasia
MLK	Mixed lineage kinase
MMP	Matrix metalloprotease
MMS	Methyl methanesulfonate
mTOR	Mechanistic target of rapamycin
NBN	Nibrin
NF- κ B	Nuclear factor κ B

NMPP1	1-naphthylmethyl-4-amino-1- <i>tert</i> -butyl-3-[<i>p</i> -methylphenyl]pyrazolo(3,4- <i>d</i>)pyrimidine
NOXA	BH3-only protein encoded by <i>Pmaip1</i>
OSM	Oncostatin M
p53	Pathway regulating and genes expressed by TP53/TRP53
PARP	Poly ADP ribose polymerase
PBS	Phosphate buffered saline
PCNA	Proliferating cell nuclear antigen
PI3K	Phosphoinositide-3-kinase
<i>Pmaip1</i>	Phorbol-12-Myristate-13-Acetate-Induced Protein 1, encodes NOXA
<i>Pou5f1</i>	POU domain, class 5, transcription factor 1, encodes OCT3/4
PR	Progesterone receptor
PTEN	Phosphatase and tensin homolog
PUMA	p53-upregulated modulator of apoptosis
RELA	v-rel avian reticuloendotheliosis viral oncogene homolog A, or p65
ROS	Reactive oxygen species
SEM	Standard error of the mean
SIRT6	Sirtuin 6
SMA	Smooth muscle actin
SNV	Single nucleotide variant
STAT	Signal transducer and activator of transcription
TAK	TGF β activated kinase
TEB	Terminal end bud
TGF β	Transforming growth factor β
TIMP	Tissue inhibitor of metalloprotease
TNBC	Triple negative breast cancer
TNF	Tumor necrosis factor
TNFR	Tumor necrosis factor receptor
TPL	Tumor progression locus
TP53	Tumor protein 53, human
TRP53	Tumor protein 53, mouse
TUNEL	Terminal deoxynucleotidyl transferase dUTP nick end labeling
UV	Ultraviolet radiation
WNT	Wingless-related integration site
ZAK	Zipper sterile- α -motif kinase

PREFACE

The work presented in this thesis was done in collaboration with the following people.

Chapter II

Pathology review by David S. Garlick, DVM (Figure II.12A, B & II.16B)

Chapter III

RNA sequencing analysis performed by Yvonne J. K. Edwards, Ph. D. (Figure III.10C, III.11, III.12)

Chapter IV

RNA sequencing analysis performed by Yvonne J. K. Edwards, Ph. D. (Figure IV.4A, IV.9A, IV.10A)

Pathology review by David S. Garlick, DVM (Figure IV.1E, F, IV.5B, & IV.15A)

PUBLICATIONS

The work presented in this thesis has resulted in the following three papers:

Girnius N, Davis RJ. JNK promotes epithelial cell anoikis by transcriptional and post-translational regulation of BH3-only proteins. (2017) *Cell Reports* 21: 1910-1921.

Girnius N, Edwards YJK, Davis RJ. The cJUN NH₂-terminal kinase (JNK) pathway contributes to mouse mammary gland remodeling during involution. (2018) *Cell Death and Differentiation*. In press.

Girnius N, Edwards YJK, Garlick DS, Davis RJ. Disruption of JNK signaling promotes the development of breast cancer. (2018) Submitted.

I also authored the following mini-review:

Girnius N, Davis RJ. TNF α -mediated cytotoxic responses to IAP inhibition are limited by the p38 α MAPK pathway. (2016) *Cancer Cell*. 29(2):131-3.

Collaborations initiated during my thesis work resulted in the following publications:

Wen HC, Avivar-Valderas A, Sosa MS, Girnius N, Farias EF, Davis RJ, Aguirre-Ghiso JA. (2011) p38alpha Signaling Induces Anoikis and Lumen Formation During Mammary Morphogenesis. *Science Signaling* 4: ra34.

Cellurale C, Girnius N, Jiang F, Cavanagh-Kyros J, Lu S, Garlick DS, Mercurio AM, Davis RJ. (2012) Role of JNK in mammary gland development and breast cancer. *Cancer Research* 72: 472-481.

You H, Padmashali RM, Ranganathan A, Lei P, Girnius N, Davis RJ, Andreadis ST. (2013) JNK regulates compliance-induced adherens junctions formation in epithelial cells and tissues. *Journal of Cell Science* 126(Pt 12):2718-29.

Harper KL, Sosa MS, Entenberg D, Hosseini H, Cheung JF, Nobre R, Avivar-Valderas A, Nagi C, Girnius N, Davis RJ, Farias EF, Condeelis J, Klein CA, Aguirre-Ghiso JA. (2016) Mechanism of early dissemination and metastasis in Her2+ mammary cancer. *Nature* 540: 588-592.

Barutcu SA, Girnius N, Vernia S, and Davis RJ. (2018) Role of the cJUN NH₂-terminal kinase (JNK) signaling pathway in starvation-induced autophagy. *Autophagy*. In press.

Jangalwe S, Kapoor VN, Xu J, Girnius N, Kennedy NJ, Edwards YJK, Welsh RM, Davis RJ, Brehm MA. (2018) Early attrition of memory T cells during inflammation and co-stimulation blockade is regulated concurrently by proapoptotic proteins Fas and Bim. Submitted.

CHAPTER I

INTRODUCTION

The cJUN NH₂-terminal Kinase (JNK) Signaling Pathway

The mitogen activated protein kinases (MAPK) allow cells to integrate signals from their environment and respond appropriately. These pathways are organized as three-tiered phosphorylation cascades with the MAPK kinase kinases (MAP3K) phosphorylating and activating the MAPK kinases (MAP2K), which then phosphorylate and activate the MAPK (Figure I.1A).

Dephosphorylation mediated by dual-specificity phosphatases enables pathway inactivation as well as crosstalk between the MAPK pathways (Farooq and Zhou 2004; Huang and Tan 2012). The MAPK are divided into 4 subgroups: extracellular-signal regulated kinase 1/2 (ERK1/2), extracellular-signal regulated kinase 5 (ERK5), p38 MAPK, and cJUN NH₂-terminal kinase (JNK). The ERK1/2 and ERK5 groups respond primarily to mitogens, though ERK5 can also be activated by stress (Nishimoto and Nishida 2006; Hoang et al. 2017). The p38 MAPK and JNK groups are primarily activated by stress stimuli (Davis 2000; Wagner and Nebreda 2009).

Recent sequencing studies have demonstrated that members of the JNK pathway are frequently mutated in human cancer. However, the role of this pathway in tumorigenesis is still not understood.

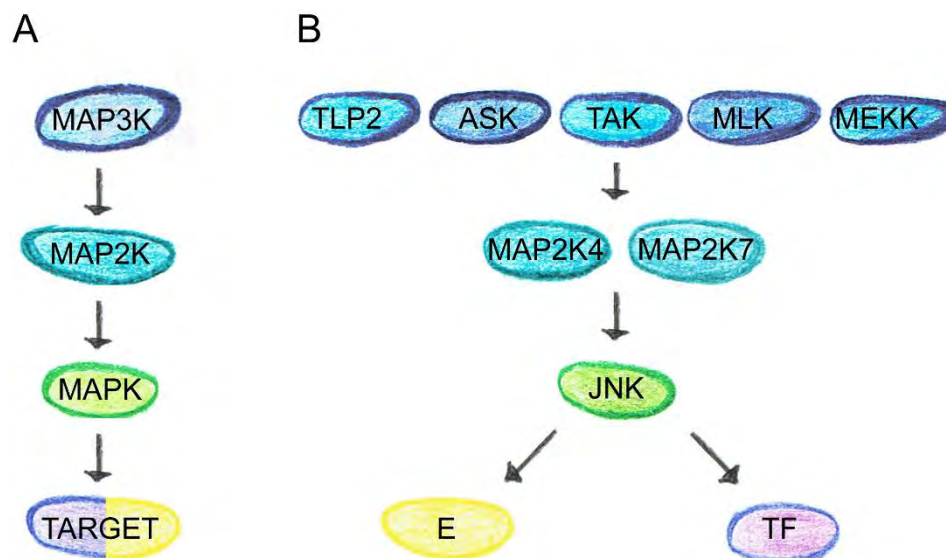


Figure I.1. The JNK signaling pathway.

A) MAPK kinase kinases (MAP3K) phosphorylate the MAPK kinases (MAP2K) that in turn phosphorylate the MAPK. Once activated, MAPK phosphorylate their targets, including transcription factors and non-transcription factors.

B) Signaling through the cJUN NH₂-terminal Kinase (JNK) pathway may be initiated by many MAP3K, including tumor promoting locus 2 (TLP2), apoptosis signal-regulating kinases (ASK), TGF β activated kinases (TAK), mixed-lineage kinases (MLK), and MAPK/extracellular signal-regulated kinase kinases (MEKK). These MAP3K can phosphorylate and activate MAP2K4 and MAP2K7 that in turn phosphorylate and activate JNK. Once activated, JNK phosphorylates its targets, including effector proteins (E; e.g., BIM) as well as transcription factors (TF; e.g., cJUN).

The JNK Signaling Cascade

JNK pathway activation occurs in response to stress stimuli, including the inflammatory cytokines TNF and IL-1, radiation, and osmotic and redox stress (Davis 2000). Studies using over-expression of proteins or dominant-negative mutants have implicated many MAP3K in the JNK pathway (Figure 1.1B), including MEKK1-4 (encoded by *MAP3K1-4*); ASK1-3 (encoded by *MAP3K5-6*, *MAP3K15*); TAK1 (encoded by *MAP3K7*); TPL2 (encoded by *MAP3K8*); and the mixed lineage kinases MLK1-4 (encoded by *MAP3K9-11*, *MAP3K21*), DLK (encoded by *MAP3K12*), ZAK (encoded by *MAP3K20*), and LZK (encoded by *MAP3K13*) (Davis 2000; Gallo and Johnson 2002; Kaji et al. 2010). However, considering that these transfection-based assays result in the activation of other MAPK pathways, the physiological relevance of these MAP3K is unclear. Studies using animals genetically ablated for the individual MAP3K will be necessary to untangle their functions, both regarding which MAP3K are in which MAPK pathway and which stimuli activate which MAP3K. For example, genetic ablation of *MAP3K1* impairs JNK activation, demonstrating that MEKK1 is indeed a component of the JNK pathway (Yujiri et al. 1998). ASK1 has also been identified as a member of the JNK pathway, as it is required for sustained JNK activation in the presence of TNF α or hydrogen peroxide (Tobiume et al. 2001). Similarly, loss of TAK1 markedly decreases JNK phosphorylation in response to LPS, TNF α , or IL1 (Shim et al. 2005) and compound loss of *Map3k10* and *Map3k11* causes impaired JNK phosphorylation in response to TNF α and

saturated fatty acids (Jaeschke and Davis 2007; Kant et al. 2011; Kant et al. 2017). Exposure of MAP3K-deficient cells to various stimuli has revealed the specialization of these proteins. Whereas MEKK2 is required for JNK activation in response to FGF2, it is dispensable for UV-mediated JNK activation (Kesavan et al. 2004).

MEKK1 was shown to activate JNK through MAP2K4 (Yang et al. 1997a), one of the two MAP2K responsible for JNK activation (Davis 2000). Phosphorylation by both MAP2K4 (on Tyr185) and MAP2K7 (on Thr183) (Figure I.1B) in the activation loop of JNK (Derijard et al. 1994; Davis 2000) is required for JNK activation (Tournier et al. 2001). Once fully activated, JNK phosphorylates Ser/Thr-Pro motifs on its targets, notably the AP1 proteins JUNB, cJUN, JUND, and ATF2, as well as other proteins (Figure I.1B) (Davis 2000). The JNK-mediated phosphorylation of cJUN on serines 63 and 73 in its activation domain increases the transcriptional activity of cJUN (Pulverer et al. 1991; Smeal et al. 1991; Adler et al. 1992). Additionally, JNK promotes the expression of cJUN and JUND (Lamb et al. 2003; Ventura et al. 2003). These findings show that regulation of cJUN and AP1 proteins by the JNK pathway enables the cell to initiate appropriate changes in gene expression in response to environmental cues.

There are three JNK genes (*MAPK8*, *MAPK9* and *MAPK10*, encoding JNK1, JNK2, and JNK3 proteins respectively) that are alternatively spliced to produce 10 different JNK isoforms with distinct substrate specificities (Gupta et

al. 1996). The JNK1 and JNK2 proteins are ubiquitously and constitutively expressed after embryonic day 7, while JNK3 is restricted to heart, testes, and brain, and is expressed after embryonic day 10 (Kuan et al. 1999). *Mapk8*^{-/-} and *Mapk9*^{-/-} mice as well as *Mapk8*^{-/-} *Mapk10*^{-/-} and *Mapk9*^{-/-} *Mapk10*^{-/-} mice are viable and fertile (Dong et al. 1998; Yang et al. 1998; Weston et al. 2004). In contrast, *Mapk8*^{-/-} *Mapk9*^{-/-} compound mutant mice die in mid-gestation (Kuan et al. 1999; Sabapathy et al. 1999). These observations together with additional genetic experiments (Tournier et al. 2000) have demonstrated that there is extensive redundancy between JNK1 and JNK2, necessitating the use of compound mutants to fully dissect the function of this pathway. The embryonic lethality of *Mapk8*^{-/-} *Mapk9*^{-/-} compound mutant mice also indicates that this pathway is essential for mammalian development.

The JNK pathway in Cell Life and Death

In times of stress, a cell must make life or death decisions. Thus, it is not surprising that JNK, a stress-activated protein, mediates a cell's decision to proliferate, senesce or die (Davis 2000; Whitmarsh and Davis 2007).

Understanding how the JNK pathway regulates these processes would provide insight into its importance during development and disease, and may inform therapeutic approaches and predict consequences of targeting the JNK pathway in the clinic. It has become clear that the JNK-regulated response to stimuli is

influenced by the cell type, genetic context, time course of activation, and environmental factors.

JNK and cell death

The JNK pathway can promote cell death in response to different stimuli.

Neuronal death following growth factor deprivation or excitotoxicity proceeds through JNK-mediated cell death pathways (Xia et al. 1995; Yang et al. 1997b). In response to ultraviolet light (UV), anisomycin, or methyl methanesulfonate , JNK initiates mitochondrial membrane depolarization and cytochrome c release to engage the apoptotic machinery (Tournier et al. 2000). However, JNK deficiency does not protect cells from FAS ligand-induced cell death, indicating that JNK is not required for the FAS/CASP8 apoptotic pathway (Tournier et al. 2000). Similarly, TNF α -induced death does not depend on the JNK pathway (Lamb et al. 2003; Das et al. 2009). Collectively, these data demonstrate that JNK selectively promotes cell death.

Cell detachment from the extracellular matrix can trigger a specialized form of apoptosis, anoikis (Frisch and Francis 1994). The role of JNK in anoikis has been controversial. Loss of JNK pathway activity, using either a JNK dominant-negative mutant (Frisch et al. 1996) or an MEKK1 dominant-negative mutant (Cardone et al. 1997), delays suspension-induced cell death. However, another study showed that a JNK dominant-negative mutant and a MAP2K4

dominant-negative mutant failed to improve cell survival, implying that JNK is not necessary for efficient cell death (Khwaja and Downward 1997). More recently, work has shown that JNK is needed for acinus lumen formation *in vitro* (Murtagh et al. 2004) and demonstrated its necessity for luminal clearance *in vivo* (Cellurale et al. 2012), suggesting that JNK is indeed needed for anoikis. Genetic models will be required to resolve this controversy.

How does JNK promote cell death? One mechanism involves JNK regulation of gene expression through its AP1 targets. Indeed, mutation of the JNK phosphorylation sites on cJUN (JUN^{AA}) renders mice more resistant to neuronal apoptosis during excitotoxicity (Behrens et al. 1999). Furthermore, cJUN induces expression of the pro-apoptotic *Hrk* (Ma et al. 2007) and *Bcl2l1* (Whitfield et al. 2001) genes that encode the BH3-only proteins HRK and BIM, respectively. However, treatment of mouse embryonic fibroblasts (MEFs) with inhibitors of mRNA and protein synthesis demonstrated that gene expression and protein synthesis were not required for the observed cell death after UV exposure (Tournier et al. 2000). Thus, JNK could promote cell death independently of gene expression.

Among the targets of JNK are the BCL2 family of proteins (Davis 2000). The anti-apoptotic BCL2-like proteins (BCL2, BCLXL, MCL1, A1, and BCLW) prevent mitochondrial membrane depolarization while the pro-apoptotic BAK/BAX-like (BAK, BAX, and BOK) and BH3-only (BAD, BID, BIK, BIM, BMF, HRK, NOXA, and PUMA) proteins induce it (Huang and Strasser 2000; Pinon et

al. 2008; Czabotar et al. 2014). Therefore, JNK could promote apoptosis by inhibiting BCL2-like proteins. Indeed, JNK phosphorylates BCL2 and BCLXL, although it has been reported that this JNK-mediated phosphorylation regulates autophagy instead of apoptosis (Wei et al. 2008). JNK also phosphorylates and inhibits the anti-apoptotic BCL2-like protein MCL1, which serves as a point of integration of pro-apoptotic signaling from JNK and pro-survival signaling from AKT (Morel et al. 2009).

JNK may also promote cell death by activating pro-apoptotic BH3-only members of the BCL2 family. JNK is reported to phosphorylate the BH3-only protein BAD to promote cell death (Donovan et al. 2002), though how this phosphorylation activates BAD is unknown. In contrast, the JNK-mediated activation of two other BH3-only proteins, BIM and BMF, is better understood. JNK phosphorylates the dynein light chain binding motif present on BIM, releasing it from sequestration and allowing it to promote BAX-mediated apoptosis (Lei et al. 2002; Lei and Davis 2003; Hubner et al. 2008; Hubner et al. 2010). The presence of a similar site on the BH3-only protein BMF, another target of JNK, suggests a similar mechanism may regulate BMF activation (Lei and Davis 2003). These phosphorylation events on anti- and pro-apoptotic BCL2 family members may account for transcription-independent JNK-mediated cell death (Tournier et al. 2000).

JNK-mediated cell death relies on inactivation of survival pathways, including AKT and ERK. The inhibitory phosphorylation of JNK on MCL1 will

only promote cell death if the AKT pathway is inactivated (Morel et al. 2009). BIM is another point of JNK and survival signal integration. Whereas JNK phosphorylation allows BIM to translocate to mitochondria and activate BAK/BAX, ERK phosphorylation induces proteasomal degradation of BIM (Ley et al. 2003; Hubner et al. 2008). Thus, the examples of BIM and MCL1 demonstrate that the pro-apoptotic signals from JNK are balanced by the pro-survival signals from AKT and ERK to decide the fate of the cell.

Clearly, JNK promotes cell elimination in response to certain stimuli. However, the absence of JNK in the developing forebrain results in increased apoptosis (Kuan et al. 1999; Sabapathy et al. 1999). Similarly, in transformed lymphoblasts (Hess et al. 2002) and in carcinogen-treated livers (Das et al. 2011) loss of JNK signaling increases cell death, indicating that JNK signaling can also contribute to cell survival. Studies of JNK-deficient MEFs demonstrated that they are more sensitive to TNF treatment than control cells (Lamb et al. 2003; Ventura et al. 2004a; Jaeschke et al. 2006; Ventura et al. 2006). A missing survival signal was *Jund*, a pro-survival protein whose expression is JNK-dependent (Lamb et al. 2003). Through JUND, the JNK pathway cooperates with the NF- κ B pathway to promote expression of *cIAP2* thereby enabling cell survival following TNF exposure (Lamb et al. 2003; Ventura et al. 2006). Moreover, the dynamics of JNK signaling determines cell survival. That is, acute JNK activation in response to TNF α treatment is important for survival signaling, while chronic JNK activation mediates cell death (Ventura et al. 2006).

JNK and cell proliferation

In addition to its role in cell death and survival, JNK regulates proliferation. Genetic studies in *Drosophila* have demonstrated that JNK pathway activation can promote cell autonomous (Igaki et al. 2006; Biteau et al. 2008) and non-autonomous (Ryoo et al. 2004; Uhlirova et al. 2005) proliferation. In mice, p38 α deficiency results in increased JNK pathway activity and increased proliferation in various cell types (Hui et al. 2007). Similarly, loss of NF- κ B activity leads to JNK activation and proliferation in the epidermis (Zhang et al. 2004). The observation that JNK-deficient MEFs undergo *Trp53*-dependent senescence further supports a positive role for JNK in proliferation (Das et al. 2007).

One means by which JNK could promote proliferation is through its major target cJUN. Loss of cJUN results in increased *Trp53* expression, delayed G1-to-S phase progression, and decreased proliferation rates (Schreiber et al. 1999). Furthermore, cJUN phosphorylation by JNK is required for cell proliferation (Behrens et al. 1999). In both the p38 α - and RelA-deficient mice that exhibit increased proliferation and JNK activity there is also increased cJUN activity, suggesting that JNK-cJUN pathway drives proliferation in these models (Zhang et al. 2004; Hui et al. 2007). Supporting this conclusion is the observation that JNK inhibition can reverse cJUN activation and hyperplasia in the epidermis of *Rela*^{-/-} animals (Zhang et al. 2004). Finally, loss of JNK in MEFs leads to

decreased levels of cJUN, which increase *Trp53* mRNA and TRP53 protein, resulting in cellular senescence (Das et al. 2007).

These findings suggest that tissues relying on proliferation to cope with high turnover or damage would require JNK signaling. However, mice lacking JNK in the intestine and colon exhibit no changes in TRP53 levels, and no decrease in proliferation or disruption to the tissue architecture (Cellurale et al. 2012). Similarly, JNK is dispensable in mammary gland transplantation assays and its loss increases proliferation of mammary epithelial cells *in vitro* (Cellurale et al. 2012). In the context of tissue injury, hepatocytes lacking JNK regenerate damaged livers comparably to controls (Das et al. 2011). This model also demonstrated that JNK deficiency in hepatocytes causes increased pro-inflammatory cytokine expression and subsequent compensatory proliferation, leading to increased tumor burden- (Das et al. 2011). This observation suggests that in the presence of liver damage, JNK deficiency causes changes in gene expression that result in an environment that supports growth. Thus, the role of JNK in proliferation is context-dependent, relying on cell type, other signaling pathways, and environmental factors.

JNK and Development

It is clear that the JNK pathway regulates cell death, survival, and proliferation. This pathway has also been shown to influence cell migration (Huang et al. 2004). It is therefore not surprising that genetic studies of the JNK pathway in flies and mice have demonstrated that it is essential during developmental morphogenesis.

The JNK Pathway in Drosophila Development

During embryonic development in *Drosophila*, two sheets of ectodermal cells migrate toward the dorsal midline and subsequently fuse to form a strong connection in a process termed dorsal closure (Ring and Martinez Arias 1993). This process requires the MAP2K7/JNK/JUN pathway (Riesgo-Escovar et al. 1996; Sluss et al. 1996). In particular, in the absence of JNK or JUN the TGF β homolog DPP is not expressed, resulting in defects in cell shape changes (Riesgo-Escovar and Hafen 1997; Sluss and Davis 1997). Re-expression of DPP partially rescues the dorsal closure defect in JNK-mutant embryos, indicating that JNK-mediated expression of DPP represents a mechanism for JNK regulation of cell migration and spreading (Riesgo-Escovar and Hafen 1997). In addition to the expression of DPP, JNK may play a role in actin polymerization and stabilization during dorsal closure (Xia and Karin 2004). Similarly, thoracic closure requires a JNK/FOS pathway for proper execution (Zeitlinger and Bohmann 1999). Furthermore, in later stages of development,

loss of JNK activity causes decreased size and malformation of imaginal discs, and delayed larval development (Agnes et al. 1999).

The JNK pathway is also required to maintain healthy epithelial cell sheets in *Drosophila* during development as well as in the adult fly. JNK-dependent cell death eliminates cells as a result of limiting amounts of morphogen, such as TGF β (Moreno et al. 2002), or as a result of oncogene expression, such as cMYC (Moreno and Basler 2004). Additionally, extrusion of epithelial cells from the epithelium results in JNK activation in these cells, leading to apoptosis (Adachi-Yamada et al. 1999; Adachi-Yamada and O'Connor 2002; Gibson and Perrimon 2005; Shen and Dahmann 2005). Collectively, these results demonstrate that the JNK pathway is important throughout development and in various tissues of the fly.

The JNK Pathway in Mammalian Development

Unlike *Drosophila*, mammals have 3 JNK genes, necessitating the study of compound knock-out mutants to establish the importance of these genes.

Mapk8^{-/-} *Mapk9*^{-/-} animals die during gestation (Kuan et al. 1999). However, *Mapk8*^{-/-} *Mapk10*^{-/-} and *Mapk9*^{-/-} *Mapk10*^{-/-} mice are healthy and fertile (Weston et al. 2004). Thus, for mammalian development, *Mapk10* is dispensable, while the ubiquitously expressed *Mapk8* and *Mapk9* are essential.

A major defect observed in *Mapk8^{-/-} Mapk9^{-/-}* animals is a failure of neural tube closure (Kuan et al. 1999; Sabapathy et al. 1999). This morphogenic process in mammals shares characteristics with dorsal and thoracic closure in *Drosophila*. JNK is also needed for expression of BMP4 during optic fissure closure through a process analogous to the DDP-driven dorsal closure mechanism in *Drosophila* (Weston et al. 2003). These results demonstrate an evolutionarily conserved role for JNK in these developmental programs, and they suggest that this role for JNK applies across different species.

The presence of a single copy of *Mapk9* does not greatly improve animal health. Studies using *Mapk8^{-/-} Mapk9^{+/-}* mice revealed that 80% die within 48 hours of birth and those surviving to adulthood are sterile (Weston et al. 2003; Weston et al. 2004). As a result of decreased EGF expression and subsequent decreased signaling through EGFR, these mice exhibit epidermal defects, including open eyes at birth. In contrast, *Mapk8^{+/-} Mapk9^{-/-}* animals were healthy and fertile, indicating some differences between JNK1 and JNK2 expression or function (Weston et al. 2004).

The eye lid closure defect in *Mapk8^{-/-} Mapk9^{+/-}* (Weston et al. 2004) was also observed in *Map3k1^{-/-}* (Yujiri et al. 2000; Zhang et al. 2003) and in epidermis-specific cJUN-knockout mice (Zenz et al. 2003). Together with the neural tube and optic fissure closure defects, these data strongly implicate JNK in the promotion of cell migration. Indeed, in addition to regulating the expression of factors that drive cell migration, JNK can phosphorylate paxillin, a

protein involved in focal adhesion turnover (Huang et al. 2003). However, JNK is dispensable in the gut and mammary gland (Cellurale et al. 2012). Also, loss of JNK in endothelial cells has no impact on their motility (Ramo et al. 2016). Thus, contrary to the widely accepted essential role of JNK in cell migration (Huang et al. 2004), its contribution to migration is likely to be more nuanced than previously thought, depending on cell type, developmental stage, and stimulus.

The development of conditional alleles for *Mapk8* and *Mapk9* has allowed dissection of JNK function in specific cell types during organismal development and in adulthood. For example, loss of the MLK2/3-JNK signaling pathway in endothelial cells impairs collateral artery formation due to decreased Dll4-Notch signaling in the JNK-deficient mice (Ramo et al. 2016). In contrast, JNK is dispensable in the gut epithelium (Cellurale et al. 2012). Similarly, T cells develop normally in the absence of JNK signaling, though their differentiation to the Th1 lineage is compromised, indicating an important role for the pathway in adulthood (Dong et al. 1998). Studies using these conditional alleles crossed to additional tissue-specific *Cre* strains will undoubtedly yield new insight into additional developmental programs regulated by this pathway.

Mammary gland biology

On the 12th day of development in the mouse, 5 pairs of placodes can be found along the milk line (Watson and Khaled 2008). These structures will become epithelial cell buds that invade into the fat pad at embryonic day 13.5, and by

embryonic day 18.5 they will become quiescent, having formed rudimentary glands (Watson and Khaled 2008). During puberty, ovarian and pituitary hormones (in particular estrogen and growth hormone) re-initiate mammary gland development, stimulating branching morphogenesis to produce a ductal tree (Sternlicht et al. 2006). Cyclic ovarian stimulation throughout adulthood leads to increased proliferation and apoptosis, resulting in the formation of tertiary branches (Fata et al. 2001). The adult ducts are composed of an epithelial bilayer, with contractile myoepithelial cells able to propel milk toward the nipple lining the outside of the duct and luminal cells capable of differentiating to milk-producing cells on the inside of the duct (Inman et al. 2015). The adult gland is now prepared for the cycle of expansion and contraction in response to pregnancy, lactation, and involution (Figure I.2).

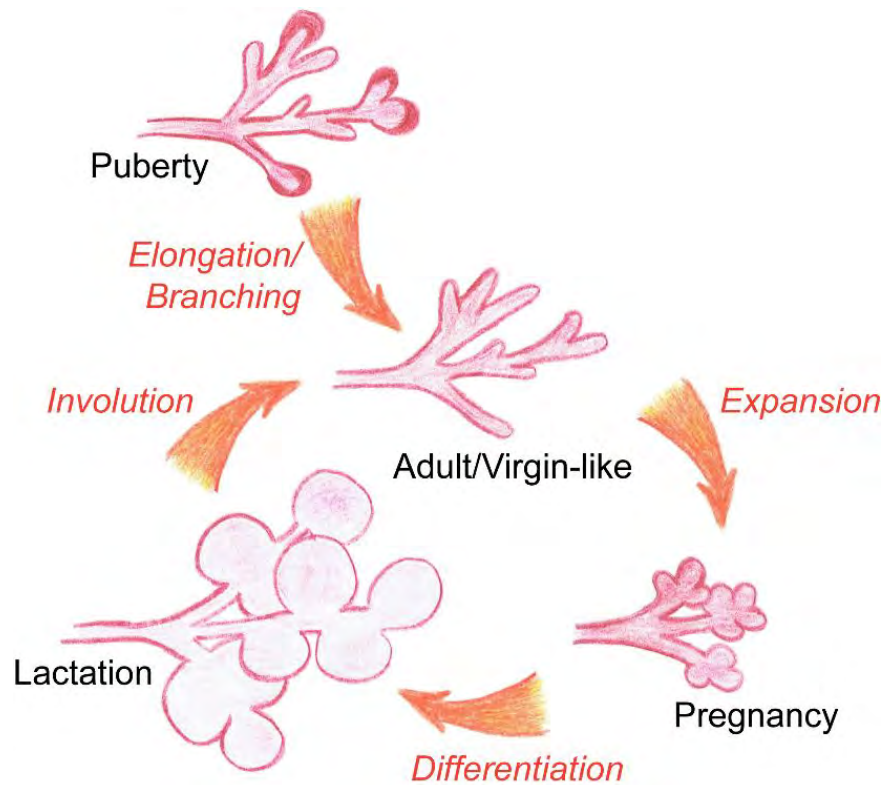


Figure I.2. The mammary gland is a dynamic organ capable of multiple cycles of expansion and contraction in adulthood.

Branching morphogenesis during puberty results in a network of ducts prepared for expansion in response to pregnancy. As pregnancy progresses to lactation, the luminal epithelial cells differentiate to alveolar cells in preparation for lactation. Upon weaning, the epithelial compartment collapses and the gland returns to a virgin-like state through the process of involution. This cycle continues throughout the life of the animal.

The fact that this cycle relies on several processes involved in tumorigenesis (proliferation, angiogenesis, matrix remodeling, and inhibition of apoptosis) indicates that tight regulation by many signaling pathways at different stages is necessary to prevent disease (Figure I.3). Among the identified regulators of branching morphogenesis is the JNK pathway (Cellurale et al. 2012). Its role in other stages of breast development has yet to be elucidated.

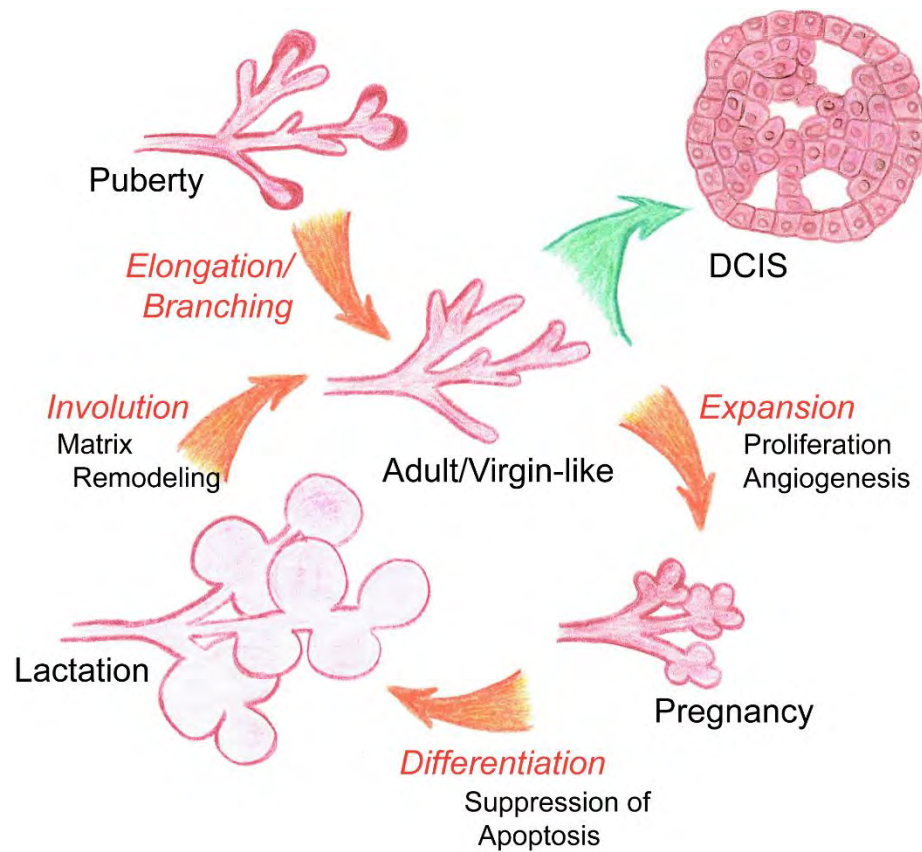


Figure I.3. Processes occurring during the normal stages of mammary gland development are also involved in carcinogenesis.

The cyclic expansion and regression of the mammary gland that occurs in response to pregnancy, parturition, and weaning involves many of the programs co-opted by transformed cells for their expansion, including proliferation, angiogenesis, suppression of apoptosis, and matrix remodeling. Thus, the epithelial cells must retain tight control of these processes to prevent the development of ductal carcinoma *in situ* (DCIS).

Mammary gland development: Puberty to Adulthood

The active sites of branching morphogenesis during puberty are the tips of the invading branches that contain the mammary stem cells (Scheele et al. 2017), bulbous structures called terminal end buds (TEB, Figure I. 4A). These structures are organized into the tip-lining cap cells and the interior body cells (Figure I.4B) (Williams and Daniel 1983). Proliferation to expand the mammary epithelium occurs in the cap cells of the TEB (Humphreys et al. 1996), while the body cells are the site of extensive apoptosis due to lack of cell attachment (anoikis) (Humphreys et al. 1996). Three-dimensional cultures of mammary epithelial cells has provided additional support for this model of lumen formation (Mailleux et al. 2008). The removal of these occluding cells leaves the luminal-myoepithelial cell bilayer (Figure I.4C & D).

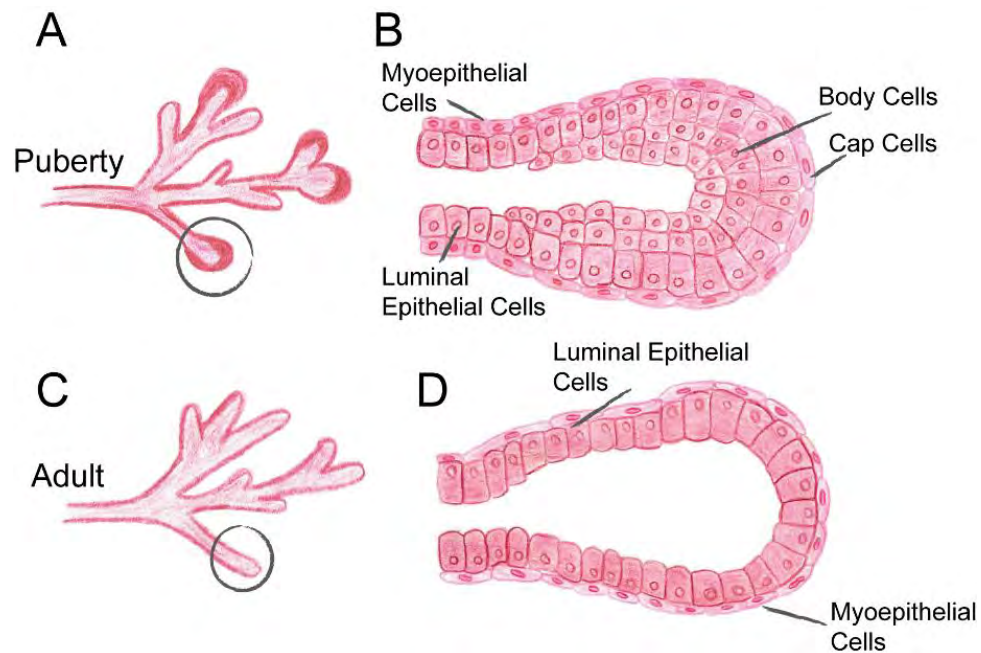


Figure I.4. Mammary gland structure during pubertal development into adulthood.

A, B) In the pubertal mammary gland (A), the tips of the ducts have bulbous, multi-layered structures called terminal end buds (circle in A). These structures are organized into the interior body cells and the tip-lining cap cells (B). While the highly proliferative cap cells expand and invade into the mammary fat pad, the body cells are cleared by apoptosis to form a single layer of luminal epithelial cells.

C, D) Terminal end buds are absent in the adult mammary gland (circle in C); the clearance of the excess cells during puberty leaves a cell bilayer with myoepithelial cells lining the outside of the duct and luminal epithelial cells lining the inside (D).

The BCL2 family of proteins are key players in luminal clearance. Over-expression of the pro-survival protein BCL2 in the mammary epithelium leads to decreased apoptosis in the TEBs (Humphreys et al. 1996) and loss of the pro-apoptotic BH3-only protein BIM causes delayed luminal clearance (Mailleux et al. 2007). Similarly, the BH3-only protein BMF is upregulated during acinar morphogenesis and promotes lumen formation (Schmelzle et al. 2007). Because there are several BH3-only proteins with partial redundancies (Huang and Strasser 2000; Pinon et al. 2008; Czabotar et al. 2014), it is likely that other members of this family are involved in luminal clearance during pubertal development.

As a regulator of BH3-only proteins, both at the level of mRNA through cJUN activation and the level of protein by phosphorylation, JNK is an appealing candidate for regulating mammary gland development. Indeed, JNK is required for proper acinus formation *in vitro* (Murtagh et al. 2004; Zhan et al. 2008; McNally et al. 2011). During this process, JNK is activated by a Scribble/bPIX/GIT1-RAC pathway and subsequently activates cJUN to induce *Bcl2l1* expression (Zhan et al. 2008). Regardless of when JNK is inhibited during acinar morphogenesis, luminal clearance is impaired, but early inhibition of JNK also disrupts cell polarization (McNally et al. 2011). This finding indicates that the JNK pathway influences different stages of acinar morphogenesis.

In vivo studies have confirmed the importance of JNK in mammary gland development. Mice with whole-body deletion of *Mapk9* exhibit increased

branching morphogenesis and an expanded luminal cell population (Cantrell et al. 2015). These perturbations resolve in adulthood; mammary glands of adult *Mapk8*^{-/-} and *Mapk9*^{-/-} mice do not have architectural or functional defects (Cellurale et al. 2010). Because MAPK8 and MAPK9 proteins serve redundant functions, it was important to examine compound mutant glands. A transplantation model in which mammary fat pads of wildtype mice were cleared and reconstituted with *Mapk8*^{Loxp/Loxp} *Mapk9*^{-/-} *Rosa-Cre*^{ERT} tissue revealed that loss of JNK proteins results in increased ductal branching, a phenotype also observed in *in vitro* organoid cultures (Cellurale et al. 2012). The TEBs of these glands also exhibited filled lumens without increased proliferation, suggesting that loss of JNK compromises anoikis (Cellurale et al. 2012). Surprisingly, JNK deficiency did not prevent epithelial cell migration into the fat pad as would have been predicted based on the observed requirement for JNK in cell migration (Huang et al. 2003).

It remains unclear how JNK regulates luminal clearance. Inhibition of the related p38 MAPK pathway during pubertal mammary gland development results in a similar phenotype to the JNK-deleted gland: occluded lumens and increased branching (Wen et al. 2011). In MEC, the p38 MAPK pathway activates ATF2 resulting in ATF2-cJUN heterodimers that increase the expression of cJUN and BIMEL (Wen et al. 2011). As an activator of AP1 proteins, JNK may employ a similar mechanism. An alternative mechanism of JNK-mediated luminal

clearance could involve BH3-only protein phosphorylation to promote cell death (Hubner et al. 2008).

Mammary gland development: Involution

During pregnancy, the hormones progesterone and prolactin are critical for additional expansion of the epithelial compartment and lobuloalveolar differentiation in preparation for lactation (Humphreys et al. 1997; Ormandy et al. 1997) (Figure I.5). Through STAT5, prolactin induces mammary epithelial cell proliferation and differentiation (Liu et al. 1997; Cui et al. 2004). However, prolactin levels drop during weaning, resulting in decreased STAT5 activity (Philp et al. 1996). Epithelial cell death, adipocyte repopulation, and extracellular matrix remodeling all occur to return the gland to a virgin-like state through the process of involution.

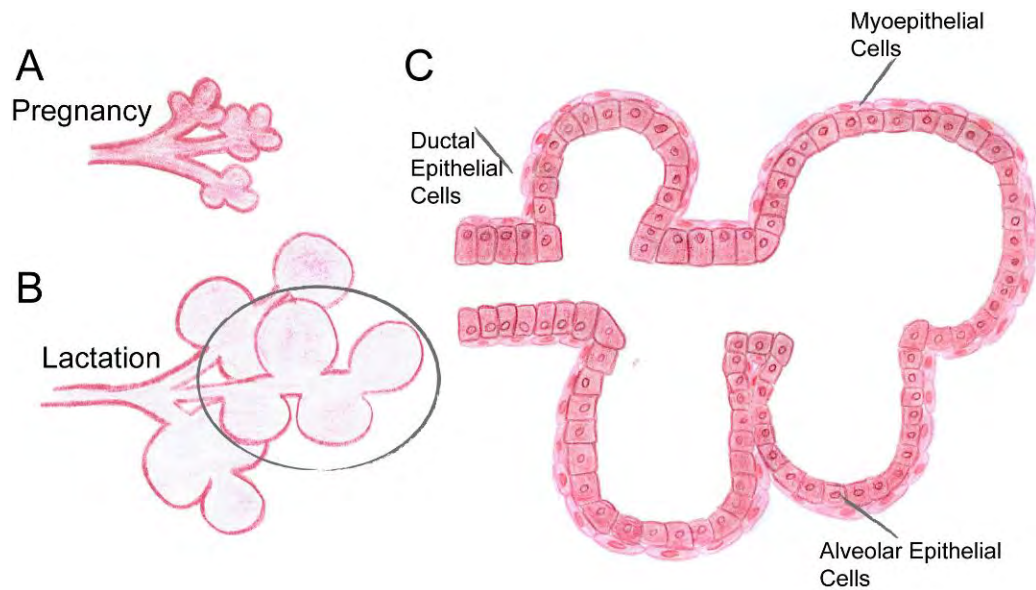


Figure I.5. Mammary gland structure during pregnancy and lactation.

A) In response to pregnancy, the mammary epithelial cells expand and differentiate in preparation for lactation.

B, C) The expanded epithelial compartment begins lactating following parturition (B). Within it, the luminal epithelial cells have differentiated to alveolar cells, forming lobuloalveolar units that are responsible for milk production (C).

Involution has distinct phases that are characterized by their reversibility and differential gene expression (Lund et al. 1996; Li et al. 1997; Stein et al. 2007). As demonstrated in sealed teat models that maintain lactogenic hormone circulation with continual nursing, milk accumulation is sufficient to induce *Bax* expression, STAT3 activation, and cell death during the first phase of involution (Li et al. 1997). The second, irreversible phase of involution is induced by decreased lactogenic hormones and is characterized by alveolar collapse and extensive remodeling of the gland (Li et al. 1997). Among the upregulated genes are proteinases, such as *Mmp3*, which promotes adipogenesis in the gland (Lund et al. 1996; Alexander et al. 2001).

Just as STAT5 maintains lactation, STAT3 is required for efficient involution (Chapman et al. 1999; Humphreys et al. 2002). In fact, loss of STAT3 not only delays involution, it also prolongs lactation even in the absence of lactogenic stimuli (Humphreys et al. 2002). During involution, there is increased expression of STAT3-activating cytokines LIF, IL6, and oncostatin M (Zhao et al. 2002; Kritikou et al. 2003; Tiffen et al. 2008). The activation of STAT3 through JAK1 induces the expression of STAT3 target genes, including the pro-apoptotic BH3-only proteins BIM and BMF (Sakamoto et al. 2016). This induction of BIM and BMF is likely functional, as loss of either delays mammary gland involution (Sakamoto et al. 2016; Schuler et al. 2016). STAT3 can also promote expression of cathepsin b and cathepsin l to induce a lysosome-mediated death

pathway in mammary epithelial cells (Kreuzaler et al. 2011; Sargeant et al. 2014).

The TGF β pathway also contributes to the involution program. Several TGF β isoforms are induced during involution, suggesting they may regulate this process (Faure et al. 2000). Indeed, loss of TGF β or SMAD3 causes decreased cell death during involution (Nguyen and Pollard 2000; Yang et al. 2002). Conversely, overexpression of TGF β 3 results in increased cell death during lactation (Nguyen and Pollard 2000).

The ability of the JNK pathway to respond to cytokines and induce cell death suggests it may participate in the involution program. Furthermore, BIM and BMF, two mediators of cell death during involution that promote the collapse of the epithelium, are targets of JNK phosphorylation (Lei et al. 2002; Lei and Davis 2003; Hubner et al. 2008; Hubner et al. 2010). Thus, JNK may promote involution by phosphorylating BIM and BMF. Alternatively, JNK may regulate the expression of genes implicated in involution, such as *Bcl2l1* (Whitfield et al. 2001) or matrix metalloproteases (Chakraborti et al. 2003), through AP1 members. Indeed, AP1 DNA binding activity is dynamically regulated by suckling: within 24 hours of removing pups AP1 DNA binding increases, and the resumption of nursing reverses this binding (Jaggi et al. 1996). Activated cJUN is still present after 3 days of involution, suggesting that it may contribute to both stages of mammary gland involution (Marti et al. 1999). Because studies of *Mapk8*^{-/-} and *Mapk9*^{-/-} mice did not reveal any defects during involution (Cellurale

et al. 2010), it will be necessary to examine compound loss of JNK in the mammary epithelium to determine the importance of this pathway in involution.

Stromal cells in mammary gland involution

The return to a quiescent mammary gland after lactation does not rely solely on epithelial cells. As the epithelial cells are removed, adipocytes must differentiate and repopulate the gland, otherwise involution is disrupted (Lund et al. 2000; Selvarajan et al. 2001). Fibroblast-like cells produce proteases to aid in gland remodeling during the second phase of involution (Lund et al. 1996). Also, immune cells, such as neutrophils and B cells, mount a response in the involuting gland that is similar to the wound healing response (Stein et al. 2004; Martinson et al. 2015).

Perhaps the most studied stromal cells in involution are macrophages. Macrophage depletion during lactation delays epithelial cell death and adipocyte repopulation during involution (O'Brien et al. 2012). The infiltrating macrophages of involuting glands express M2 markers, arginase 1 and mannose receptor (O'Brien et al. 2010). These macrophages along with the other infiltrating immune cells produce an environment that resembles the wound healing response, both in the type of infiltrating cell and the timing of the cells' arrival (Martinson et al. 2015). Macrophage infiltration of involuting breast tissue has been observed in humans as well (O'Brien et al. 2010). Even after regression of

the epithelial compartment, macrophages are present at elevated levels (Jindal et al. 2014).

Inflammation characterized by M2 macrophages promotes cancer by providing beneficial cytokines and aiding tissue remodeling (Melief and Finn 2011). Also, collagen deposition that occurs during remodeling can promote tumor cell growth and invasion (Lyons et al. 2011). Thus, involution creates an environment conducive to tumorigenesis in which human tumor cells thrive (Lyons et al. 2011). Indeed, women diagnosed with breast cancer within 5 years of pregnancy have a poorer prognosis than nulliparous women (Schedin 2006). Additional work is needed to understand involution in order to develop therapeutic approaches for women who develop post-partum breast cancer.

JNK and Cancer

Cellular transformation involves co-opting normal processes to promote cell survival and expansion (Hanahan and Weinberg 2011). The PI3K/AKT (Yuan and Cantley 2008), RAS (Downward 2003), and p53 (Halazonetis et al. 2008; Vousden and Prives 2009) pathways are frequently used by cells to escape the regulatory mechanisms checking their growth.

Sequencing of human tumors and tumor-derived cell lines has implicated the JNK pathway in cancer. Deletions or loss of heterozygosity of *MAP2K4*, one of the upstream activators of JNK, were found in a subset of human tumor cell

lines, suggesting that this gene is a tumor suppressor (Teng et al. 1997). With increased sequencing of human tumors, more evidence has been found for the JNK pathway's involvement in this disease. A study focused on serine/threonine kinase mutations in colorectal cancers also identified *MAP2K4* mutations (Parsons et al. 2005). Yet another study found mutations in *MAPK8* and *MAPK9* as well as *MAP2K7* in different human tumors (Greenman et al. 2007). While these sequencing studies implicate the JNK pathway in human cancer, the functional relevance of these mutations in tumorigenesis is unknown.

JNK pathway: tumor promoting or suppressing?

The examination of JNK in *Drosophila* models revealed different roles for the JNK pathway. The JNK pathway was able to suppress tumorigenesis by eliminating cells that had lost polarity due to mutations in genes like *scribble* (Brumby and Richardson 2003; Uhlirova et al. 2005; Igaki et al. 2006; Igaki et al. 2009). However, in the context of activated RAS, JNK took on oncogenic roles and was required for the invasive and metastatic behavior of cells (Igaki et al. 2006; Uhlirova and Bohmann 2006). These experiments supported a role for the JNK pathway in cancer.

The major target of JNK is the proto-oncogene cJUN. Since the JNK pathway activates cJUN, it would be predicted that JNK promotes cancer. Indeed, the oncogene RAS causes increased JNK activity and phosphorylation of

cJUN on Ser63 and Ser73, the JNK target sites (Pulverer et al. 1991; Smeal et al. 1991; Derijard et al. 1994). Furthermore, these phosphorylation sites on cJUN contribute to RAS- or FOS-driven transformation (Behrens et al. 2000). Similarly, ERBB2-driven transformation of mammary epithelial cells was reported to rely on the JNK/cJUN pathway (Guo et al. 2006). These observations suggest that JNK activity drives cancer.

In contrast to the reported tumor-promoting function of JNK, aging studies of *Trp53^{+/-} Mapk8^{-/-}* and *Trp53^{+/-} Mapk9^{-/-}* mice showed enhanced tumor formation compared to *Trp53^{+/-}* controls (Cellurale et al. 2010). Furthermore, an *in vivo* KRAS^{G12D}-driven model of lung cancer (Cellurale et al. 2011) as well as a transplantation model of breast cancer (Cellurale et al. 2012) demonstrated that JNK was dispensable during oncogenesis if *Trp53* was deleted. In fact, JNK loss together with *Trp53* deletion accelerated tumor formation (Cellurale et al. 2011; Cellurale et al. 2012). These data contrast with the observed requirement for JNK in transformation and demonstrate that the JNK pathway plays context-specific roles during tumorigenesis.

Cancer stem cells and the JNK Pathway

As a regulator of transcription factors, it is likely that JNK signaling may impinge on genes that modulate cell differentiation. Inactivation of the JNK pathway together with *Pten* loss in prostate epithelial cells results in large tumors that form

more rapidly than in mice only deficient for *Pten* (Hubner et al. 2012).

Characterization of the tumor cells revealed that the prostate cancer cells without a functional JNK pathway had an expanded stem cell-like population relative to controls, indicating that JNK pathway inhibition in prostate epithelial cells may promote cancer by expanding the stem cell compartment (Hubner et al. 2012). This observation contrasts with the reported requirement for JNK signaling to maintain cancer stem cell activity in triple negative breast cancer cell lines (Xie et al. 2017). This discrepancy may be due to the means of pathway inactivation (i.e. genetic inactivation of JNK versus small molecule or siRNA targeting of JNK) or the tissue being studied. Nevertheless, both studies indicate that the JNK pathway can influence the stem cell compartment.

More generally, these observations indicate that the JNK pathway may regulate terminal cell differentiation and in doing so may impact tumorigenesis. Indeed, JNK is known to be required for proper embryonic stem cell differentiation (Xu and Davis 2010). In both the mammary gland and in mammary tumors, loss of JNK2 expands ER-positive cells and results in increased ER-associated proliferation (Cantrell et al. 2015). Similarly, mice with activated KRAS and no functional JNK pathway showed accelerated acinar-to-ductal metaplasia in the pancreas (Davies et al. 2014). This result suggests that the JNK pathway prevents cells from differentiating to a cell type more susceptible to transformation. Thus, JNK enables cells to retain acinar

differentiation, making them refractory to KRAS-driven transformation and pancreatic ductal adenocarcinoma (Davies et al. 2014).

JNK and DNA damage

The acquisition of advantageous mutations marches cells down the path of transformation; therefore sensing and repairing lesions in the DNA are key tumor suppressive processes (Hanahan and Weinberg 2011). These mutations can occur after exposure to environmental sources of DNA damage, such as ionizing radiation, ultraviolet light, and chemotherapeutic drugs, or from cell-intrinsic sources. For example, insults to DNA occur as a result of metabolic processes that generate reactive oxygen species (ROS) (Kryston et al. 2011). In settings of chronic inflammation, increased cell proliferation in the presence of ROS results in increased mutagenesis (Grivennikov et al. 2010). Oncogene activation can also increase DNA double strand breaks due to increased replication stress (Halazonetis et al. 2008).

In the presence of DNA damage, sensing proteins activate the PI3K family members ATM/ATR to engage the appropriate repair pathway (Ciccia and Elledge 2010). DNA damage also causes phosphorylation of the histone H2AX protein at serine 139 to promote the assembly of factors that mediate repair (Ciccia and Elledge 2010). JNK has been implicated in the phosphorylation of H2AX at this site (Lu et al. 2006; Boege et al. 2017) and JNK inhibition resulted

in decreased DNA damage repair signaling (Boege et al. 2017). In the presence of oxidative stress, JNK is activated and it phosphorylates SIRT6, resulting in SIRT6 binding to DNA and recruiting PARP for double strand break (DSB) repair (Van Meter et al. 2016). JNK can also phosphorylate DGCR8 to promote transcriptional-coupled nucleotide exchange repair (Calses et al. 2017). The involvement of JNK in the DNA damage response suggests that JNK-deficient tumors will exhibit increased genomic instability. Indeed, *Mapk9*^{-/-} tumor cells experience replicative stress and have increased aneuploidy relative to controls (Chen et al. 2010).

JNK activity in response to various genotoxic agents has also been examined. For example, the DNA alkylating agent MMS strongly activates JNK (Wilhelm et al. 1997). In *Mapk8*^{-/-} *Mapk9*^{-/-} MEFs, MMS treatment results in growth arrest rather than cell death (Tournier et al. 2000). Cisplatin treatment also results in JNK activation (Sanchez-Perez et al. 1998; Hayakawa et al. 2004; Helbig et al. 2011), with prolonged JNK activation leading to increased cell death (Chen et al. 1996; Sanchez-Perez et al. 1998). However, cisplatin treatment of breast carcinoma cells also causes a JNK-dependent induction of a substantial number of genes involved in DNA repair (Hayakawa et al. 2004). Thus, JNK activation during cisplatin treatment may enable cells to repair damaged DNA and survive, suggesting that pathway inhibition may sensitize cells to cisplatin.

JNK in breast cancer

In the breast, transformation goes through different stages with hyperplasia leading to ductal carcinoma *in situ*, or DCIS (Bombonati and Sgroi 2011). Two models exist for the subsequent filling of the ductal lumen observed in DCIS:

- (1) Transformed cells translocate to the luminal space and, having overcome anoikis, proliferate there. The increased cell number causes the observed ductal occlusion (Taraseviciute et al. 2010; Leung and Brugge 2012; Pradeep et al. 2012).
- (2) Cell proliferation results in chords of polarized and unpolarized cells spanning the lumen, creating secondary lumina. These structures eventually collapse, resulting in a filled duct (Halaoui et al. 2017).

The resulting breast tumors are classified according to the expression of estrogen receptor (ER) and progesterone receptor (PR), and HER2 amplification, which informs therapeutic approaches (American Cancer Society 2013). Triple negative breast cancers are characterized by lack of ER/PR expression or HER2 amplification and as a result must be treated using chemotherapy which, while beneficial, is less specific (Perou 2011). Gene expression studies have been performed on breast cancer samples to more thoroughly classify these tumors to better understand the disease and its subtypes, to predict clinical outcomes, and to uncover potential therapeutic targets (van 't Veer et al. 2002; Sorlie et al. 2003).

Studies focusing on human breast cancer have found that *MAP2K4* and *MAP3K1* are mutated in human breast cancer (Cancer Genome Atlas 2012; Stephens et al. 2012). In fact, *MAP2K4* and *MAP3K1* are among the most frequently mutated genes in this disease (Nik-Zainal et al. 2016a). A mutation in *MAP2K7*, the gene encoding the other upstream activator of JNK, was also found in a triple negative breast cancer (Wang et al. 2014). The types of mutations identified in these proteins suggest that they result in a loss of protein function (Kan et al. 2010; Banerji et al. 2012; Ellis et al. 2012). A comparison of invasive lobular carcinoma with invasive ductal carcinoma revealed that *MAP3K1* and *MAP2K4* mutations are more frequent in the latter disease, indicating that different breast cancers show a preference for JNK pathway mutations (Ciriello et al. 2015). Collectively, these data implicate the JNK pathway in human breast cancer, but they do not provide insight into how JNK influences cellular transformation.

To address this gap in knowledge, mouse models have been used to examine the role of JNK in breast cancer. Whole-body *Mapk9* deletion in the presence of MMTV-driven polyoma middle T antigen resulted in earlier tumor formation and increased tumors per mouse relative to control animals (Chen et al. 2010). In the context of *Trp53* deficiency, whole-body loss of either *Mapk8* or *Mapk9* resulted in similar tumor spectrums forming with the same kinetics in *Trp53^{-/-}*, *Trp53^{-/-} Mapk8^{-/-}*, and *Trp53^{-/-} Mapk9^{-/-}* mice (Cellurale et al. 2010). However, a comparison of *Trp53^{+/-}*, *Trp53^{+/-} Mapk8^{-/-}* and *Trp53^{+/-} Mapk9^{-/-}* mice

revealed that loss of either JNK isoform reduced tumor-free survival (Cellurale et al. 2010). Additionally, loss of either JNK1 or JNK2 increased the percentage of breast tumors relative to *Trp53*^{-/-} controls (Cellurale et al. 2010).

Because the JNK1 and JNK2 proteins are largely redundant (Tournier et al. 2000), both genes must be deleted to understand the role of this pathway in breast cancer. Considering that compound loss of JNK results in embryonic lethality (Kuan et al. 1999; Sabapathy et al. 1999), a conditional deletion approach is necessary. In a mammary gland transplantation model in which tumors were driven by KRAS activation and *Trp53* deletion, compound JNK loss significantly increased mammary tumor formation (Cellurale et al. 2012). These findings agree with the whole body knock-out studies of JNK in breast cancer (Cellurale et al. 2010; Chen et al. 2010). Additional studies of more human relevant breast cancer models are warranted to better appreciate the role of the JNK pathway in cancer.

Cell-specific Functions of JNK in Cancer

The immune system actively participates in cancer development by both suppressing and promoting the disease (Hanahan and Weinberg 2011; Schreiber et al. 2011). Immune cells prevent tumorigenesis by removing mutant cells and suppressing inflammation; however tumors eventually break through this barrier (Schreiber et al. 2011). Through the recruitment of M2 macrophages, Th2 and

Treg cells, and the exclusion of Th1 cells and M1 macrophages, tumor cells establish an environment that promotes growth and tissue remodeling (Melief and Finn 2011). In addition to influencing cellular transformation in the epithelial cells of a particular tissue, JNK signaling may influence tumorigenesis through immune cells. Indeed, the JNK pathway is important for immune cell differentiation and function (Dong et al. 1998; Yang et al. 1998; Conze et al. 2002; Han et al. 2013).

A role for the JNK pathway in macrophages during carcinogenesis has been identified in hepatocellular carcinoma (HCC), a tumor that relies on an inflammatory environment for its development. While whole-body *Mapk8*^{-/-} mice develop fewer chemically induced HCC lesions than controls (Sakurai et al. 2006; Hui et al. 2008), *Mapk8* deletion in hepatocytes results in increased tumor burden (Das et al. 2011). Simultaneous loss of JNK in parenchymal and non-parenchymal cells of the liver recapitulated the observations made in the whole-body knock-out, indicating that loss of JNK in stromal cells is key for the development of HCC (Das et al. 2011). Furthermore, JNK expression in hematopoietic cells, not hepatocytes, is needed for hepatitis (Das et al. 2009). The observations that JNK is needed for M1 macrophage cytokine expression and is involved in macrophage polarization, led to the hypothesis that HCC development relies on macrophage JNK (Han et al. 2013). Indeed, JNK expression in macrophages is required for the expression of pro-inflammatory cytokines and tumor formation in a model of HCC (Han et al. 2016). These

observations may apply to other tumor types, like breast cancer, that also recruit macrophages to enable disease progression (Lin et al. 2002; Qian and Pollard 2010).

In addition to illustrating a tumor-promoting role for JNK signaling in macrophages, these findings highlight the importance of targeted JNK deletion to study its role in cancer. Studies of whole-body deletion of *Mapk8* or *Mapk9* that have examined the importance of JNK in breast cancer (Cellurale et al. 2010; Chen et al. 2010; Cantrell et al. 2015) may have come to erroneous conclusions because of JNK deficiency in other cell types. Genetically engineered mouse models that target JNK deletion to the mammary epithelium will be necessary to elucidate the role of this pathway in breast cancer.

Rationale and Objectives

The frequent mutation of JNK pathway components in breast cancer necessitates an understanding of its involvement in normal and diseased states of the mammary gland. Overcoming anoikis and surviving in luminal spaces is an early step in transformation (Taraseviciute et al. 2010; Leung and Brugge 2012; Pradeep et al. 2012). Initial studies found evidence supporting (Frisch et al. 1996) and refuting (Khwaja and Downward 1997) a role for JNK during this form of cell death. However, studies of acinar morphogenesis and mammary gland development indicate that JNK is required for luminal clearance (McNally et al. 2011; Cellurale et al. 2012). In Chapter II, I resolve the controversy regarding the requirement for JNK in epithelial cell anoikis and show that JNK promotes this cell death through transcriptional and post-translational regulation.

I next examined the role of the JNK pathway in mammary gland involution following lactation (Chapter III). While the STAT3 (Chapman et al. 1999; Humphreys et al. 2002) and TGF β (Nguyen and Pollard 2000) pathways are known to regulate the return to a virgin-like state, it is likely that other pathways also contribute to this process. The stress-activated MAP kinases are known to participate in mammary gland biology, making them prime candidates (Avivar-Valderas et al. 2014). For example, JNK regulates branching morphogenesis and luminal clearance during pubertal development, demonstrating its importance in mammary gland biology (Cellurale et al. 2012). Furthermore, JNK and its AP1 targets are activated during involution (Jaggi et al. 1996; Marti et al.

1999). These observations suggested that JNK signaling to AP1 members may be involved in the involution program. I found that JNK was required for efficient mammary gland involution and for the expression of a large number of genes involved in this process. Furthermore, this promotion of involution was independent of STAT3 or TGF β signaling.

Finally, I addressed the question of JNK pathway involvement in breast cancer (Chapter IV). Sequencing studies of human tumors have demonstrated that the pathway is frequently mutated in breast cancer (Nik-Zainal et al. 2016a), but the importance of these mutations has not been tested. *In vivo* studies of JNK in breast cancer had used whole-body loss of either *Mapk8* or *Mapk9* (Cellurale et al. 2010; Chen et al. 2010) leaving open the question of how complete JNK pathway inactivation restricted to mammary epithelial cells influences disease progression. While the mammary gland transplantation assays partially addressed this question, these tumors developed in the presence of a compromised immune system and were driven by an oncogene not frequently observed in human breast cancer (Cellurale et al. 2012). Thus, I used conditional gene ablation to delete JNK in the mammary epithelium. I found that JNK loss was sufficient for genomic instability and carcinogenesis. Additional studies in a murine model of breast cancer confirmed that JNK plays a tumor suppressive role in breast cancer, and suggested its main function is to prevent tumor initiation rather than to produce a more aggressive tumor phenotype.

CHAPTER II

JNK PROMOTES EPITHELIAL CELL ANOIKIS BY TRANSCRIPTIONAL AND POST-TRANSLATIONAL REGULATION OF BH3-ONLY PROTEINS

Abstract

Developmental morphogenesis, tissue injury, and oncogenic transformation can cause the detachment of epithelial cells. These cells are eliminated by a specialized form of apoptosis (anoikis). While the processes that contribute to this form of cell death have been studied, the underlying mechanisms remain unclear. Here I tested the role of the cJUN NH₂-terminal kinase (JNK) signaling pathway using murine models with compound JNK-deficiency in mammary and kidney epithelial cells. These studies demonstrated that JNK is required for efficient anoikis *in vitro* and *in vivo*. Moreover, JNK-promoted anoikis required pro-apoptotic members of the BCL2 family of proteins. I show that JNK acts through a BAK/BAX-dependent apoptotic pathway by increasing BIM expression and phosphorylating BMF leading to death of detached epithelial cells.

Introduction

Multicellular organisms rely on apoptosis to remove excess cells, mediate cell turnover, and clear damaged cells in order to prevent disease (Fuchs and Steller 2011). Improper regulation of cell death is implicated in pathogenic processes, including cancer (Hanahan and Weinberg 2011). Gaining an understanding of the pathways that mediate these forms of cell death is therefore critically important.

Pro-apoptotic BCL2-family proteins, including BAK/BAX-like proteins and BH3-only proteins, can initiate cell death, while anti-apoptotic BCL2-family proteins can suppress cell death (Huang and Strasser 2000; Pinon et al. 2008; Czabotar et al. 2014). BAK and BAX can release cytochrome c from mitochondria, thereby committing cells to apoptosis (Jurgensmeier et al. 1998; Narita et al. 1998). Anti-apoptotic BCL2-like proteins can prevent BAK and BAX activation, while pro-apoptotic BH3-only members of the BCL2 family can initiate BAK/BAX-mediated cell death. Multiple signaling pathways target the BCL2-family proteins, and the balance of these signals determines whether a cell initiates apoptosis (Puthalakath and Strasser 2002). The stress-activated c-JUN NH₂-terminal kinase (JNK) pathway (Davis 2000) is one of these signaling mechanisms (Tournier et al. 2000). Pro-apoptotic targets of JNK signaling include the BH3-only proteins BIM and BMF that can initiate BAK/BAX-dependent apoptotic cell death (Lei et al. 2002; Lei and Davis 2003; Hubner et al. 2008; Hubner et al. 2010).

Anoikis – apoptosis induced by epithelial cell detachment – is implicated in the luminal clearance of developing mammary glands (Humphreys et al. 1996), involution of lactating mammary glands (Boudreau et al. 1995), and cancer metastasis (Douma et al. 2004). The initiation of anoikis is induced by the disruption of epithelial cell interactions with the cell matrix (Frisch and Francis 1994; Frisch and Screaton 2001; Reginato et al. 2003). The role of JNK in anoikis is controversial because it has been reported that JNK is essential (Frisch et al. 1996) and also that JNK is dispensable (Khwaja and Downward 1997) for epithelial cell apoptosis in response to detachment. This controversy has yet to be resolved. More recent studies suggest that JNK may promote epithelial cell anoikis *in vitro* (Zhan et al. 2008; McNally et al. 2011) and *in vivo* (Cellurale et al. 2012).

The purpose of this study was to rigorously test the role of JNK in anoikis using compound ablation of the *Mapk8* and *Mapk9* genes that encode the JNK1 and JNK2 protein kinases (Han et al. 2013) and pharmacological inhibition using a highly specific small molecule (Zhang et al. 2012). These *loss-of-function* studies demonstrated that JNK signaling is required for epithelial cell anoikis. Conversely, *gain-of-function* studies using constitutively activated JNK demonstrated that JNK signaling promotes anoikis. Mechanistic analysis demonstrated that JNK-promoted anoikis requires the pro-apoptotic BCL2-family proteins BAK/BAX and the BH3-only proteins BIM and BMF. I show that JNK-induced BIM expression and JNK-mediated phosphorylation of BMF lead to

engagement of the BAK/BAX apoptosis pathway that causes death of detached epithelial cells.

Results

JNK promotes epithelial cell anoikis

To test the role of the JNK pathway during epithelial cell anoikis, I examined the effect of JNK inhibition using a small molecule (JNK-IN-8) that selectively and potently blocks JNK activity (Zhang et al. 2012). Normal human mammary epithelial cells were treated with JNK-IN-8 or solvent (DMSO) and then cultured in suspension (1 h or 48 h). The number of apoptotic (Annexin V⁺ 7-AAD⁻) cells was measured by flow cytometry. Suspension culture (48 h) caused a large increase in apoptosis (anoikis) that was strongly suppressed following treatment with the JNK inhibitor (Figure II.1A-D). Gene expression analysis performed on attached and suspended cells demonstrated JNK-dependent expression of pro-apoptotic genes that encode BH3-only members of the BCL2 family, including *BBC3*, *BIK*, *BCL2L11*, *HRK*, and *PMAIP1* (Figure II.1E).

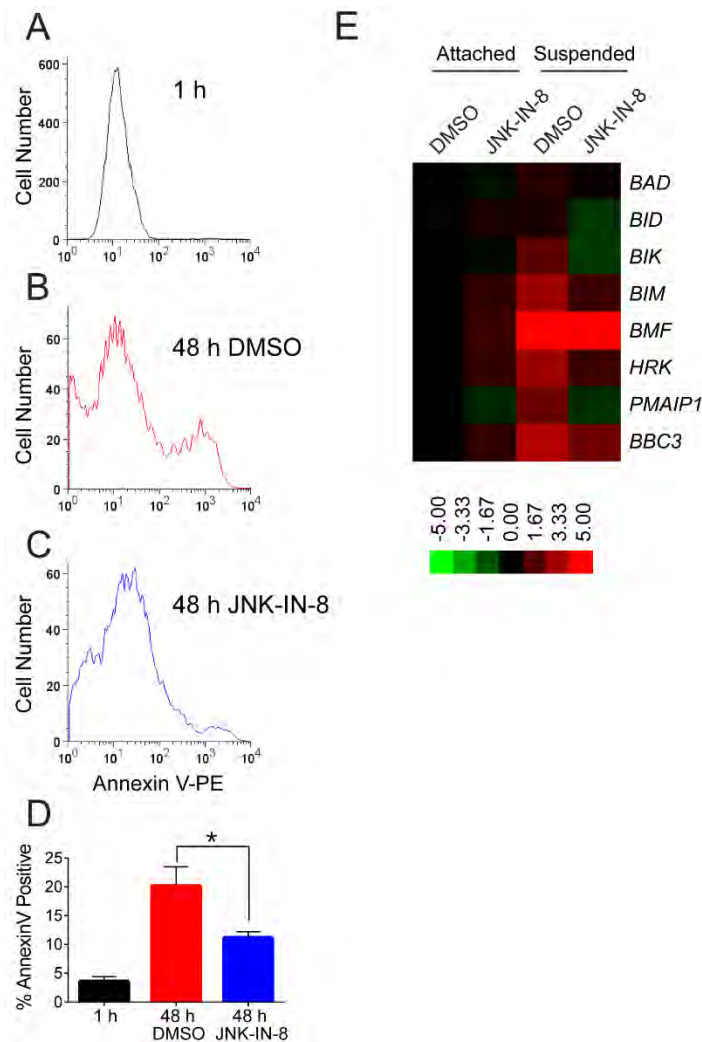


Figure II.1. JNK promotes anoikis of human mammary epithelial cells.

A - C) Human mammary epithelial cells (HMEC) were cultured in suspension for 1 h (A) or 48 h (B,C). The effect of JNK inhibition was examined by incubating the cells with solvent (DMSO) (B) or 2 μ M JNK-IN-8 (C). The cells were stained with Annexin V-PE and 7AAD and examined by flow cytometry. The 7AAD⁻ cell population was gated and examined for Annexin V staining intensity. Representative flow cytometry data are presented.

D) Apoptotic cells (Annexin V⁺ (AnxV⁺) and 7AAD⁻) were quantitated (mean \pm SEM of 5 independent experiments; * $p < 0.05$).

E) HMEC were cultured in suspension for 24 h in the absence or presence of JNK-IN-8. BH3-only gene expression was quantitated using RT-PCR. Mean values are represented as a heatmap (n=3).

To obtain genetic evidence for a role of JNK in epithelial cell anoikis, I examined the effect of *Mapk8* (encodes JNK1) and *Mapk9* (encodes JNK2) gene ablation in primary murine kidney epithelial cells. Immunoblot analysis of Control (*Mapk8*^{+/+} *Mapk9*^{+/+}) and JNK^{KO} (*Mapk8*^{-/-} *Mapk9*^{-/-}) cells confirmed that JNK was expressed in Control, but not JNK^{KO}, epithelial cells (Figure II.2A). I examined anoikis of Control and JNK^{KO} epithelial cells caused by suspension culture (1 h or 24 h). Colony formation assays demonstrated that JNK deficiency promoted epithelial cell survival (Figure II.2B). Quantitation of apoptotic (Annexin V⁺ 7-AAD⁻) cells using flow cytometry (Figure II.2C) and activation of the apoptosis effector caspase 3 by cleavage (Figure II.2D) confirmed that JNK is required for efficient epithelial cell anoikis.

To test whether JNK promotes anoikis, I examined the effect of conditional expression of constitutively activated JNK using epithelial cells transduced with a doxycycline-inducible lentiviral vector that expresses Flag-Mkk7β2-Jnk1α1 (JNK1^{CA}). Immunoblot analysis confirmed that treatment with doxycycline induced the expression of JNK1^{CA} (Figure II.2E). When cultured in suspension (1 h or 24 h), JNK1^{CA} expression in epithelial cells caused an increase in the number of apoptotic (Annexin V⁺ 7-AAD⁻) cells detected by flow cytometry (Figure II.2F). These data demonstrate that JNK functions to promote anoikis.

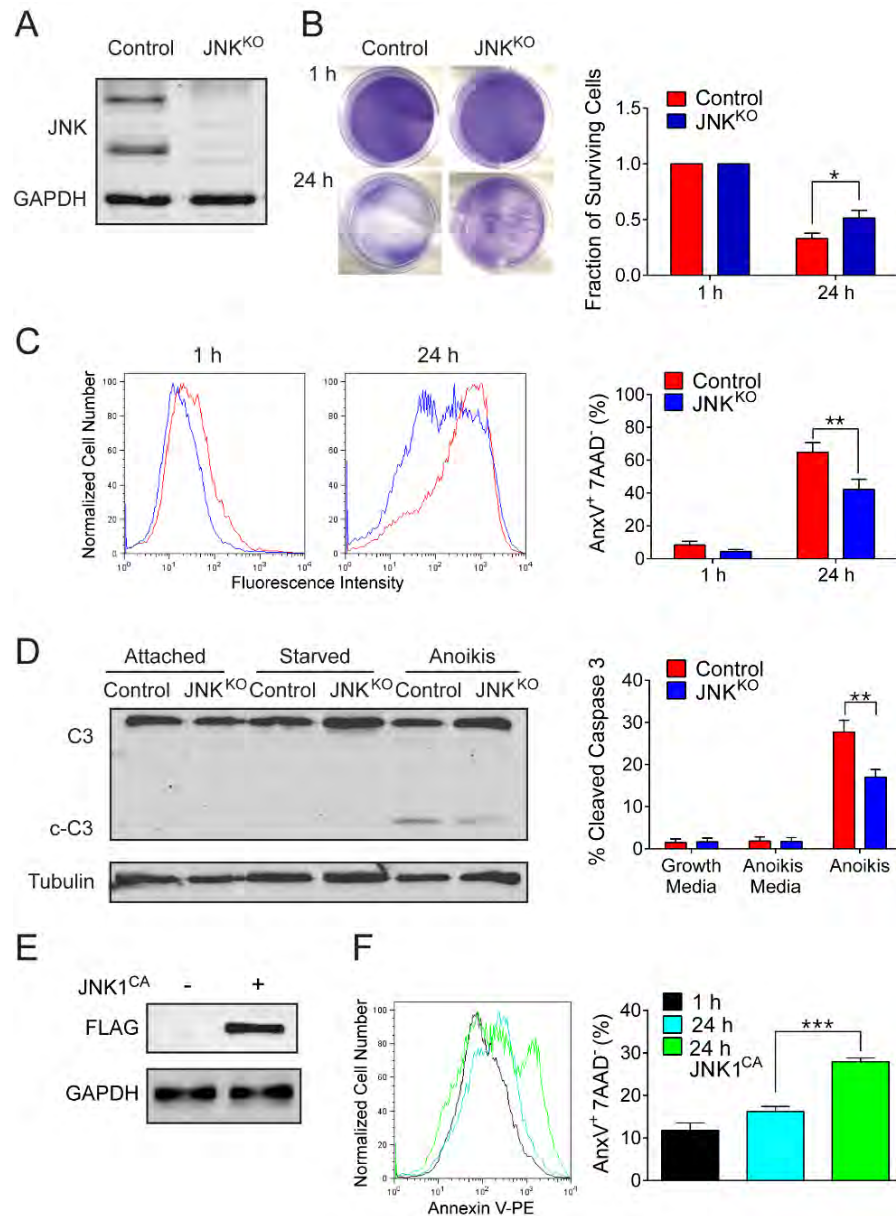


Figure II.2. JNK promotes anoikis of murine epithelial cells.

A) *Mapk8*^{LoxP/LoxP} *Mapk9*^{-/-} *RosaCre*^{ERT} mouse kidney epithelial cells were treated with 4-hydroxytamoxifen to generate *Mapk8*^{Δ/Δ} *Mapk9*^{-/-} cells (JNK^{KO}). JNK expression by Control (*RosaCre*^{ERT}) and JNK^{KO} cells was examined by immunoblot analysis.

B) Control and JNK^{KO} mouse kidney epithelial cells were replated after suspension (1 h or 24 h) and stained with crystal violet. Representative images of cultures are presented. The fraction of surviving cells was quantitated by staining with crystal violet (mean ± SEM; n=3; * p<0.05).

C) Control (red) and JNK^{KO} (blue) mouse kidney epithelial cells were cultured in suspension (1 h or 24 h). Representative flow cytometry data are presented. Apoptotic Control and JNK^{KO} cells (Annexin V⁺ (AnxV⁺) and 7AAD⁻) were quantitated by flow cytometry (mean \pm SEM; n=4; ** p<0.001).

D) Extracts prepared from Control and JNK^{KO} mouse kidney epithelial cells (attached, attached and starved 24 h, and anoikis 24 h) were examined by immunoblot analysis of caspase 3 (C3), cleaved caspase 3 (c-C3), and α Tubulin. The data were quantitated (mean and SEM; n=3; ** p<0.01).

E, F) Control mouse kidney epithelial cells were transduced with an empty vector or a vector that expresses constitutively activated JNK1 (Flag-Mkk7 β 2-Jnk1 α 1 (JNK1^{CA})), treated with doxycycline, and examined by immunoblot analysis using antibodies to FLAG and GAPDH (E). The epithelial cells were cultured in suspension (1 h or 24 h) and apoptotic cells (Annexin V⁺ (AnxV⁺) and 7AAD⁻) were quantitated by flow cytometry (F) (mean \pm SEM; n=4; *** p<0.001). Representative flow cytometry data are also presented.

MLK2/3 are dispensable for epithelial cell anoikis

JNK activation requires phosphorylation by both MAP2K4 and MAP2K7 (Tournier et al. 2001). Upstream of these MAP kinase kinases are the MAP kinase kinase kinases (MAP3K), including the mitogen-activated protein/ERK kinase kinases (MEKK), apoptosis signal-regulating kinase (ASK), TGF β -activated kinase 1 (TAK), tumor-progression locus 2 (TPL2), and mixed lineage kinases (MLK) (Davis 2000). These kinases respond to different stimuli and can activate different subsets of MAPK pathways. Knock-out studies have demonstrated that ASK1 (Tobiume et al. 2001), TAK1 (Shim et al. 2005), MEKK1 (Yujiri et al. 1998), MEKK2 (Kesavan et al. 2004), and MLK2 and MLK3 (Jaeschke and Davis 2007; Kant et al. 2011; Kant et al. 2017) are members of the JNK pathway.

To test the involvement of the mixed lineage kinases in anoikis, I placed Control and *Map3k10*^{-/-} *Map3k11*^{-/-} (encoding MLK2 and MLK3; MLK2/3^{KO}) cells into suspension culture (1 h and 24 h). Both genotypes experienced a similar increase in cell death following 24 h of suspension (Figure II.3), indicating that these MAP3K are not involved in the JNK-mediated response to cell suspension.

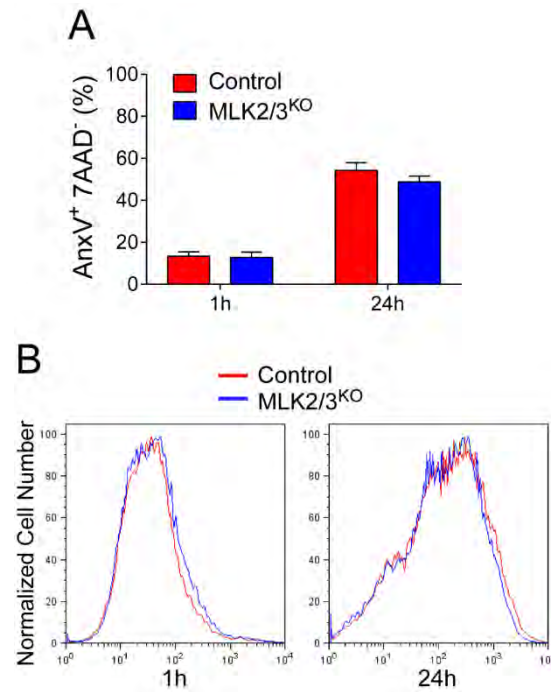


Figure II.3. MLK2 and 3 proteins are not essential for epithelial cell anoikis.

A, B) Control and *Map3k10*^{-/-} *Map3k11*^{-/-} (MLK2/3^{KO}) cells were cultured in suspension (1 h or 24 h). Apoptotic cells (Annexin V⁺ (AnxV) 7AAD⁻) were quantitated using flow cytometry. Graph shows mean \pm SEM (Control n=4, MLK2/3^{KO} n=8) (A). A representative flow cytometry plot is presented (B).

JNK-promoted anoikis is mediated by the BAK/BAX pathway

I next sought to understand how JNK promotes anoikis. Cell detachment activates autophagy, leading to enhanced survival (Fung et al. 2008).

Furthermore, the JNK pathway can regulate autophagy, though this regulation may be cell-type specific (Wei et al. 2008; Xu et al. 2011; Barutcu et al. In press).

Thus, I examined autophagy in attached and suspended (4 h) Control and JNK^{KO} kidney epithelial cells. Suspension culture resulted in increased levels of LC3B II in Control cells, indicating that anoikis induced autophagy (Figure II.4). However, no JNK-dependent changes in LC3B II accumulation were detected (Figure II.4).

This observation suggests that alterations in the regulation of autophagy is unlikely to account for the increased survival of JNK^{KO} kidney epithelial cells.

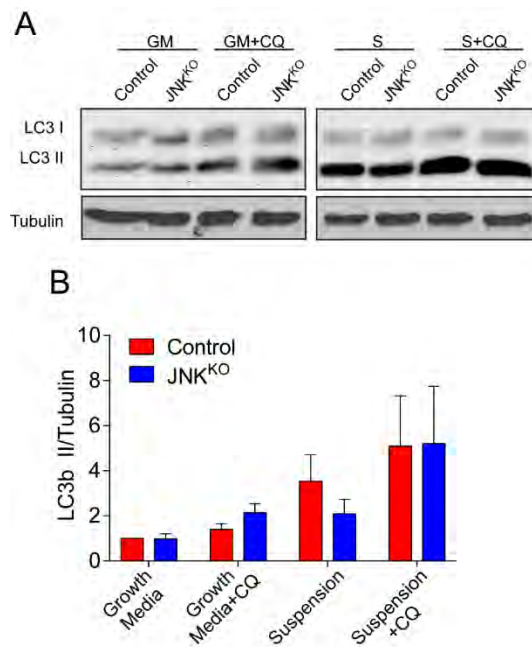


Figure II.4. Autophagy induction is comparable in Control and JNK^{KO} cells.

A, B) Control and JNK^{KO} cells were cultured in growth media without (GM) or with (GM+CQ) 25 μ M chloroquine, or were placed in suspension culture without (S) or with (S+CQ) 25 μ M chloroquine. Cell lysates were subjected to immunoblot analysis with antibodies for LC3B and α Tubulin. A representative blot is presented (A). Two independent experiments were quantified and the mean \pm SEM was plotted with conditions normalized to the Control cells in growth media (B).

It is established that the pro-apoptotic BCL2 family proteins BAK and BAX play a central role in apoptotic cell death (Lindsten et al. 2000; Wei et al. 2001). To test whether this pathway contributes to anoikis, I examined the effect of suspension culture (1 h and 24 h) on Control and *Bak1^{-/-} Bax^{-/-}* (BAK/BAX^{KO}) epithelial cells. I found that BAK/BAX-deficiency greatly decreased the number of apoptotic (Annexin V⁺ 7-AAD⁻) cells detected by flow cytometry following epithelial cell detachment (Figure II.5A). BAK and BAX are therefore key players in anoikis.

To test whether BAK/BAX contribute to JNK-promoted anoikis, I examined BAK/BAX^{KO} epithelial cells transduced with a lentiviral vector that conditionally expresses JNK1^{CA}. Expression of JNK1^{CA} in doxycycline-treated BAK/BAX^{KO} epithelial cells was confirmed by immunoblot analysis (Figure II.5B). Examination of BAK/BAX^{KO} epithelial cell suspension cultures demonstrated that JNK1^{CA} expression did not cause increased anoikis (Figure II.5C). Together, these data demonstrate that JNK-promoted anoikis is mediated by the BAK/BAX pathway.

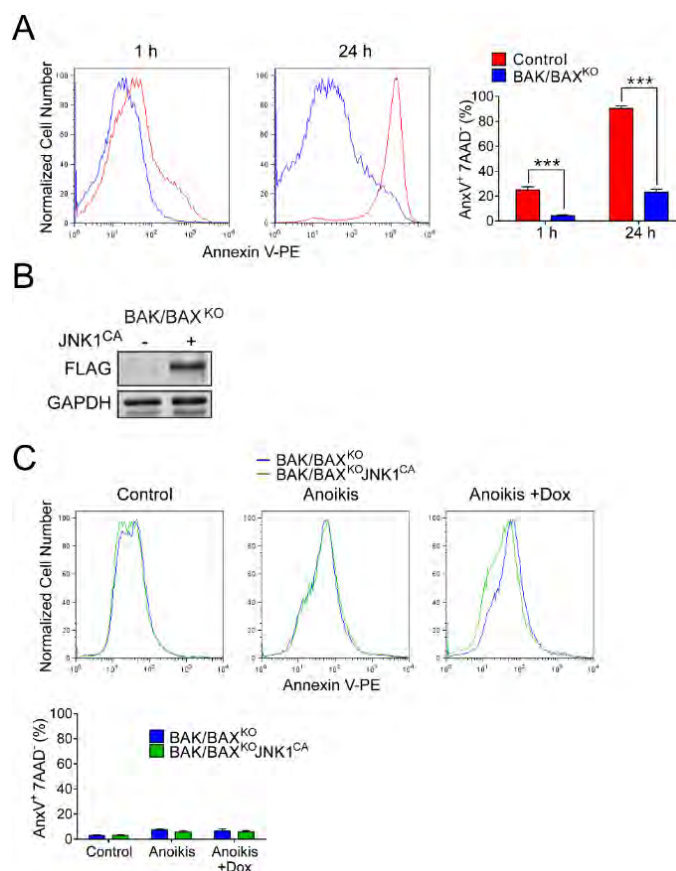


Figure II.5. BAK and BAX are required for JNK-promoted anoikis.

A) Control and *Bak1*^{-/-} *Bax*^{-/-} (BAK/BAX^{KO}) mouse kidney epithelial cells were cultured in suspension (1 h or 24 h) and apoptotic cells (Annexin V⁺ (AnxV⁺) and 7AAD⁻) were quantitated by flow cytometry (mean ± SEM; n=3; *** p<0.001). Representative flow cytometry data are also presented.

B, C) BAK/BAX^{KO} kidney epithelial cells were transduced with an empty vector or a vector that expresses constitutively activated Flag-tagged JNK1 (JNK1^{CA}), treated with doxycycline, and examined by immunoblot analysis using antibodies to FLAG and GAPDH (B). The cells were cultured in suspension (1 h or 24 h) and apoptotic cells (Annexin V⁺ (AnxV⁺) and 7AAD⁻) were quantitated by flow cytometry (C). The data shown are the mean ± SEM; n=3). Representative flow cytometry data are also presented.

BH3-only proteins promote epithelial cell anoikis *in vitro*

The BAK/BAX pathway of cell death can be engaged by BH3-only members of the BCL2 protein family by interacting with pro-survival BCL2-family proteins (Zong et al. 2001; O'Neill et al. 2016). I found that anoikis was not associated with increased BAK or BAX expression (Figure II.6A). Consequently, BAK/BAX-mediated cell death may be initiated by either increased pro-apoptotic BH3-only protein function and/or decreased pro-survival BCL2 family protein function.

I examined the potential role of pro-survival members of the BCL2 family. Gene expression studies demonstrated decreased expression of *Bcl2* and *Bcl2l1* during anoikis of primary murine epithelial cells (Figure II.6B). Increased expression of pro-survival BCL2 family genes was not detected in JNK^{KO} epithelial cells (Figure II.6B) and therefore cannot account for the resistance of JNK^{KO} epithelial cells to anoikis (Figure II.2).

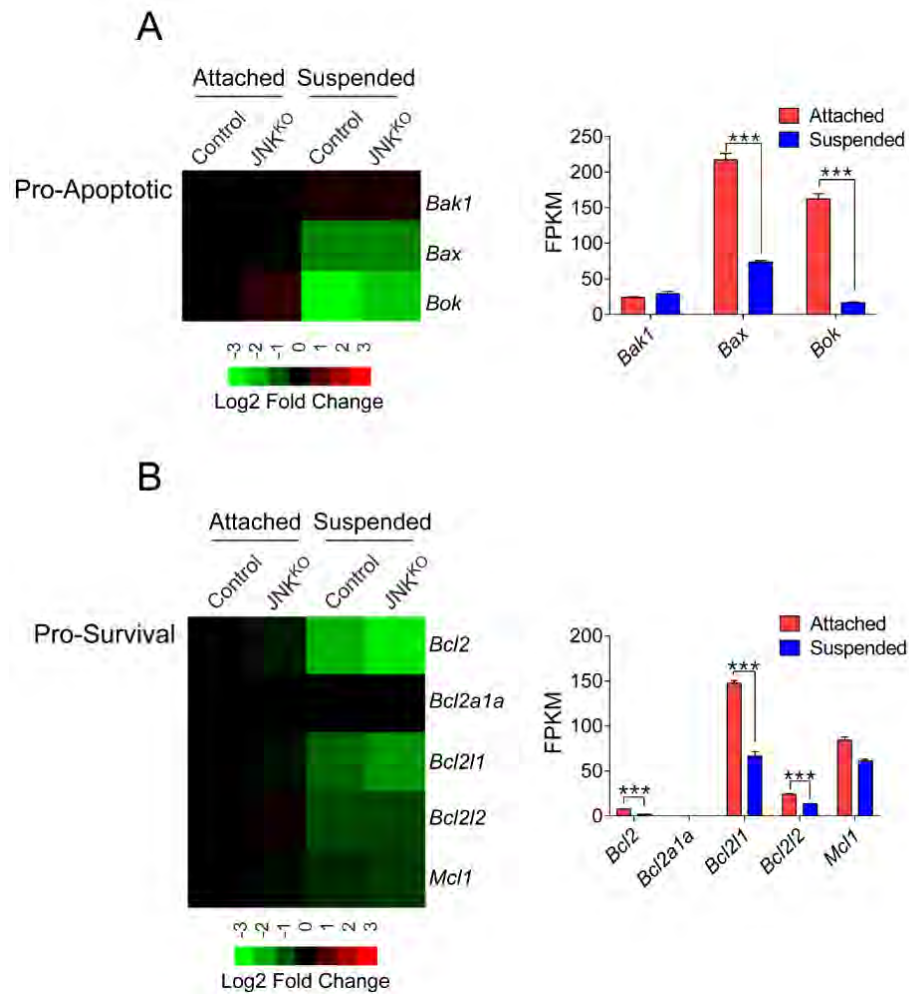


Figure II.6. BCL2 family gene expression in suspended epithelial cells.

A, B) RNA-seq analysis of attached and suspended (4 h) Control and JNK^{ko} cells was performed. Expression of pro-apoptotic (A) and pro-survival (B) BCL2 family genes is presented as a heat map with samples normalized to the attached Control. Bar graphs show the mean fragments per kilobase of exon model per million mapped fragments (FPKM) \pm SEM (n=3 replicates per condition).

Expression of the anti-apoptotic BCL2 family member MCL1 is regulated by ubiquitin-mediated degradation promoted by the AKT-regulated GSK3 signaling pathway (Maurer et al. 2006). I therefore performed immunoblot analysis to examine survival signaling pathways and MCL1 expression during anoikis. I found that suspension culture caused decreased activation of the ERK and AKT signaling pathways and decreased expression of MCL1 protein (Figure II.7). However, JNK-deficiency caused no change in MCL1 protein abundance (Figure II.7). Together, these data demonstrate that decreased expression of pro-survival BCL2 family member MCL1 protein likely contributes to anoikis, but this mechanism is not targeted by JNK to promote anoikis.

I also examined the role of pro-apoptotic BH3-only members of the BCL2 family in JNK-promoted apoptotic cell death during anoikis. Gene expression analysis demonstrated that the expression of *Bcl2l1* (encoding BIM), *Bmf*, and *Hrk* were increased during epithelial cell anoikis (Figure II.8A). However, only very low levels of *Hrk* gene expression were detected (Figure II.9A). This analysis indicates that BIM and BMF may mediate the effects of JNK on anoikis. However, studies of gene expression by JNK^{KO} epithelial cells demonstrated that only the *Bcl2l1* gene (not the *Bmf* gene) exhibited JNK-dependent expression during anoikis (Figure II.7, II.8A & II.9B). Thus, JNK promotes BIM expression during anoikis.

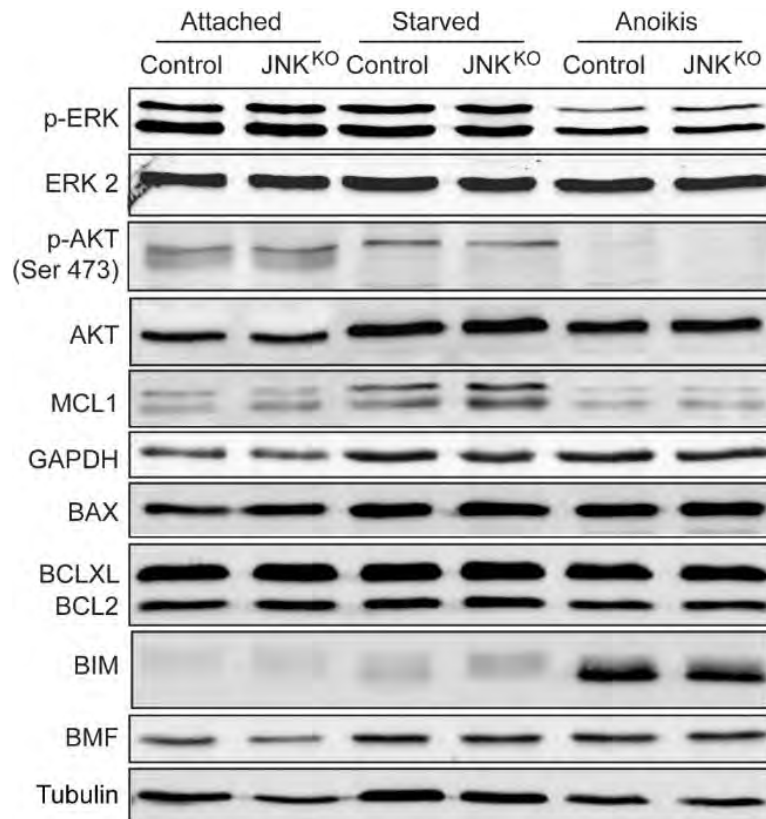


Figure II.7. Anoikis causes JNK-independent decreased expression of MCL-1.

Attached, attached and starved (24 h), and suspended (24 h) Control and JNK^{KO} epithelial cells were examined by immunoblot analysis by probing with antibodies to phospho-ERK (p-ERK), ERK2, phospho-Ser⁴⁷³ AKT (p-AKT), AKT, MCL1, GAPDH, BAX, BCLXL, BCL2, BIM, BMF, and α Tubulin. A representative blot of 3 independent experiments is presented. The subtle change in BIM protein levels observed between Control and JNK^{KO} cells after 24 h of suspension contrasts with the dramatic changes observed in *Bcl2/11* mRNA expression after 4 h of suspension (Figures II.8 & II.9). This discrepancy likely reflects additional expression of BIM in the intervening time in suspension culture and accounts for the ability of JNK-deficient cells to die at a later time point.

To test the role of BIM and BMF in anoikis, I prepared primary epithelial cells from Control mice (*Bcl2l11*^{+/+} *Bmf*^{+/+}), BIM^{KO} mice (*Bcl2l11*^{-/-} *Bmf*^{+/+}), and BMF^{KO} mice (*Bcl2l11*^{+/+} *Bmf*^{-/-}). I also prepared primary epithelial cells from BIM/BMF^{KO} mice (*Bcl2l11*^{-/-} *Bmf*^{-/-}) because it has previously been established that BIM and BMF have partially redundant functions (Hubner et al. 2010; Labi et al. 2014). These cells were cultured in suspension (1 h and 24 h) to test the effect of BIM and BMF-deficiency on anoikis. Colony formation assays demonstrated that BIM-deficiency, but not BMF-deficiency, significantly increased survival following suspension culture (Figure II.8B). Similarly, BIM-deficiency, but not BMF-deficiency, suppressed cleavage and subsequent activation of the apoptosis effector caspase 3 during anoikis (Figure II.8C). However, both BIM-deficiency and BMF-deficiency significantly decreased the number of apoptotic (Annexin V⁺ 7-AAD⁻) cells detected by flow cytometry during anoikis (Figure II.8D). These data indicate that while BIM and BMF can both contribute to anoikis, BIM (which exhibits JNK-dependent expression) plays a key role during anoikis, while BMF (which is expressed by a JNK-independent mechanism) most likely plays a partially redundant role.

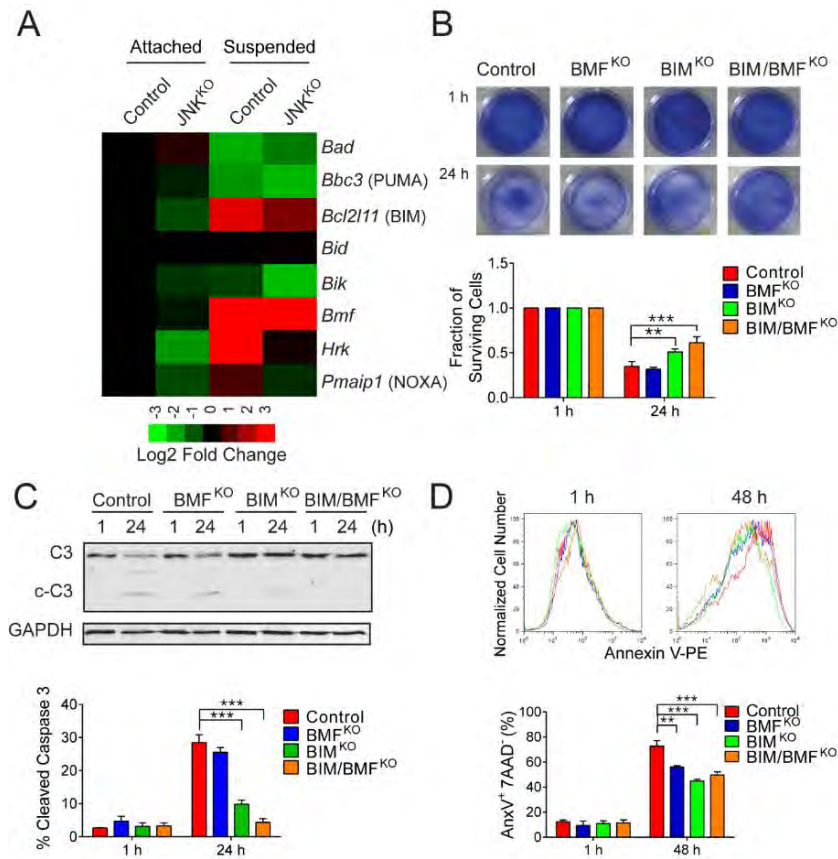


Figure II.8. Anoikis causes JNK-dependent increased expression of BH3-only genes.

A) Attached and suspended (4 h) Control and JNK^{KO} mouse kidney epithelial cells were examined by RNA-seq analysis. The expression of BH3-only genes is presented using a heat map with samples normalized to the attached Control epithelial cells (mean, n=3).

B) Control (n=9), *Bmf*^{-/-} (BMF^{KO}, n=9), *Bcl2l11*^{-/-} (BIM^{KO}, n=12), and compound mutant *Bmf*^{-/-} *Bcl2l11*^{-/-} (BIM/BMF^{KO}, n=10) kidney epithelial cells were cultured in suspension (1 h or 24 h). Epithelial cell viability was tested by colony formation assays and quantitated by staining with crystal violet (mean ± SEM; ** p<0.01, *** p<0.001). Representative images of cultures are also presented

C) Kidney epithelial cells were cultured in suspension (1 h or 24 h) and extracts were examined by immunoblot analysis of caspase 3 (C3), cleaved caspase 3 (c-C3), and GAPDH. The data were quantitated (mean and SEM; n=2; *** p<0.001).

D) Kidney epithelial cells were cultured in suspension (1 h or 48 h) and apoptotic cells (Annexin V⁺ (AnxV⁺) and 7AAD⁻) were quantitated by flow cytometry (mean and SEM; Control n=6, BMF^{KO} n=4, BIM^{KO} n=4, BIM/BMF^{KO} n=6; ** p<0.01, *** p<0.001). Representative flow cytometry data are also presented.

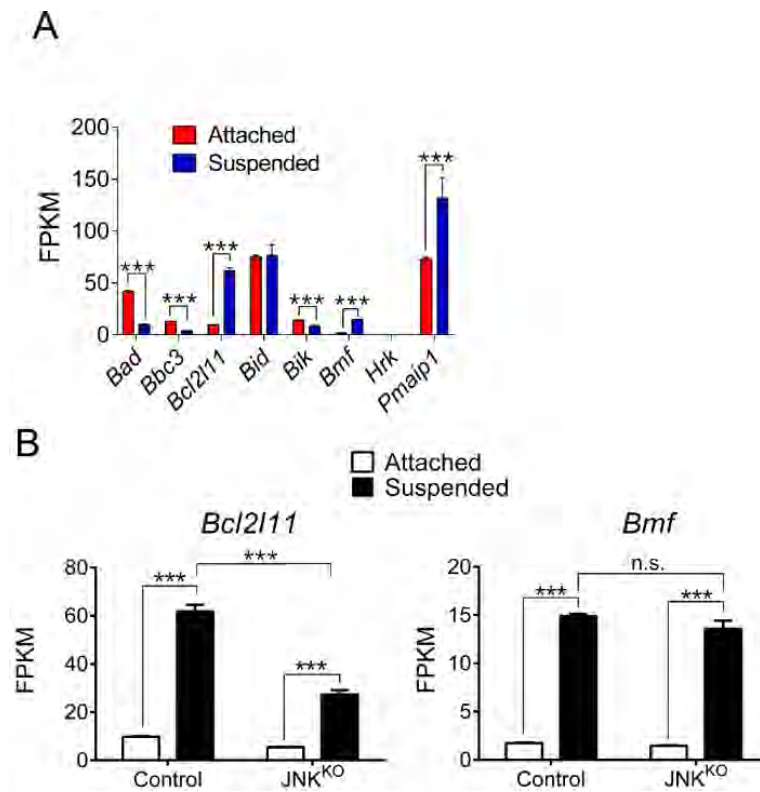


Figure II.9. BH3-only gene expression by suspended epithelial cells.

A) RNA-seq analysis of Control (WT) mouse epithelial cells cultured in suspension (4 h) was performed. BH3-only gene expression is presented as FPKM values of BH3-only mRNA (mean \pm SEM of 3 independent experiments; ** $p < 0.01$, *** $p < 0.001$).

B) The expression of *Bcl2l1* and *Bmf* mRNA by Control and JNK^{KO} epithelial cells is presented as FPKM values (mean \pm SEM of 3 independent experiments; n. s., $p > 0.05$; ***, $p < 0.001$).

BIM and BMF-deficiency in epithelial cells causes resistance to JNK-promoted anoikis

To confirm that BIM and BMF mediate the effects of JNK to promote anoikis, I examined the effect of compound BIM and BMF-deficiency in epithelial cells that conditionally express JNK1^{CA}. Activated JNK was expressed using a doxycycline-inducible lentiviral vector (Figure II.10A). JNK-promoted anoikis in control (*Bcl2l1*^{+/+} *Bmf*^{+/+}) epithelial cells was detected by flow cytometry of Annexin V staining (Figure II.10B, C). However, this JNK-promoted anoikis was suppressed in *Bcl2l1*^{-/-} *Bmf*^{-/-} (BIM/BMF^{KO}) epithelial cells (Figure II.10B, C).

The low level of JNK-promoted anoikis detected in BIM/BMF^{KO} epithelial cells may be caused by the increased expression of other BH3-only proteins. Indeed, I found that constitutively activated JNK caused increased expression of *Hrk* (Figure II.11A) and *Pmaip1* (encodes NOXA, Figure II.11B) mRNA by epithelial cells in suspension culture. It is therefore possible that HRK and NOXA may also contribute to anoikis caused by constitutively activated JNK. However, studies of wild-type epithelial cells demonstrated that anoikis was associated with very low levels of *Hrk* mRNA expression (Figure II.9A) and only modest changes in *Pmaip1* mRNA expression (Figure II.8A). These data suggest that BIM and BMF are the major physiological targets of JNK signaling and that very high levels of activated JNK may also engage additional pathways, such as the NOXA pathway.

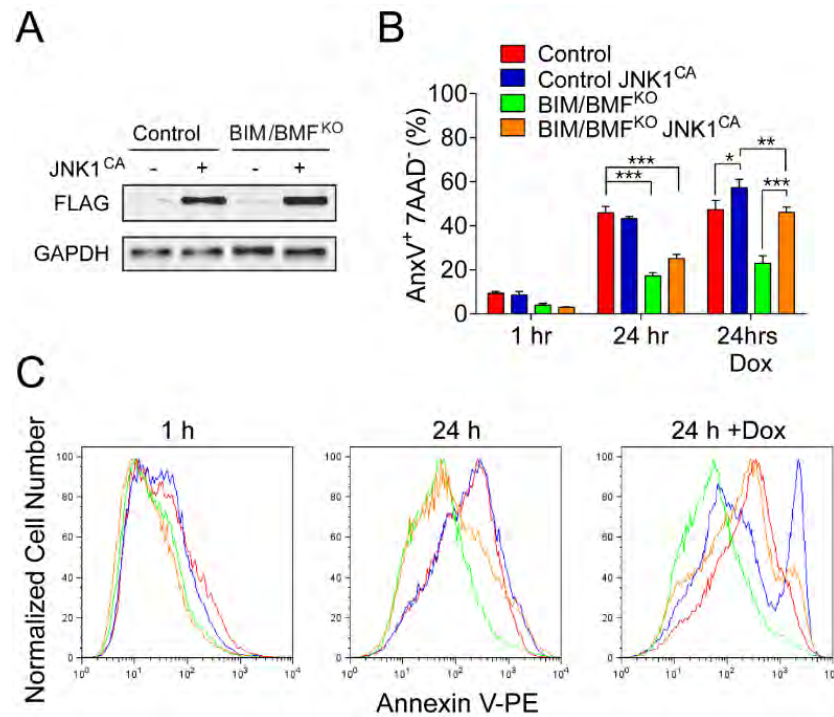


Figure II.10. BIM and BMF contribute to JNK-promoted anoikis.

A) Control and BIM/BMF^{KO} mouse kidney epithelial cells expressing doxycycline (Dox)-inducible FLAG-tagged constitutively active JNK (JNK1^{CA}) were cultured in suspension (1 h or 24 h) in medium supplemented without or with doxycycline. The expression of FLAG-JNK1^{CA} and GAPDH was examined by immunoblot analysis.

B, C) The epithelial cells were cultured in suspension (1 h or 24 h) and apoptotic cells (Annexin V⁺ (AnxV⁺) and 7AAD⁻) were examined by flow cytometry (mean \pm SEM; n=6; * p<0.05, ** p<0.01, *** p<0.001) (B). Representative flow cytometry data are presented (C).

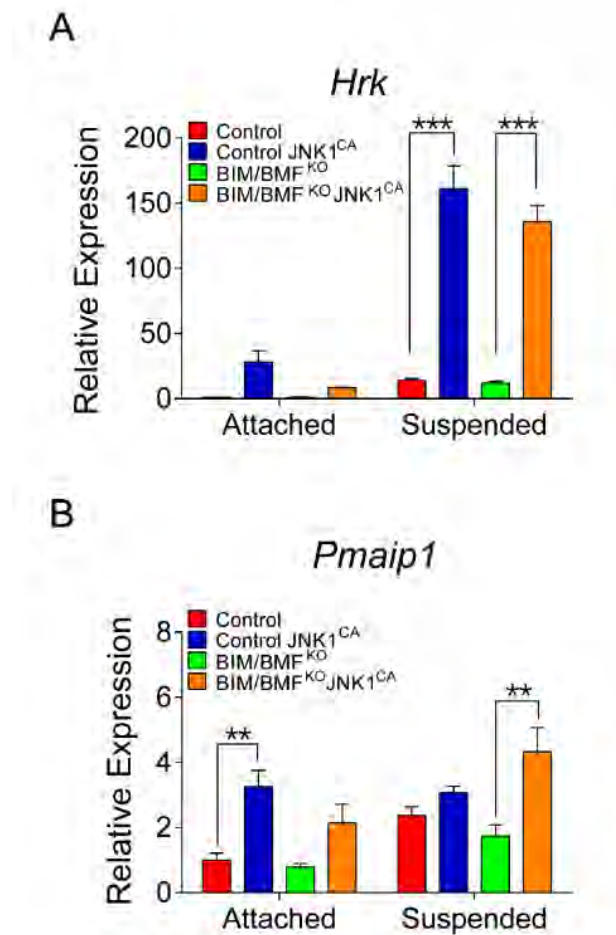


Figure II.11. Constitutively activated JNK1 causes increased expression of the BH3-only genes *Hrk* and *Pmaip1*.

A,B) Control and BIM/BMF^{KO} mouse epithelial cells expressing doxycycline (Dox)-inducible FLAG-tagged constitutively active JNK (JNK1^{CA}) were cultured in suspension (1 h or 4 h) in medium supplemented with doxycycline. RNA was isolated from attached cells and suspended cells (4 h) and used to measure *Hrk* mRNA (A) and *Pmaip1* mRNA (B) expression (mean \pm SEM of 3 independent experiments; ** $p < 0.01$, *** $p < 0.001$).

BIM and BMF are required for epithelial cell anoikis *in vivo*

It is established that lumen formation in terminal end buds (TEBs) and ducts is mediated by apoptosis (Humphreys et al. 1996) and that defective anoikis causes TEB/ductal occlusion (Mailleux et al. 2007). Interestingly, JNK-deficiency is associated with TEB/ductal occlusion (Cellurale et al. 2012), suggesting that JNK signaling in the breast epithelium may be required for developmental anoikis. Previous studies have established roles for BIM and BMF in mammary acinar formation (Mailleux et al. 2007; Schmelzle et al. 2007). To elucidate the relative roles of BIM and BMF in this form of anoikis *in vivo*, I examined murine mammary gland development. I found that BMF-deficiency caused no major defects in mammary gland development of young (5-6 week-old) or mature (6 month old) mice (Figure II.12A,B & II.13A), although BMF-deficiency was found to cause increased duct extension in young mice compared with Control mice (Figure II.13B). In contrast, young BIM-deficient mice exhibited a marked defect in duct extension (Figure II.13B) and occlusion of TEB and ducts (Figure II.12A and II.13A) compared with Control mice. Duct occlusion in mature BIM^{KO} mice was not observed (Figure II.12B). Interestingly, the developmental defects detected in compound mutant BIM/BMF^{KO} mice were more severe than those detected in either BIM^{KO} mice or BMF^{KO} mice. Compared with BIM^{KO} mice, young BIM/BMF^{KO} mice exhibited a larger duct extension defect and significantly greater occlusion of TEB and ducts (Figure II.12A & II.13). Moreover, the duct occlusion phenotype persisted in mature BIM/BMF^{KO} mice (Figure II.12B) and

was not associated with increased proliferation, as monitored by PCNA staining (Figure II.12C & II.13C). These data demonstrate that BIM plays a key role during mammary gland development, and confirm the conclusion that the anoikis functions of BIM are partially redundant with BMF.

The mammary epithelium is composed of keratin 5⁺ myoepithelial cells that form the exterior surface of ducts and keratin 8⁺ luminal epithelial cells that form the interior surface of ducts (Deugnier et al. 2002). To determine which of these cell types occluded the ducts of BIM/BMF^{KO} mice, I stained tissue sections with antibodies to keratin 5 and keratin 8. Both myoepithelial and luminal cells contributed to luminal occlusion in young mice (Figure II.14A), but I primarily found luminal cells in the occluded lumens of mature mice (Figure II.14B). Thus, while myoepithelial and luminal epithelial cells are initially retained within the ducts of the developing mammary glands of BIM/BMF^{KO} mice, it is the luminal epithelial cells that persist in mature mice (Figure II.14).

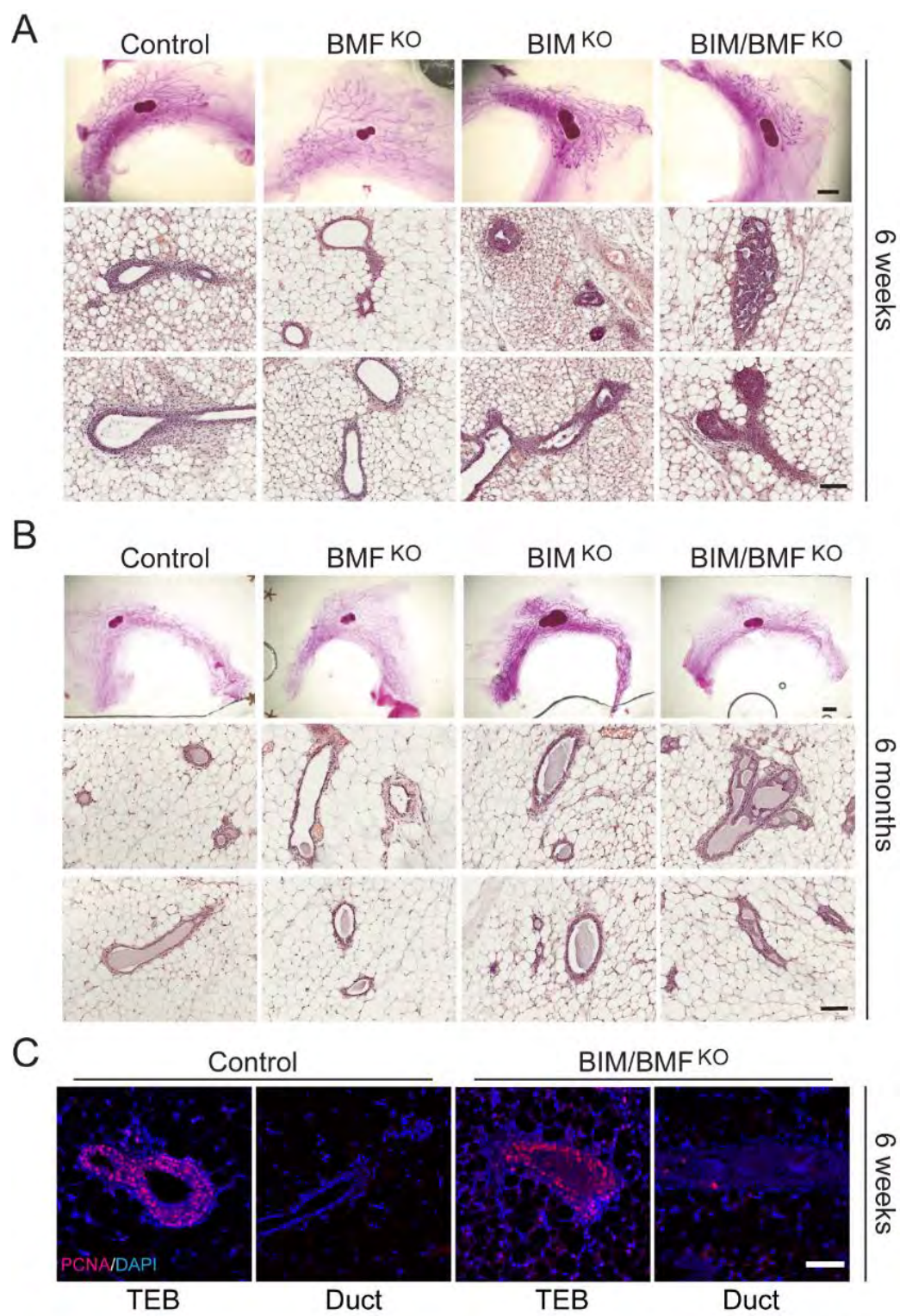


Figure II.12. BIM and BMF contribute to normal mammary gland development.

A,B) Representative carmine alum-stained whole-mount mammary glands (*upper panels*, scale bar = 2 mm) and hematoxylin and eosin stained sections (*middle and lower panels*, scale bar = 100 μ m) from 6 week-old (A) and 6 month-old (B) mice are presented.

C) Representative sections of mammary glands from 6 week-old mice were stained with DAPI (blue) and an antibody to PCNA (red). 5 Control mice and 7 BIM/BMF^{KO} mice were examined. Sections showing ducts and terminal end buds (TEB) are presented. Scale bar = 75 μ m.

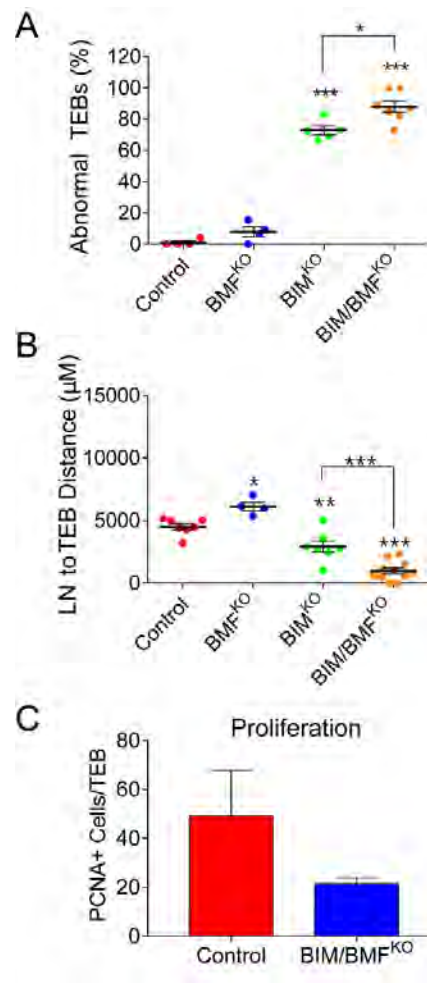


Figure II.13. BIM/BMF^{KO} compound mutant mice exhibit impaired mammary gland development.

A) Terminal end buds (TEBs) in whole-mounts of mammary glands from 6 week-old animals were examined. Abnormal TEBs with filled lumens were counted. Ten to thirty TEBs were examined per animal (mean \pm SEM; $n = 4\sim7$ mice; * $p < 0.05$, ** $p < 0.01$, *** $p < 0.001$).

B) The distance from the lymph node to terminal end buds was measured in mammary glands from 6 week-old mice (mean \pm SEM; $n = 4\sim11$ mice; * $p < 0.05$, *** $p < 0.001$).

C) Glands from 6 week-old animals were stained with PCNA to measure cell proliferation. PCNA-positive cells in terminal end buds were counted (mean \pm SEM; $n = 5$ Control mice, $n = 6$ BIM/BMF^{KO} mice). No significant ($p > 0.05$) differences were detected.

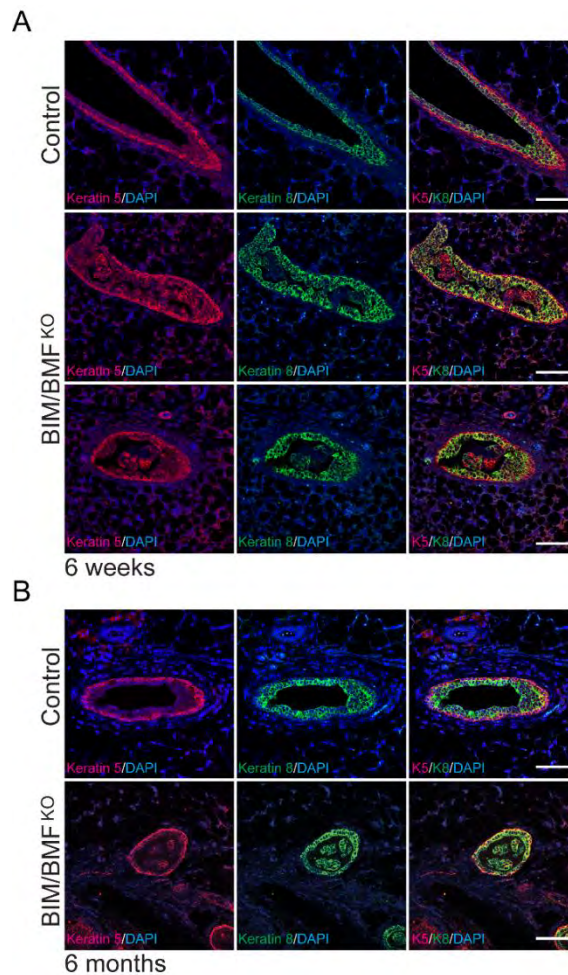


Figure II.14. Basal and luminal cells occlude ducts of BIM/BMF^{KO} mammary glands.

A, B) Representative sections of mammary glands from Control (upper panels) and BIM/BMF^{KO} (lower panels) mice were stained with antibodies against keratin 5 (red) and keratin 8 (green), and counterstained with DAPI. Scale bars = 75 μm. Six week-old (A) and 6 month-old (B) mice are presented.

Role of BIM and BMF phosphorylation during anoikis

The anoikis phenotypes of *Mapk8*^{-/-} *Mapk9*^{-/-} (JNK^{KO}) epithelial cells (Figure II.2) and *Bcl2l1*^{-/-} *Bmf*^{-/-} (BIM/BMF^{KO}) epithelial cells (Figure II.8) are similar. It is possible that this observation reflects the finding that both BIM and BMF are phosphorylated by JNK (Lei and Davis 2003; Hubner et al. 2008; Hubner et al. 2010). To test whether JNK-mediated phosphorylation of BIM and BMF contributes to JNK-dependent anoikis, I isolated primary epithelial cells from mice harboring point mutations in the *Bcl2l1* and *Bmf* genes at the JNK phosphorylation sites Thr¹¹² on BIM and Ser⁷⁴ on BMF (Hubner et al. 2008; Hubner et al. 2010). I also examined a *Bcl2l1* mutant that is resistant to ERK-promoted proteasomal degradation due to mutations at the ERK phosphorylation sites Ser⁵⁵, Ser⁶⁵, and Ser⁷³ (BIM^{3SA}) (Hubner et al. 2008). I found that mutation of the ERK phosphorylation sites on BIM caused no change in epithelial cell anoikis monitored by flow cytometry analysis of 7-AAD/Annexin V staining (Figure II.15A). Similarly, mutation of the JNK phosphorylation site Thr¹¹² (replacement with Ala) caused no change in anoikis, including studies using epithelial cells on a sensitized genetic background (*Bmf*^{-/-}) (Figure II.15A, B). In contrast, mutation of the BMF phosphorylation site Ser⁷⁴ (replacement with Ala) caused decreased anoikis *in vitro* (Figure II.15C), but caused only limited ductal occlusion *in vivo* (Figure II.16).

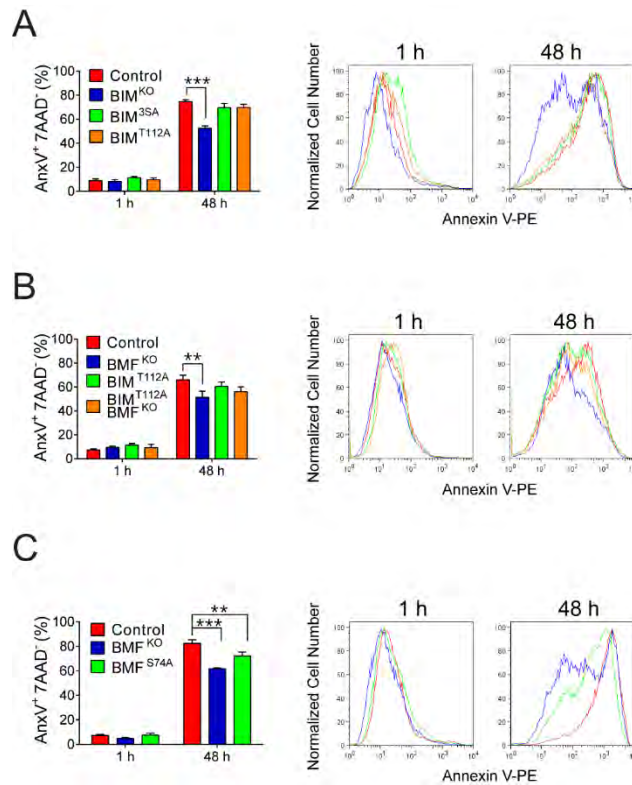


Figure II.15. Phosphorylation of BMF, but not BIM, contributes to JNK-promoted anoikis.

A) Control, *Bcl2l1*^{-/-} (BIM^{KO}), *Bcl2l1*^{Ser55,65,73A/Ser55,65,73A} (BIM^{3SA}), and *Bcl2l1*^{T112A/T112A} (BIM^{T112A}) kidney epithelial cells were cultured in suspension (1 h or 48 h). Apoptotic cells (Annexin V⁺ (AnxV⁺) and 7AAD⁻) were quantitated by flow cytometry (mean ± SEM; n=6; ** p<0.01, *** p<0.001). Representative flow cytometry plots are presented.

B) Control, *Bmf*^{-/-} (BMF^{KO}), *Bcl2l1*^{T112A/T112A} (BIM^{T112A}), and *Bmf*^{-/-} *Bcl2l1*^{T112A/T112A} (BMF^{KO} BIM^{T112A}) kidney epithelial cells were cultured in suspension (1 h or 48 h). Apoptotic cells (Annexin V⁺ (AnxV⁺) and 7AAD⁻) were quantitated by flow cytometry (mean ± SEM; n=6; ** p<0.01, *** p<0.001). Representative flow cytometry plots are presented.

C) Control, *Bmf*^{-/-} (BMF^{KO}), and *Bmf*^{S74A/S74A} (BMF^{S74A}) mouse kidney epithelial cells were cultured in suspension (1 h or 48 h). Apoptotic cells (Annexin V⁺ (AnxV⁺) and 7AAD⁻) were quantitated by flow cytometry (mean ± SEM; n=6; ** p<0.01, *** p<0.001). Representative flow cytometry plots are presented.

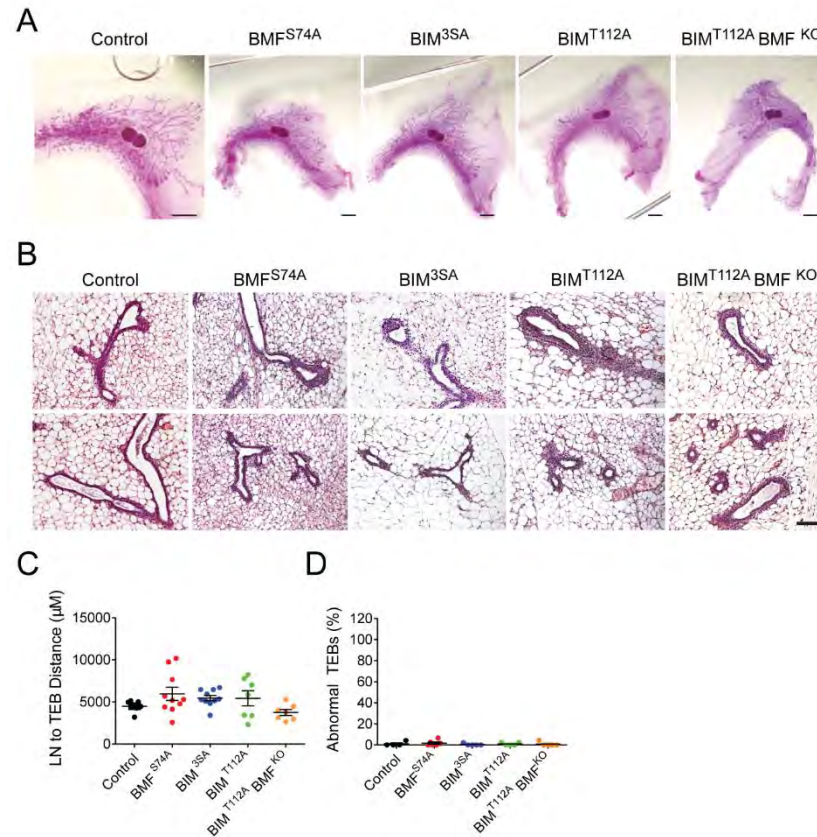


Figure II.16. Mammary gland development in mice with defects in JNK-mediated BIM and BMF phosphorylation.

A,B) Representative carmine alum-stained whole mounts (A) and hematoxylin & eosin-stained sections (B) of mammary glands from 6-week-old Control (WT), BMF^{S74A}, BIM^{3SA}, BIM^{T112A}, and BIM^{T112A} BMF^{KO} mice are presented. Scale bars = 2 mm (A) and 100 μm (B).

C) The distance from the terminal end buds (TEBs) to the lymph node (LN) was measured (mean ± SEM; n = 7~10 mice). No statistically significant differences were detected (p>0.05).

D) The number of abnormal TEBs with filled lumens were counted. Ten to thirty TEBs were examined per animal (mean ± SEM; n = 7~10 mice). No statistically significant differences were detected (p>0.05).

Collectively, these data indicate that BIM and BMF phosphorylation is not essential for anoikis. Indeed, BIM phosphorylation at these sites appears to play no role in anoikis. However, phosphorylation of BMF on Ser⁷⁴, a site targeted by JNK, partially contributes to anoikis. I conclude that BMF phosphorylation (but not BIM phosphorylation) may contribute to cell death following epithelial cell detachment.

Discussion

Genetic studies of epithelial cell sheet development in *Drosophila* demonstrate a role for extrusion and death of compromised cells. This extrusion mechanism causes the removal of cells from the epithelial cell sheet and JNK activation in the detached epithelial cells subsequently causes apoptosis (Adachi-Yamada et al. 1999; Adachi-Yamada and O'Connor 2002; Gibson and Perrimon 2005; Shen and Dahmann 2005). Similarly, competition between cells in epithelial cell sheets for limiting amounts of morphogen (e.g. a TGF β ligand) (Moreno et al. 2002) or cell-intrinsic fitness (e.g. cMYC expression) (Moreno and Basler 2004) can cause JNK-dependent elimination of compromised cells. These mechanisms not only ensure normal development of epithelial cell sheets, but also act to suppress tumor formation (Brumby and Richardson 2003; Uhlirova et al. 2005; Igaki 2009). JNK therefore plays a key role in epithelial cell sheet development. Nevertheless, the mechanism of pro-apoptotic signaling by JNK in *Drosophila* is unclear.

Mammalian studies of the role of JNK in epithelial cell detachment and death (anoikis) are controversial because early studies using dominant-negative over-expression approaches in MDCK epithelial cells were interpreted both to support a required role for JNK in anoikis (Frisch et al. 1996) and to refute a role of JNK in anoikis (Khwaja and Downward 1997). More recently, studies using the drug SP600125, that inhibits JNK and many other protein kinases (Bain et al. 2003), indicated that JNK may be required for acinar formation and luminal

clearance by human MCF10A mammary epithelial cells (McNally et al. 2011). This observation suggested that JNK may play a role in anoikis. This was later supported by studies of murine mammary gland development using mice with wild-type or compound mutant *Mapk8*^{-/-} *Mapk9*^{-/-} mammary epithelial cells that demonstrated a requirement of JNK for the luminal clearance of mammary ducts and terminal end buds by apoptosis (anoikis) (Cellurale et al. 2012). The present study extends these findings to demonstrate a requirement for JNK in anoikis of human and murine primary epithelial cells (Figures II.1 & II.2).

This requirement for JNK in anoikis contrasts with the observation that JNK does not contribute to other forms of apoptosis, including cell death mediated by the cell surface receptors FAS and TNFR1 (Tournier et al. 2000; Lamb et al. 2003; Das et al. 2009). These observations indicate that JNK plays a selective role in apoptosis. This is illustrated by the finding that constitutively activated JNK does not cause apoptosis of attached epithelial cells, but constitutively activated JNK promotes apoptosis of detached epithelial cells (Figures II.2 & II.10).

I demonstrate that the mechanism of JNK signaling to cause anoikis requires the pro-apoptotic BCL2 family proteins BAK and BAX (Figure II.5) and the pro-apoptotic BH3-only proteins BIM and BMF (Figure II.8). *Gain-of-function* studies using conditional expression of constitutively activated JNK demonstrated that the JNK-promoted anoikis detected in wild-type epithelial cells was suppressed in BAK/BAX^{KO} epithelial cells (Figure II.5) or BIM/BMF^{KO} epithelial

cells (Figure II.10). The residual cell death detected in BAK/BAX^{KO} and BIM/BMF^{KO} cells may reflect partial compensation by the related pro-apoptotic proteins BOK (Figure II.6) and NOXA (Figures II.8 & II.9), respectively. Together, these data establish the BH3-only proteins BIM and BMF as mediators of JNK-promoted anoikis caused by activation of the cell intrinsic BAK/BAX mitochondrial apoptosis pathway.

Whereas BIM and BMF co-operate to cause anoikis, BIM plays a key role while the pro-apoptotic functions of BMF are partially redundant with BIM (Figure II.8). This co-operation is illustrated by the finding that compound mutant BIM/BMF^{KO} mice exhibited a larger duct extension defect and significantly greater occlusion of TEB and ducts compared with BIM^{KO} mice or BMF^{KO} mice (Figure II.12A & II.13). Moreover, unlike BIM^{KO} mice or BMF^{KO} mice, the duct occlusion phenotype persisted in mature BIM/BMF^{KO} mice (Figure II.12B). These functions of BIM and BMF are consistent with previous observations demonstrating co-operative roles of BIM and BMF during cell death (Hubner et al. 2010; Labi et al. 2014; Sakamoto et al. 2016). Moreover, these roles are consistent with the established functions of BIM and BMF during mammary acinar development (Mailleux et al. 2007; Schmelzle et al. 2007).

Two mechanisms may account for the activation of BIM and BMF by JNK signaling:

- 1) Anoikis is associated with markedly increased expression of both BIM and BMF (Figure II.8A). The increased expression of BIM, but not BMF, was JNK-

dependent (Figure II.9B). Indeed, it is established that the JNK target cJUN strongly promotes the expression of BIM (Whitfield et al. 2001). This JNK-dependent increase in BIM expression may account for the requirement of both JNK and BIM for anoikis.

2) BIM and BMF are substrates that are phosphorylated by activated JNK (Lei and Davis 2003; Hubner et al. 2008; Hubner et al. 2010). Studies of mice with germ-line point mutations in BIM phosphorylation sites (Ser⁵⁵, Ser⁶⁵, Ser⁷³ or Thr¹¹²) demonstrated that BIM phosphorylation was not required for anoikis (Figure II.15A, B). In contrast, studies of mice with a germ-line point mutation in BMF at the JNK phosphorylation site Ser⁷⁴ demonstrated that BMF phosphorylation was required for efficient anoikis (Figure 11.15C).

Collectively, these data establish that JNK promotes anoikis by increasing BIM expression and by phosphorylating BMF. It is possible that these roles of BIM and BMF are augmented by effects of JNK on other BH3-only proteins, including HRK and NOXA (Figure II.8A). HRK is expressed at extremely low levels in primary epithelial cells, but does exhibit increased JNK-dependent expression during anoikis (Figures II.8A & II.9A). This JNK-dependent HRK expression may reflect the targeting of the *Hrk* gene by the cJUN transcription factor (Ma et al. 2007). Nevertheless, the very low level of HRK expression in epithelial cells indicates that HRK may only contribute to anoikis under specialized circumstances. NOXA is expressed by epithelial cells and this expression is modestly increased during anoikis (Figure II.8). NOXA may

therefore contribute to anoikis under some conditions, particularly when a threshold amount of BH3-only protein is required to promote anoikis.

Interestingly, the expression of HRK and NOXA are increased when epithelial cells expressing constitutively activated JNK are cultured in suspension (Figure II.11). It is therefore possible that BIM and BMF mediate the pro-anoikis effects of moderate levels of JNK activation in detached epithelial cells and that very high levels of JNK activity may additionally recruit JNK-dependent expression of NOXA to promote efficient anoikis.

Genetic analysis of *Drosophila* indicates that JNK plays a role in tumor suppression by promoting the elimination of compromised epithelial cells (Brumby and Richardson 2003; Uhlirova et al. 2005; Igaki 2009; Igaki et al. 2009; Ohsawa et al. 2011). This observation suggests that JNK may play a similar role in mammalian epithelial cells. Thus, loss of JNK function by epithelial cells may lead to survival in luminal spaces and the subsequent acquisition of additional mutations that may cause cancer. Indeed, JNK-deficiency enhances tumor formation in a transplantation model of breast cancer (Cellurale et al. 2012). Moreover, sequencing of human tumors has revealed that two upstream components of the JNK pathway (MAP2K4 and MAP3K1) are frequently mutated in human cancer (Stephens et al. 2012; Nik-Zainal et al. 2016a). Whether these human mutations contribute to cancer development is unclear. Studies to test this hypothesis are therefore warranted.

In conclusion, I have demonstrated that JNK is required for efficient anoikis of detached human and mouse epithelial cells. I show that JNK causes increased BIM expression and phosphorylation of BMF following epithelial cell detachment. These BH3-only proteins act as mediators of JNK-promoted anoikis that engage the cell intrinsic BAK/BAX mitochondrial apoptosis pathway.

Materials and Methods

Mice

Bmf^{-/-} mice (RRID:IMSR_JAX:011024), *Bmf*^{S74A/S74A} mice (RRID:IMSR_JAX:011022), *Bcl2l1*^{T112A/T112A} mice (RRID:IMSR_JAX:011026), *Bcl2l1*^{S55,65,73A/S55,65,73A} mice (RRID:IMSR_JAX:011025), (Hubner et al. 2008; Hubner et al. 2010), *Map3k10*^{-/-} *Map3k11*^{-/-} mice (Kant et al. 2011), and *Mapk8*^{LoxP/LoxP} *Mapk9*^{-/-} *RosaCre*^{ERT} mice (Das et al. 2007) have been previously described. C57BL/6J mice (Stock # 000664; RRID:IMSR_JAX:000664), B6;129-*Gt(ROSA)26Sor*^{tm1(cre/ERT)Nat}/J mice (Stock # 004847; RRID:IMSR_JAX:004847) (Badea et al. 2003), and B6.129S1-*Bcl2l1*^{tm1.1Ast}/J mice (Stock # 004525; RRID:IMSR_JAX:004525) (Bouillet et al. 1999)) were obtained from The Jackson Laboratories. Virgin females (age 6 weeks and 6 months) were used for mammary gland studies. Both male and female mice (age 8 weeks) were used to establish kidney epithelial cells. The mice were housed in a specific pathogen-free facility accredited by the American Association of Laboratory Animal Care. All animal studies were approved (A-1032) by the Institutional Animal Care and Use Committee of the University of Massachusetts Medical School.

Cell culture

Tertiary human mammary epithelial cells were purchased and maintained in MammaryLife Media (Lifeline Cell Technology). Primary murine kidney epithelial cells were prepared (Follit et al. 2008) using kidneys from mice (8 week-old)

digested at 37°C (<2 h) with 0.1% collagenase, 0.1% trypsin, and 150 mM NaCl in Dulbecco's modified Eagle's medium (DMEM) (Life Technologies). These cells were maintained in DMEM/F12 media containing 10% fetal bovine serum and supplemented with 150 mM urea plus 150 mM NaCl. Wild-type and *Bak1*^{-/-} *Bax*^{-/-} (BAK/BAX^{KO}) epithelial cells were obtained from Applied Biological Materials (ABM Inc) and maintained in DMEM media containing 10% fetal bovine serum. *Rosa-Cre^{ERT}* kidney epithelial cells were treated with 1 µM 4-hydroxytamoxifen (24 h) to ablate floxed alleles.

Immunoblot Analysis

Cell lysates were prepared using Triton lysis buffer (20 mM Tris [pH 7.4], 1% Triton X-100, 10% glycerol, 137 mM NaCl, 2 mM EDTA, 25 mM β-glycerophosphate, 1 mM sodium orthovanadate, 1 mM phenylmethylsulfonyl fluoride, and 10 µg/mL of aprotinin plus leupeptin). Extracts (30 µg) were subjected to immunoblot analysis with antibodies to Caspase 3 (Cell Signaling Technology Cat# 9662 RRID:AB_331439; dilution 1:500), LC3B (Cell Signaling Technology, Cat#2775), ERK2 (Santa Cruz Biotechnology Cat# sc-1647; RRID:AB_627547; dilution 1:1000), Flag (Sigma-Aldrich Cat# F3165 RRID:AB_259529; dilution 1:5000), GAPDH (Santa Cruz Biotechnology Cat# sc-25778; RRID:AB_10167668; dilution 1:1000), JNK (R & D Systems Cat# AF1387 RRID:AB_2140743R&D; dilution 1:1000), p-ERK (Cell Signaling Technology Cat# 9101 RRID:AB_2315114; dilution 1:1000), AKT (Cell Signaling Technology

Cat# 9272 RRID:AB_329827; dilution 1:1000), p-Ser473 AKT (Cell Signaling Technology Cat# 9271 RRID:AB_329825; dilution 1:1000), MCL1 (Rockland Cat# 600-401-394S RRID:AB_11179937; dilution 1:2000), BAX (Abcam Cat# ab32503 RRID:AB_725631; dilution 1:5000), BCLXL (Abcam Cat# ab32370 RRID:AB_725655; dilution 1:2000), BCL2 (Abcam Cat# ab182858 RRID:AB_2715467; dilution 1:2000), BMF (Abcam Cat# ab181148 RRID:AB_2715466; dilution 1:1000), BIM (Abcam Cat# ab32158 RRID:AB_725697), and α Tubulin (Sigma-Aldrich Cat# T5168; RRID:AB_477579). Immune complexes were detected with IRDye 680LT conjugated-donkey anti-mouse IgG antibody (LI-COR Biosciences Cat# 926-68022 RRID:AB_10715072) and IRDye 800CW conjugated-goat anti-rabbit IgG (LI-COR Biosciences Cat# 926-32211 RRID:AB_621843), and quantitated using the Odyssey infrared imaging system (LI-COR Biosciences).

Analysis of mRNA

RNA was isolated using the RNeasy kit (Qiagen). RNA quality (RIN > 9) was verified using a Bioanalyzer 2100 System (Agilent Technologies). Total RNA (10 μ g) was used to prepare each RNA-seq library by following the manufacturer's instructions (Illumina). Three independent libraries were examined for each condition. The cDNA libraries were sequenced by Illumina Hi-Seq with a paired-end 40-bp format. These RNA-seq data have been deposited in the Gene Expression Omnibus (GEO) database with accession number GSE88856.

Reads from each sample were aligned to the mouse genome (UCSC genome browser mm10 build) using TopHat2 (Kim et al. 2013). The average number of aligned reads per library was > 30,000,000. Gene expression was quantitated as fragments per kilobase of exon model per million mapped fragments (FPKM) using Cufflinks (Trapnell et al. 2010). Differentially expressed genes were identified using the Cufflinks tools Cuffmerge and Cuffdiff.

The expression of mRNA was also examined by quantitative RT-PCR analysis using a Quantstudio 12K Flex machine (Life Technologies). TaqMan® assays were used to quantify *BAD* (Hs00188930_m1), *BBC3* (Hs00248075_m1), *BID* (Hs01026792_m1), *BIK* (Hs00154189_m1), *BCL2L11* (Hs00708019_s1), *BMF* (Hs00372937_m1), *HRK* (Hs02621354_s1), and *PMAIP1* (Hs00560402_m1), *Bad* (Mm00432042_m1), *Bbc3* (Mm00519268_m1), *Bcl2l11* (Mm00437797_m1), *Bid* (Mm00432073_m1), *Bik* (Mm00476123_m1), *Bmf* (Mm00506773_m1), *Hrk* (Mm01208086_m1), and *Pmaip1* (Mm00451763_m1) mRNA (Life Technologies). The relative mRNA expression was normalized by measurement of the amount of 18S RNA in each sample using Taqman® assays (catalog number 4308329; Life Technologies).

Anoikis Assay

Tertiary human mammary epithelial cells were suspended (4×10^5 cells/ml) in MammaryLife media (Lifeline Cell Technology) containing 0.5% methylcellulose (Sigma) in poly-HEMA (Sigma) coated plates. Murine kidney epithelial cells were

suspended (1.2×10^5 cells/ml) in serum-free DMEM/F12 media supplemented with 0.5% methylcellulose in poly-HEMA coated plates. To study autophagic flux during suspension, cells were treated with 25 μ M chloroquine diphosphate (Fluka Biochemika). Where indicated, cells were treated with 2 μ M JNK-in-8 (Millipore) at 24 h prior to the anoikis assay. Cell death was measured using colony formation assays and by measurement of Annexin V-staining.

Colony Formation Assay

Cells were washed with PBS, replated in 24-well plates, and cultured (24 h) prior to fixation (100% methanol, -20°C) and staining with 0.1% crystal violet dissolved in 20% methanol / 80% PBS. The cells were imaged using a Zeiss SteREO Discovery.V12 microscope and quantitated by extracting the crystal violet dye with 10% acetic acid and measurement of the absorbance at 590 nm (Tecan Instruments).

Flow Cytometry

The flow cytometry data were deposited in Flow Repository with accession number FR-FCM-ZYCR. Cells were washed twice with PBS and stained with phycoerythrin-conjugated Annexin V and 7-aminoactinomycin D (7-AAD) using the PE Annexin apoptosis detection kit I (BD Pharmingen #559763) and examined by flow cytometry using a FACSCalibur (BD Biosciences) to quantitate the apoptotic (Annexin V⁺ 7-AAD⁻) population. 7-AAD⁺ cells were gated using

single-stained controls. The Annexin V⁺ and Annexin V⁻ populations were defined using cells suspended for 1 hr. The data obtained were analyzed using FlowJo version 9.7.6 (Tree Star).

Mammary Gland Analysis

The 4th inguinal mammary glands were harvested from 6-week old and 6-month old virgin female mice. Whole mount preparations were fixed with formalin, stained with carmine alum, and imaged using a Zeiss SteREO Discovery.V12 microscope. Sections (5 µm) were prepared using tissue fixed in 10% formalin that was dehydrated and embedded in paraffin. A board-certified pathologist examined sections stained with hematoxylin & eosin and imaged using a Zeiss AxioVert 200M. Sections were also stained with antibodies against keratin 5 (BioLegend Cat# 905501 RRID:AB_2565050; 1:50 dilution) and keratin 8 (Developmental Studies Hybridoma Bank Cat# TROMA-I RRID:AB_531826; 1:100 dilution), and immune complexes were detected using AlexaFluor 546 conjugated-goat anti-rabbit IgG (H+L) antibody (Molecular Probes Cat# A11035 RRID:AB_143051) and AlexaFluor 488 conjugated-goat anti-rat IgG (H+L) antibody (Molecular Probes Cat# A11006 RRID:AB_141373) and counterstained with 2-(4-amidinophenyl)-1 h -indole-6-carboxamide (DAPI). Proliferating cells were stained using the endogenous biotin blocking kit (Thermo Fisher Scientific E21390), biotin-conjugated PCNA antibody (Thermo Fisher Scientific Cat# 13-3940 RRID:AB_2533; dilution 1:50), and AlexaFluor 633-conjugated streptavidin

(Thermo Fisher Scientific Cat# S-21375 RRID:AB_2313500).

Immunofluorescence was examined using a Leica SP2 confocal microscope.

Plasmids

The plasmid pCDNA3-Flag-MKK7 β 2-Jnk1 α 1 (Lei et al. 2002) has been previously described. The Flag-MKK7 β 2-Jnk1 α 1 cDNA fragment was excised by PCR using the primers 5'-

AAACCGCGGGCCGCCACCATGGACTATAAGGACGATGA-3' and 5'-

AAATCTAGATCACTGCTGCACCTGTGCTAAAGGAG-3', restricted using *Sac*II

and *Xba*I, and cloned into the *Sac*II and *Xba*I sites of the entry vector

pEN_Tmirc3 (Addgene plasmid # 25748 (Shin et al. 2006)) before insertion,

using Gateway Technology, into the lentiviral vector pSLIK-Hygro (Addgene

plasmid # 25737 (Shin et al. 2006)) to create the vector pSLIK- Flag-MKK7 β 2-

Jnk1 α 1-Hygro.

Transduction assays

HEK293T cells (American Type Culture Collection Cat # CRL-3216) were

transfected with 7.5 μ g each of the packaging plasmids pMD2.G (Addgene

plasmid #12259 (Naldini et al. 1996)) and psPAX2 (Addgene plasmid # 12260

(Naldini et al. 1996)) plus 10 μ g of pSLIK-Hygro or pSLIK- Flag-MKK7 β 2-Jnk1 α 1-

Hygro using Lipofectamine 2000 (Life Technologies). The culture supernatant

was collected at 24 h post-transfection and filtered (0.45 μ m). Primary epithelial cells were transduced (x2) with the lentivirus plus polybrene (8 μ g/ml). The transduced epithelial cells were selected at 48 h post-infection using medium supplemented with 8 μ g/ml hygromycin (Life Technologies). The cells were maintained in selection medium with tetracycline-free fetal bovine serum (Clontech). To induce expression of the MKK7-JNK1 fusion protein, the cells were treated with 1 μ g/ml doxycycline (24 h).

Statistical Analysis

Data are presented as the mean and standard error. The n values provided in the figure legends correspond to the number of independent experiments for studies using cultured cells or the number of animals examined. Statistical analysis was performed using GraphPad Prism version 6 (GraphPad Software). Pair-wise comparisons of data with similar variance were performed using a t-test to determine significance ($p < 0.05$). Pair-wise comparisons of data with unequal variance were performed using Welch's unpaired t-test to determine significance ($p < 0.05$). When more than two populations were compared ANOVA with Bonferroni's test was used to determine significance with an assumed confidence interval of 95%.

CHAPTER III

THE JNK PATHWAY CONTRIBUTES TO MOUSE MAMMARY GLAND REMODELING DURING INVOLUTION

Abstract

Involution returns the lactating mammary gland to a quiescent state after weaning. The mechanism of involution involves collapse of the mammary epithelial cell compartment. To test whether the cJUN NH₂-terminal kinase (JNK) signal transduction pathway contributes to involution, I established mice with JNK deficiency in the mammary epithelium. I found that JNK is required for efficient involution. JNK deficiency did not alter the STAT3/5 or SMAD2/3 signaling pathways that have been previously implicated in this process. Nevertheless, JNK promotes the expression of genes that drive involution, including matrix metalloproteases, cathepsins, and BH3-only proteins. These data demonstrate that JNK plays a key role in mammary gland involution post-lactation.

Introduction

The mammary gland is dynamically regulated by circulating hormones and paracrine/autocrine cytokines during post-natal development. Estrogen promotes ductal development by epithelial cells in the mammary gland after puberty (Mallepell et al. 2006; Feng et al. 2007). In contrast, progesterone and prolactin are critically required for the epithelial development of alveoli and subsequent milk production by the mammary gland in response to pregnancy (Horseman et al. 1997; Humphreys et al. 1997; Ormandy et al. 1997). Weaning causes milk stasis, decreased circulating concentrations of prolactin, and increased expression of cytokines that activate the JAK1/STAT3 signaling pathway, including leukemia inhibitory factor (LIF) (Kritikou et al. 2003), interleukin 6 (IL6) (Zhao et al. 2002), and oncostatin M (OSM) (Tiffen et al. 2008). LIF may serve to initiate STAT3 activation that engages an autocrine pathway sustained by STAT3-induced OSM expression (Tiffen et al. 2008). The switch from prolactin-stimulated STAT5 activation to LIF/IL6/OSM-stimulated STAT3 activation drives remodeling (involution) of the mammary gland, including collapse of the epithelial cell compartment and replacement by adipose tissue, to enable return to a quiescent state (Chapman et al. 1999; Cui et al. 2004).

The requirement of the LIF/JAK1/STAT3 pathway for mammary gland involution is strongly supported by studies of knockout mice. Deficiency of LIF (Kritikou et al. 2003), JAK1 (Sakamoto et al. 2016), or STAT3 (Li et al. 1997) causes a similar delay in mammary gland involution. Targets of STAT3 signaling

include pathways of lysosome-mediated cell death involving cathepsins (Kreuzaler et al. 2011) and mitochondrion-mediated apoptotic pathways mediated by members of the BCL2 family (Schmelzle et al. 2007; Sakamoto et al. 2016; Schuler et al. 2016). Indeed, it is established that the *Bcl2l1* and *Bmf* genes that encode the pro-apoptotic BH3-only proteins BIM and BMF are direct targets of STAT signaling (Sakamoto et al. 2016; Schuler et al. 2016). Increased *Bcl2l1* and *Bmf* gene expression during involution may result from loss of transcriptional repression by STAT5 and increased transcriptional activity mediated by STAT3 (Sakamoto et al. 2016; Schuler et al. 2016). The importance of *Bcl2l1* and *Bmf* gene induction is confirmed by analysis of knockout mice that show delayed involution (Sakamoto et al. 2016; Schuler et al. 2016). The BH3-only proteins BAD and NOXA are also implicated in involution, but studies of BAD-deficient (*Bad*^{-/-}) mice and NOXA-deficient (*Pmaip1*^{-/-}) mice demonstrate that these BH3-only proteins are not essential for involution (Schuler et al. 2016).

Although the LIF/IL6/OSM – JAK1 – STAT3 signaling pathway plays a key role in involution, this pathway appears to function in collaboration with other signaling pathways that contribute to involution, including TGF β (Nguyen and Pollard 2000). Several TGF β isoforms are expressed at low levels during lactation, but are greatly induced during involution (Faure et al. 2000). It is therefore likely that TGF β signaling during involution may contribute to remodeling of the extracellular matrix during involution and TGF β may also contribute to mammary epithelial cell death. Indeed, deficiency of TGF β 3

(Nguyen and Pollard 2000) or Smad3 (Yang et al. 2002) causes decreased cell death during involution, while the forced expression of TGF β 3 causes increased cell death during lactation (Nguyen and Pollard 2000).

Other signaling pathways might also contribute to the involution response. For example, loss of survival signaling (e.g. AKT and ERK) caused by cell detachment and loss of signaling by integrins and receptor tyrosine kinases may promote cell death (Frisch and Francis 1994; Frisch and Screaton 2001; Reginato et al. 2003). Similarly, increased signaling by stress-activated MAP kinases (Davis 2000; Cuadrado and Nebreda 2010; Avivar-Valderas et al. 2014) may promote cell death during involution. Indeed, it is established that the stress-activated protein kinases p38 MAP kinase (Wen et al. 2011) and cJUN NH₂-terminal kinase (JNK) (Cellurale et al. 2012; Girnius and Davis 2017b) can promote anoikis of mammary epithelial cells. However, it is not known whether these stress-activated MAP kinases contribute to the involution response.

The purpose of this study was to test whether JNK contributes to mammary gland remodeling during the involution response. JNK is activated during involution and has been mechanistically implicated in the involution response (Marti et al. 1999). Interestingly, JNK can promote cell death mediated by BH3-only proteins (BMF and BIM) (Tournier et al. 2000; Lei et al. 2002; Lei and Davis 2003; Hubner et al. 2008; Hubner et al. 2010) that are known to contribute to cell death during involution (Schmelzle et al. 2007; Sakamoto et al. 2016; Schuler et al. 2016). Two JNK isoforms (JNK1 and JNK2) with partially

redundant functions are expressed in the mammary epithelium. Developmental studies demonstrate that these JNK isoforms are required for anoikis and the clearance of cells from mammary ducts and terminal end buds (Cellurale et al. 2012; Girnius and Davis 2017b). Indeed, deficiency of JNK1 plus JNK2 in the mammary epithelium (but not deficiency of JNK1 or JNK2 alone (Cellurale et al. 2010)) causes ductal occlusion by suppressing anoikis (Cellurale et al. 2012; Girnius and Davis 2017b). Thus, JNK is required for normal mammary gland development and could contribute to involution.

Previous studies have established that involution defects were not observed in mice lacking JNK1 or JNK2 (Cellurale et al. 2010). I therefore examined mice with compound deficiency of JNK1 plus JNK2 in the mammary epithelium. These JNK-deficient mice exhibited delayed involution. Moreover, JNK deficiency caused major disruption of the gene expression program that mediates involution. Together, these data demonstrate that JNK contributes to the normal mammary gland involution response.

Results

JNK is required for efficient mammary gland involution

To study mice with compound disruption of the *Mapk8* gene (encodes JNK1) plus the *Mapk9* gene (encodes JNK2) in the mammary epithelium, I established Control (JNK^{WT}) mice (*Wap-Cre*^{+/+}) and JNK-deficient (JNK^{KO}) mice (*Wap-Cre*^{+/+} *Mapk8*^{LoxP/LoxP} *Mapk9*^{LoxP/LoxP}). *Wap-Cre* expression is induced in the mammary epithelium during lactation (Wagner et al. 1997) and I found *Cre*-mediated recombination in mammary epithelial cells (Figure III.1.A). Analysis of genomic DNA demonstrated efficient ablation of the *Mapk8* and *Mapk9* genes in the mammary glands of lactating JNK^{KO} mice (Figure III.1.B, C).

To test the role of JNK in involution, I examined JNK^{WT} and JNK^{KO} dams that nursed litters for 9 days. Involution was initiated by removal of the pups (involution day 0). Microscopic analysis of tissue sections at this stage demonstrated no differences between the mammary glands of JNK^{WT} and JNK^{KO} mice (Figure III.2 & III.3). After 3 days of involution, the JNK^{WT} glands exhibited collapse of alveolar structures and the reappearance of adipocytes. In contrast, analysis of the JNK^{KO} glands demonstrated the presence of distended alveoli and no reappearance of adipocytes (Figure III.2 & III.3). After 7 days of involution, the JNK^{WT} glands had returned to a virgin-like state, while JNK^{KO} glands still had an expanded epithelial compartment with many collapsed alveoli (Figure III.2 & III.3). However, on day 14 after the initiation of involution, no differences were detected between the tissue architecture (Figure III.2 & III.3) or epithelial cell

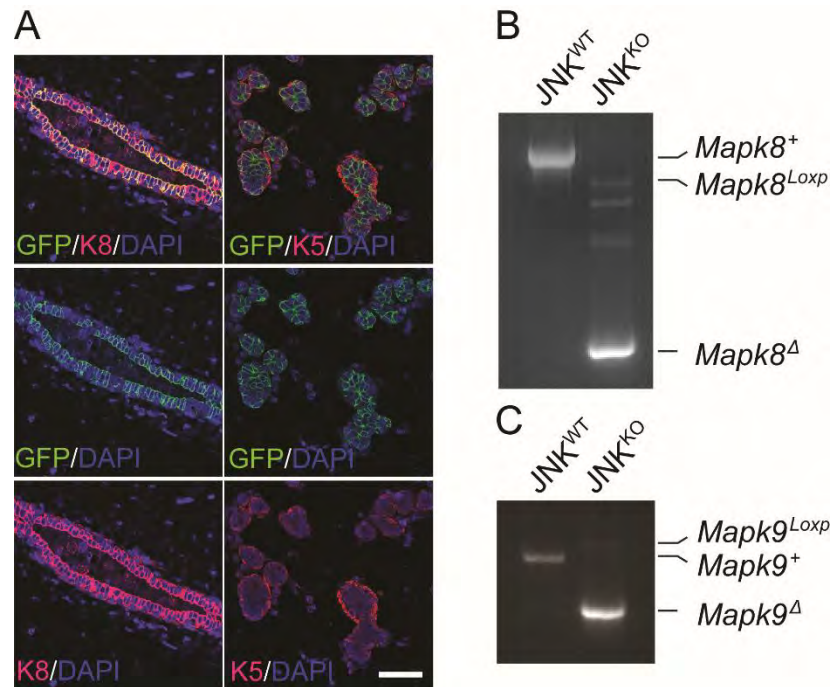


Figure III1. *Mapk8* and *Mapk9* gene disruption in luminal mammary epithelial cells.

(A) Sections of mammary glands prepared from single parous female *Wap-Cre*^{+/+} *Rosa*^{mT/mG} reporter mice were stained with antibodies to GFP, keratin 5 (K5), or keratin 8 (K8), and then counter-stained with DAPI. The GFP antibody stains *Cre*⁺ cells in the reporter mice. The images presented are representative of sections prepared from mammary glands of 7 mice. Scale bar = 50 μ m.

(B, C) *Cre*-mediated recombination of *Mapk8*^{Loxp} (B) and *Mapk9*^{Loxp} (C) alleles was confirmed by PCR analysis of genomic DNA isolated from mammary epithelial cells isolated from mice after 10 days of lactation.

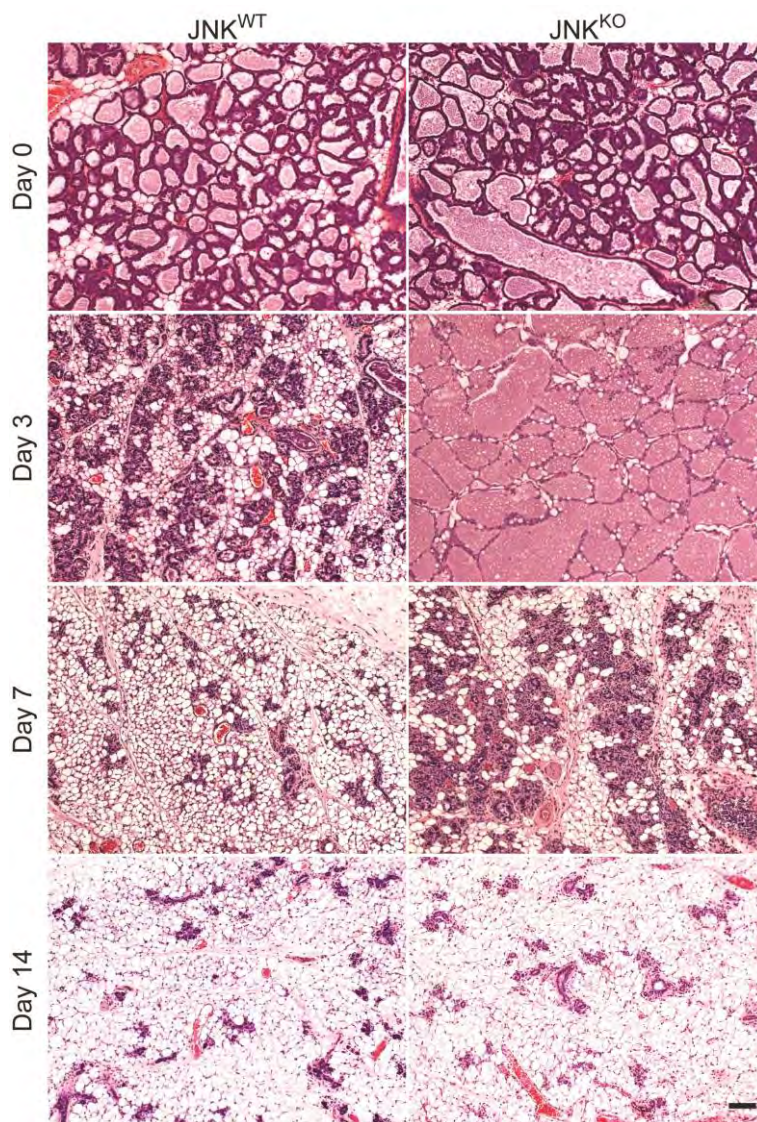


Figure III.2. JNK is required for efficient mammary gland involution.

Sections of #4 mammary glands from JNK^{WT} and JNK^{KO} mice on involution day 0, 3, 7 and 14 were stained with H&E. The images presented are representative of sections prepared from the mammary glands of 5 JNK^{WT} mice and 5 JNK^{KO} mice for each condition. Scale bar = 100 μ m.

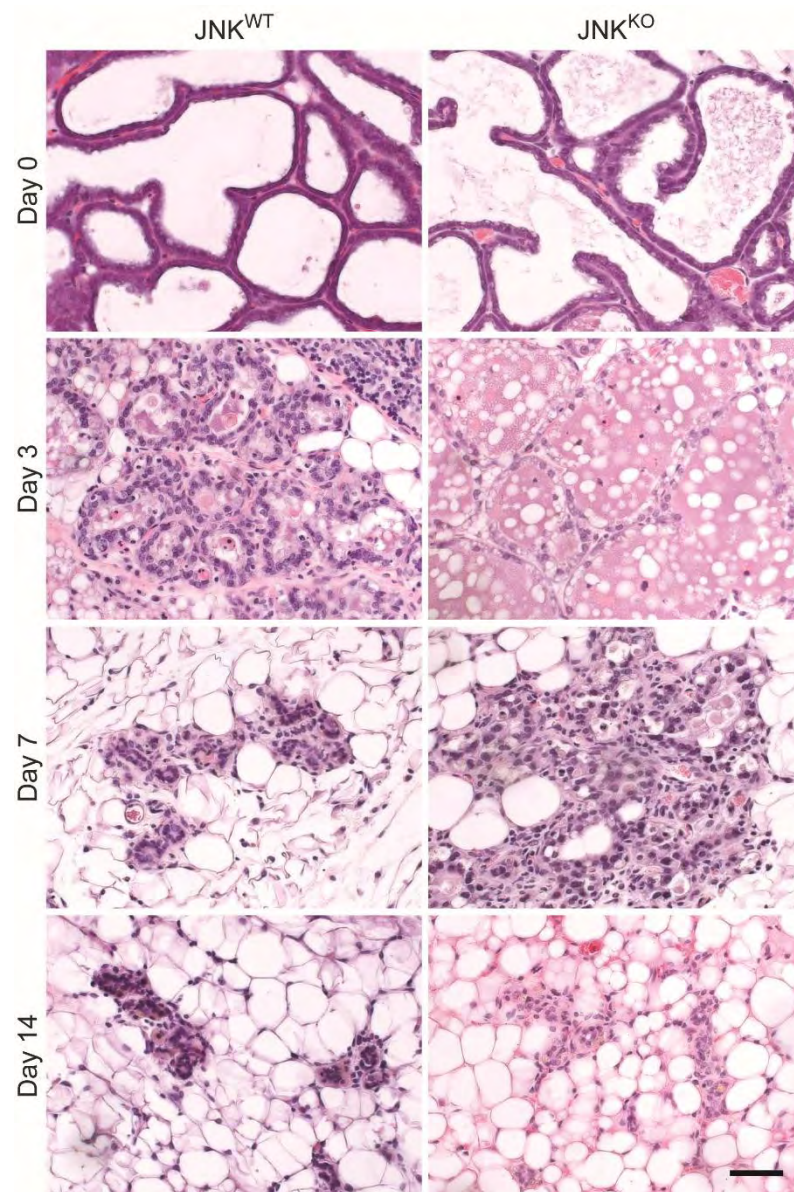


Figure III.3. JNK is required for mammary gland involution.

Sections of mammary glands from JNK^{WT} and JNK^{KO} female mice on day 0, 3, 7, and 14 of involution were stained with H&E. The images are representative of sections taken from 5 JNK^{WT} mice and 5 JNK^{KO} mice for each condition. Scale bar = 50 μ m.

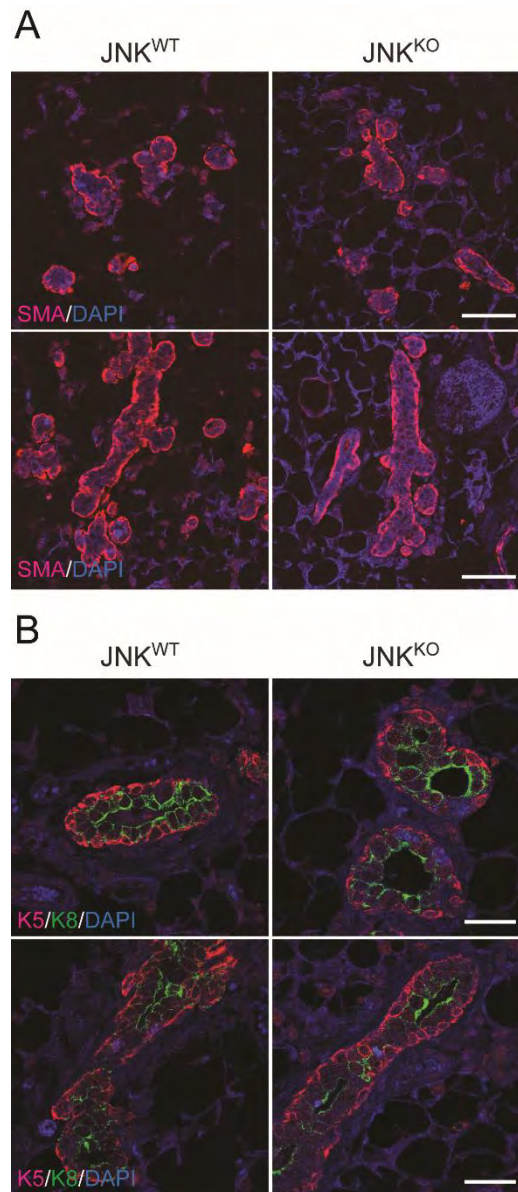


Figure III.4. Epithelial cell populations in mammary glands after involution.

(A, B) Mammary gland sections were stained with antibodies to smooth muscle actin (SMA, a) or with antibodies to keratin 5 and 8 (K5 and K8, b), and counterstained with DAPI. Representative images are presented. Scale bars = 50 μ m (A) and 30 μ m (B).

populations (Figure III.4) of mammary glands from JNK^{WT} and JNK^{KO} mice.

These findings demonstrate that JNK-deficiency delays involution, indicating that JNK is required for the proper execution of this process.

JNK promotes epithelial cell death during involution

To test whether JNK regulates epithelial cell death in mammary glands during involution, I performed immunohistochemistry using an antibody specific for cleaved caspase 3. On involution day 0, few cleaved caspase 3 positive (c-C3⁺) cells were detected in the mammary glands of JNK^{WT} and JNK^{KO} mice (Figure III.5A). However, on day 3 of involution a substantial increase in the number of c-C3⁺ cells was found in the glands of JNK^{WT} mice, but not JNK^{KO} mice (Figure III.5A). In contrast, large numbers of c-C3⁺ cells were found in both JNK^{WT} and JNK^{KO} mice on day 7 of involution (Figure III.6). These data indicate that JNK deficiency delays cell death during involution. To confirm this conclusion, I examined terminal deoxynucleotidyl transferase dUTP nick end labeling (TUNEL) of cells on day 3 of involution. In agreement with the c-C3 data, there were reduced numbers of TUNEL⁺ cells in glands from JNK^{KO} mice compared with JNK^{WT} mice (Figure III.5B). Thus, JNK-deficiency causes delayed epithelial cell death in the involuting mammary gland.

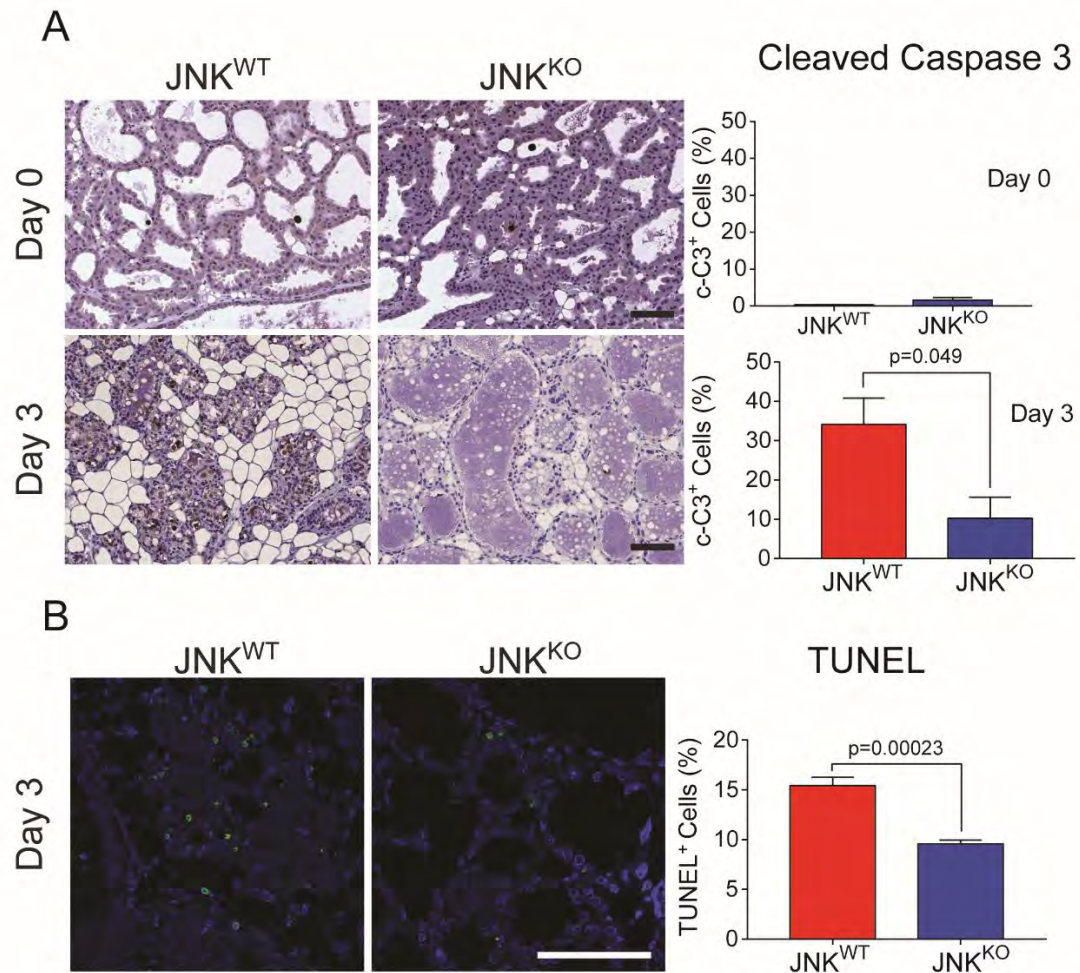


Figure III.5. JNK-deficiency suppresses cell death during involution.

(A) Sections of #4 mammary glands from single parous female mice on involution day 0 or on involution day 3 were stained with an antibody to cleaved caspase 3 (c-C3) and counter-stained with hematoxylin. Representative images are presented. c-C3⁺ cells were quantitated in 6 fields (40x) per section and presented as the % of total cells (mean \pm SEM; JNK^{WT} 0 day n=5, JNK^{WT} 3 day n=4, JNK^{KO} 0 day n=4, JNK^{KO} 3 day n=6 mice). Scale bar = 100 μ m.

(B) Sections of #4 mammary glands from mice on involution day 3 were stained by TUNEL assay and counter-stained with DAPI. Representative images are presented. TUNEL⁺ cells were quantitated in 6 fields (40x) per section and presented as the % of total cells (mean \pm SEM; JNK^{WT} n=4, JNK^{KO} n=5 mice). Scale bar = 50 μ m.

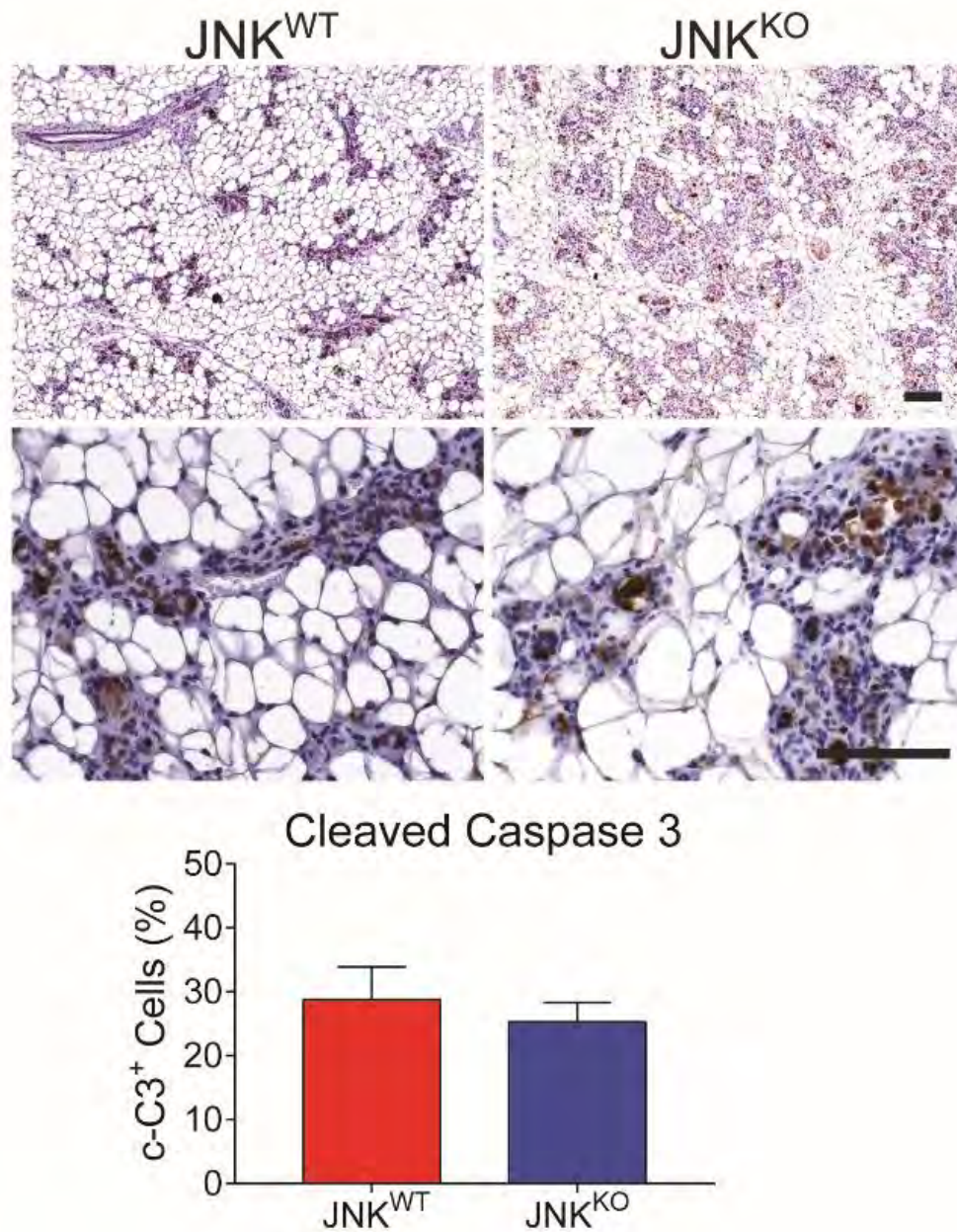


Figure III.6. Caspase 3 activation in mammary glands after 7 days of involution.

Sections prepared from mammary glands of 5 JNK^{WT} mice and 5 JNK^{KO} mice on day 7 of involution were stained with an antibody to cleaved caspase 3 (c-C3⁺). Representative images are presented. c-C3⁺ cells were quantitated in 6 fields (40x) per section and presented as the % of total cells (mean \pm SEM; n = 5 mice; p>0.05). Scale bars = 100 μ m.

Effect of JNK deficiency on STAT and SMAD transcription factors

The delayed involution observed in JNK^{KO} mice may be caused by changes in the key transcription factors that regulate this process. It is established that decreased activation of SMAD2/3 or STAT3, or increased STAT5 activation, may cause delayed involution (Chapman et al. 1999; Cui et al. 2004). I therefore examined the activation state of these transcription factors by immunohistochemistry using antibodies to the activating sites of phosphorylation. Studies of phospho-STAT3 (Figure III.7A), phospho-STAT5 (Figure III.8A), and phospho-SMAD2/3 (Figure III.8B) revealed similar staining of sections prepared from mammary glands of JNK^{WT} and JNK^{KO} mice on day 3 of involution. Indeed, quantitation of phospho-STAT3 immunofluorescence revealed no significant difference between JNK^{WT} and JNK^{KO} glands (Figure III.7B). Immunoblot analysis performed on tissue lysates supported this conclusion (Figure III.7C). Strikingly, the induction of *Socs3*, a STAT3 target gene, was evident after 3 days of involution and was un-affected by JNK deficiency (Figure III.7D). These data demonstrate that the delayed involution caused by JNK deficiency did not reflect disruption of the signaling pathways that regulate the STAT3/5 or SMAD2/3 transcription factors.

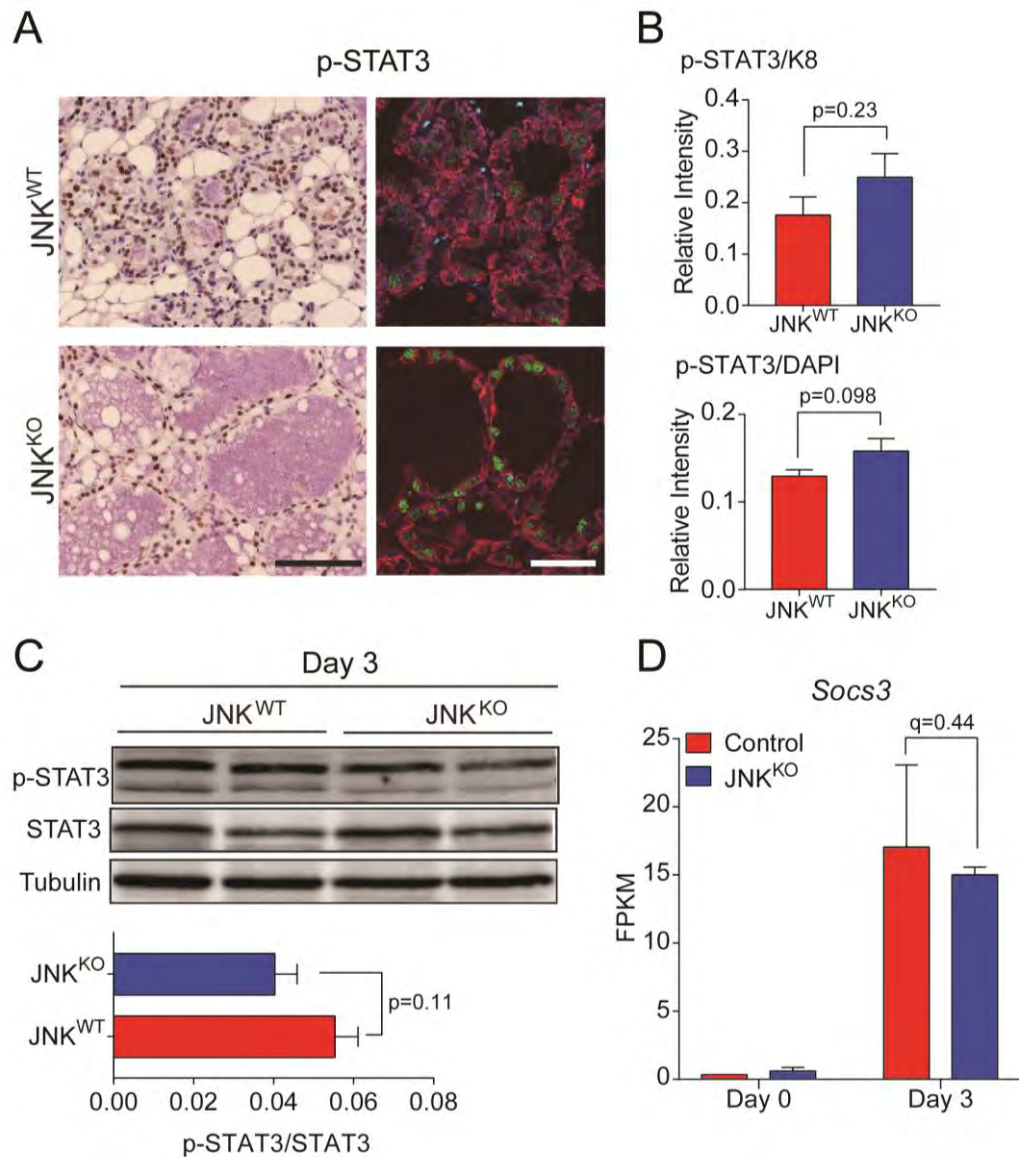


Figure III.7. STAT3 signaling is not disrupted in JNK^{KO} glands.

(A) Immunohistochemistry (*left*, scale bar = 100 μ m) and immunofluorescence (*right*, scale bar = 30 μ m) were performed on sections prepared from #4 mammary glands of single parous female mice on involution day 3 ($n=5$ JNK^{WT} mice and $n=4$ JNK^{KO} mice) using an antibody to phospho-STAT3 (p-STAT3) and counter-stained with hematoxylin or DAPI, respectively. An antibody to keratin 8 (K8) was used to label epithelial cells during immunofluorescence staining. Representative images are presented.

(B) K8, p-STAT3, and DAPI fluorescence intensities of involution day 3 glands from JNK^{WT} (n=5 mice) and JNK^{KO} (n=4 mice) were quantitated and p-STAT3 intensity was normalized to K8 and DAPI fluorescence intensity. No significant differences between JNK^{WT} and JNK^{KO} glands were detected ($p>0.05$).

(C) Protein extracts prepared from involution day 3 mammary glands were examined by immunoblot analysis by probing with antibodies to p-STAT3, STAT3 and Tubulin. Two representative mice are presented. The quantitative data presented are the mean \pm SEM (n=9 JNK^{WT} mice and n=5 JNK^{KO} mice). No significant differences between JNK^{WT} and JNK^{KO} glands were detected ($p>0.05$).

(D) The mRNA expression of *Socs3* measured by RNA-seq analysis is presented as the mean fragments per kilobase of exon model per million mapped fragments (FPKM) \pm SEM; n=3 JNK^{WT} and 3 JNK^{KO} mice per condition). No significant differences between JNK^{WT} and JNK^{KO} glands were detected ($q>0.05$).

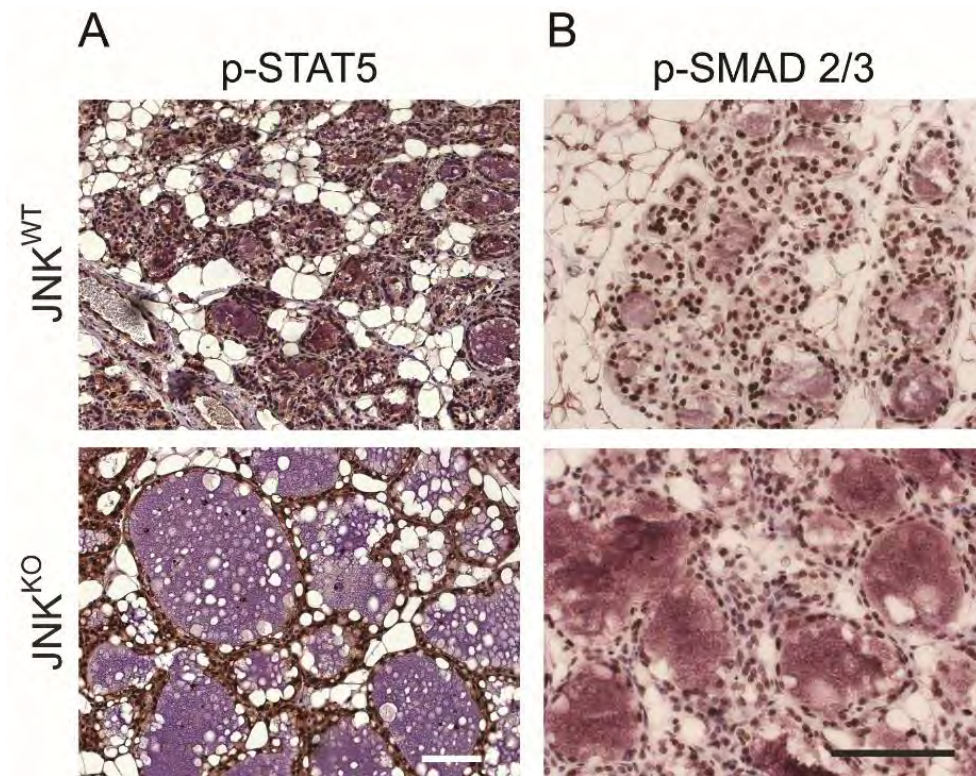


Figure III.8. JNK deficiency does not alter STAT5 or SMAD2/3 activation during involution.

(A, B) Sections prepared from mammary glands of 5 JNK^{WT} mice and 5 JNK^{KO} mice on involution day 3 were stained with an antibody to p-STAT5 (a) or p-SMAD2/3 (b) and counterstained with hematoxylin. Representative images are presented. Scale bars = 100 μ m.

Effect of JNK deficiency on AP1 transcription factors

Major targets of JNK signaling include members of the Activator Protein 1 (AP1) group of transcription factors that are phosphorylated and activated by JNK (Davis 2000) and have been implicated in involution (Jaggi et al. 1996; Marti et al. 1999). The AP1 family includes members of the JUN and FOS groups, as well as some members of the ATF group of transcription factors. I therefore examined the expression of these AP1-related transcription factors in mammary glands of JNK^{WT} and JNK^{KO} mice on day 0 and day 3 of involution by mRNA sequencing (Figure III.9A). Involution in JNK^{WT} mice caused significantly increased expression of many of these AP1-related transcription factors, including *Atf3*, *Atf5*, *Atf7*, *Fos*, *FosB*, *FosL1*, *FosL2*, *Jun*, *JunB*, and *JunD* (Figure III.9A). Comparison of JNK^{WT} and JNK^{KO} mice demonstrated no significant differences in AP1-related transcription factor expression on day 0 of involution (Figure III.9A). However, on involution day 3 the increased expression of *Atf3*, *FosL2*, *Jun*, and *JunD* detected in JNK^{WT} mice was suppressed in JNK^{KO} mice (Figure III.9B-E). Thus, JNK-deficiency causes a selective defect in the AP1-related transcription factor response during involution that is mediated by ATF3, FOSL2, cJUN, and JUND. This observation may be mechanistically relevant to involution because AP1 transcription factor function has been implicated in mammary gland involution (Marti et al. 1999).

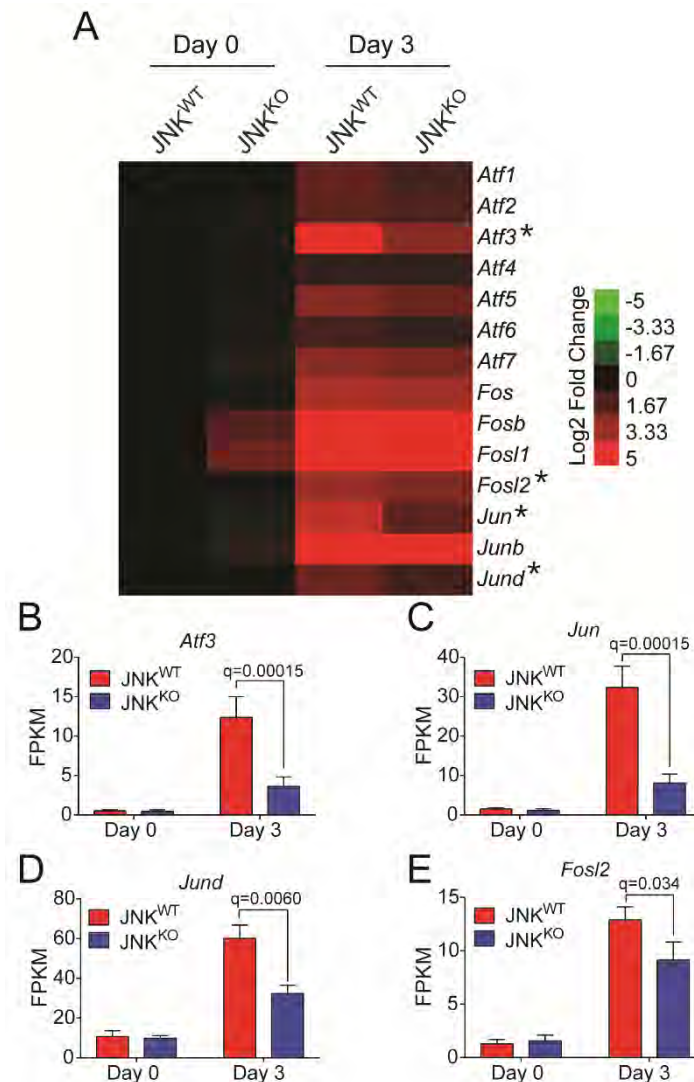


Figure III.9. JNK-deficiency suppresses the increase in AP1-related transcription factor expression during involution.

(A) Heatmap representation of RNA-seq data showing AP1-related transcription factor gene expression. Asterisks denote genes that are differentially expressed ($q < 0.05$) between JNK^{WT} and JNK^{KO} mammary glands on involution day 3 (mean; $n=3$ JNK^{WT} and $n=3$ JNK^{KO} mice for each condition)

(B-E) The mRNA expression of *Atf3* (B), *Jun* (C), *Jund* (D), and *Fosl2* (E) measured by RNA-seq analysis is presented as mean FPKM \pm SEM; $n=3$ JNK^{WT} and $n=3$ JNK^{KO} mice for each condition.

JNK deficiency disrupts involution-associated gene expression

Comparison of gene expression on day 0 and day 3 of involution demonstrated that 10,358 genes were differentially expressed in JNK^{WT} mammary glands ($\log_2|\text{Fold Change}| > 1$; $q < 0.01$) (Figure III.10A). A similar number of genes (10,071) were differentially expressed in JNK^{KO} mammary glands (Figure III.10A) and 8,620 genes were co-regulated in both JNK^{WT} and JNK^{KO} mammary glands during involution (Figure III.10A). However, 1,688 genes were differentially expressed only in JNK^{WT} mice and 1,401 genes were differentially expressed only in JNK^{KO} mice. These data demonstrate that involution is associated with major changes in gene expression and that JNK deficiency causes dysregulation of a large fraction (26%) of these genes.

Comparison of RNA expression in mammary glands of JNK^{WT} and JNK^{KO} mice on involution day 0 demonstrated differential expression of 134 genes ($\log_2|\text{Fold Change}| > 1$; $q < 0.01$) (Figure III.10B), indicating that JNK deficiency causes only small changes in gene expression in the lactating mammary gland. In contrast, comparison of JNK^{WT} and JNK^{KO} mice demonstrated 2,236 differentially expressed genes on involution day 3 (Figure III.10B) and only 92 genes were co-regulated during both normal lactation and involution (Figure III.10B). These data indicate that while JNK deficiency causes few changes in gene expression in the lactating mammary gland, JNK deficiency causes major changes in gene expression during involution. The majority of this differential

RNA expression (~94%) corresponded to genes that encode proteins (Figure III.11).

To characterize involution-associated gene expression in JNK^{WT} and JNK^{KO} mammary glands, I performed k-means clustering on the 12,862 genes that were differentially expressed in any of the pairwise comparisons (Figure III.10C). Cluster 1 included genes that were up-regulated during involution (day 3) in JNK^{WT} mice and were more strongly up-regulated in JNK^{KO} mice. This cluster was highly enriched for ribosomal genes ($p_{\text{adj}}=1.88 \times 10^{-98}$; Figure III.10D). Clusters 2/3 included genes that were highly up-regulated during involution in JNK^{WT} mice and modestly up-regulated in JNK^{KO} mice (Cluster 2) or were not up-regulated in JNK^{KO} mice (Cluster 3). Both clusters were enriched for metabolic pathways ($p_{\text{adj}} < 10^{-71}$), while Cluster 2 showed additional enrichment for genes involved in RNA metabolism (Figure III.10D). There was no striking enrichment of pathways in Cluster 4, which contained genes down-regulated in both JNK^{WT} and JNK^{KO} mice during involution (Figure III.10D). Thus, while JNK is dispensable for the regulation of a limited number of genes during involution (Cluster 4), the loss of JNK greatly affects the expression of other involution-associated genes (Clusters 1, 2 and 3).

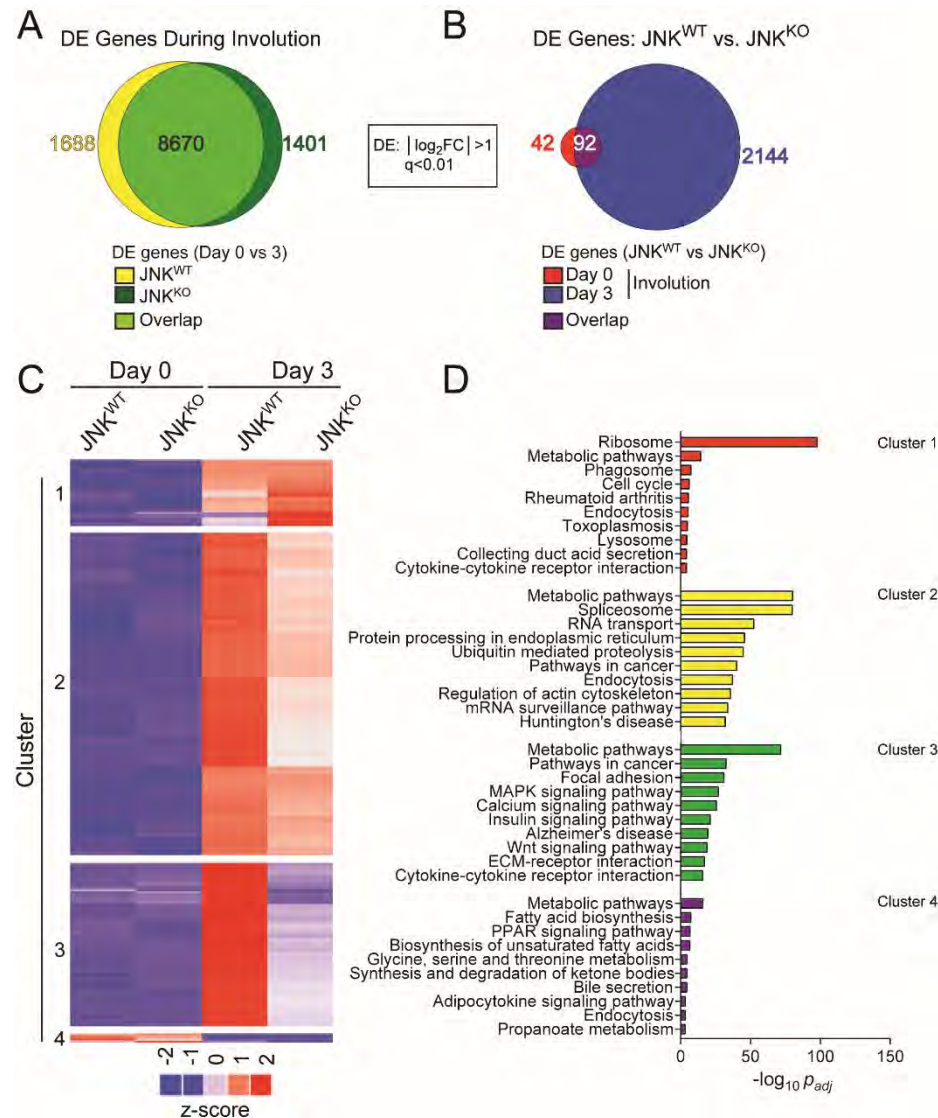


Figure III.10. JNK promotes involution-associated gene expression.

(A, B) RNA-seq analysis of mammary glands of JNK^{WT} and JNK^{KO} mice on involution day 0 or day 3 is presented as a Venn diagram of the number of differentially expressed (DE) genes ($\log_2|\text{Fold Change}| > 1$; $q < 0.01$; $n = 3$ JNK^{WT} and $n = 3$ JNK^{KO} mice for each condition).

(C) The heatmap presents k-means clustering ($k = 4$) of DE genes in at least one pairwise comparison between JNK^{WT} and JNK^{KO} mammary glands on involution day 0 or day 3.

(D) Gene set enrichment analysis was performed on the 4 gene clusters. The 10 KEGG pathways identified with lowest p_{adj} -value are presented.

A

Biological Group	Mean Reads	Mean Read Mapping Rate
JNK ^{WT} Day 0	66,439,000	98.3 %
JNK ^{KO} Day 0	63,476,000	98.1 %
JNK ^{WT} Day 3	61,129,000	97.9 %
JNK ^{KO} Day 3	64,328,000	98.0 %

B

JNK ^{WT}		
Biotype	Frequency	Differentially Expressed
Protein Coding	22,580	9,882
Pseudogene	5,850	413
lincRNA	1,762	108
Processed Transcript	621	57
Antisense	1,443	32
miRNA	1,768	11
snoRNA	1,453	10
misc RNA	529	4
Polymorphic pseudogene	15	3
rRNA	299	2
Mt tRNA	8	1
Sense Intronic	86	1
Sense Overlapping	8	1
	36,422	10,525

C

JNK ^{KO}		
Biotype	Frequency	Differentially Expressed
Protein Coding	22,583	9,468
Pseudogene	5,850	457
lincRNA	1,762	94
Processed Transcript	621	51
Antisense	1,443	33
snoRNA	1,453	9
miRNA	1,768	8
misc RNA	529	6
Polymorphic pseudogene	15	4
rRNA	299	3
Sense Intronic	86	1
Sense Overlapping	8	1
	36,417	10,135

Figure III.11. Summary of RNA sequencing analysis.

(A) RNA sequencing analysis of mammary glands isolated from JNK^{WT} and JNK^{KO} mice is summarized. Each biological group comprises 3 independent replicates.

(B, C) Biotypes were determined for both detected gene expression and genes that are differentially expressed ($\log_2|\text{Fold Change}| > 1$, $q < 0.01$) between day 0 and day 3 of involution in JNK^{WT} mice (B) and JNK^{KO} mice (C).

The requirement of JNK for normal involution-associated gene expression (Figure III.10) may be a secondary consequence of delayed involution and suppression of this developmental program of gene expression. Alternatively, these involution-associated genes may be directly targeted by JNK. To explore these two possible mechanisms, I compared the presence of AP1 binding sites (defined by ENCODE ChIP-seq analysis of cJUN and JUND (Mouse et al. 2012)) near genes that are developmentally regulated during involution in a JNK-dependent manner with genes that are not significantly regulated by JNK. This analysis demonstrated significant enrichment of cJUN and JUND binding sites ($p=2 \times 10^{-16}$) with approximately 35% of the JNK-regulated genes during involution (Figure III.12). However, the remaining 65% of the JNK-regulated genes lack cJUN/JUND binding sites (Figure III.12). The JNK-regulated expression of these genes may reflect targeting of other transcription factors by JNK or represent a consequence of delayed involution.

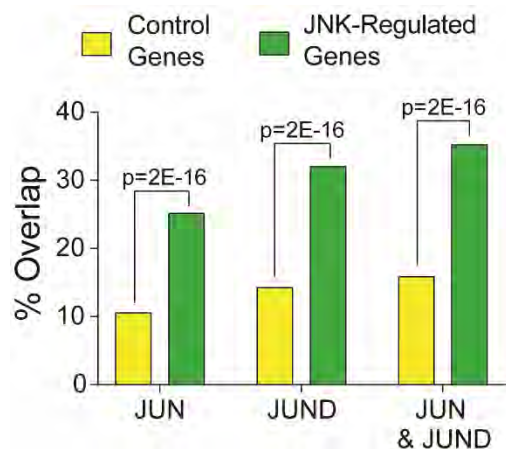


Figure III.12. Enrichment of AP1 binding sites with genes that exhibit JNK-dependent expression during involution.

Genes expressed in a JNK-dependent manner (green) or JNK-independent manner (yellow) after 3 days of involution (Figure III.10) were compared with genes identified by ChIP-Seq analysis (cJUN, JUND, or JUN plus JUND) to determine overlap between JNK-dependent gene expression and genes with AP1 binding sites. Pearson's Chi-squared test was used to determine statistical significance.

JNK promotes the expression of genes that remodel the mammary gland during involution

It is established that matrix metalloproteinases (MMPs) are involved in remodeling the extracellular matrix (Page-McCaw et al. 2007). Interestingly, differentially expressed genes with enrichment of cJUN/JUND binding include several *Mmp* genes that may contribute to mammary gland involution (Figure III.10C; Figure III.12). Indeed, *Mmp3* is implicated in both mammary gland development and involution (Lund et al. 1996; Page-McCaw et al. 2007). I found that JNK deficiency markedly suppressed the increased *Mmp3* expression detected in JNK^{WT} mice on involution day 3 (Figure III.13), consistent with the observation that JNK^{KO} mice exhibit delayed involution (Figure III.2 & III.3). I also found that the expression of *Mmp2*, *Mmp9*, *Mmp11*, *Mmp12*, *Mmp13*, and *Mmp14* were significantly decreased in JNK^{KO} mice compared with JNK^{WT} mice after 3 days of involution (Figure III.13).

Alterations in the tissue inhibitors of metalloproteases (TIMPs) could also impact mammary gland involution. Indeed, *Timp1* overexpression results in more rapid adipocyte repopulation of the gland, while *Timp3* loss can promote epithelial cell apoptotic signaling (Alexander et al. 2001; Hojilla et al. 2011). Unexpectedly, I found that *Timp2* and *Timp3* expression was increased during involution in JNK^{WT} mice and that this was suppressed in JNK^{KO} mice (Figure III.13).

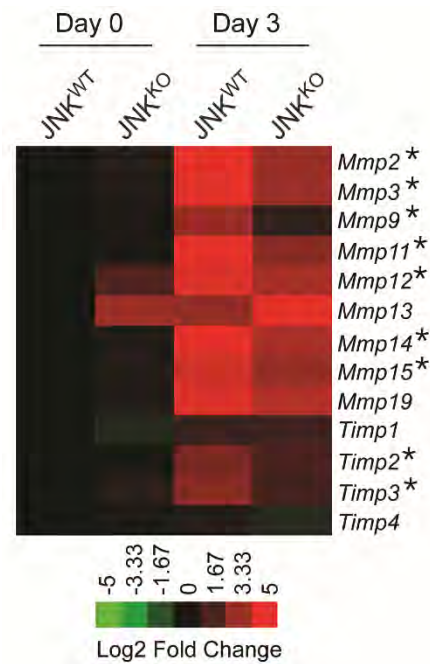


Figure III.13. Mammary gland expression of *Mmp* and *Timp* genes.

Heatmap representation of RNA-seq data showing *matrix metalloproteinase* and *tissue inhibitor of metalloproteinase* gene expression. Asterisks denote genes that are differentially expressed (q<0.05) between JNK^{WT} and JNK^{KO} mammary glands on involution day 3 (mean; n=3 JNK^{WT} and n=3 JNK^{KO} mice for each condition).

Epithelial cell death during involution is caused, in part, by a lysosomal pathway mediated by Cathepsins (Kreuzaler et al. 2011) and it is established that increased *Ctsb* (encodes Cathepsin B) and *Ctsl* (encodes Cathepsin L) expression, together with reduced expression of *Serpina3g* (encodes the protease inhibitor Spi2A), contribute to STAT3-induced involution (Chapman et al. 1999; Kreuzaler et al. 2011). Interestingly, the *Ctsb* gene binds the AP1 transcription factors cJUN / JUND and therefore might exhibit JNK-dependent expression (Figure 5 & S7). Indeed, I found that the expression of *Ctsb* was increased on involution day 3 in JNK^{WT} mice and that this increased expression was suppressed in JNK^{KO} mice (Figure III.14A). A similar pattern of expression was observed for *Ctsl* (Figure III.14B). In contrast, JNK deficiency caused no significant change in *Serpina3g* expression during involution (Figure III.14C). Thus, reduced Cathepsin expression may contribute to the delayed involution phenotype caused by JNK-deficiency.

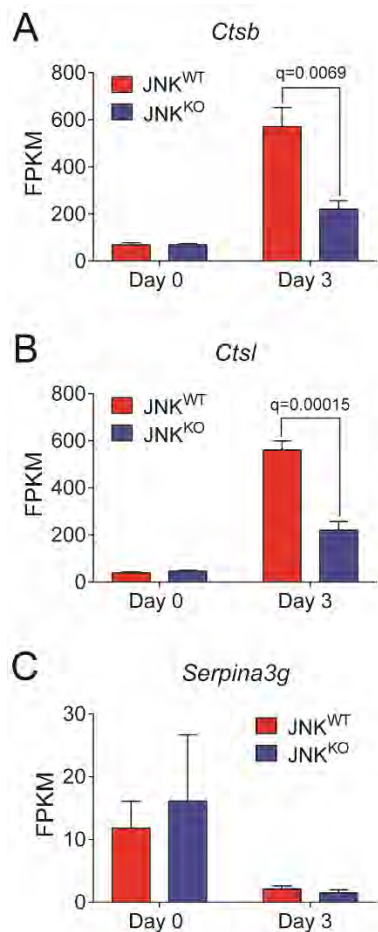


Figure III.14. Mammary gland expression of cathepsin.

(A-C) The mRNA expression of *Ctsb* (A), *Ctsl* (B), and *Serpina3g* (C) was measured by RNA-seq analysis. The data are presented as mean FPKM \pm SEM; n=3 JNK^{WT} and n=3 JNK^{KO} mice for each condition).

Epithelial cell death during involution is also caused by the mitochondrion-mediated apoptotic pathway induced by members of the BCL2 family (Schmelzle et al. 2007; Sakamoto et al. 2016; Schuler et al. 2016). Previous studies have implicated a key role for the BH3-only gene *Bcl2l1* (encodes BIM) in the promotion of epithelial cell death during the involution response (Sakamoto et al. 2016; Schuler et al. 2016). Moreover, it is established that the *Bcl2l1* gene is regulated by AP1 transcription factor binding to the promoter (Whitfield et al. 2001; Biswas et al. 2007). I therefore anticipated that *Bcl2l1* gene expression may depend on JNK. Indeed, I found that involution caused increased expression of *Bcl2l1* mRNA in the mammary glands of JNK^{WT} mice during involution and that this response was suppressed in JNK^{KO} mice (Figure III.15A,C). The increased expression of *Bik* detected in JNK^{WT} mice was also suppressed in JNK^{KO} mice (Figure III.15A,B,D). In contrast, expression of the pro-apoptotic BH3-only genes *Bad*, *Bbc3*, *Bid*, *Bmf*, *Bnip3*, *Bnip3l*, and *Pmaip1* was similar in the involuting mammary glands of JNK^{KO} and JNK^{WT} mice (Figures III.15A & III.16).

Collectively, these data demonstrate that the delayed involution defect in JNK-deficient mice is associated with dysregulation of the gene expression program that promotes involution.

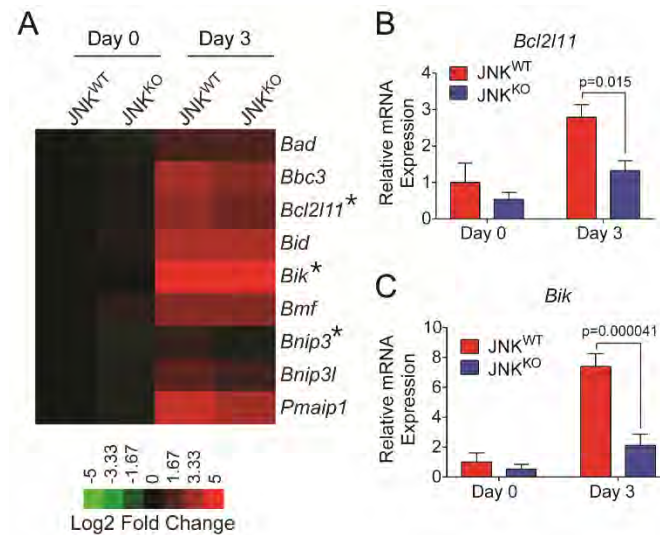


Figure III.15. JNK-deficiency suppresses the expression of pro-apoptotic BH3-only genes.

(A) Heatmap representation of RNA-seq data showing pro-apoptotic BH3-only gene expression. Asterisks denote genes that are differentially expressed ($q < 0.05$) between JNK^{WT} and JNK^{KO} mammary glands on involution day 3 (mean; $n = 3$ JNK^{WT} and $n = 3$ JNK^{KO} mice for each condition).

(B-D) Quantitative RT-PCR was performed on RNA isolated from mammary glands on involution day 0 and day 3. The relative expression of *Bcl2l1* (B) and *Bik* (C) mRNA was measured using Taqman® assays (mean \pm SEM; JNK^{WT} 0 days $n = 6$ mice, JNK^{WT} 3 days $n = 8$ mice, JNK^{KO} 0 days $n = 6$ mice, JNK^{KO} 3 days $n = 6$ mice).

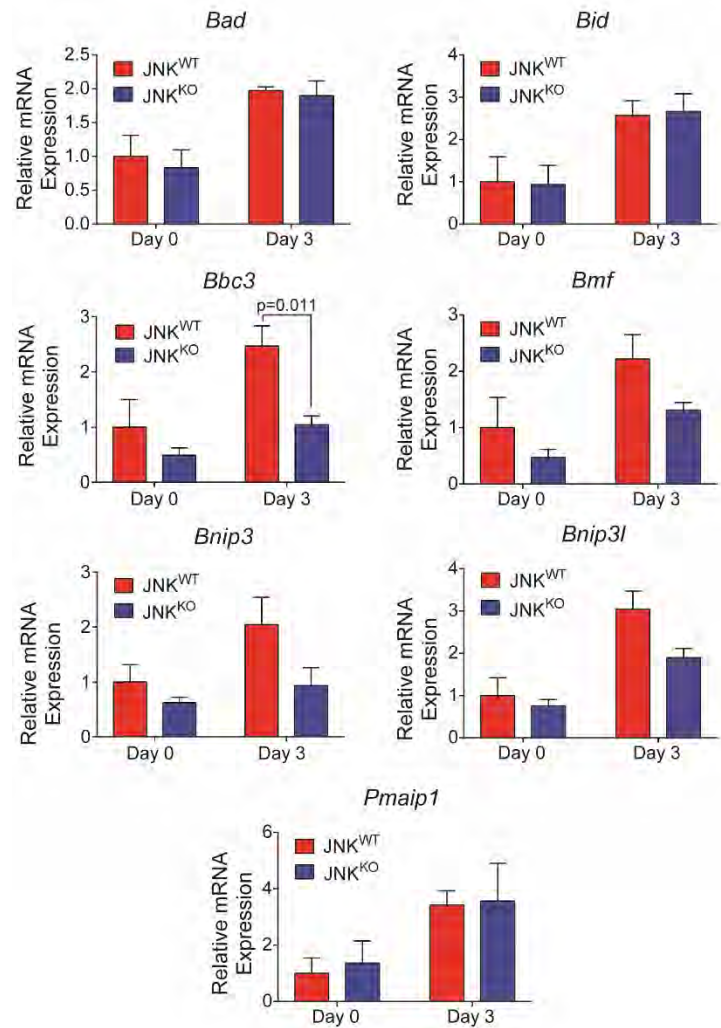


Figure III.16. Mammary gland expression of BH3-only genes.

Quantitative RT-PCR was performed on RNA isolated from mammary glands on involution day 0 and day 3. The relative expression of *Bad*, *Bbc3*, *Bid*, *Bmf*, *Bnip3*, *Bnip3l*, and *Pmaip* mRNA was measured using Taqman[®] assays (mean \pm SEM; JNK^{WT} 0 days n = 6, JNK^{WT} 3 days n = 8, JNK^{KO} 0 days n = 6, JNK^{KO} 3 days n = 6 mice).

Discussion

Weaning initiates the process of mammary gland involution that causes collapse of the epithelial cell compartment and its replacement by adipose tissue. Here I demonstrate that the JNK signaling pathway plays a key role in the involution response. This program of mammary gland remodeling involves differential expression of 10,385 genes (Figure III.10). I show that 26% of this gene expression program requires JNK (Figure III.10).

Previous studies have demonstrated that involution is associated with activation of JNK (Marti et al. 1999) and increased AP1 transcription factor activity (Jaggi et al. 1996; Marti et al. 1999). My analysis shows that JNK deficiency in the mammary epithelium suppresses the involution response mediated by increased expression of *Atf3*, *Fosl2*, *Jun*, and *Jund* (Figure III.9). Indeed, approximately 35% of JNK-regulated gene expression during involution is associated with the presence of AP1 binding sites (Figure III.12). These data confirm that the JNK/AP1 signaling axis plays an important role during involution (Jaggi et al. 1996; Marti et al. 1999). However, the remaining 65% of JNK-regulated expression during involution is not associated with genes in close proximity to AP1 binding sites. Some of this JNK-mediated regulation may be caused by AP1 binding to sites localized to distant enhancer elements, but there may also be roles for other JNK-regulated transcription factors (Davis 2000). It is also possible that some JNK-dependent gene expression may represent a consequence of a delayed involution response.

Examples of genes that may be directly targeted by JNK signaling during involution include matrix metalloproteases (Figure III.13) that are regulated by AP1, including JUN (Chakraborti et al. 2003; Yan and Boyd 2007), and are implicated in both epithelial cell death (Talhouk et al. 1991) and adipocyte repopulation (Alexander et al. 2001) during involution. Indeed, JNK-regulated *Mmp* expression may contribute to epithelial cell detachment during involution. A second example is represented by *Ctsb* and *Ctsl* which encode Cathepsins that promote lysosomal cell death during involution and are targeted by AP1 (Figures III.10 & III.12). A third example is represented by pro-apoptotic BH3-only members of the BCL2 family (Figure III.15) that can promote epithelial cell apoptosis during involution, including *Bcl2l1* that is required for normal involution (Sakamoto et al. 2016; Schuler et al. 2016) and is a JNK/AP1 target gene (Whitfield et al. 2001; Biswas et al. 2007; Girnius and Davis 2017b). Defects in the expression of these genes most likely contribute to the delayed involution observed in mice with JNK deficiency in the mammary epithelium (Figure III.2).

It is established that STAT3 is a key driver of the involution response (Li et al. 1997). Interestingly, STAT3 target genes that are required for cell death during involution, including *Ctsb* and *Bcl2l1*, are also targets of AP1 transcription factors. For example, the *Bcl2l1* promoter binds both STAT3 (Sakamoto et al. 2016) and AP1 (Whitfield et al. 2001; Biswas et al. 2007; Girnius and Davis 2017b) at independent sites. The combinatorial actions of

these transcription factors on the same promoter may lead to a synergistic increase in gene expression. This mechanism would account for the non-redundant functions of STAT3 and JNK/AP1 in the expression of these involution-related genes.

The discovery that JNK plays a major role in mammary gland involution suggests that other members of the MAP kinase group of signaling proteins may also contribute to involution. Indeed, the ERK pathway is activated during early involution and may contribute to mammary gland remodeling (Zhao et al. 2002). For example, STAT3, a master regulator of involution, is phosphorylated and inhibited by ERK (Chung et al. 1997). Moreover, the BH3-only protein BIM is required for involution (Schuler et al. 2016) and is down-regulated by ERK-mediated phosphorylation and ubiquitin-mediated degradation (Ley et al. 2003; Hubner et al. 2008). Studies to test whether the ERK pathway contributes to involution are therefore warranted.

The p38 MAP kinases represent another group of MAP kinases that is implicated in involution (Avivar-Valderas et al. 2014). It is established that p38 α MAP kinase plays a key role in luminal mammary epithelial cell fate by regulating RUNX1 expression in progenitor cells (Del Barco Barrantes et al. 2017). The p38 MAP kinase pathway therefore plays an important role in mammary gland development. Moreover, p38 MAP kinase promotes epithelial cell anoikis and clearance of occluded mammary gland ducts by increasing the expression of the BH3-only protein BIM (Wen et al. 2011). Since BIM is required for normal

mammary gland remodeling during involution (Schuler et al. 2016), it is therefore possible that p38 MAP kinase contributes to the involution response. This prediction remains to be tested.

It is interesting that there are functional similarities between the JNK and p38 MAP kinases in mammary epithelial cells. For example, both p38 MAP kinase (Wen et al. 2011) and JNK (Girnius and Davis 2017b) can promote mammary epithelial cell anoikis by increasing the expression of BIM by an AP1 transcription factor-dependent mechanism. It is likely that the non-redundant functions of p38 MAP kinase and JNK are mediated by different repertoires of AP1-related transcription factors. For example, ATF2 is preferentially phosphorylated and activated by p38 MAP kinase while JUN is phosphorylated by JNK in mammary epithelial cells (Avivar-Valderas et al. 2014). Moreover, JNK is required for the expression of the AP1-related transcription factors ATF3, FOSL2, JUN, and JUND during involution (Figure III.9). It is likely that p38 MAP kinase leads to the activation of a different group of AP1-related transcription factors. JNK and p38 MAP kinase may therefore act in a non-redundant manner to regulate AP1-dependent gene expression. These separate signaling functions of p38 MAP kinase and JNK can lead to different pathological consequences; for example, p38 MAP kinase increases (Del Barco Barrantes et al. 2017) and JNK decreases (Cellurale et al. 2012) mammary tumor development.

In summary, I show that JNK promotes mammary gland involution by a mechanism that is independent of changes in STAT3/5 or SMAD2/3

phosphorylation. Loss of JNK signaling causes delayed involution, reduced expression of AP1 transcription factors, and dysregulation of gene expression. Collectively, my analysis identifies JNK as a key signaling pathway that promotes mammary gland involution.

Materials and Methods

Mice

Mapk8^{LoxP/LoxP} mice and *Mapk9*^{LoxP/LoxP} mice have been previously described (Das et al. 2007; Han et al. 2013). B6.129(Cg)-Gt(ROSA)26Sor^{tm4}(ACTB-tdTomato,-EGFP)^{Lu0}/J mice (Muzumdar et al. 2007) (RRID:IMSR_JAX:007676) and B6.Cg-Tg(Wap-cre)11738Mam/JK^{nu} mice (Wagner et al. 1997) (RRID:IMSR_JAX:008735) were purchased from Jackson Laboratories. Female mice were bred at age 10-12 wks. Mammary glands from single-parous females were harvested at 0, 3, 7, and 14 days after forced weaning following 9 days of lactation. The mice were housed in a specific pathogen-free facility accredited by the American Association of Laboratory Animal Care (AALAC). The animal studies were approved by the Institutional Animal Care and Use Committee at the University of Massachusetts Medical School.

Genomic DNA analysis

The polymerase chain reaction (PCR) amplimers 5'-CTCTGCTGCCTCCTGGCTTCT-3', 5'-CGAGGCGGATCACAAGCAATA-3' and 5'-TCAATGGGCGGGGGTCGTT-3' were used to detect presence of the *mTmG* (250 bp) and WT alleles (330 bp). The amplimers 5'-TTACTGACCGTACACCAAATTTGCCTGC-3' and 5'-CCTGGCAGCGATCGCTATTTTCCATGAGTG-3' were used to detect the *Cre*⁺ allele (450 bp). The amplimers 5'-AGGATTTATGCCCTCTGCTTGTC-3' and 5'-

GACCACTGTTCCAATTTCCATCC-3' were used to detect the *Mapk8*⁺ (540 bp) and *Mapk8*^{LoxP} (330 bp) alleles. The amplimers 5'-GTTTTGTAAAGGGAGCCGAC-3' and 5'-CCTGACTACTGAGCCTGGTTTCTC-3' were used to detect the *Mapk9*⁺ (224 bp) and *Mapk9*^{LoxP} alleles (264 bp). The amplimers 5'-CCTCAGGAAGAAAGGGCTTATTTC-3' and 5'-GAACCACTGTTCCAATTTCCATCC-3' were used to detect the *Mapk8*⁺ (1550 bp), *Mapk8*^{LoxP} (1,095 bp), and the *Mapk8*^Δ alleles (395 bp). The amplimers 5'-GGAATGTTTGGTCCTTTAG-3', 5'-GCTATTCAGAGTTAAGTG-3', and 5'-TTCATTCTAAGCTCAGACTC-3' were used to detect the *Mapk9*^{LoxP} (560 bp) and *Mapk9*^Δ alleles (400 bp).

Mammary Gland Analysis

Female mice were euthanized and mammary glands #2-5 were harvested, fixed in 10% formalin, dehydrated, and embedded in paraffin. Sections (5 μm) were cut and stained with hematoxylin and eosin (H&E) for analysis. Additional sections of #4 glands were stained with antibodies against cleaved-caspase-3 (1:100; Cell Signaling Technology Cat# 9662 RRID:AB_331439), phospho-STAT3 (1:400; Cell Signaling Technology Cat# 9145 RRID:AB_2491009), phospho-STAT5 (1:50; Abcam Cat# ab32364 RRID:AB_778105), phospho-SMAD2/3 (1:200; Santa Cruz Biotechnology Cat# sc-11769-R), smooth muscle actin (Millipore Sigma Cat# A2547, RRID:AB_476701; 1:100 dilution), keratin 5 (BioLegend Cat# 905501 RRID:AB_2565050; 1:50 dilution), keratin 8 (DSHB

Cat# TROMA-I RRID:AB_531826; 1:100 dilution), and GFP (Thermo Fisher Cat# A21311 RRID:AB_221477). Immunohistochemistry was performed using a biotinylated goat anti-IgG antibody (Biogenex Cat# HK340-5K) plus streptavidin-conjugated horseradish peroxidase (Vector Laboratories Cat# PK-6100) and 3,3'-diaminobenzidine (Vector Laboratories Cat# SK-4100). Sections were counterstained with hematoxylin (Thermo Fisher). Images were acquired using a Zeiss Axiovert microscope. Immunofluorescence was performed using AlexaFluor 546 conjugated-goat anti-rabbit IgG (H+L) antibody (Thermo Fisher Cat# A11035 RRID:AB_143051), AlexaFluor 488 conjugated-goat anti-rabbit IgG (H+L) antibody (Thermo Fisher Cat# A-11008 RRID:AB_143165), AlexaFluor 633 conjugated-goat anti-mouse IgG (H+L) antibody (Thermo Fisher Cat# A-21052, RRID:AB_141459), AlexaFluor 633 conjugated-goat anti-rat IgG (H+L) antibody (Thermo Fisher Cat# A-21094, RRID:AB_141553), or AlexaFluor 488 conjugated-goat anti-rat IgG (H+L) antibody (Thermo Fisher Cat# A11006 RRID:AB_141373), and counterstained with 2-(4-amidinophenyl)-1H-indole-6-carboxamide (DAPI). TUNEL staining was performed following the manufacturer's recommendations (Sigma Cat# 11684795910). Fluorescence images were acquired using a Leica SP2 confocal microscope.

Immunofluorescence staining of phospho-STAT3 was quantitated using ImageJ (Schneider et al. 2012) on 10-15 images per mouse; the amount of phospho-STAT3 was normalized to keratin 8 or DAPI fluorescence and the mean value per mouse was calculated. Sections were examined in a blinded fashion for

days 0, 3, 7 and 14 of involution. However, the marked histological differences on involution day 3 prevented blinded analyses.

Immunoblot Analysis

Tissue lysates from #2-3 glands were prepared using Triton lysis buffer (20 mM Tris [pH 7.4], 1% Triton X-100, 10% glycerol, 137 mM NaCl, 2 mM EDTA, 25 mM β -glycerophosphate, 1 mM sodium orthovanadate, 1 mM phenylmethylsulfonyl fluoride, and 10 μ g/mL of aprotinin plus leupeptin). Extracts (30 μ g) were subjected to immunoblot analysis with antibodies to STAT3 (Cell Signaling Technology Cat# 9139 RRID:AB_331757; dilution 1:1000), phospho-STAT3 (Cell Signaling Technology, Cat# 9145 RRID:AB_2491009; dilution 1:2000), and α Tubulin (Sigma-Aldrich Cat# T5168; RRID:AB_477579). IRDye 680LT conjugated-donkey anti-mouse IgG antibody (LI-COR Biosciences Cat# 926-68022 RRID:AB_10715072) and IRDye 800CW conjugated-goat anti-rabbit IgG (LI-COR Biosciences Cat# 926-32211 RRID:AB_621843) were used to detect immune complexes, and these were quantitated using the Odyssey infrared imaging system (LI-COR Biosciences).

Mammary epithelial cell isolation

Mammary epithelial cells were isolated as previously described (Kittrell et al. 1992; Novaro et al. 2003) with minor modifications (Cellurale et al. 2012). Briefly, lymph nodes were removed and whole mammary glands were placed in

DMEM/F12 supplemented with penicillin/streptomycin and nystatin. The glands were washed once in PBS before being minced and placed in DMEM/F12 containing 0.2% trypsin, 0.2% collagenase A, 5% fetal calf serum, and 5µg/ml gentamicin (2 h) on a rotator at 37°C. Cells and organoids were pelleted by centrifugation at 1,500 rpm (10 min). The fatty layer was transferred to a second tube and dispersed with pipetting while the pellet was resuspended in DMEM/F12. The pellet and fatty layer were centrifuged again at 1,500 rpm (10 min) and combined in one tube prior to incubation (2~5 mins at 25°C with shaking) in DMEM/F12 supplemented with 10 µg/ml DNase I. The cells were centrifuged at 1,500 rpm (10 min) and resuspended in 10 ml of DMEM/F12. The epithelial cells and organoids were briefly (0.2 min) centrifuged at 1,500 rpm 6-7 times and resuspended in fresh DMEM/F12 to wash out fibroblasts.

RT-PCR analysis

The expression of *Bad* (Mm00432042_m1), *Bbc3* (Mm00519268_m1), *Bcl2l11* (Mm00437797_m1), *Bmf* (Mm00506773_m1), *Bid* (Mm00432073_m1), *Bik* (Mm00476123_m1), *Bnip3* (Mm01275601_g1), *Bnip3l* (Mm00786306_s1), and *Pmaip1* (Mm00451763_m1) mRNA and *18S* RNA (4308329) was measured using TaqMan® assays using QuantStudio 12K Flex machine (Thermo Fisher). The amount of mRNA was normalized to the amount of *18S* detected in the same sample.

RNA-seq analysis

Mammary glands #2-5 were flash frozen in liquid nitrogen and RNA was isolated using the RNeasy kit with DNase treatment (Qiagen). RNA quality (RIN>8) was confirmed using a Bioanalyzer 2100 (Agilent Technologies). Libraries were constructed according to the manufacturer's instructions using the NeoPrep kit (Illumina). Paired-end RNA sequencing with reads (40 bp) were performed using a NextSeq500 (Illumina). Three independent libraries were analyzed for each condition. These RNA-seq data were deposited in the Gene Expression Omnibus (GEO) database with accession number GSE89495. FastQC (version 0.10.1) (Andrews 2010) was used to generate sequence quality reports. Poor quality reads, adapter sequence and reads less than 20 bp were removed using Trimmomatic (version 0.36) (Bolger et al. 2014). The pre-processed Illumina paired-end Fastq datasets were aligned to the mouse reference genome (Ensembl GRCm38). Alignment was performed using Bowtie2 (v 2.2.1.0) (Langmead and Salzberg 2012) and Tophat2 (v 2.0.14) (Kim et al. 2013). Samtools (version 0.0.19) (Li et al. 2009) and IGV (version 2.3.60) (Thorvaldsdottir et al. 2013) were used for indexing the alignment files and viewing the aligned reads respectively. Gene expression was quantitated as fragments per kilobase of exon model per million mapped fragments (FPKM) using Cufflinks (v 2.2.1) (Trapnell et al. 2010; Trapnell et al. 2012) and differential expression was identified using the Cuffmerge and Cuffdiff tools. The library normalization method used for Cuffdiff was set to "classic-fpkm" and the

dispersion method was set to “per-condition”. Cummebund (version 2.4.1) (Trapnell et al. 2012) was used to assess replicate concordance between sample groups. Gene set enrichment analysis was performed using differentially expressed gene lists with the WEB-based GENE SeT AnaLysis Toolkit (Webgestalt) (Wang et al. 2013) by selecting the KEGG database and viewing the 10 pathways with lowest p_{adj} -value.

Clustering analysis

The complex heatmap package (version 1.12.0) (Gu et al. 2016) was used to cluster RNA-seq data (Figure III.10C). The “clustering distance rows” parameter was set to “maximum”; the “clustering method rows parameter” was set to “ward.D”. Genes were included in the clustering analysis if they were differentially expressed ($\log_2|\text{Fold Change}| > 1$; $q < 0.01$) between one or more pairwise group comparisons. Over 12,000 genes together with the gene expression levels were examined by k-means ($k=4$) clustering.

Enrichment analysis

I used RNA-seq data (Figure 5) and Mouse ENCODE ChIPSeq datasets (Mouse et al. 2012) (accession numbers GSM912901 and GSM912902) to evaluate the overlap between genes that were non-differentially expressed or differentially expressed between JNK^{WT} and JNK^{KO} on involution day 3 (Figure III.10C), and genes that bind the transcription factors cJUN and JUND. Peaks that passed the

irreproducible discovery rate at a threshold of 2% were selected from the ENCODE project. The Mouse ENCODE ChIPSeq bed files with mm10 coordinates were entered as input into PAVIS (Huang et al. 2013) and the nearest genes to the peaks from the ChIPSeq data were annotated. The “genome assembly” and the “gene set” were set to “Ensembl GRCm38” and “mm10 all genes” respectively. The upstream distance from the transcription start site and the downstream distance from the transcript termination site were each set to 20,000 bp. The intersections between the differentially expressed genes (identified by RNA-seq analysis (Figure III.10C)) and the genes that bind the transcription factors JUN and JUND (identified using ENCODE ChIP-seq data) were identified using Interactivenn (<http://www.interactivenn.net/>) (Heberle et al. 2015). Statistical significance between two groups was determined by Pearson’s Chi-squared test.

Statistical Analysis

Data are presented as the mean and standard error. Statistical analysis was performed using GraphPad Prism version 7 (GraphPad Software, La Jolla). ANOVA with Bonferroni’s test was used to determine significance with an assumed confidence interval of 95%. The significance of pair-wise comparisons was determined using Students T-test ($p < 0.05$). The false discovery rate (q value) was obtained by applying the Benjamini-Hochberg method to the p-value.

CHAPTER IV

THE cJUN NH₂-TERMINAL KINASE (JNK) SIGNALING PATHWAY PREVENTS BREAST CANCER INITIATION

Abstract

Breast cancer is the most commonly diagnosed malignancy in women. Analysis of breast cancer genomic DNA indicates frequent *loss-of-function* mutations in components of the cJUN NH₂-terminal kinase (JNK) signaling pathway. Since JNK signaling can promote cell proliferation by activating the AP1 transcription factor, this apparent association of reduced JNK signaling with tumor development is unexpected. I examined the effect of JNK deficiency in the murine breast epithelium. Loss of JNK signaling was sufficient for genomic alterations and the development of breast cancer. Moreover, JNK deficiency rapidly accelerated tumorigenesis in a murine model of breast cancer. This tumor suppressive function was not mediated by a role of JNK in the growth of established tumors, but by a requirement of JNK to prevent tumor initiation. Together, these data identify JNK pathway defects as “driver” mutations that promote the acquisition of mutations and tumor initiation.

Introduction

Breast cancer is the most frequently diagnosed tumor in women (Siegel et al. 2015). The etiology of breast cancer has been studied in detail, but the causes of breast cancer remain incompletely understood. Nevertheless, it is established that familial breast cancers result from germ-line mutations that increase the risk of cancer development (Afghahi and Kurian 2017). Examples of inherited mutations that can cause breast cancer predisposition include *ATM*, *BRCA1/2*, *CDH1*, *CHEK2*, *NBN*, and *TP53*. Moreover, sporadic mutation of these and other genes promote the development of non-familial breast cancer (Hanahan and Weinberg 2011). Changes in the tumor genome are therefore important for breast cancer development (Hanahan and Weinberg 2011).

Recent advances in breast cancer genome analysis have led to significant progress towards the identification of sporadic mutations in breast cancer (Kan et al. 2010; Cancer Genome Atlas 2012; Ellis et al. 2012; Shah et al. 2012; Stephens et al. 2012; Wang et al. 2014; Ciriello et al. 2015; Nik-Zainal et al. 2016b). These genetic changes include “driver” mutations that promote tumor development and “passenger” mutations that do not functionally contribute to the tumor phenotype. Genes mutated in familial cancer syndromes constitute a prime example of “driver” mutations that can contribute to cancer development. The presence of “passenger” mutations complicates the analysis of cancer genomes for the development of targeted tumor therapy. For example, some “driver” mutations cause genetic instability (e.g. *ATM*, *BRCA1/2*, *CHEK2*, *NBN* and

TP53) that can result in the accumulation of additional mutations in developing tumors.

Computational methods have been employed to distinguish “driver” and “passenger” mutations based on mutation frequency (Parmigiani et al. 2009), gene function in pathways (Lin et al. 2007; Wendl et al. 2011), level of gene expression (Berger et al. 2016) and predictions based on gene function (Kaminker et al. 2007; Carter et al. 2009; Youn and Simon 2011) and protein interactions (Cerami et al. 2010; Babaei et al. 2013). These computational approaches to identify “driver” mutations have been complemented by functional siRNA screens on breast tumor cell lines (Sanchez-Garcia et al. 2014; Marcotte et al. 2016). Collectively, these approaches have led to the identification of “driver” mutations in human cancer, but it is likely that many more “driver” mutations remain to be discovered (Garraway and Lander 2013).

Examples of “driver” mutations in breast cancer include the *TP53*, *PIK3CA*, and *PTEN* genes. Mutational inactivation of *PTEN* or activation of *PI3K* increases AKT / mTOR signaling that promotes growth, proliferation, and survival (Yuan and Cantley 2008), while mutation of *TP53* promotes cell survival and proliferation (Vousden and Prives 2009). The appreciation of the importance of these pathways in cancer has spurred research into potential therapies (Yuan and Cantley 2008; Vousden and Prives 2009). These well-established “driver” mutations contribute to the etiology of breast cancer. In contrast, the role of some other highly mutated genes in breast cancer is unclear.

One frequently mutated pathway in breast cancer is the cJUN NH₂-terminal kinase (JNK) pathway (Garraway and Lander 2013). The JNK pathway is a three-tiered cascade that includes a MAP kinase kinase kinase (MAP3K) that phosphorylates and activates MAP kinase kinases (MAP2K) that, in turn, phosphorylate and activate JNK (Davis 2000). This pathway requires two MAP2K isoforms that co-operate to activate JNK by phosphorylation on tyrosine (by MAP2K4) and threonine (by MAP2K7) (Tournier et al. 2001). The sequencing of breast tumor genomic DNA has revealed mutations in genes that encode members of this pathway, including *MAP3K1*, *MAP2K4*, and *MAP2K7* (Kan et al. 2010; Banerji et al. 2012; Cancer Genome Atlas 2012; Ellis et al. 2012; Shah et al. 2012; Stephens et al. 2012; Wang et al. 2014; Ciriello et al. 2015; Nik-Zainal et al. 2016b). The genetic changes include frequent deletion of the gene locus and mutations that cause protein truncation and loss of protein kinase activity. This analysis suggests that breast cancer is associated with loss of JNK signaling. Indeed, since AKT phosphorylates and inactivates MAP2K4 (Park et al. 2002), breast cancer “driver” mutations that activate AKT (e.g. *PTEN* and *PI3K*) also cause loss of JNK signaling. The JNK signaling pathway may therefore be suppressed in many breast cancers.

The association of breast cancer with reduced JNK signaling represents a correlation. What is the significance of *loss-of-function* JNK pathway mutations? Are these “driver” or “passenger” mutations? The purpose of this study was to test the role of JNK signaling in breast cancer development. I found that loss of

JNK signaling was sufficient for breast cancer development in a mouse model with JNK deficiency in mammary epithelial cells. Furthermore, JNK deficiency accelerated tumor formation in a murine model of breast cancer. I conclude that the frequent *loss-of-function* JNK pathway mutations in breast tumors represent “driver” mutations that promote breast cancer development. This finding presents opportunities for therapeutic intervention in patients with breast cancer.

Results

Disruption of JNK signaling is sufficient for breast cancer development

Loss-of-function mutations in the JNK signaling pathway (e.g. *MAP3K1*, *MAP2K4*, and *MAP2K7*) are implicated in the etiology of breast cancer (Kan et al. 2010; Banerji et al. 2012; Cancer Genome Atlas 2012; Ellis et al. 2012; Shah et al. 2012; Stephens et al. 2012; Wang et al. 2014; Ciriello et al. 2015; Nik-Zainal et al. 2016b). These potential “driver” mutations in breast cancer cause disruption of JNK signaling. To test whether JNK pathway disruption influences breast cancer development, I examined the effect of JNK-deficiency in the mammary epithelium. The JNK1 (encoded by *Mapk8*) and JNK2 (encoded by *Mapk9*) isoforms exhibit partially redundant functions (Davis 2000). I therefore examined compound JNK deficiency in the mammary epithelium using control (ME^{WT}) mice (*Mapk8*^{LoxP/LoxP} *Mapk9*^{LoxP/LoxP}) and JNK-deficient (ME^{KO}) mice (*Wap-Cre*^{-/+} *Mapk8*^{LoxP/LoxP} *Mapk9*^{LoxP/LoxP}). Lactation induces *Wap-Cre* expression (Wagner et al. 1997). Studies using *Rosa26*^{mTmG+/-} female reporter mice demonstrated *Cre*-mediated recombination in keratin 8 (CK8) positive luminal epithelial cells (Figure IV.1A), but not in keratin 5 (CK5) positive myoepithelial cells (Figure IV.1B).

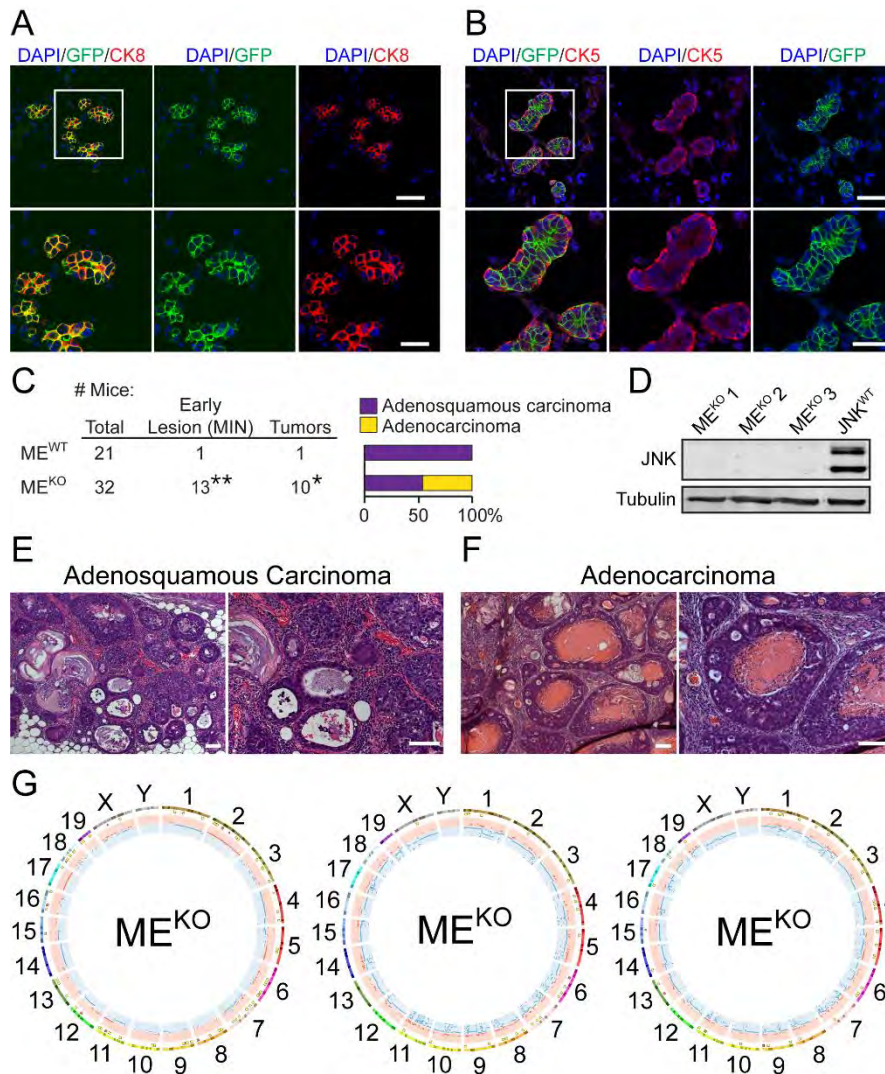


Figure IV.1. JNK deficiency in mammary epithelial cells is sufficient for tumor formation and the acquisition of mutations.

A, B) Mammary gland tissue sections were prepared from parous *Wap-Cre^{+/-} Rosa26^{mTmG^{+/-}}* female mice (n=6). These sections were stained with antibodies to keratin 8 (CK8, red (A)) or keratin 5 (CK5, red (B)), and GFP (green), and counterstained with DAPI (blue). Representative images are presented (*upper panel*, scale bar=48 μ M). Boxed area was magnified (*lower panel*, scale bar=24 μ M).

C) Summary of the study cohort showing the total number of *Mapk8^{LoxP/LoxP} Mapk9^{LoxP/LoxP}* (ME^{WT}) and *Wap-Cre^{+/-} Mapk8^{LoxP/LoxP} Mapk9^{LoxP/LoxP}* (ME^{KO}) mice examined, the number of mice exhibiting mammary intraepithelial neoplasia (MIN) or tumors (*p<0.05, **p<0.01, Fisher's exact test) (*left panel*). The type of carcinoma is presented (*right panel*).

D) Extracts prepared from ME^{KO} and *Wap-Cre*^{+/-} *Trp53*^{LoxP/LoxP} (JNK^{WT}) tumor cells were subjected to immunoblot analysis using antibodies to JNK and α -Tubulin.

E, F) Representative hematoxylin and eosin (H&E) -stained sections of adenosquamous carcinomas (E) and adenocarcinomas (F) from ME^{KO} females are presented. Scale bar=100 μ m.

G) Exome sequencing was performed on ME^{KO} tumor cell lines (n=3). Mammary tissue from a virgin female of the same genotype (*WapCre*^{+/-} *Mapk8*^{LoxP/LoxP} *Mapk9*^{LoxP/LoxP}) was used as the reference genome. Circos plots showing copy number variations (CNVs) in ME^{KO} tumor cells are presented. The outermost ring shows chromosome ideograms. The next track indicates high (red) and moderate (yellow) impact single nucleotide variants and indels marked by rectangles and triangles, respectively. The innermost track shows chromosome amplifications and deletions, with red and blue lines indicating chromosomal fragments present at $\log_2(\text{ratio Tumor/Normal}) > 0.2$ or $\log_2(\text{ratio Tumor/Normal}) < -0.2$, respectively.

I examined ME^{WT} and ME^{KO} female mice to determine whether JNK deficiency is sufficient for breast tumor development. Studies of a cohort of 21 control ME^{WT} mice identified one palpable breast tumor (adenosquamous carcinoma) in a 78 wk old mouse (Figure IV.1C). In addition, mammary intraepithelial neoplasia (MIN) was detected in one ME^{WT} mouse during microscopic analysis of tissue sections following necropsy. In contrast, the incidence of MIN lesions (41% of mice; $p < 0.01$; Fisher's Exact Test) and palpable breast tumors (31% of mice, median age 80 wk; $p < 0.05$; Fisher's Exact Test) in ME^{KO} mice was significantly greater than ME^{WT} mice (Figure IV.1C). Immunoblot analysis confirmed that the ME^{KO} tumor cells do not express JNK proteins (Figure IV.1D). These data indicate that JNK deficiency is sufficient to promote breast tumor development.

Microscopic analysis of tumor sections demonstrated the presence of adenosquamous carcinoma in ME^{WT} mice, but both adenocarcinoma and adenosquamous carcinoma were detected in ME^{KO} mice (Figure IV.1C,E,F). The adenocarcinomas were primarily CK8 positive and variably expressed estrogen receptor (ER) and progesterone receptor (PR), while the adenosquamous carcinomas expressed CK5 and did not express ER (Figure IV.2A, B). CK8 expression by ME^{KO} adenocarcinomas is consistent with both a luminal epithelial cell origin and the expression of *Wap-Cre* in luminal epithelial cells (Figure IV.1A,B). In contrast, CK5 expression by the ME^{KO} adenosquamous carcinomas

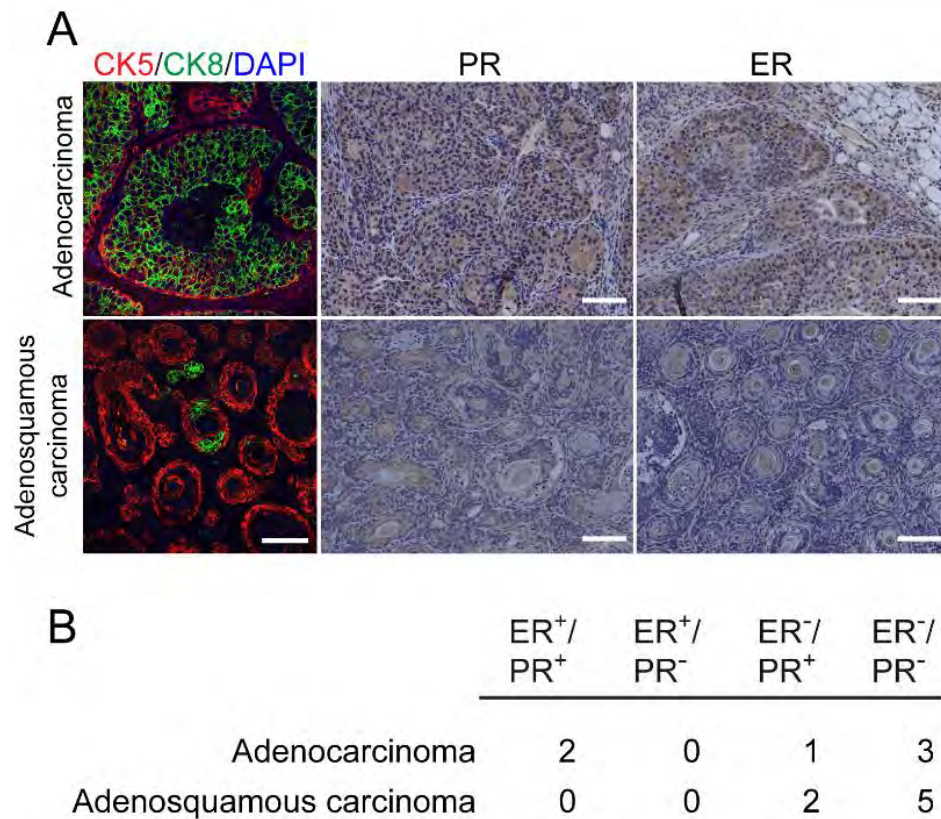


Figure IV.2. Expression of estrogen and progesterone receptors in breast tumors caused by JNK deficiency in the mammary epithelium.

A, B) Representative adenocarcinoma (*upper panel*) and adenosquamous carcinoma (*lower panel*) sections stained for progesterone receptor (PR), estrogen receptor (ER) (Scale bar=100 μ m), and cytokeratin 8 (CK8, green) and cytokeratin 5 (CK5) (Scale bar=50 μ m) are presented (A). Sections were counter-stained with hematoxylin or DAPI. Adenocarcinomas (AC) and adenosquamous carcinomas (ASC) were scored for hormone receptor positivity (B).

suggests that these tumor cells partially differentiate to express a marker of myoepithelial cells.

JNK deficiency impairs genome maintenance and alters gene expression

The JNK pathway has been implicated in genome maintenance (Lu et al. 2006; Van Meter et al. 2016; Calses et al. 2017). To test whether JNK deficiency caused defects in genome stability, I examined the exome sequences of three independent ME^{KO} breast tumor cell lines (Figures IV.1D & IV.3A). This analysis demonstrated single nucleotide variants (SNVs) and short insertions / deletions (Indels) (Figure IV.1G), including SNVs and Indels that resulted in frame shifts and truncations within gene coding regions (Figure IV.3B,C). Moreover, many chromosome segment amplifications and deletions (copy number variations, CNVs) were detected (Figure IV.1G). These data demonstrate that JNK signaling promotes genome maintenance.

A

Biological Group	Project ID	Sample ID	Mean SNVs	Mean Indels
JNK ^{WT} (2)	PRJNA401332	SAMN07602920-1	332	138
Control	PRJNA401332	SAMN07605063		
ME ^{KO} (3)	PRJNA401332	SAMN07602922-4	113	9
Control	PRJNA401332	SAMN07605064		
JNK ^{KO} (6)	PRJNA401332	SAMN07602925-30	193	67
Control	PRJNA401332	SAMN07605065		

B**High Impact SNVs**

JNK ^{WT}	ME ^{KO}	JNK ^{KO}
<i>2210408121Rik</i>	<i>Adcy5</i>	<i>Akr1c13</i>
<i>Alms1</i>	<i>Ctnnb1</i>	<i>Aplf</i>
<i>Apcs</i>	<i>Def8</i>	<i>Brix1</i>
<i>Clu</i>	<i>Gm906</i>	<i>Cep295</i>
<i>Gpr98</i>	<i>Neb</i>	<i>Dennd4a</i>
<i>H1foo</i>	<i>Olfr455</i>	<i>Gc</i>
<i>Heph11</i>	<i>Sptb</i>	<i>Gm10436</i>
<i>Hmcn1</i>	<i>Tex14</i>	<i>Mgst1</i>
<i>Rbm10</i>		<i>Pet2</i>
<i>Robo1</i>		<i>Prickle1</i>
<i>Shroom4</i>		<i>Rapgef4</i>
<i>Sptan1</i>		<i>Socs4</i>
<i>Stam2</i>		<i>Ssbp2</i>
<i>St6galnac1</i>		<i>Zmpste24</i>
<i>Ttc14</i>		
<i>Zfand4</i>		

C**High Impact Indels**

JNK ^{WT}	ME ^{KO}	JNK ^{KO}
<i>Abcc3</i>	<i>Dsccl</i>	<i>Cd300c</i>
<i>Cd300c</i>	<i>Gpr112</i>	<i>Elfn2</i>
<i>Cml3</i>	<i>Olfr1066</i>	<i>Foxr1</i>
<i>Dnajc2</i>	<i>Wac</i>	<i>Gm2056</i>
<i>Fdxr</i>		<i>Gm5039</i>
<i>Tagap</i>		<i>Grin3a</i>
<i>Tagap1</i>		<i>Kcnn3</i>
<i>Ttc14</i>		<i>Mcf2</i>
<i>Zxdc</i>		<i>Mocs2</i>
		<i>Nom1</i>
		<i>Prpf38b</i>
		<i>Ptpdc1</i>
		<i>Tctn3</i>
		<i>Tjap1</i>
		<i>Tlr1</i>
		<i>Vmn1r7</i>
		<i>Vmn1r8</i>
		<i>Zfp709</i>

Figure IV.3. Summary of exome sequence data.

A) The NCBI SRA accession information (Project ID and Sample ID) for the exome sequence data is presented. The mean number of single nucleotide variants (SNVs) and insertions/deletions (Indels) is shown for each tumor genotype. An examination of frequent nucleotide changes revealed that ME^{KO} tumor cells favored G to A (2/3 tumor cell lines) and JNK^{KO} favored C to T (4/6 tumor cell lines) replacements, but no favored replacements were identified in JNK^{WT} tumor cells.

B, C) High impact SNVs (B) and Indels (C) identified in JNK^{WT} (n=2), ME^{KO} (n=3) and JNK^{KO} (n=6) cells. No well-established driver mutations were found among the high impact indels or SNVs identified and there were no recurring mutations within or across genotypes.

I compared gene expression profiles of three independent ME^{KO} tumor-derived cell lines and three independent primary *Wap-Cre*^{-/+} mammary epithelial cell (MEC) preparations. RNA-seq analysis identified 2,218 differentially expressed genes ($q < 0.05$, $|\log_2 \text{Fold Change}| > 0.75$) that formed two clusters (Figure IV.4A). Gene set enrichment analysis (GSEA) using the KEGG database revealed that both clusters were highly enriched for “Pathways in Cancer” (Figure IV.4B). Cluster 1 was also enriched for “Focal Adhesion”, while Cluster 2 was enriched for “Metabolic Pathways” and “p53 Signaling” (Figure IV.4B). As expected, JNK deficiency caused reduced expression of AP1 transcription factors (Ventura et al. 2003) in ME^{KO} tumor cells compared with primary MEC (Figure IV.4C). Ingenuity Pathway Analysis (IPA) identified a significant increase in “WNT/ β -Catenin Pathway” activity (Figure IV.4D). This finding is consistent with the observed enrichment of WNT signaling genes in GSEA (Figure 2B, Cluster 2), including increased expression of *Wnt7b* and *Wnt10a* (Figure IV.4E) and increased expression of the WNT target genes *Axin2*, *Ccnd1*, and *Myc* in ME^{KO} cells compared with MEC (Figure IV.4F). These data suggest that ME^{KO} tumors may exploit the WNT pathway to maintain proliferation.

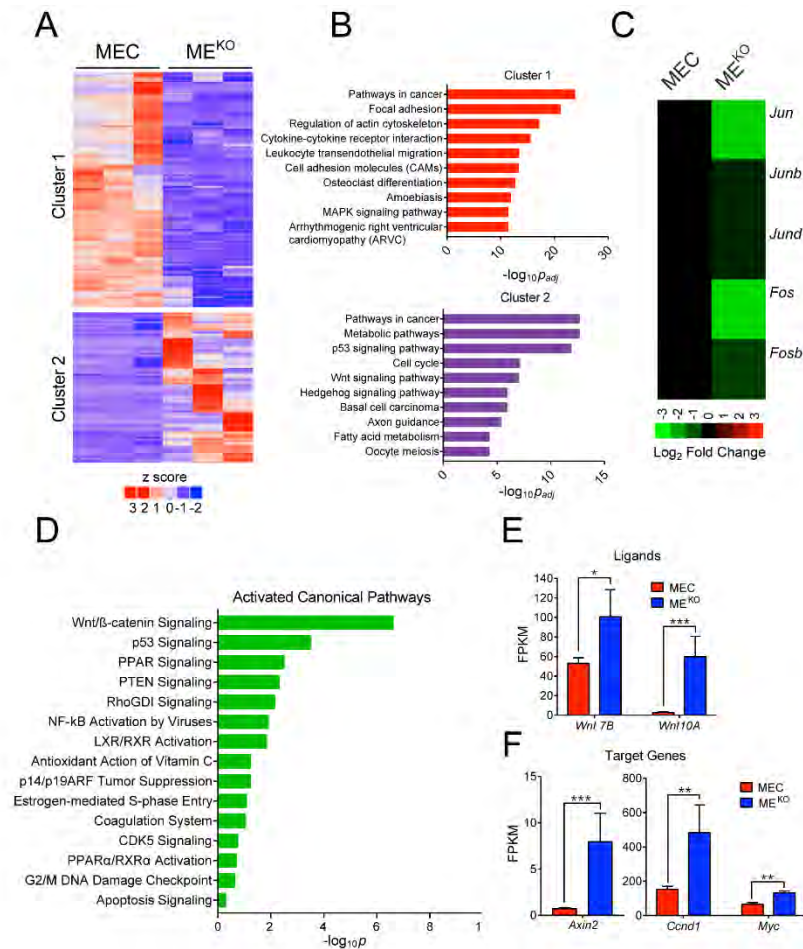


Figure IV.4. JNK deficiency is sufficient to promote tumor-associated gene expression.

A-D RNA-seq analysis was performed using primary mammary epithelial cells (MEC, $n=3$) and ME^{KO} tumor cell lines ($n=3$). K-means clustering was performed on differentially expressed genes and is presented as a heatmap (A). Gene set enrichment analysis using the KEGG database was performed on genes from each of the clusters. The pathways with the 10 lowest p_{adj} values are presented (B). The mean expression *Jun*, *Junb*, *Jund*, *Fos*, and *Fosb* mRNA is presented as a heatmap (C). Ingenuity Pathway analysis of the RNA-seq data was used to predict signaling pathway activity (D).

E *Wnt7b* and *Wnt10a* expression in MEC ($n=3$) and ME^{KO} tumor cells ($n=3$) is presented as the mean fragments per kilobase of exon model per million mapped fragments (FPKM) \pm SEM (* $q < 0.05$, *** $q < 0.001$).

F WNT target gene expression (*Axin2*, *Ccnd1*, and *Myc*) in MEC ($n=3$) and ME^{KO} ($n=3$) cells is presented as FPKM (mean \pm SEM; ** $q < 0.01$, *** $q < 0.001$).

JNK deficiency rapidly accelerates tumor development in a mouse model of breast cancer

The observation that JNK deficiency is sufficient for breast tumorigenesis (Figure IV.1) suggests that defects in JNK signaling may accelerate tumor development in a sensitized genetic background. To test this hypothesis, I examined the genetic interaction between JNK inactivation and loss of TRP53. Since *TP53* is the most frequently mutated gene in human breast cancer, this model is relevant to human disease (Nik-Zainal et al. 2016b).

I established TRP53-deficient (JNK^{WT}) mice (*Wap-Cre*^{-/+} *Trp53*^{LoxP/LoxP}) and TRP53/JNK compound mutant (JNK^{KO}) mice (*Wap-Cre*^{-/+} *Trp53*^{LoxP/LoxP} *Mapk8*^{LoxP/LoxP} *Mapk9*^{LoxP/LoxP}). Loss of JNK on the TRP53 deficient background dramatically accelerated tumor formation (Figure IV.5A). Histological examination of the JNK^{WT} and JNK^{KO} tumors confirmed that the majority of lesions were adenocarcinomas (Figure IV.5B & IV.6A). JNK^{WT} and JNK^{KO} tumors presented with variable ER and PR staining patterns (Figures IV.5C & IV.6B). Moreover, both JNK^{WT} and JNK^{KO} tumor cells primarily expressed the luminal marker CK8, rather than the myoepithelial cell marker CK5, consistent with a luminal epithelial cell origin (Figure IV.5C). Tumor latency did not correlate with parity (Figure IV.7A) and litter sizes were comparable across the genotypes (Figure IV.7B). However, JNK deficiency in the maternal mammary epithelium caused a substantial decrease in pup survival after the first litter (Figures IV.7C).

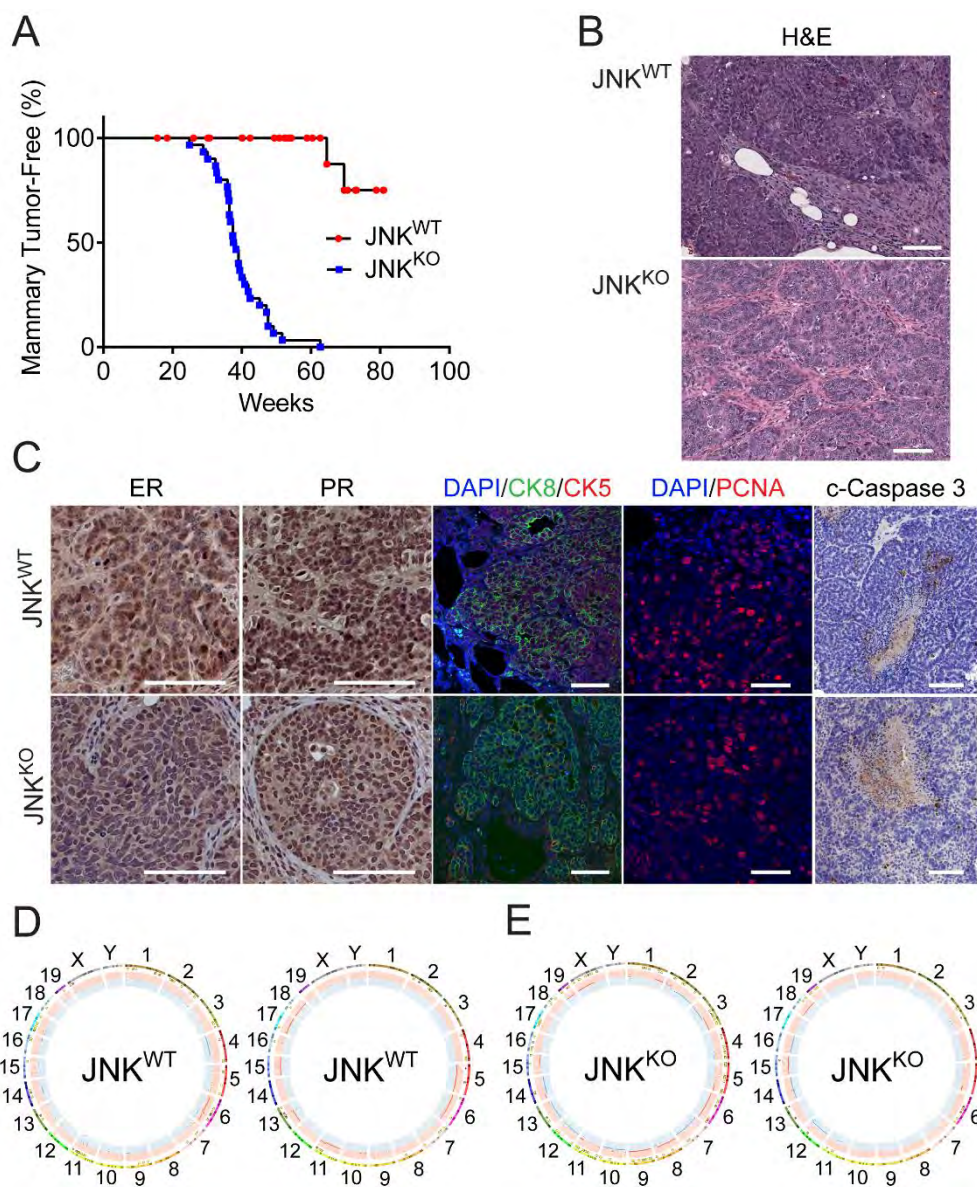


Figure IV.5. JNK deficiency accelerates tumor formation in a mouse model of breast cancer.

A Mammary tumor-free survival was monitored in $Wap-Cre^{-/-} Trp53^{LoxP/LoxP}$ (JNK^{WT}) mice and $Wap-Cre^{-/-} Trp53^{LoxP/LoxP} Mapk8^{LoxP/LoxP} Mapk9^{LoxP/LoxP}$ (JNK^{KO}) mice. Animals euthanized before a palpable mammary tumor had formed were censored in the log-rank analysis ($p < 0.0001$).

B) Tissue sections were prepared from mammary tumors. Representative images of H&E-stained sections from JNK^{WT} (*upper panel*) and JNK^{KO} (*lower panel*) mice are presented. Scale bar=100 μ m.

C) Adenocarcinoma tissue sections from JNK^{WT} mice (*upper panel*) and JNK^{KO} mice (*lower panel*) were stained with antibodies to (from left to right) estrogen receptor (ER), progesterone receptor (PR), keratins 5 (red) and 8 (green) (CK5 and CK8 respectively), PCNA (Scale bars=50 μ m), and cleaved caspase 3 (Scale bar=100 μ m). Immunofluorescent stains were counterstained with DAPI, and peroxidase-based staining was counterstained with hematoxylin.

D, E) Exome sequencing was performed on JNK^{WT} (n=2) and JNK^{KO} (n=6) tumor cell lines. Mammary tissue from a virgin female of the same genotype (*WapCre*^{-/+} *Trp53*^{LoxP/LoxP} for JNK^{WT} and *WapCre*^{-/+} *Trp53*^{LoxP/LoxP} *Mapk8*^{LoxP/LoxP} *Mapk9*^{LoxP/LoxP} for JNK^{KO}) was used as the reference genome. Representative Circos plots showing CNVs are presented for JNK^{WT} (D) and JNK^{KO} (E) tumor cells. The outermost ring shows chromosome ideograms. The next track indicates high (red) and moderate (yellow) impact single nucleotide variants and indels marked by rectangles and triangles, respectively. The innermost track shows chromosome amplifications and deletions, with red and blue lines indicating chromosomal fragments present at $\log_2(\text{ratio Tumor/Normal}) > 0.2$ or $\log_2(\text{ratio Tumor/Normal}) < -0.2$, respectively.

A

	JNK ^{WT}	JNK ^{KO}
Total mice	31	35
Tumor-bearing mice	11	35
Adenocarcinoma	5	38
Adenosquamous Carcinoma	1	3
Sarcoma	5	4
Lymphoma	1	0
MammaryTumor Latency (<i>Wks</i>)	67	39

B

	ER ⁺ PR ⁺	ER ⁺ PR ⁻	ER ⁻ PR ⁺	ER ⁻ PR ⁻
JNK ^{WT}	3/5 (60)	0	2/5 (40)	0
JNK ^{KO}	9/38 (24)	3/38 (5)	17/38 (45)	10/38 (26)

Figure IV.6. Tumors in JNK^{KO} mice are primarily adenocarcinomas and display a spectrum of hormone receptor expression patterns.

A) The JNK^{WT} and JNK^{KO} mouse cohorts are summarized.

B) Adenocarcinomas from JNK^{WT} and JNK^{KO} mice were stained for PR and ER and scored for expression. Numbers in parentheses indicate percentages.

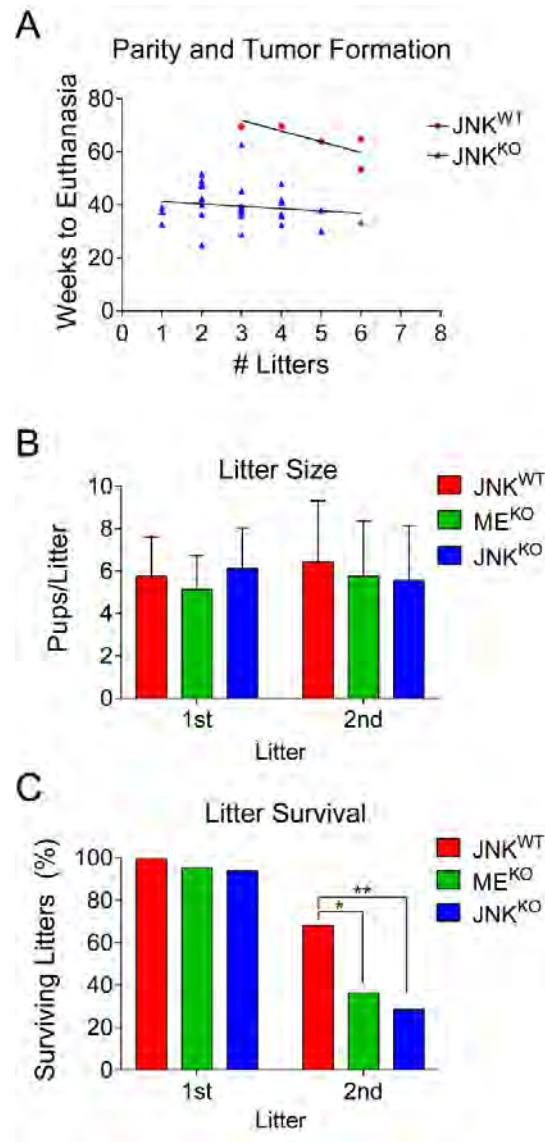


Figure IV.7. Tumor latency in JNK^{WT} and JNK^{KO} mice is not influenced by parity.

A) The number of litters born to JNK^{WT} and JNK^{KO} females was plotted against the time of euthanasia. Only females that developed mammary carcinomas were included in this analysis. No correlation was found between parity and tumor development.

B) The number of pups in the first and second litters of JNK^{WT} (*Wap-Cre*^{-/+} *Trp53*^{LoxP/LoxP}), ME^{KO} (*Wap-Cre*^{-/+} *Mapk8*^{LoxP/LoxP} *Mapk9*^{LoxP/LoxP}), and JNK^{KO} (*Wap-Cre*^{-/+} *Trp53*^{LoxP/LoxP} *Mapk8*^{LoxP/LoxP} *Mapk9*^{LoxP/LoxP}) dams that survived to weaning was counted (mean ± SEM). No significant differences were detected (p>0.05), indicating that females of all three genotypes had similar lactation histories.

C) The percentage of litters surviving to weaning age was monitored for JNK^{WT}, ME^{KO}, and JNK^{KO} dams (*p<0.05, **p<0.01).

To test whether JNK deficiency promotes tumorigenesis by disrupting the balance of proliferation and cell death, I stained tumor tissue sections with antibodies to detect the proliferation marker PCNA and the apoptotic marker cleaved caspase 3. No differences were detected in PCNA-stained sections, indicating that JNK^{KO} tumors were not more proliferative than JNK^{WT} tumors (Figure IV.5C). Similarly, I did not detect differences in cleaved caspase 3 staining between JNK^{WT} and JNK^{KO} tumors (Figure IV.5C). Collectively, these data show that JNK deficiency causes significantly accelerated disease progression without greatly changing the tumor phenotype.

To assess whether there are differences in mutational load, and to determine if there are recurring mutations or chromosomal alterations associated with the different tumor genotypes, I performed exome sequencing of JNK^{WT} and JNK^{KO} tumor cell lines (Figures IV.5D,E & IV.8A). SNVs and Indels resulting in frame shifts, truncations, and splice site mutations were identified (Figure IV.3B,C). CNV analysis demonstrated that chromosome 6 was amplified and no chromosome was consistently deleted in JNK^{WT} tumor cells (Figure IV.5D). Chromosome 6 was also amplified in some (two of six) JNK^{KO} tumor cells (Figures IV.5E & IV.8A). The proto-oncogene *Kras* resides on chromosome 6 and CNV analysis demonstrated that the *Kras* locus was recurrently amplified in JNK^{WT} tumor cells (Figures IV.5D & IV.8A) and was more highly expressed (Figure IV.8B).

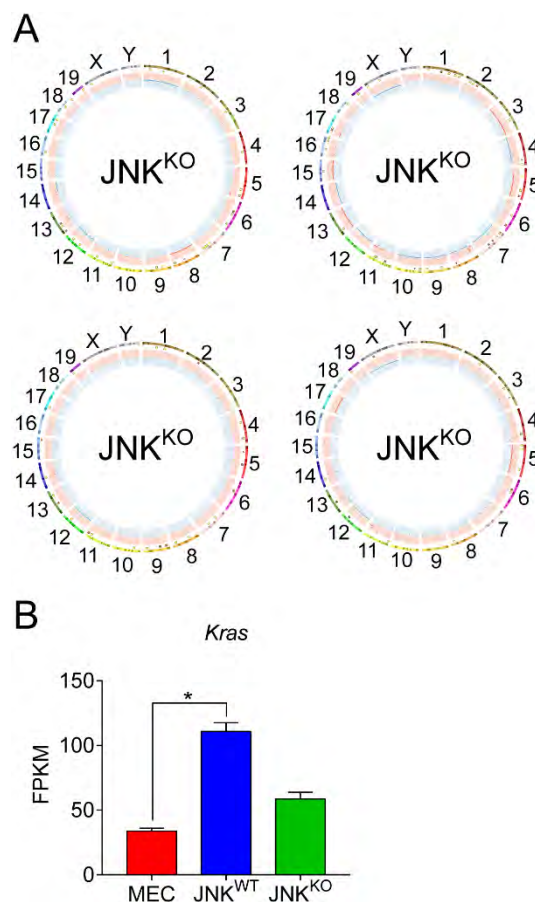


Figure IV.8. Exome sequencing of Control and JNK deficient tumor cells.

A) Circos plots showing copy number variations (CNV) in additional JNK^{KO} tumor cell lines are presented. The outermost ring shows chromosome ideograms. The next track indicates high (red) and moderate (yellow) impact single nucleotide variants and indels marked by rectangles and triangles, respectively. The innermost track shows chromosome amplifications and deletions, with red and blue lines indicating chromosomal fragments present at $\log_2(\text{ratio Tumor/Normal}) > 0.2$ or $\log_2(\text{ratio Tumor/Normal}) < -0.2$, respectively.

B) *Kras* expression in MEC (n=3), JNK^{WT} (n=2), and JNK^{KO} (n=2) cells was measured by RNA sequencing and is presented as mean FPKM \pm SEM (* $q < 0.05$).

Effects of JNK deficiency on tumor-associated gene expression

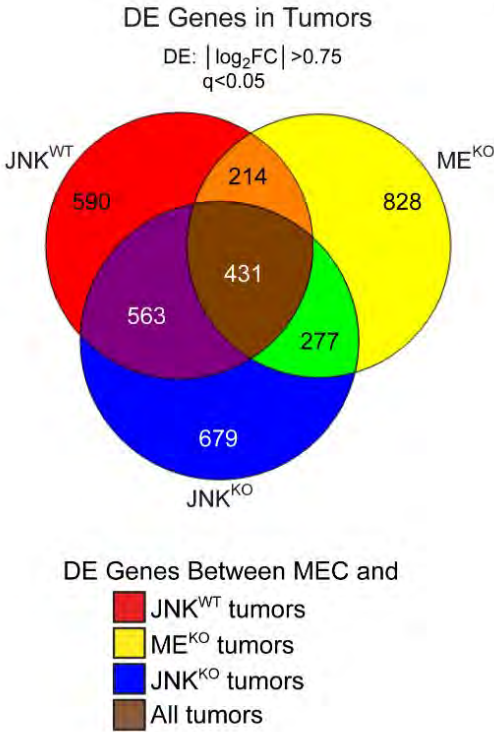
I performed RNA-seq on primary mammary epithelial cells (MEC) and tumor cells (Figure IV.9A) to test whether JNK deficiency caused changes in tumor-associated gene expression. An examination of genes differentially expressed ($|\log_2\text{Fold Change}| > 0.75$; $q < 0.05$) in tumor cells compared to MEC revealed distinct gene expression patterns between JNK^{WT}, JNK^{KO}, and ME^{KO} tumor cells (Figure IV.10A & IV.9B). GSEA using the KEGG database (Figure IV.10B) demonstrated that up-regulated genes in JNK-deficient tumors were enriched for “Metabolic Pathways” (Clusters 1 & 2), while genes up-regulated in JNK^{WT} tumors were enriched for “Cytokine-Cytokine Receptor Interactions” (Cluster 3). In contrast, down-regulated genes in all of the tumor cells were enriched for “Focal Adhesion Proteins” (Cluster 4). These data indicate that JNK deficiency selectively alters a subset of tumor-associated gene expression.

To understand how JNK deficiency may alter tumor signaling pathways, I used IPA to predict pathway activation status by examining differential expression between each tumor type and MEC. The pathways were ranked by Activation z-Score (total $-\log_{10} p$ of Fisher’s exact test across the tumors) and the top 100 were considered (Figure IV.9C). Two dominant categories emerged from the comparative analysis: down-regulated “Chemokine/Cytokine Signaling”; and down-regulated “Integrin/Cytoskeleton Signaling” (Figure IV.10C).

A

Biological Group		GEO Accession	Sample ID	Platform	Mean Reads	Read Length	Mean Read Mapping Rate
MEC	(3)	GSE100581	GSM2687426-8	2x150, NextSeq 500	39x10 ⁶	40-50	99.5 %
JNK ^{WT}	(2)	GSE92560	GSM2432256-7	1x40, HiSeq 2000	40x10 ⁶	40-50	96.9 %
ME ^{KO}	(3)	GSE100581	GSM2687429-31	2x150, NextSeq 500	40x10 ⁶	40-50	99.7 %
JNK ^{KO}	(2)	GSE92560	GSM2432258, GSM2432260	1x40, HiSeq 2000	40x10 ⁶	40-50	96.4 %

B



C

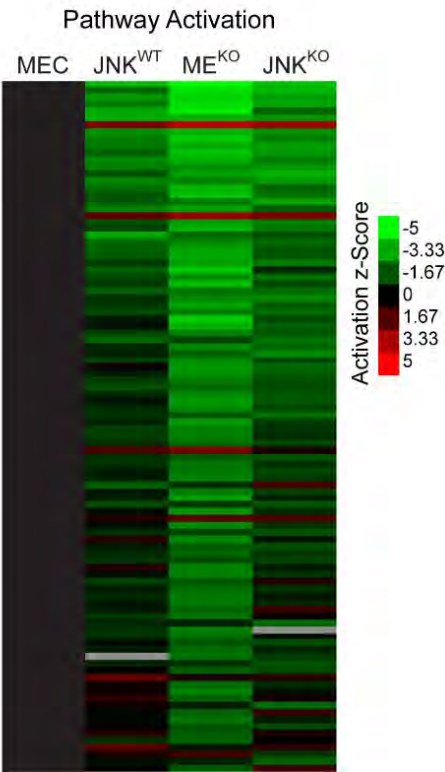


Figure IV.9. Gene expression analysis of control and JNK deficient tumor cells.

A) Summary of the RNA sequencing data together with database accession information (GEO accession numbers and Sample ID). The number of samples per biological group is shown in parentheses.

B) Venn diagram showing differentially expressed (DE) genes in JNK^{WT} (n=2), ME^{KO} (n=3), and JNK^{KO} (n=2) tumors compared to MEC (n=3).

C) Ingenuity Pathway Analysis was used to predict pathway activation and inhibition in JNK^{WT} (n=2), ME^{KO} (n=3), and JNK^{KO} (n=2) tumor cells. The heatmap shows pathways ranked (top to bottom) by their score (total $-\log_{10}p$ of Fisher's exact test across the tumors). The top 100 pathways are shown. Coloring corresponds to the activation z-Score, with green representing inhibited pathways and red activated pathways. A cutoff of score=1.31 was set (equates to $p=0.049$; Fisher's exact test).

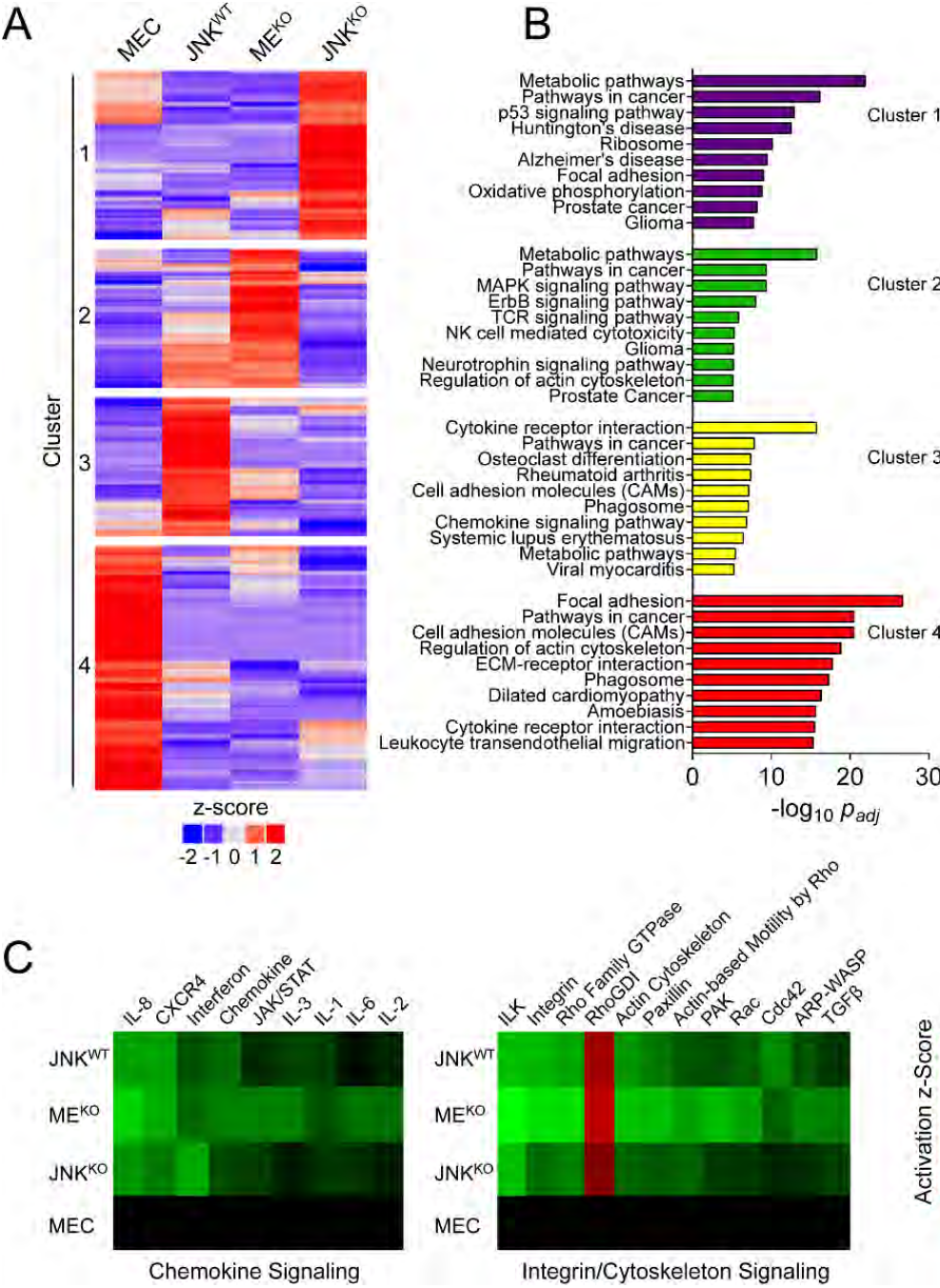


Figure IV.10. RNA-seq analysis demonstrates that a sub-set of tumor-associated gene expression requires JNK.

A, B) RNA isolated from primary mammary epithelial cells (MEC, n=3) and also JNK^{WT} (n=2), ME^{KO} (n=3), and JNK^{KO} (n=2) tumor cell lines was sequenced. The heatmap presents k-means clustering (k=4) of genes differentially expressed in any of the pairwise comparisons ($q < 0.05$, $|\log_2 \text{Fold Change}| > 0.75$; mean) (A). Gene set enrichment analysis was performed on each of the four clusters using the KEGG database (B). The pathways with the lowest p_{adj} values for each cluster are presented.

C) Comparative analysis was performed on genes differentially expressed between MEC and each of the tumor cell lines using Ingenuity Pathway Analysis (IPA). Heatmaps show the predicted activation (Activation z-score) of canonical pathways involved in immune (*left panel*) and integrin/cytoskeleton (*right panel*) signaling ranked by score. A cutoff score=1.31 was set (equates to $p=0.049$; Fisher's exact test).

I also examined signaling pathways by immunoblot analysis. Studies of JNK^{WT} tumor cells demonstrated the presence of a functional JNK signaling pathway, including stress-induced phosphorylation of both JNK and cJUN (Figure IV.11A). However, JNK was not detected in JNK^{KO} tumor cells (Figure IV.11B). The activation state of other MAPK pathways (ERK and p38) and the AKT pathway were similar between JNK^{WT} and JNK^{KO} tumor cells (Figure IV.11B).

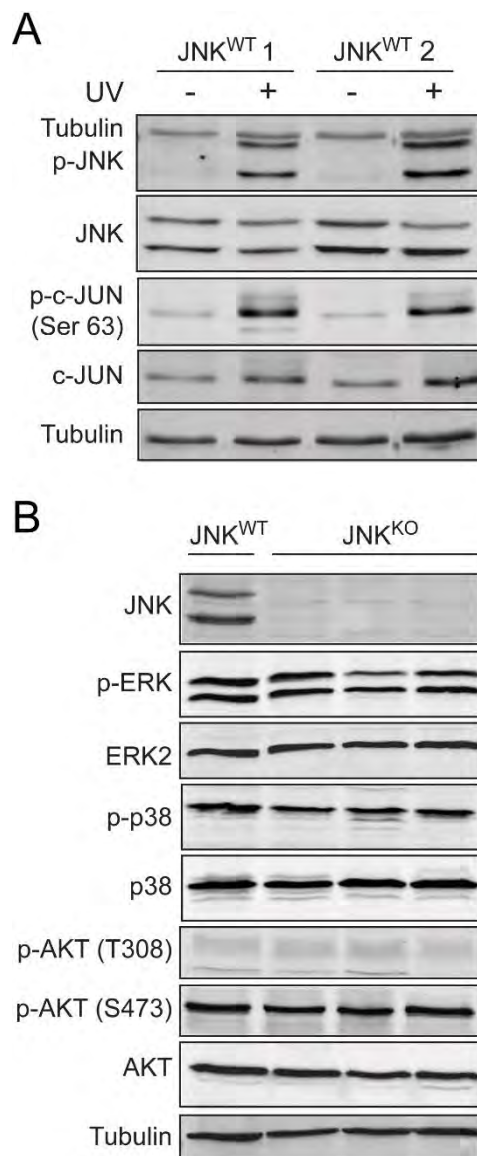


Figure IV.11. Comparison of signaling pathways in control and JNK deficient tumor cells.

A) Two independently-derived JNK^{WT} tumor cell lines (JNK^{WT} 1 and JNK^{WT} 2) were left untreated (-) or were exposed (+) to 60 J/m² ultraviolet light. Lysates from these cells were harvested at 30 min post-irradiation and were examined by immunoblot analysis by probing with antibodies to α -Tubulin, p-JNK, JNK, p-cJUN, and cJUN.

B) JNK^{WT} (n=2) and JNK^{KO} (n=6) tumor cell lines were cultured and protein lysates were prepared for immunoblot analysis. Lysates were probed for JNK, p-ERK, ERK2, p-p38, p38, p-AKT (T308), p-AKT (S473), AKT, and α -Tubulin. Representative blots showing one JNK^{WT} cell line and three JNK^{KO} cell lines are presented.

JNK deficiency does not increase tumor stem cell activity

The increased tumor burden caused by JNK deficiency may reflect a role of JNK in tumor stem cells. To examine this potential role of JNK, I monitored mammosphere formation and maintenance using JNK^{WT} and JNK^{KO} tumor cells. No evidence of increased mammosphere propagation by the JNK^{KO} tumor cells was obtained (Figure IV.12A,B). Moreover, I did not detect enhanced sphere formation by ME^{KO} tumor cells (Figure IV.13A,B). Staining of agarose-embedded JNK^{WT} and JNK^{KO} mammospheres revealed a similar organization with peripheral CK5⁺ cells and central CK8⁺ cells (Figure IV.12C). Finally, the expression of stem cell markers (*Bmi1*, *Nanog*, and *Pou5f1*) was not significantly different between JNK^{WT} and JNK^{KO} mammospheres (Figure IV.12D). This analysis does not support the conclusion that differences in cancer stem cell activity account for the accelerated tumor formation by JNK^{KO} mice compared with JNK^{WT} mice.

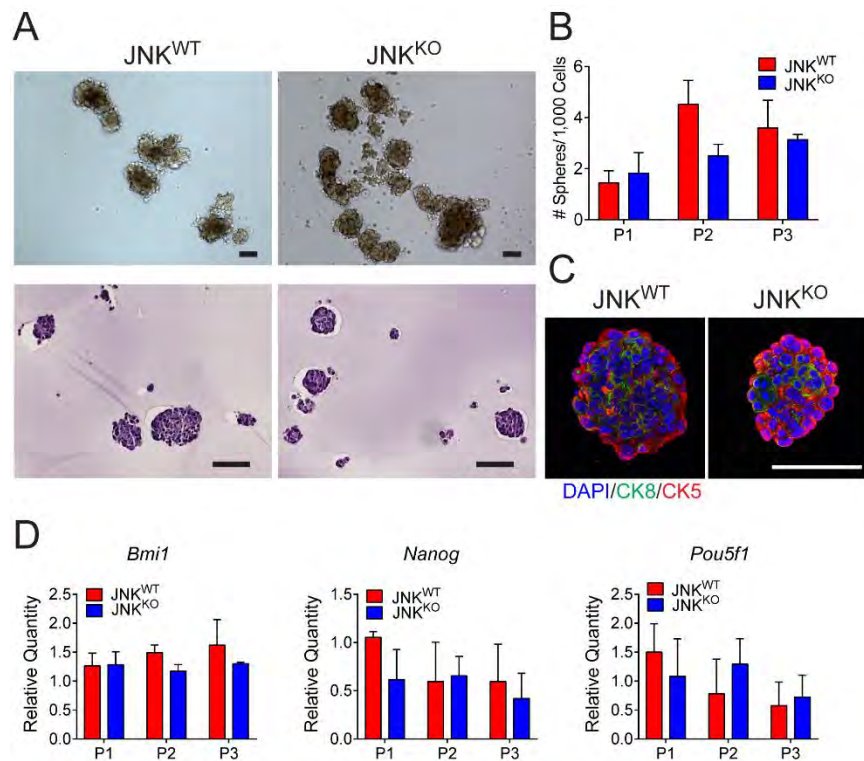


Figure IV.12. Stem cell populations are comparable in JNK^{WT} and JNK^{KO} tumor cells.

A) JNK^{WT} and JNK^{KO} tumor cells formed mammospheres when grown in suspension. Representative phase contrast (*upper panel*) and H&E-stained agarose-embedded sphere sections (*lower panel*) are presented. Scale bar=100 μ m.

B) The number of mammospheres formed per 1,000 plated cells each passage (P) was quantitated for JNK^{WT} and JNK^{KO} tumor cells. Two independent cell lines were tested for each genotype. The data presented are the mean \pm SEM (n=3 independent experiments; **p<0.01).

C) Representative agarose-embedded mammosphere sections stained with antibodies to keratin 5 (CK5, red) and keratin 8 (CK8, green), and counterstained with DAPI are presented. Scale bar=50 μ m.

D) RNA was isolated from JNK^{WT} and JNK^{KO} tumor cell mammospheres at different passages to quantify mRNA expression of *Bmi1*, *Nanog*, and *Pou5f1*. Two independent cell lines were tested for each genotype. The data presented are the mean \pm SEM (n=2 independent experiments). No significant differences were observed (p>0.05).

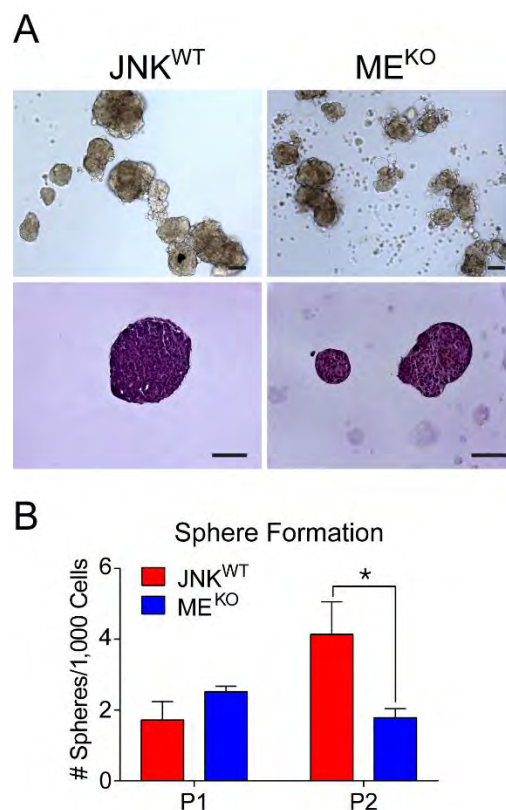


Figure IV.13. JNK-deficient tumor cells do not exhibit enhanced tumor stem cell activity.

A) JNK^{WT} (n=2) and ME^{KO} (n=3) tumor cells grown in suspension formed mammospheres. Representative phase contrast (*upper panel*) and agarose-embedded H&E-stained sections (*lower panel*) are shown. Scale bar= 100 μ m.

B) Sphere formation per 1,000 cells plated over 2 passages (P) was quantitated for JNK^{WT} and ME^{KO} tumor cells (mean \pm SEM of 3 independent experiments, *p<0.05).

JNK deficiency does not increase tumor cell proliferation, but does promote survival

Transformed cells co-opt cellular processes to block anti-proliferative and death mechanisms while increasing cell proliferation, invasion, and migration (Hanahan and Weinberg 2011). A change in one of these processes may account for the increased tumor burden detected in JNK^{KO} mice. No differences between JNK^{WT} and JNK^{KO} tumor cell proliferation were detected (Figure IV.14A). Similarly, I found no difference in JNK^{WT} and JNK^{KO} tumor cell migration during wound healing (Figure IV.14B) or in response to a serum gradient (Figure IV.14C). Moreover, JNK^{WT} and JNK^{KO} tumor cell invasion through matrigel-coated membranes (Figure IV.14C) and collagen I-filled wounds (Figure IV.14D) was similar. These data demonstrate that JNK deficiency does not alter breast tumor cell proliferation, invasion, or migration. Consistent with this conclusion, I found no differences between the growth of JNK^{WT} and JNK^{KO} tumor cells in orthotopically transplanted syngeneic mice (Figure IV.14E-G).

While many properties of JNK^{WT} and JNK^{KO} tumor cells are similar (Figure IV.14A-G), I did detect some JNK-dependent differences in the tumor cell phenotype (Figure IV.14H-J). Thus, JNK^{KO} tumor cells formed more colonies than JNK^{WT} tumor cells when grown in soft agar (Figure IV.14H,I) and JNK^{KO} cells exhibited greater resistance to anoikis than JNK^{WT} tumor cells (Figure IV.14J). These data indicate that JNK deficiency can promote tumor cell survival.

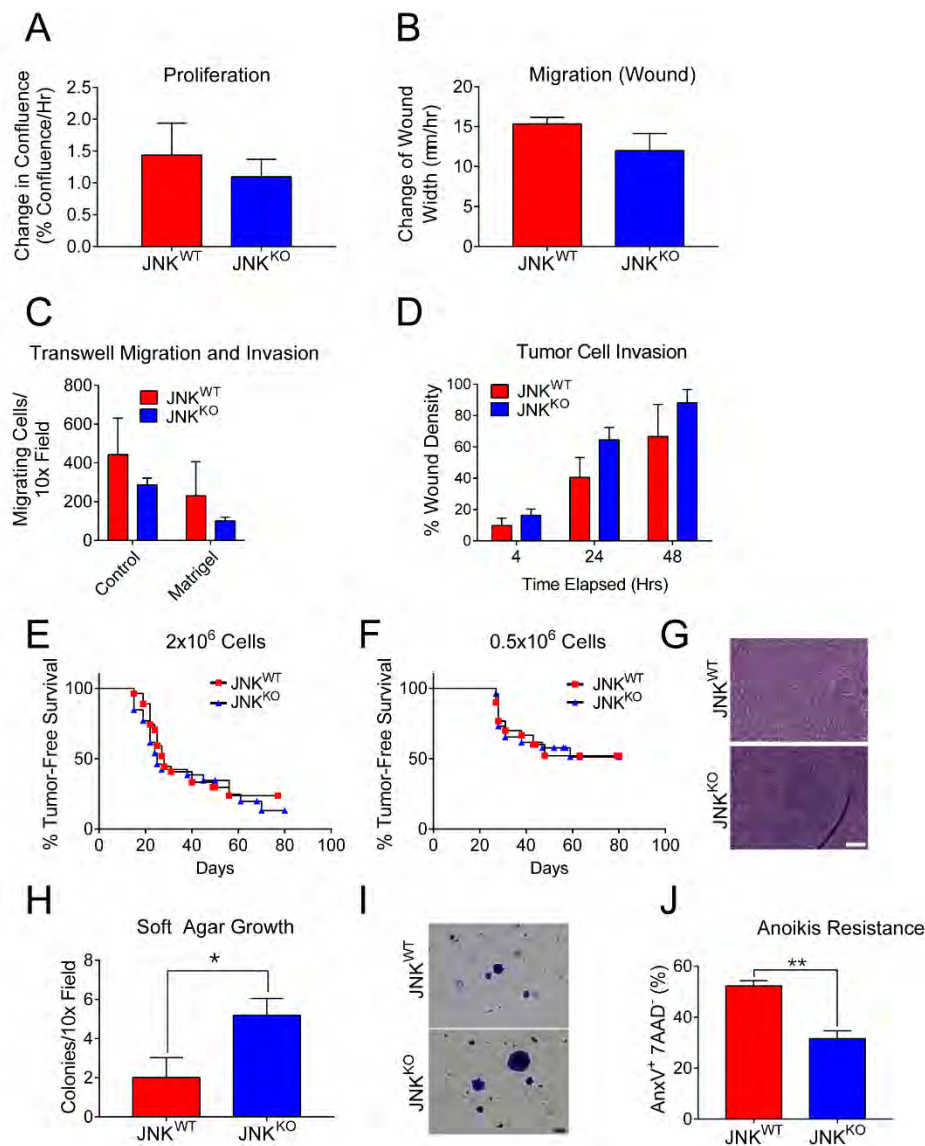


Figure IV.14. JNK^{WT} and JNK^{KO} tumor cells exhibit similar phenotypes.

A) JNK^{WT} (n=2) and JNK^{KO} (n=6) tumor cell lines were cultured (8 h) in growth media and the change in confluence was measured using an IncuCyte ZOOM (mean ± SEM). No significant differences (p>0.05) were observed. Similar data were obtained in four independent experiments.

B) Monolayers of JNK^{WT} (n=2) and JNK^{KO} (n=4) cells were wounded and cell migration rates were assessed by measuring the change in wound width 48 h after wounding using an IncuCyte ZOOM (mean ± SEM). No significant differences (p>0.05) were observed. Similar data were obtained in two independent experiments.

C) JNK^{WT} (n=2) and JNK^{KO} (n=6) tumor cell chemotaxis in response to a serum gradient in the absence (Control) or presence of Matrigel was examined (mean \pm SEM). No significant differences were observed ($p>0.05$). Similar data were obtained in two independent experiment.

D) Monolayers of JNK^{WT} (n=2) and JNK^{KO} (n=3) tumor cells were wounded, overlaid with 0.5mg/ml collagen I in growth serum, and cultured for up to 48 h in media containing 2% serum. Tumor cell migration into the collagen-filled wound was quantitated by measuring cell density in the initial wound area using an IncuCyte ZOOM (mean \pm SEM). No significant differences were observed ($p>0.05$). Similar data were obtained in two independent experiments.

E-G) Orthotopic transplantation of JNK^{WT} and JNK^{KO} tumor cells (two independent cell lines per genotype) into the mammary fat pads of 26 (JNK^{WT}) and 27 (JNK^{KO}) syngeneic mice was performed using 2×10^6 (E). Orthotopic transplantation of 0.5×10^6 cells was performed using 30 (JNK^{WT}) and 26 (JNK^{KO}) syngeneic wild-type hot mice (F). No significant differences were observed ($p>0.05$). Representative H&E stained tumor sections from JNK^{WT} (*upper panel*) and JNK^{KO} (*lower panel*) tumors are presented (G). Scale bar=100 μ M.

H, I) JNK^{WT} (n=4) and JNK^{KO} (n=9) tumor cell lines were cultured in soft agar and colony formation was quantitated (mean \pm SEM; $*p<0.05$) (H). Similar data were obtained from 2 independent experiments and representative images of crystal violet-stained colonies are presented (I). Scale bar=100 μ M.

J) JNK^{WT} (n=7) and JNK^{KO} (n=16) tumor cell lines were cultured in suspension (24 h) and apoptotic cells (7AAD⁻ annexin V⁺) were quantified by flow cytometry (mean \pm SEM; $*p<0.05$). Similar data were obtained in two independent experiments.

JNK deficiency causes early disease initiation

Comparative studies of JNK^{WT} and JNK^{KO} tumor cells demonstrated that JNK-deficiency does not contribute to differences in proliferation, migration, or invasion phenotypes *in vitro* (Figure IV.14A-D) or to tumor growth in orthotopically transplanted syngeneic mice (Figure IV.14E-G). I therefore considered the possibility that JNK may influence tumor initiation rather than the function of fully developed tumor cells. To test this hypothesis, I examined sections of mammary glands from female mice at 18 weeks after gene ablation. JNK^{WT} mice presented normal mammary gland morphology (Figure IV.15A). In contrast, multifocal mammary intraepithelial neoplasia (MIN) was observed in JNK^{KO} glands (Figure IV.15A). The presence of MIN lesions in young JNK^{KO} mice indicates that JNK-deficient mammary epithelial cells exhibit defects in apical-basal polarity, a hallmark of mammary tumor development (Zhan et al. 2008; Halaoui et al. 2017). Moreover, it is likely that mammary tumor development is further promoted by the increased survival of JNK^{KO} cells *in vitro* (Figure IV.14H-J) and increased proliferation of JNK^{KO} epithelial cells compared with JNK^{WT} epithelial cells *in vivo* (Figure IV.15B,C). These data indicate that one physiological function of JNK in mammary epithelial cells is to suppress breast cancer development by preventing the initiation of carcinogenesis.

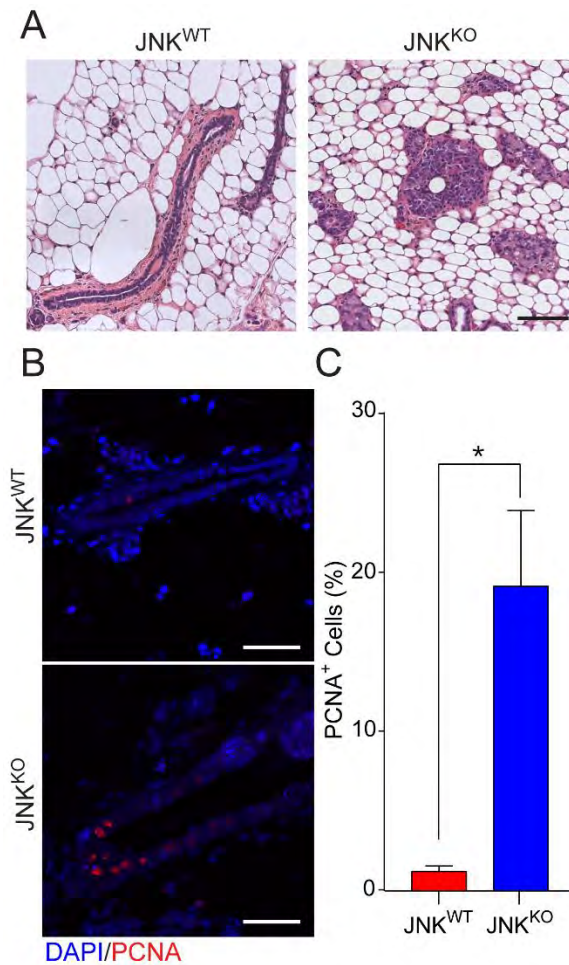


Figure IV.15. JNK deficiency promotes early disease lesions.

A) Eighteen weeks after gene deletion, tissue sections were prepared from mammary glands of JNK^{WT} (n=5) and JNK^{KO} (n=12) female mice. Representative H&E-stained sections are presented. Scale bar=100 μ m.

B, C) Proliferation was examined in mammary glands at 18 weeks after gene ablation-by staining tissue sections with an antibody to PCNA (JNK^{WT} n=4, JNK^{KO} n=5). Representative PCNA-stained and DAPI counter-stained glands are presented (B, Scale bar=50 μ m). The percent of PCNA+ cells was quantified (mean \pm SEM, *p<0.05) (C).

Discussion

The frequent mutation of the JNK pathway in human breast cancer (including the genes *MAP3K1*, *MAP2K4*, and *MAP2K7*) implicates reduced JNK signaling in the etiology of mammary carcinoma (Kan et al. 2010; Banerji et al. 2012; Cancer Genome Atlas 2012; Ellis et al. 2012; Shah et al. 2012; Stephens et al. 2012; Wang et al. 2014; Ciriello et al. 2015; Nik-Zainal et al. 2016b). Mutation of *Mapk8* (encodes JNK1) and *Mapk9* (encodes JNK2) is not frequently detected, most likely because of the functional redundancy of these JNK isoforms (Davis 2000). In contrast, *MAP2K4* and *MAP2K7* serve as non-redundant activators of JNK and mutation of either *MAP2K4* or *MAP2K7* causes JNK inhibition (Tournier et al. 2001). Similarly, *MAP3K1* acts in a non-redundant manner to activate JNK (Yujiri et al. 2000). Tumor-associated ablation or mutation of these genes therefore causes JNK inhibition. Moreover, JNK signaling is also inhibited by phosphorylation of *MAP2K4* by AKT (Park et al. 2002) in breast tumors with AKT activation caused by “driver” mutations in *PTEN* or *PIK3CA* (Garraway and Lander 2013). Suppression of JNK signaling is therefore a characteristic of many breast cancers. Nevertheless, the significance of JNK pathway inactivation in breast cancer is unclear (Cellurale et al. 2010; Chen et al. 2010; Cellurale et al. 2012). Here I demonstrate that loss of JNK signaling is sufficient for murine breast cancer development (Figure IV.1). Furthermore, JNK deficiency accelerated tumor development in a murine model of breast cancer (Figure IV.5).

The frequent JNK pathway *loss-of-function* mutations in human breast cancer may therefore represent “driver” mutations that promote tumor development.

I find that JNK loss plays a key role at the early stages of breast cancer development by promoting mammary gland neoplasia (Figure IV.15). This observation likely accounts for the effect of mutational inactivation of JNK signaling to promote tumor development (Figures IV.1 & IV.5). In contrast to this tumor-suppressive role of JNK during early stages of carcinogenesis (Figure IV.15), JNK does not markedly influence the late-stage tumor phenotype (Figure IV.14). Thus, JNK does not change tumor cell proliferation, invasion or migration *in vitro* or tumor formation in orthotopically transplanted mice *in vivo* (Figure IV.14). However, JNK deficiency does repress tumor cell anoikis and promotes growth in soft agar *in vitro* (Figure IV.14). JNK therefore plays a major role in early tumor development, but only a minor role in established tumors.

An important question relates to the mechanism of breast tumor suppression by the JNK signaling pathway. Part of the mechanism may reflect the pro-apoptotic role of JNK (Tournier et al. 2000). Mutations in key genes can enable epithelial cell survival in the luminal space, resulting in ductal carcinoma *in situ* (DCIS) and cancer (Taraseviciute et al. 2010; Leung and Brugge 2012; Pradeep et al. 2012; Halaoui et al. 2017). Indeed, JNK has been shown to be required for efficient epithelial cell death in response to cell detachment (anoikis) *in vitro* and JNK deficiency results in occluded mammary ducts *in vivo* (Cellurale et al. 2012; Girnius and Davis 2017a). However, this mechanism may not be

sufficient to account for tumor formation caused by JNK deficiency (Figure IV.1) or the observed acceleration of tumor formation caused by JNK deficiency in a mouse model of breast cancer (Figure IV.5). For example, both JNK and p38 MAPK promote mammary gland epithelial cell anoikis by a BIM-dependent mechanism and are required for luminal clearance of mammary ducts (Wen et al. 2011; Cellurale et al. 2012; Girnius and Davis 2017a), but JNK inhibition promotes breast cancer (Figures IV.1 & IV.5) while p38 MAPK pathway inhibition suppresses breast cancer development and the dissemination of metastatic tumor cells (Harper et al. 2016; Del Barco Barrantes et al. 2018; Gawrzak et al. 2018). These data indicate that anoikis defects and ductal occlusion by detached epithelial cells caused by stress-activated MAPK inhibition is not sufficient for tumor formation. This reasoning implicates a second pathway of JNK-mediated suppression of mammary tumor development.

Insight into JNK-mediated tumor suppression was obtained from the analysis of tumor genomic DNA. I found that JNK deficiency resulted in the accumulation of SNVs, Indels, and CNVs (Figure IV.1G). It is likely that these genetic changes caused by JNK deficiency contribute to tumor development. This accumulation of mutations reflects the function of JNK to promote genome maintenance in response to stress. Examples include JNK-mediated phosphorylation of SIRT6 to stimulate double-stranded DNA break repair (Van Meter et al. 2016) and JNK-mediated phosphorylation of DGCR8 to induce transcription-coupled nucleotide excision repair (Calses et al. 2017). Loss of JNK

signaling would therefore be expected to cause defects in DNA repair that result in increased genomic instability. Indeed, my analysis demonstrates that JNK deficiency in the mammary epithelium is sufficient to cause genomic alterations (Figure IV.1G) and breast cancer (Figure IV.1C).

The identification of JNK pathway mutations as “driver” mutations for breast cancer was not anticipated. For example, the JNK pathway can promote cell proliferation and survival through regulation of AP1 transcription factors (Lamb et al. 2003; Ventura et al. 2003; Das et al. 2007). Indeed, the JNK/JUN signaling pathway may promote the proliferation of some breast tumor cells *in vitro* (Guo et al. 2006; Xie et al. 2017). It is therefore possible that JNK signaling may have pro-oncogenic functions in certain tumor types or under specific conditions (Whitmarsh and Davis 2007). Nevertheless, my analysis establishes that a major role of JNK signaling in the breast epithelium is tumor suppression (Figures IV.1 & IV.5). This role of JNK signaling is consistent with the discovery of frequent JNK pathway gene ablation and mutation in human breast cancer (Kan et al. 2010; Banerji et al. 2012; Cancer Genome Atlas 2012; Ellis et al. 2012; Shah et al. 2012; Stephens et al. 2012; Wang et al. 2014; Ciriello et al. 2015; Nik-Zainal et al. 2016b).

My analysis demonstrates that JNK deficiency in the mammary epithelium is sufficient to cause breast cancer in mice and that JNK deficiency causes rapid acceleration of tumor development in a mouse model of breast cancer. These observations indicate that JNK can act as a tumor suppressor for breast cancer

development. Inactivating mutation of genes that encode JNK pathway components may therefore promote human breast cancer. This conclusion presents an opportunity for therapeutic intervention in patients with breast cancer.

Materials and Methods

Mice

Mapk8^{LoxP/LoxP} Mapk9^{LoxP/LoxP} mice have been previously described (Han et al. 2013). C57BL6/J (RRID:IMSR_JAX:000664), B6129-TG(Wap-cre)11738Mam/J (RRID:IMSR_JAX:008735) (Wagner et al. 1997), B6.129P2-*Trp53^{tm1Brn}*/J (RRID:IMSR_JAX:008462) (Marino et al. 2000), and B6.129(Cg)-Gt(ROSA)26Sor^{tm4}(ACTB-tdTomato,-EGFP)Luo/J mice (RRID:IMSR_JAX:007676) (Muzumdar et al. 2007) were purchased from The Jackson Laboratories. All mice were on a C57BL6/J strain background and were randomly assigned to groups. Female mice were bred at 10-12 weeks of age and monitored for tumor development by palpation following weaning. Reasons for euthanasia included a mass of 1 cm in diameter, ulceration due to the tumor, poor health, or weight loss (>20% body weight). The animals were housed in a specific pathogen-free facility accredited by the American Association of Laboratory Animal Care (AALAC).

Tumor-derived Cell Lines

Tumors were harvested and placed in DMEM/F12 containing 1% penicillin/streptomycin and 1% nystatin (Thermo Fisher Scientific). The tissue was washed with phosphate-buffered saline (PBS), minced, and digested (37°C for up to 2 h, shaking) in DMEM containing 2mg/ml collagenase, 0.1% trypsin, and 1% penicillin/streptomycin. Following digestion, cells were pelleted and re-suspended in DMEM/F12 supplemented with 2% bovine growth serum and 1%

penicillin/streptomycin, then plated on collagen I (Thermo Fisher Scientific Cat# A1048301) coated dishes. After two passages, the cells were plated on standard tissue culture dishes and maintained in Growth Medium (DMEM/F12 supplemented with 10% fetal bovine serum plus 1% penicillin/streptomycin) prior to cryogenic storage.

Genotype Analysis

Genomic DNA was genotyped using a PCR-based method. *Mapk8^{LoxP}* (540 bp) and *Mapk8⁺* (330 bp) were detected using amplimers 5'-AGGATTTATGCCCTCTGCTTGTC-3' and 5'-GACCACTGTTCCAATTTCCATCC-3'. *Mapk9^{LoxP}* (264 bp) and *Mapk9⁺* (224 bp) were detected using amplimers 5'-GTTTTGTAAAGGGAGCCGAC-3' and 5'-CCTGACTACTGAGCCTGGTTTCTC-3'. *Trp53^{LoxP}* (370 bp) and *Trp53⁺* (288 bp) were detected using amplimers 5'-AGCACATAGGAGGCAGAGAC-3' and 5'-CACAAAAACAGGTAAACCCAG-3'. *Cre⁺* (450 bp) was detected using amplimers 5'-T TACTGACCGTACACCAAATTTGCCTGC-3' and 5'-CCTGGCAGCGATCGCTATTTTCCATGAGTG-3'. *Mapk8^Δ* (395 bp), *Mapk8⁺* (1550 bp), and *Mapk8^{LoxP}* (1,095 bp) were detected using amplimers 5'-CCTCAGGAAGAAAGGGCTTATTTC-3' and 5'-GAACCACTGTTCCAATTTCCATCC-3'. *Mapk9^Δ* (400 bp) and *Mapk9^{LoxP}* (560 bp) were detected using 5'-GGAATGTTTGGTCCTTTAG-3', 5'-GCTATTCAGAGTTAAGTG-3', and 5'-TTCATTCTAAGCTCAGACTC-3'. *Trp53^Δ*

(612 bp) was detected using amplimers 5'-GAAGACAGAAAAGGGGAGGG-3' and 5'-CACAAAAACAGGTAAACCCAG-3'.

Orthotopic Transplantation

Tumor-derived cell lines were screened for common pathogens using the Rapidmap panel 21 (Taconic). The cells were pelleted and washed 5 times with PBS before resuspension at a final concentration of 2×10^6 or 0.5×10^6 cells/40 μ l of PBS. A 26 gauge needle was used to inject the cells into the thoracic mammary gland. The presence of tumors was monitored weekly and palpable tumors were measured using calipers. Mice meeting euthanasia criteria or mice that remained 80 days post-inoculation were euthanized.

Cell Proliferation

Cells were seeded in 96-well plates (1,000 cells/well) and cultured in an IncuCyte Zoom (Essen Bioscience). The cells were kept in growth media and fed every 2 days for the duration of the assay. Images were taken every 4h and cell confluence was measured at these time points.

Soft Agar Growth

Agarose (Lonza) was dissolved in water (4% or 2% (w/v) solution) and autoclaved. The 4% agarose was mixed with growth media to yield a 1% agarose solution, which was plated and allowed to solidify (4°C). Tumor cells in growth

media (100,000/ 6cm dish) were mixed with the 2% agarose to a final concentration of 0.5% agarose, and overlaid onto the solidified 1% agarose. The cells were fed with Growth Medium every 3~4 days for the duration of the assay. After 3 weeks, the cells were fixed with 100% methanol (-20°C) and stained with 0.1% crystal violet dissolved in 20% methanol / 80% PBS. Images were taken using a Zeiss AxioVert 200M. Six 10x-fields/plate were used to quantify colony formation using FIJI software (Schindelin et al. 2012).

Mammosphere Assay

Tumor cells were seeded 25,000/ml in a 24-well ultra-low attachment plate in DMEM/F12 media containing 1% penicillin/streptomycin, B27 supplement (1:50), 20 ng/ml bFGF, 2.5 µg/ml insulin, and 20 ng/ml EGF. Six wells were plated for each cell line. Three to four days later, before passaging, colonies larger than 50 µm were counted using a Zeiss AxioVert 200M microscope. The spheres were dissociated by incubation (15 min) with 0.25% trypsin (Thermo Fisher Scientific) with pipetting. The digestion was terminated by addition of 0.5% soybean trypsin inhibitor (ATCC) and single cells were plated. Spheres used for embedding in agarose or for RNA isolation were treated similarly, but were cultured in 100 mm ultra-low attachment dishes. Spheres prepared for embedding were resuspended in 4% agarose (IBI Scientific Cat# IB70050), and fixed in 10% formalin before processing.

Anoikis Assay

Tumor cells were suspended in serum-free DMEM/F12 media with 0.5% methylcellulose (Millipore-Sigma), placed in poly-HEMA (Millipore-Sigma) coated plates (1.2×10^5 cells/ml), and incubated for 24 h. After incubation, the cells were washed twice with PBS, then stained with phycoerythrin-conjugated Annexin V and 7-aminoactinomycin D (7-AAD) using the PE annexin apoptosis detection kit I (BD Pharmingen #559763). A FACSCalibur (BD Bioscience) was used to quantify the apoptotic cells (7AAD⁻ Annexin V⁺). Single-stained controls were used to gate 7AAD⁻ and 7AAD⁺ cells while cells suspended for 1 h were used to define the annexin V⁺ and annexin V⁻ populations. FlowJo version 9.7.6 (Tree Star) was used to analyze the data (Girnius and Davis 2017a).

Wound Healing

Tumor cells were seeded at a density of 100,000 cells/well in a 96-well ImageLock plate (Essen Bioscience) and allowed to adhere overnight. The following day, a Wound Maker (Essen Bioscience) was used to scratch the confluent monolayers of cells. The cells were washed 2 times with PBS and then maintained in serum-free media for the remainder of the assay. Invasion assays were performed using cells plated in 96-well ImageLock plates coated with 300 µg/ml collagen I. Cells adhered overnight, were scratched using a WoundMaker, and washed twice with media before being placed on ice (5 min). The cells were then overlaid with growth media containing collagen I (0.5 mg/ml). The cells

were incubated (30min at 37°C) to solidify the collagen prior to the addition of DMEM/F12 supplemented with 2% FBS. All plates were imaged every 4h using an IncuCyte Zoom (Essen Bioscience).

Transwell Migration

Tumor cells (30,000 cells/well) were plated in triplicate using Growth Medium in transwells with 8 µm pores (Millipore Sigma) and allowed to adhere. For invasion assays, inserts coated with Matrigel (Millipore Sigma) were rehydrated according to the manufacturer's instructions before plating cells. To create a serum gradient, media from the upper chambers was replaced with serum-free media. Cells were allowed to migrate for 16-20 h. Remaining cells in the upper chambers were removed with a cotton swab, then the inserts were fixed with 100% methanol (20 min, -20°C), washed 3 times with PBS, and stained with 2-(4-amidinophenyl)-1H-indole-6-carboxamide (DAPI). The insert membranes were removed with a scalpel and mounted on a slide for examination using a Zeiss Axiovert 200M microscope. Two to three images at 10x magnification were taken for each membrane. FIJI was used to quantify the migrating cells (Schindelin et al. 2012).

Histological Analysis

Mammary glands #2-5 were harvested, fixed in 10% formalin, dehydrated, and embedded in paraffin. Hematoxylin and eosin-stained sections (5 µm) were

reviewed by a board-certified veterinary pathologist to identify and classify proliferative lesions (Cardiff et al. 2000). To detect proliferation, sections were treated with the endogenous biotin blocking kit (Thermo Fisher Scientific E21390); prior to incubation with a biotin-conjugated antibody to PCNA (Thermo Fisher Scientific Cat# 13-3940 RRID:AB_2533; dilution 1:50), and an AlexaFluor 633-conjugated streptavidin (Thermo Fisher Scientific Cat# S-21375 RRID:AB_2313500). For PCNA quantification 49-50 fields were examined across JNK^{WT} (n=4) and JNK^{KO} (n=5) mice. PCNA positive duct cells were normalized to the total number of duct cells in the field examined. Additional sections were stained with cleaved-caspase-3 (Cell Signaling Technology Cat# 9662 RRID:AB_331439; 1:100), keratin 5 (BioLegend Cat# 905501 RRID:AB_2565050; 1:50), keratin 8 (DSHB Cat# TROMA-I RRID:AB_531826; 1:100), GFP (Thermo Fisher Scientific Cat# A21311 RRID:AB_221477; 1:100), estrogen receptor (Santa Cruz Biotechnology Cat# sc-542 RRID:AB_631470; 1:500), and progesterone receptor (Santa Cruz Biotechnology Cat# sc-538 RRID:AB_632263; 1:300). For immunohistochemistry, a biotinylated rabbit antibody (Biogenex Cat# HK340-5K) in conjunction with streptavidin-conjugated horseradish peroxidase (Vector Laboratories Cat# PK-6100) and 3,3'-diaminobenzidine (Vector Laboratories Cat# SK-4100) was used to detect the primary antibody. Sections were then counterstained with hematoxylin (Fisher Scientific) and pictures were taken using a Zeiss Axiovert. AlexaFluor 546 conjugated-goat anti-rabbit IgG (H+L) antibody (Thermo Fisher Scientific Cat#

A11035 RRID:AB_143051) and AlexaFluor 488 conjugated-goat anti-rat IgG (H+L) antibody (Thermo Fisher Scientific Cat# A11006 RRID:AB_141373) were used to detect immune complexes in co-staining experiments. These sections were counterstained with DAPI and immunofluorescence was examined using a Leica SP2 confocal microscope.

Immunoblot Analysis

Cell lysates were prepared using Triton lysis buffer (20 mM Tris [pH 7.4], 1% Triton X-100, 10% glycerol, 137 mM NaCl, 2 mM EDTA, 25 mM β -glycerophosphate, 1 mM sodium orthovanadate, 1 mM phenylmethylsulfonyl fluoride, and 10 μ g/mL of aprotinin and leupeptin). Extracts (30 μ g) were examined by immunoblot analysis by probing with antibodies to phospho-ERK (Cell Signaling Technology Cat# 9101 RRID:AB_2315114), ERK2 (Santa Cruz Biotechnology Cat# sc-1647 RRID:AB_627547), phospho-JNK (Cell Signaling Technology Cat# 9255 RRID:AB_2307321), JNK (R & D Systems Cat# AF1387 RRID:AB_2140743R&D), p38 (Cell Signaling Technology Cat# 9212 RRID:AB_330713), phospho-p38 (Cell Signaling Technology Cat# 9211 also 9211L, 9211S RRID:AB_331641), phospho-JUN (S63) (Cell Signaling Technology Cat# 9261L RRID:AB_2130159), JUN (Santa Cruz Biotechnology Cat# sc-1694 RRID:AB_631263), p-AKT (T308) (Cell Signaling Technology Cat# 5106S RRID:AB_836861), p-AKT (S473) (Cell Signaling Technology Cat# 9271 RRID:AB_329825), AKT (Cell Signaling Technology Cat# 9272

RRID:AB_329827), and α -Tubulin (Millipore-Sigma Cat# T5168 RRID:AB_477579). IRDye 680LT conjugated-donkey anti-mouse IgG antibody (LI-COR Biosciences Cat# 926-68022 RRID:AB_10715072) and IRDye 800CW conjugated-goat anti-rabbit IgG (LI-COR Biosciences Cat# 926-32211 RRID:AB_621843) were used to detect and quantitate immune complexes with the Odyssey infrared imaging system (LI-COR Biosciences).

Exome Sequencing

Genomic DNA was isolated from cancer cell lines using the DNEasy kit, including RNase treatment (Qiagen). For each genotype, a control sample was generated by isolating genomic DNA from mammary glands of a virgin mouse of the same genotype. Whole exome sequencing libraries were prepared using the Agilent SureSelect XT library preparation kit. DNA (OD_{260/280} 1.7-2.0 and OD_{260/230} >2.0) was sheared using a Covaris LE220. End-repaired, adenylated DNA fragments were ligated to Illumina sequencing adapters and amplified by PCR. Exome capture was performed using the Agilent SureSelect Mouse All Exon (50 mb) capture probe set; captured exome libraries were enriched by PCR. Final libraries were quantified using the KAPA Library Quantification Kit (KAPA Biosystems), Qubit Fluorometer (Life Technologies) and Agilent 2100 BioAnalyzer, and were sequenced on an Illumina HiSeq2500 machine using 2x125 bp cycles. Single nucleotide variants were reported as the union of SNVs called by muTect (Cibulskis et al. 2013), Strelka (Saunders et al. 2012), and

LoFreq (Wilm et al. 2012) and indels were reported as the union of indels called by Strelka, somatic versions of Pindel (Ye et al. 2009) and Scalpel (Narzisi et al. 2014). ExomeCNV was run with default settings using mm10 reference to generate copy-number calls (Sathirapongsasuti et al. 2011). The segmentation and log2 ratios from ExomeCNV output were used to identify amplified, deleted and copy-neutral regions. Log2 thresholds of >0.2 and <-0.2 were used to label a segment as amplified or deleted, respectively, and the segments were visualized (Krzywinski et al. 2009). Bedtools (Quinlan and Hall 2010) was run to identify genes overlapping copy-number segments.

Analysis of mRNA Expression

Cellular RNA was isolated using the RNeasy kit with DNase treatment (Qiagen) and RNA quality (RIN >9) was confirmed using the Bioanalyzer 2100 system (Agilent Technologies). Libraries were constructed according to the manufacturer's instructions (Illumina). Two to three libraries were analyzed for each condition. Single-end sequencing with reads of 40 bp reads (for JNK^{WT} and JNK^{KO}) was performed on a HiSeq 2000 platform and paired-end sequencing with 150 bp reads (for MEC and ME^{KO}) was performed on a NextSeq500 platform (Figure IV.4) (Illumina). Poor quality reads, adapter sequences, and reads less than 40 bp were removed using Trimmomatic (version 0.36) (Bolger et al. 2014). First, the MEC and ME^{KO} biological groups were analyzed (Figure IV.4). Second, to adequately compare the four biological groups (MEC, ME^{KO}, JNK^{WT}, and

JNK^{KO}), seqtk was used to sample sequences averaging 40 million single-end reads per sample (Figure IV.9A) (Li 2017). Reads were aligned to the mouse genome mm10 using Bowtie2 (v 2-2.1.0) (Langmead and Salzberg 2012) and Tophat2 (v 2.0.14) (Kim et al. 2013). Samtools (version 0.0.19) (Li et al. 2009) and IGV (version 2.3.60) (Thorvaldsdottir et al. 2013) were used for indexing the alignment files and viewing the aligned reads respectively. Cufflinks (v 2.2.1) (Trapnell et al. 2010; Trapnell et al. 2012) was used to quantitate gene expression as fragments per kilobase of exon model per million mapped fragments (FPKM); differential expression was identified using the Cufflinks tools, Cuffmerge and Cuffdiff. Cummerbund version 2.4.1 (Trapnell et al. 2012) was used to assess replicate concordance. The complex heatmap package version 1.12.0 (Gu et al. 2016) was used to generate heatmaps of differentially expressed ($q < 0.05$, $|\log_2 \text{Fold Change}| > 0.75$) genes. Gene set enrichment analysis was performed on differentially expressed genes using the WEB-based GEne SeT AnaLysis Toolkit (Webgestalt) (Wang et al. 2013) with the KEGG database. Ingenuity Pathway Analysis (Qiagen) was used to predict pathway activation based on differentially expressed genes. The top 100 pathways ranked by score (the sum across tumor genotypes of $-\log_{10}$ p-value calculated by Fisher's exact test) were identified. Treeview (Java) (Saldanha 2004) was used to make heatmaps showing pathway activation z-scores.

The expression of mRNA was also determined by RT-PCR using a Quantstudio 12K Flex machine (Thermo Fisher Scientific). TaqMan[®] assays were

used to quantify the expression of *Bmi1* (Mm03053308_g1), *Pou5f1* (Mm03053917_g1), and *Nanog* (Mm02019550_s1). Relative expression was normalized to the expression of 18S RNA in each sample using Taqman® assays (catalog number 4308329; Thermo Fisher Scientific).

Quantification and Statistical Analysis

Data are presented as the mean and standard error. Statistical analysis was performed using GraphPad Prism version 7 (GraphPad Software). ANOVA with Bonferroni's test was used to determine significance with an assumed confidence interval of 95%. Two-tailed, unpaired t-test with Welch's correction was used for pairwise comparisons. Chi-squared was used to determine differences in litter survival and Fisher's exact test was used to determine differences in tumor or MIN incidence. Kaplan-Meier analysis of mammary tumor-free survival was performed using the log-rank test. Statistical significance was defined as $p < 0.05$.

Data Availability

The raw data has been deposited in the Mendeley repository (<https://data.mendeley.com/datasets/fzygb8drwc/draft?a=136fb1fa-23b4-4272-adc4-76800ee14b4c>) . The RNA-seq raw data files have been deposited with NCBI; GEO accession numbers GSE100581 and GSE92560. The exome sequence data were deposited with NCBI; SRA accession number PRJNA401332.

CHAPTER V

DISCUSSION AND FUTURE DIRECTIONS

Discussion

The JNK pathway is required during developmental morphogenesis and its de-regulation can promote disease (Davis 2000; Manning and Davis 2003). The context-specific responses of this pathway require systematic characterization of its roles in different cell types under varied conditions. To this end, I sought to study the importance of JNK in epithelial cells. In particular, I focused on aspects of mammary gland biology to elucidate how JNK signaling may participate in breast carcinogenesis. I found that suspended epithelial cells require JNK for efficient anoikis (Chapter II). Also, JNK in the mammary epithelium promotes cell death during post-lactational involution, and its absence results in substantial disruption of the involution gene expression program (Chapter III). Finally, JNK loss is sufficient for mammary carcinogenesis and accelerates transformation in a model of breast cancer (Chapter IV). Collectively, this work furthers our understanding of how JNK promotes cell death and it establishes the JNK pathway as a regulator of mammary epithelial cells at several stages of mammary gland development (Figure V.1).

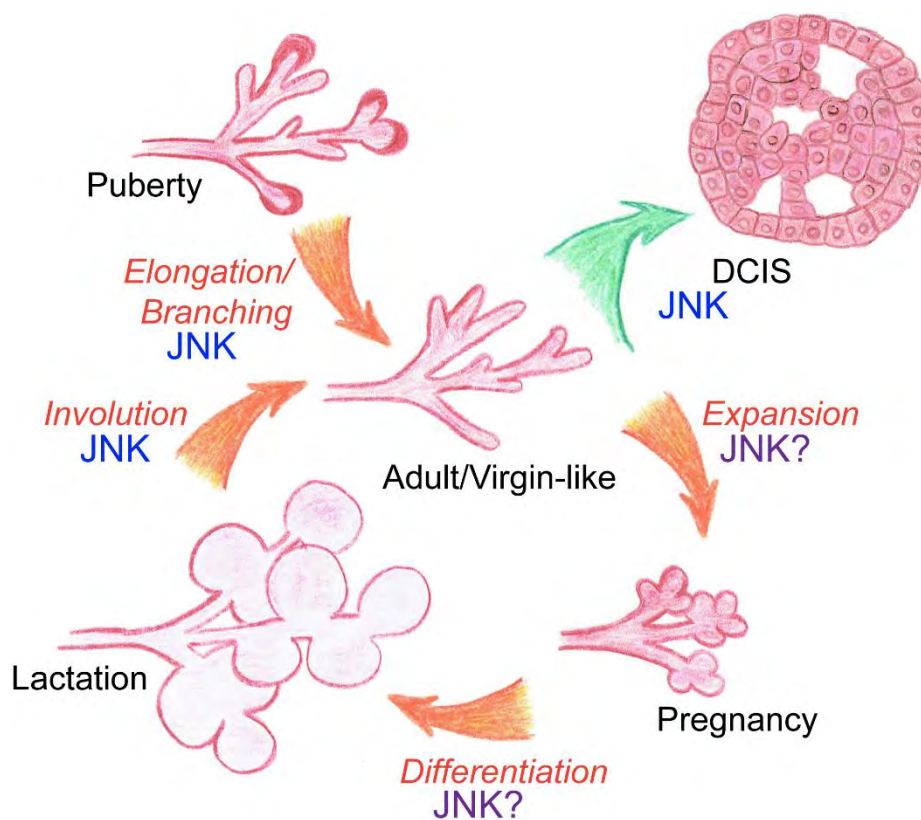


Figure V.1. JNK participates in several aspects of mammary gland biology.

Prior to these studies, the requirement of JNK for branching morphogenesis and luminal clearance had been established. In the current body of work, I show that JNK in the mammary epithelium suppresses carcinogenesis and promotes involution after lactation. Additional work will be needed to determine if JNK contributes to the development of the gland during pregnancy and lactation.

Anoikis – suspension-induced cell death – is important in the mammary gland for ductal clearance during pubertal development (Humphreys et al. 1996). It is also a barrier that transformed cells must overcome during disease initiation to expand into luminal spaces (Taraseviciute et al. 2010; Leung and Brugge 2012; Pradeep et al. 2012) and during metastasis to travel to distant sites (Douma et al. 2004). Among the proteins involved in anoikis are the pro-apoptotic BH3-only proteins BIM and BMF (Reginato et al. 2003; Maillieux et al. 2007; Schmelzle et al. 2007) that can initiate cell death by promoting BAK/BAX-mediated cytochrome c release from mitochondria (Huang and Strasser 2000; Pinon et al. 2008; Czabotar et al. 2014).

The ability of the JNK pathway to mediate cell death and survival decisions make it an appealing candidate for regulating anoikis. However, JNK responses to stress stimuli are selective, as JNK is required for UV-induced apoptosis, but does not contribute to cell death mediated by the FAS and TNFR1 cell surface receptors (Tournier et al. 2000; Lamb et al. 2003; Das et al. 2009). Early studies testing the importance of JNK in anoikis used dominant-negative mutants and arrived at contradicting conclusions (Frisch et al. 1996; Khwaja and Downward 1997). In later studies, *in vitro* acinar formation assays (Zhan et al. 2008; McNally et al. 2011) as well as observations from mammary gland development (Cellurale et al. 2012) showed that JNK pathway inactivation results in luminal infilling, supporting a role for JNK in anoikis. Using chemical inhibition and genetic ablation of JNK, I demonstrate that JNK indeed promotes anoikis

(Figures II.1 & II.2). Furthermore, JNK regulation of anoikis occurs in both human and murine cells, indicating a conserved function for JNK during this process.

JNK-mediated anoikis relies on activating the BIM/BMF-BAK/BAX pathway (Figures II.5 & II.10). Previous work showed that JNK activates BIM and BMF by phosphorylating dynein light chain binding motifs to promote their translocation to mitochondria where they activate BAK/BAX (Lei et al. 2002; Lei and Davis 2003; Hubner et al. 2008; Hubner et al. 2010). Mutation of this site on BMF (Ser⁷⁴ to Ala) increases cell survival during suspension (Figure II.15). However, mutating the analogous site on BIM (Thr¹¹² to Ala) did not result in increased survival during cell suspension (Figure II.15), indicating that JNK phosphorylation of BIM at Thr¹¹² is not required for anoikis.

Altering gene expression through AP1 transcription factors such as cJUN constitutes another mechanism by which JNK could promote anoikis (Davis 2000). Indeed, *Bcl2l1* (encoding BIM) is a cJUN target gene (Whitfield et al. 2001). In the absence of JNK activity, suspended cells expressed lower levels of *Bcl2l1* mRNA (Figure II.1E & II.8) and BIM protein (Figure II.7), while *Bmf* mRNA levels were independent of JNK (Figure II.1E & II.8). Suspension culture also did not alter BMF protein levels (Figure II.7), suggesting that BMF participation in anoikis is regulated by its cellular localization. Collectively, these data show that JNK promotes anoikis at the level of transcription (*Bcl2l1*) and protein phosphorylation (BMF) (Figure V.2).

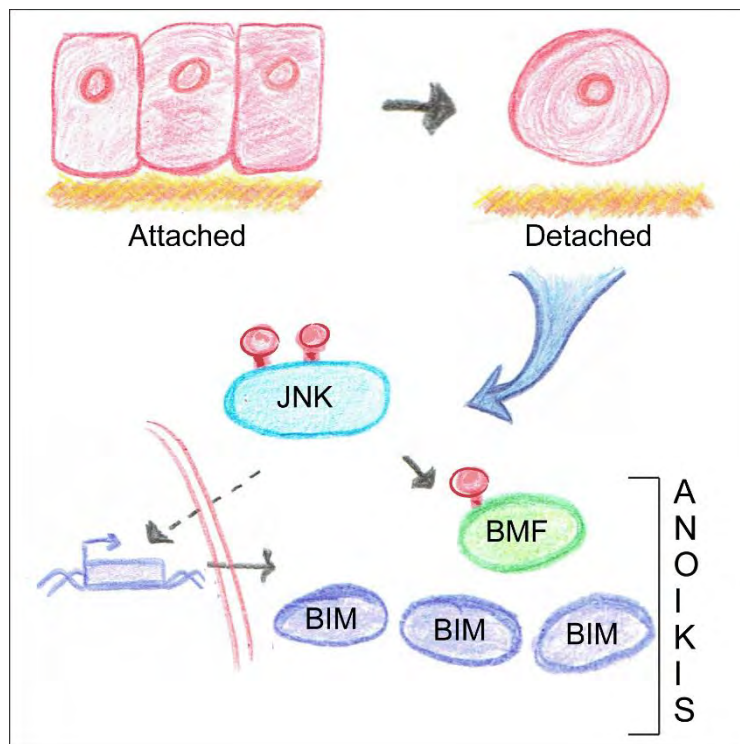


Figure V.2. JNK promotes anoikis through transcriptional regulation of BIM and phosphorylation of BMF.

When epithelial cells become detached, activated JNK can increase expression of BIM and phosphorylate BMF to induce anoikis. Thus, transcription factor and non-transcription factor targets of JNK contribute to its regulation of suspension-induced death.

The JNK-dependent expression of *Bcl2/11* appears to be a general phenomenon. Both human mammary epithelial cells (Figure II.1E) and mouse kidney epithelial cells (Figure II.8A & II.9B) require JNK to induce *Bcl2/11* during anoikis. JNK was also needed for *Bcl2/11* induction during mammary gland involution (Figure III.15A, C). Furthermore, the similar phenotypes observed in developing JNK-deficient (Cellurale et al. 2012) and BIM-deficient (Figure II.12A & Mailloux et al. 2007) mammary glands suggests that these proteins may participate in the same pathway during lumen formation in terminal end buds (TEB). However, elimination of the JNK phosphorylation site on BIM (Thr¹¹² replacement with Ala) did not result in occluded TEBs (Figure II.16), indicating that phosphorylation of this site is not needed for luminal clearance. Together, these observations suggest that JNK-mediated BIM expression also constitutes part of the TEB clearance program.

The transcription factor responsible for JNK-mediated *Bcl2/11* induction during anoikis and involution was not identified. However, cJUN, a major target of JNK (Davis 2000) and a positive regulator of *Bcl2/11* expression in neurons (Whitfield et al. 2001), is an appealing candidate. In the context of involution, two additional pieces of evidence implicate cJUN: (1) cessation of suckling increases phosphorylation cJUN and AP1 DNA binding activity (Jaggi et al. 1996), and (2) the differentially expressed genes in involuting JNK^{KO} glands show significant enrichment for cJUN/JUND binding sites (Figure III.12).

The JNK-dependent expression of *Bcl2l1* in the involuting mammary gland may partially account for the promotion of involution by JNK (Figure III.2 & III.3). However, the involution defect in JNK^{KO} mice (Figure III.2) is more severe than the defect observed in *Bcl2l1*^{-/-} mice (Sakamoto et al. 2016; Schuler et al. 2016), indicating that JNK loss affects additional proteins. Indeed, of the more than 10,000 genes that are differentially expressed during involution, 26% rely on an active JNK pathway (Figure III.10A).

Among the groups of genes that exhibit JNK-dependent expression (Figure III.10C) and cJUN/JUND binding (Figure III.12) are matrix metalloproteases (Figure III.13) and cathepsins (Figure III.14), both of which promote involution (Lund et al. 1996; Kreuzaler et al. 2011). JNK deficiency during involution also resulted in decreased expression of the AP1 members ATF3 and FOSL2 (Figure III.9). Thus, these transcription factors may contribute to the delayed gland remodeling observed in JNK^{KO} glands (Figure III.2 & III.3). These observations indicate that JNK is a major regulator of the gene expression program that enables mammary gland remodeling after lactation.

In addition to elucidating developmental processes, studying the pathways that lead to cell death advances our understanding of carcinogenesis. Overcoming anoikis is considered an early step in tumor development (Taraseviciute et al. 2010; Leung and Brugge 2012; Pradeep et al. 2012). Inhibition of anoikis is also necessary for tumor cell metastasis (Douma et al. 2004). Thus, the ability of JNK to promote anoikis suggests that it may suppress

cancer. Indeed, in my breast cancer model, JNK loss on a sensitized background accelerates disease initiation (Figure IV.4A). These JNK-deficient tumor cells are largely similar to cells isolated from control tumors (Figure IV.14). However, JNK-deficient tumor cells have increased survival in suspension and they form more colonies in soft agar (Figure IV.14E-G). These observations indicate that loss of JNK in tumor cells reduces their sensitivity to anoikis. Furthermore, JNK-deficient mice exhibit mammary epithelial cell proliferation into the lumens earlier than Controls (Figure IV.15B, C). Considering that members of the JNK pathway are frequently mutated in human breast cancer (Nik-Zainal et al. 2016a), these observations have important implications for understanding disease initiation and progression.

The roles of the JNK pathway during puberty (Cellurale et al. 2012), involution (Chapter III), and mammary carcinogenesis (Chapter IV) illustrate its importance in mammary gland biology. However, the role of JNK in the gland during pregnancy and lactation has yet to be established (Figure V.1). My observation that female mice lacking JNK in their mammary epithelium have difficulty supporting litters after the first litter (Figure IV.5) suggests there may be a defect in the mammary glands of these mice. Whereas JNK deficiency does not impair mammary epithelial cell proliferation during pubertal development (Cellurale et al. 2012), it may be involved in the expansion of the epithelial compartment that occurs during pregnancy. The role that JNK plays in cell survival (Lamb et al. 2003) may also be important during pregnancy and

lactation, when the epithelial cells must resist premature involution. Alternatively, JNK pathway loss may affect the differentiation state of the epithelial cells, resulting in lactation defects. Indeed, the JNK pathway is involved in lineage-specific differentiation of embryonic stem cells (Xu and Davis 2010). It also has been shown to restrict stem cell populations (Hubner et al. 2012) and regulate differentiation (Davies et al. 2014) in adult tissues. In the mammary glands of *Mapk9*^{-/-} mice, the luminal epithelial cell population is expanded (Cantrell et al. 2015). My data showing transdifferentiation of mammary epithelial cells that have lost JNK (Figure IV.2A) provides additional evidence that this pathway may influence mammary epithelial cell fate. In addition to affecting the cycle of lactation and involution, this role for JNK could have implications for mammary carcinogenesis.

The studies described herein have focused exclusively on the importance of JNK in epithelial cells. However, the intricate crosstalk of epithelial and stromal cells regulates all stages of mammary biology and disease. Disruption of JNK signaling in these stromal cells might also impact involution and mammary carcinogenesis. For example, interleukin 6, a factor that promotes mammary gland involution (Zhao et al. 2002), has been shown to exhibit JNK-dependent expression in both macrophages and adipocytes (Sabio et al. 2008; Han et al. 2013). Similarly, JNK in macrophages induces the expression of inflammatory cytokines that are required for carcinogenesis in a model of hepatocellular carcinoma (Das et al. 2011; Han et al. 2016). Since breast carcinogenesis also

exploits macrophages to promote disease progression (Lin et al. 2002; Qian and Pollard 2010), this role for JNK in macrophages may apply to this disease.

Studies of JNK in the mammary stroma will likely reveal additional contributions of JNK to mammary gland biology, extending beyond its function in mammary epithelial cells.

This work has resolved the controversy surrounding the role of JNK in anoikis, uncovered an unappreciated role for JNK in involution, and established JNK as a tumor suppressor in the mammary epithelium. These types of studies are important for our understanding of when and how the JNK pathway functions. Since JNK inhibitors are being tested in the clinic, new insights into this pathway are crucial to develop better and safer therapies.

Future Directions

The work described herein has established a role for JNK in anoikis and demonstrated that JNK is involved in several aspects of mammary gland biology. While these studies have advanced our understanding of this pathway and mammary gland biology, they have also provided additional questions that form the basis of future work in these fields.

Future studies of JNK in anoikis:

(1) Hypothesis: Additional BH3-only proteins compensate for BIM and BMF in suspended, constitutive JNK-expressing BIM/BMF^{KO} cells.

In suspension culture, cell death increases in BIM/BMF^{KO} cells expressing the constitutively active JNK compared to vector controls (Figure II.10). This finding suggests that other BH3-only proteins compensate for BIM and BMF. To identify these compensating proteins, CRISPR/Cas9 gene editing could be used in BIM/BMF^{KO} cells to delete additional BH3-only proteins before inducing expression of the constitutively active JNK.

(2) Hypothesis: JNK-dependent expression of *Bcl2/11* through cJUN is a major contributor to anoikis.

Both chemical inhibition (Figure II.1E) and genetic ablation of JNK (Figure II.8A & II.9B) results in decreased *Bcl2/11* expression. Future studies could clarify the

importance of transcriptional regulation by JNK during anoikis and confirm that this regulation occurs through cJUN. Treatment of Control and JNK^{KO} cells with actinomycin D to inhibit transcription and cyclohexamide to inhibit translation would establish the importance of gene expression during anoikis. To specifically address the question of whether *Bcl2l1* expression is important for anoikis, a lentiviral vector expressing an inducible *Bcl2l1* could be introduced into JNK^{KO} kidney epithelial cells and the expression of *Bcl2l1* could be titrated to achieve levels present in suspended Control cells. Suspension culture experiments using the JUN point mutant (JUN^{AA}) that lacks the JNK phosphorylation sites (Behrens 1999) would determine the importance of JNK-mediated JUN activation in survival and gene induction during anoikis. Finally, ChIP assays examining cJUN binding of *Bcl2l1* would demonstrate that cJUN indeed regulates *Bcl2l1* expression in suspended kidney epithelial cells.

(3) Hypothesis: Cell death during suspension requires MAP2K4 and MAP2K7.

JNK is activated by MAP2K4 and MAP2K7 (Davis 2000). While both kinases are required for full activation of JNK, they do exhibit selectivity for certain stimuli (Tournier et al. 2001). Subjecting *Rosa-Cre^{ERT} Map2k4^{LoxP/LoxP}*, *Rosa-Cre^{ERT} Map2k7^{LoxP/LoxP}*, and *Rosa-Cre^{ERT} Map2k4^{LoxP/LoxP} Map2k7^{LoxP/LoxP}* cells to suspension culture and monitoring JNK activation, cell death, and gene expression would determine the relative contributions of these kinases to anoikis.

(4) Hypothesis: MAP3K1 is required for JNK activation and JNK-induced anoikis.

The upstream signals that activate JNK in response to anoikis remain unknown. Using a genetic approach, I determined that the MAP3Ks MLK2 and MLK3 are dispensable for epithelial cell anoikis (Figure II.3) indicating some other MAP3K is responsible for JNK pathway activation. MEKK1, another MAP3K, is a member of the JNK pathway that has been implicated in anoikis (Cardone et al. 1997). Using MEKK1-null cells (Yujiri et al. 1998), the role of this MAP3K in anoikis could be confirmed. To determine if MEKK1 signals through JNK during suspension, JNK activation in MEKK1-null and control cells could be examined. Assuming the MEKK1-deficient cells exhibit delayed anoikis, the constitutively active JNK could be used to rescue anoikis in these cells. This approach should be employed to assay the involvement of additional MAP3K, including MEKK2 (Kesavan et al. 2004), TAK1 (Shim et al. 2005), and ASK1 (Tobiume et al. 2001). It may be necessary to examine compound deficiencies of different combinations of the MAP3K because they can be partially redundant (Kant et al. 2011).

Future studies of JNK in mammary gland development:

(1) Hypothesis: JNK-mediated expression of *Bcl2l1* through cJUN contributes to TEB clearance.

Whole-mammary gland JNK loss leads to increased ductal branching and inhibits luminal cell clearance during pubertal mammary gland development (Cellurale et al. 2012). Gene expression analysis performed on a selection of genes in

Control and JNK-deficient mammary epithelial cells revealed changes in expression; however these expression changes could not explain the observed phenotype (Cellurale et al. 2012). It is known that loss of *Bcl2/11* leads to filled TEB (Figure II.12 & II.13) (Mailleux et al. 2007). Also, *Bcl2/11* is down-regulated in JNK-deficient cells (Figure II.8A, II.9B, & III.15A, B). Collectively, these observations suggest that decreased *Bcl2/11* expression in JNK-deficient TEB epithelial cells contributes to luminal infilling. Gene expression analysis of Control and JNK-deficient pubertal mammary glands would reveal if *Bcl2/11* expression is also decreased in this context. Rescuing the occluded lumen phenotype in transplanted JNK-deficient mammary glands using a doxycycline-inducible *Bcl2/11* could confirm the importance of JNK-mediated BIM expression. Furthermore, examining mammary gland development in JUN^{AA} (Behrens et al. 1999) mutant females would determine if a JNK/c-JUN pathway is involved in TEB luminal clearance.

(2) Hypothesis: The JNK pathway contributes to embryonic development of the mammary epithelium.

The JNK pathway is required for embryonic development (Kuan et al. 1999; Sabapathy et al. 1999). It also promotes developmental processes, including closure of the eyelids and the optic fissure (Weston et al. 2003; Weston et al. 2004). The role of JNK at this stage of mammary gland development is unknown. Because JNK-deficiency is embryonic lethal (Kuan et al. 1999; Sabapathy et al. 1999), a conditional deletion strategy must be applied. CRE

recombinase expression driven by the *Krt14* promoter has been used to assess the importance of other proteins in embryonic mammary gland development (Watson and Khaled 2008). Thus, *Krt14-Cre⁺ Mapk8^{LoxP} Mapk9^{LoxP}* mice could be generated to target JNK deletion to the developing mammary epithelium. Previous studies of JNK in development suggest that the JNK-deficient epithelial cells may exhibit a migration defect (Kuan et al. 1999; Sabapathy et al. 1999; Weston et al. 2003; Weston et al. 2004). However, JNK is dispensable for the migration of kidney epithelial cells *in vitro* (Appendix A) and of gut and mammary epithelial cells *in vivo* (Cellurale et al. 2012). Furthermore, unlike previously reported (Huang et al. 2003), JNK is not required for paxillin phosphorylation to promote migration (Appendix A). An understanding of JNK during mammary gland development at this stage would advance our understanding of the role of JNK in various cellular processes. These studies could also provide insight into the role of JNK during the development of branched epithelia.

(3) Hypothesis: The JNK pathway contributes to mammary gland development and function during pregnancy and lactation.

I observed that the percentage of surviving litters decreases with each subsequent pregnancy for females lacking JNK in their mammary epithelium (Figure IV.5). This observation suggests a defect in epithelial cell expansion and alveolar differentiation during pregnancy, or a lactation defect. Gland morphology should be examined in late pregnancy and at parturition to determine whether JNK loss has prevented the elaboration and expansion of the ductal

network. Furthermore, the differentiation of luminal cells to alveolar cells should be confirmed. Gene expression analysis could determine if any genes involved in milk production or secretion have been impacted by JNK loss.

Future studies of JNK in involution

(1) Hypothesis: JNK phosphorylation of cJUN rather than BIM and BMF regulates involution.

Which JNK targets are key for the progression of involution is unknown. Since BIM and BMF are JNK targets that have been implicated in involution (Sakamoto et al. 2016; Schuler et al. 2016), they are appealing candidates. Subjecting the BIM^{T112A} and BMF^{S74A} mutant mice to involution studies would determine if JNK phosphorylation of either of these effectors is important for cell death during the remodeling process. These experiments could also provide evidence of the physiological relevance of these phosphorylation sites *in vivo*. However, the *Bcl2l11*^{-/-} and *Bmf*^{-/-} involution phenotypes (Schuler et al. 2016) are not as dramatic as the phenotype observed in JNK^{KO} animals (Figure III.2), suggesting that JNK regulation of these proteins will not account for the involution defect in JNK^{KO} animals. Instead, JNK phosphorylation of transcription factors is the more likely means of regulating gland remodeling. This activation of transcription factors by JNK would account for the de-regulated gene expression program in JNK^{KO} glands during involution (Figure III.10). The finding that the JNK-

dependent genes are highly enriched for cJUN binding sites implicates this AP1 member (Figure III.12). Involution studies together with gene expression analysis using the JUN^{AA} mutant could assess the importance of JNK-mediated JUN phosphorylation in involution.

(2) Hypothesis: The AP1 members *Jun*, *Jund*, *Atf3*, and *Fos/2* are responsible for the JNK-dependent gene expression program during involution.

The expression of *Jun*, *Jund*, *Atf3*, and *Fos/2* was significantly decreased in JNK^{KO} glands during involution (Figure III.9). To determine the relevance of this down-regulation and establish the relative contributions of these transcription factors to the involution response, mice expressing conditional *Jun* (Behrens et al. 2002), *Atf3* (Taketani et al. 2012), and *Fos/2* (Karreth et al. 2004) genes could be used. Similarly, mice expressing conditional *Jund* should be generated to study the role of JUND in involution.

(3) Hypothesis: Loss of JNK in mammary epithelial cells affects gene expression in the epithelium and stroma.

In my approach, I used whole tissue lysates for RNA isolation and sequencing. The next step is to systematically dissect gene expression in different cell populations of the involuting gland. This goal can be achieved by crossing reporter mice, for example *Rosa^{mTmG}* mice (Muzumdar et al. 2007), to the JNK^{KO} and Control animals and purifying epithelial cells before RNA isolation in order to determine which genes are directly affected by JNK loss. Similarly, the

Rosa^{NuTRAP} (Roh et al. 2017) allele could be used to isolate epithelial cell mRNA and nuclei. Comparing the gene expression changes in epithelial cells to changes in the whole tissue lysate could suggest which changes occur indirectly in other cell types as a consequences of JNK loss in epithelial cells. Examples of non-epithelial changes could include different rates of repopulation by adipocytes, changes in immune cell infiltrates, or altered gene expression in stromal cells due to aberrant signals from epithelial cells as a result of JNK loss. Further sorting of cells for RNA isolation could be done based on cell surface markers.

(4) Hypothesis: JNK ablation in stromal cells of the mammary gland will disrupt involution.

Adipocytes and macrophages participate in mammary gland remodeling after lactation by secreting factors that can promote involution (O'Brien et al. 2010; O'Brien et al. 2012; Martinson et al. 2015). An example of a secreted factor implicated in promoting involution is IL6, although the source of IL6 has not been determined (Zhao et al. 2002; O'Brien et al. 2012). Interestingly, *Il6* exhibits JNK-dependent expression in adipocytes and macrophages (Sabio et al. 2008; Han et al. 2013). Studies of mice with JNK-deficient adipocytes and myeloid cells could determine the importance of JNK in these cell types during involution. Additionally, these studies could provide more insight into the source of IL6 and determine if it is expressed in a JNK-dependent manner during involution.

(5) Hypothesis: The ERK and p38 MAPK pathways are regulators of involution.

The importance of JNK during involution suggests that the other MAPK pathways may also participate in this process. For example, the p38 MAPK pathway induces BIM expression during anoikis and is required for luminal clearance during pubertal mammary gland development (Wen et al. 2011). Furthermore, it plays a role in luminal epithelial cell fate (Del Barco Barrantes et al. 2018). The ERK pathway is also likely to contribute to involution. It is activated during early involution (Zhao et al. 2002) and it can phosphorylate STAT3 (Chung et al. 1997). These observations together with my data regarding JNK in involution suggest that similar studies should be performed to establish the roles of ERK and p38 MAPK during involution.

Future studies of JNK in breast cancer:

(1) Hypothesis: The early lesions in Control and JNK-deficient mammary glands exhibit gene expression and mutational load differences.

Despite the dramatic acceleration of tumor onset in the absence of JNK (Figure IV.4A), JNK-deficient tumors closely resemble Control tumors. This observation suggests that the early stages of carcinogenesis account for the different phenotypes. Thus, analysis of these early lesions could be performed to gain insight into the mechanism of JNK tumor suppression. These studies could include RNA sequencing to examine gene expression changes and pathway

deregulation, and DNA sequencing to determine genomic stability. The *Rosa^{mTmG}* (Muzumdar et al. 2007) allele could be used to label the mammary epithelial cells for isolation. Alternatively, the *Rosa^{NuTRAP}* (Roh et al. 2017) allele could be introduced into the mice to directly isolate the mRNA and nuclei.

(2) Hypothesis: *Map2k4* loss in the mammary epithelium accelerates carcinogenesis on a sensitized background.

Mutations in *MAP2K4* and *MAP3K1* are frequently found in human breast cancer (Cancer Genome Atlas 2012; Stephens et al. 2012; Nik-Zainal et al. 2016a). However, JNK mutations are not. The reason for this may be that the ubiquitously expressed JNK1 and JNK2 proteins have largely redundant functions. It is likely that deletion of *Map2k4* in this model would result in accelerated tumor formation. However, MAP2K4 has additional targets. Studies of *Map2k4*-deficient mammary epithelial cells and conditional mice will further uncover the role of this mutation in human disease. Such studies considered in the context of my data from JNK-deficient tumors could inform the contributions of additional pathways (e.g., p38 MAPK) to mammary carcinogenesis.

(3) Hypothesis: The role of JNK in carcinogenesis depends on the genetic context.

My studies demonstrate that epithelial cell JNK suppresses breast cancer. This finding is somewhat surprising given that JNK activates an oncogene (cJUN) and that other oncogenes, such as ERBB2, may rely on JNK activity (Guo et al.

2006). Furthermore, unpublished data from our lab suggest that mammary epithelial cells expressing activated ERBB2 require JNK for acinus formation in Matrigel. To test if JNK is a tumor suppressor in other genetic backgrounds, the conditional JNK alleles can be crossed to a mouse expressing *ErbB2*-IRES-*Cre* under the control of the MMTV promoter (Ursini-Siegel et al. 2008). In this mouse, JNK loss would be targeted to *ErbB2*-expressing mammary epithelial cells, and breast tumor formation could be compared to the *ErbB2*-IRES-*Cre* animals.

(4) Hypothesis: JNK loss promotes tumor cell metastasis.

The ability of JNK to promote anoikis in epithelial cells and tumor cells suggests that loss of JNK may promote metastasis. By crossing the JNK conditional alleles into a breast cancer model with reported metastasis, I could assay its importance in this process. E-cadherin loss has been shown to increase metastasis of breast tumors in mice (Derksen et al. 2006). Thus, cohorts of *Wap-Cre*^{-/+} *Trp53*^{LoxP/LoxP} and *Wap-Cre*^{-/+} *Trp53*^{LoxP/LoxP} *Mapk8*^{LoxP/LoxP} *Mapk9*^{LoxP/LoxP} mice with additional E-cadherin loss could be examined. To determine if JNK loss in human breast cancer increases metastasis, a study could be performed examining the correlation between metastasis and *MAP2K4* or *MAP3K1* mutations.

(5) Hypothesis: JNK loss in tumor cells will increase cell sensitivity to certain treatments.

Cancer therapies are becoming personalized, with tumor mutations informing treatment strategies. One example of this type of approach is the administration of PARP inhibitors to patients with *BRCA1/2* mutations (Sonnenblick et al. 2015). The loss of *BRCA1/2* inactivates homologous recombination in tumor cells and the addition of PARP inhibitors renders them incapable of resolving DNA damage, leading to tumor cell death. The JNK pathway has also been implicated in genome maintenance (Chen et al. 2010; Van Meter et al. 2016; Calses et al. 2017) and in the expression of DNA damage response proteins following cisplatin treatment (Hayakawa et al. 2004). Thus, tumors that have lost JNK pathway activity through mutations may be more susceptible to certain genotoxic drugs. I have initiated studies examining this possibility (Appendix B).

(6) Hypothesis: JNK inhibitors can improve the response of cells to therapies currently used in the clinic.

Co-treatment with a JNK inhibitor may sensitize tumor cells to drugs already used in the clinic, either by inactivating DNA damage repair (previous hypothesis) or by an alternative mechanism. Indeed, combined JNK and RAF inhibitor treatment in melanoma cells that express the mutant BRAF^{V600E} protein results in a substantial increase in cell death relative to RAF inhibitors alone (Fallahi-Sichani et al. 2015). Similarly, in triple negative breast cancer cells, co-treatment of lapatinib and JNK inhibitors results in enhanced cell death (Ebelt et al. 2017).

While promising, these findings are restricted to a small subset of tumor types. Exploring additional drug combinations with JNK inhibitors in more tumor cell lines is therefore warranted. I have initiated these studies (Appendix B).

(7) Hypothesis: JNK expression in myeloid cells is required for carcinogenesis.

JNK loss in macrophages can prevent hepatocellular carcinoma due to decreased inflammation (Das et al. 2011; Han et al. 2016). Macrophages and the associated inflammation are implicated in breast cancer (Lin et al. 2002; Qian and Pollard 2010). It is unknown if JNK deficiency in macrophages would similarly suppress breast cancer. Myeloid cell-specific JNK loss in breast cancer models could assay the impact of myeloid JNK on mammary carcinogenesis.

Final Conclusion

In conclusion, I have established that JNK promotes anoikis and is a key player in mammary gland biology. In addition to regulating normal mammary gland development, JNK suppresses carcinogenesis in the breast epithelium. These studies have answered several questions in the field and uncovered exciting new avenues of research. Confirming these observations in humans will be an important next step.

APPENDIX A

JNK IS DISPENSABLE FOR EPITHELIAL CELL MIGRATION

Abstract

Developmental morphogenesis, maintenance of tissue architecture, healing, invasion, and metastasis all require cell movement. The cJUN NH₂-terminal kinase (JNK) pathway is required for the proper execution of several developmental processes that rely on cell migration. This observation led to mechanistic studies that implicated JNK as a positive regulator of focal adhesion turnover through phosphorylation of paxillin. However, JNK is dispensable during mammary epithelial cell migration through the fat pad and for gut epithelial cell migration along villi. These conflicting results indicate that the role of JNK in cell migration may be more nuanced than previously appreciated. Using a genetic ablation strategy in epithelial cells, I assayed the importance of JNK in migration. I found that JNK is dispensable for both cell migration and paxillin phosphorylation in kidney epithelial cells. Additionally, conditioned media from JNK-deficient cells did not promote Control cell migration. These observations indicate that the role of JNK in migration has been over-simplified and warrants additional study.

Introduction

Cell migration is critical during developmental morphogenesis and tissue homeostasis. Dorsal closure in *Drosophila* requires migration of epithelial cells to join at the dorsal midline (Ring and Martinez Arias 1993). Analogous processes occur during mammalian developmental morphogenesis to close the neural tube and optic fissure (Morriss-Kay 1981; Weston et al. 2003). In the pubertal mammary gland, branching morphogenesis involves luminal and myoepithelial cell migration to elaborate the ductal network (Ewald et al. 2008). Defects in cell motility would prevent the proper execution of these processes.

Cell motility depends on dynamic assembly and disassembly of cell adhesions (Webb et al. 2002). These adhesions contain many proteins, including paxillin, which coordinates signaling through its numerous binding sites and docking motifs (Schaller 2001). Phosphorylation of paxillin at serine 178 prevents focal adhesions from forming, keeping cells poised to migrate (Huang et al. 2003). The cJUN NH₂-terminal kinase (JNK) has been shown to phosphorylate this site, and JNK inhibition results in decreased paxillin phosphorylation and consequent reduced cell motility (Huang et al. 2003).

There are 2 ubiquitously expressed JNK proteins, JNK1 and JNK2 (encoded by *Mapk8* and *Mapk9*), as well as the neuronally-restricted JNK3 (encoded by *Mapk10*) (Davis 2000). JNK1 and JNK2 are largely redundant (Tournier et al. 2000), although there is evidence for differences between their

function or expression (Weston et al. 2004). JNK activation requires phosphorylation by both MAP kinase kinase 4 (MAP2K4) and MAP kinase kinase 7 (MAP2K7) (Tournier et al. 2001). These MAP2K are activated by a number of MAP kinase kinase kinases, or MAP3K (Davis 2000).

Developmental defects observed in JNK pathway-deficient animals support a role for this pathway in cell migration. Mice that lack MAP3K1, one of the MAP3K in the JNK pathway, are born with their eyes open (Yujiri et al. 2000; Zhang et al. 2003). Similarly, reduced JNK protein levels (Weston et al. 2004) or deletion of the JNK target cJUN (Zenz et al. 2003) prevents eyelid closure in mice due to decreased EGFR pathway activity. During embryonic development, the JNK pathway is required for neural tube closure in mice and dorsal closure in *Drosophila* (Riesgo-Escovar et al. 1996; Sluss et al. 1996; Riesgo-Escovar and Hafen 1997; Kuan et al. 1999; Sabapathy et al. 1999).

These observations together with the mechanistic studies demonstrating paxillin phosphorylation by JNK (Huang et al. 2003) and *in vitro* experiments employing JNK inhibitors and dominant-negative mutants (Huang et al. 2004) have led to the conclusion that the JNK pathway is required for cell migration (Xia and Karin 2004). However, in several cell types JNK is dispensable for migration, including intestinal and mammary epithelial cells (Cellurale et al. 2012), mouse embryonic fibroblasts (MEFs) (Ventura et al. 2004b), and endothelial cells (Ramo et al. 2016). Furthermore, in neurons JNK activity impedes, rather than promotes, cell migration through MARCKSL1-mediated

actin stabilization (Bjorkblom et al. 2012). These data refute the notion that JNK is required for migration.

To determine the importance of JNK in epithelial cell migration, I used kidney epithelial cells in which JNK was genetically ablated. A comparison of paxillin phosphorylation in Control and JNK-deficient cells revealed no defects in the mutant cells, suggesting that another protein may compensate for JNK. Additionally, loss of JNK in these cells did not result in a migration defect and instead enhanced cell migration under certain conditions. These findings indicate that the role of JNK in epithelial cell migration is not as simple as previously concluded (Xia and Karin 2004).

Results

Paxillin phosphorylation at serine 178 is present in JNK-deficient cells

To study the role of JNK in cell migration, I used the previously described *Rosa-Cre^{ERT/+} Mapk8^{LoxP/LoxP} Mapk9^{-/-}* kidney epithelial cells (Girnius and Davis 2017a). Treatment with 4-hydroxy tamoxifen ablates *Mapk8*, resulting in JNK-deficient cells (JNK^{KO}). Because JNK deficiency can induce cellular senescence (Das et al. 2007) or increased proliferation (Cellurale et al. 2012), I monitored Control (*Rosa-Cre^{ERT/+}*) and JNK^{KO} cell growth. Cell proliferation was comparable between genotypes whether cells were cultured in the presence or absence of serum (Figure A.1A). Likewise, bromodeoxyuridine (BrdU) incorporation at the leading edge of a wound was no different between JNK^{KO} and Control cells (Figure A.1B).

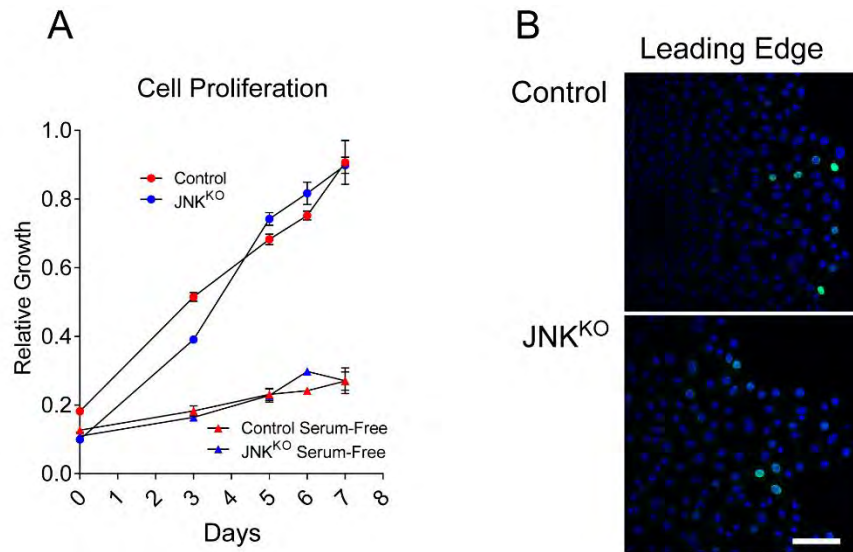


Figure A.1. JNK-deficient cells proliferate comparably to Control cells.

A) *Rosa-Cre^{ERT/+}* (Control) and *RosaCre^{ERT/+} Mapk8^{LoxP/LoxP} Mapk9^{-/-}* (JNK^{KO}) kidney epithelial cells were cultured in growth media and serum-free media. Cell proliferation was monitored by crystal violet stain at 0, 3, 5, 6, and 7 days, and the growth relative to day 0 was calculated (mean \pm SEM; n=2-3). Similar data was obtained from 2 additional experiments.

B) Confluent monolayers of Control and JNK^{KO} cells on coverslips were wounded, incubated with bromodeoxyuridine (BrdU, 10 μ M) for 4 h, then stained with an antibody for BrdU and counterstained with DAPI. Scale bar = 75 μ m.

A proposed mechanism for JNK promotion of migration involves phosphorylation of serine 178 on paxillin by JNK, allowing turnover of focal adhesions (Huang et al. 2003). To examine paxillin phosphorylation in the kidney epithelial cells, I irradiated Control and JNK^{KO} cells with ultraviolet (UV) light to activate the JNK pathway and performed immunoblot analysis for Paxillin phosphorylated on serine 178. Paxillin phosphorylation was dramatically induced in Control cells 60 minutes after UV exposure (Figure A.2A). Interestingly, JNK^{KO} cells also had substantially elevated levels of phospho-Ser178 Paxillin at 60 minutes after UV exposure (Figure A.2A). Furthermore, phosphorylated Paxillin was also evident in Control and JNK^{KO} cells 30 minutes post-UV exposure (Figure A.2B), indicating that JNK is not necessary for this phosphorylation event.

To determine whether the JNK pathway was necessary for paxillin phosphorylation in another cell type, I exposed JNK pathway-inactivated *Map2k4*^{-/-} *Map2k7*^{-/-} immortalized MEFs to UV. Phosphorylation of serine 178 on paxillin was evident in the Control cells following UV exposure (Figure A.2C). *Map2k4*^{-/-} *Map2k7*^{-/-} MEFs also exhibited paxillin phosphorylation, albeit at lower levels than the Control cells indicating less phosphorylation or increased de-phosphorylation (Figure A.2C). These results indicate that another kinase (or kinases) is able to phosphorylate paxillin on Ser¹⁷⁸. Thus, JNK is not required for phosphorylation of Paxillin at Ser¹⁷⁸.

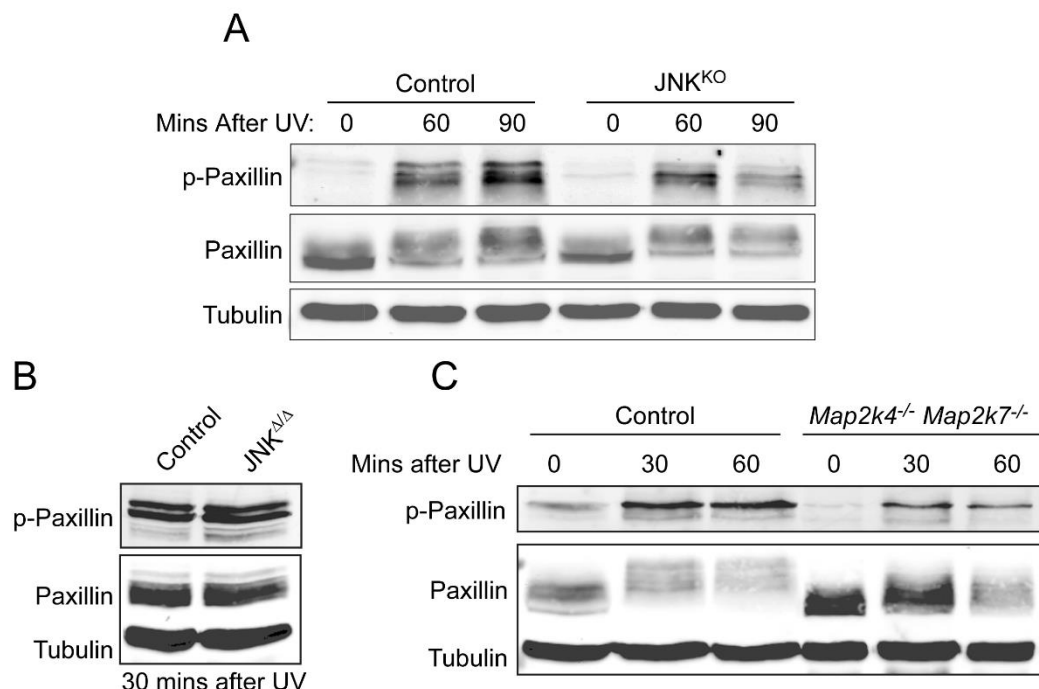


Figure A.2 Paxillin is phosphorylated at serine 178 in cells despite JNK pathway inactivation.

A) Control and JNK^{KO} kidney epithelial cells were exposed to 60 J/m² of ultraviolet light (UV) and cultured for the indicated times before cell lysates were prepared. Immunoblot analysis was performed using antibodies for Paxillin phosphorylated at serine 178 (p-Paxillin), Paxillin, and JNK. α -Tubulin served as a loading control.

B) Cell lysates were made from Control and JNK^{KO} kidney epithelial cells 30 minutes after UV (60 J/m²) exposure. Immunoblot analysis for Paxillin and p-Paxillin. α -Tubulin served as a loading control.

C) Immortalized Control and Map2k4^{-/-} Map2k7^{-/-} mouse embryonic fibroblasts were cultured post-UV exposure for the indicated times. Immunoblot analysis was performed on cell lysates using antibodies for Paxillin and p-Paxillin. α -Tubulin served as a loading control.

JNK is not required for cell migration

The observation that JNK is not required for Paxillin phosphorylation suggested that the JNK^{KO} kidney epithelial cells would not exhibit a migration defect. To test this hypothesis, confluent monolayers of Control and JNK^{KO} cells growing on collagen I, collagen IV, fibronectin, or laminin were scratched with a pipet tip and monitored for infilling of the scratched area. In these “wound healing assays”, the epithelial cells moved as sheets to “heal” the wound made by scratching. The Control cells had closed approximately 20-30% of the original wound 24 h after assay initiation, regardless of the surface coating (Figure A.3A). While the JNK^{KO} cells migrating on collagen I and laminin coated surfaces had healed similarly to Control cells after 24 h, the JNK^{KO} cells migrating on collagen IV, fibronectin, or tissue culture dishes healed wounds faster than Control cells (Figure A.3A). Analysis of wound healing after 48 h of migration showed that JNK^{KO} cells migrating on any of the tested substrates healed more of the original wound area than Control cells (Figure A.3B). Continuous monitoring of wound closure (4 h intervals) similarly showed that JNK-deficient cells migrated more rapidly than Control cells (Figure A.3C).

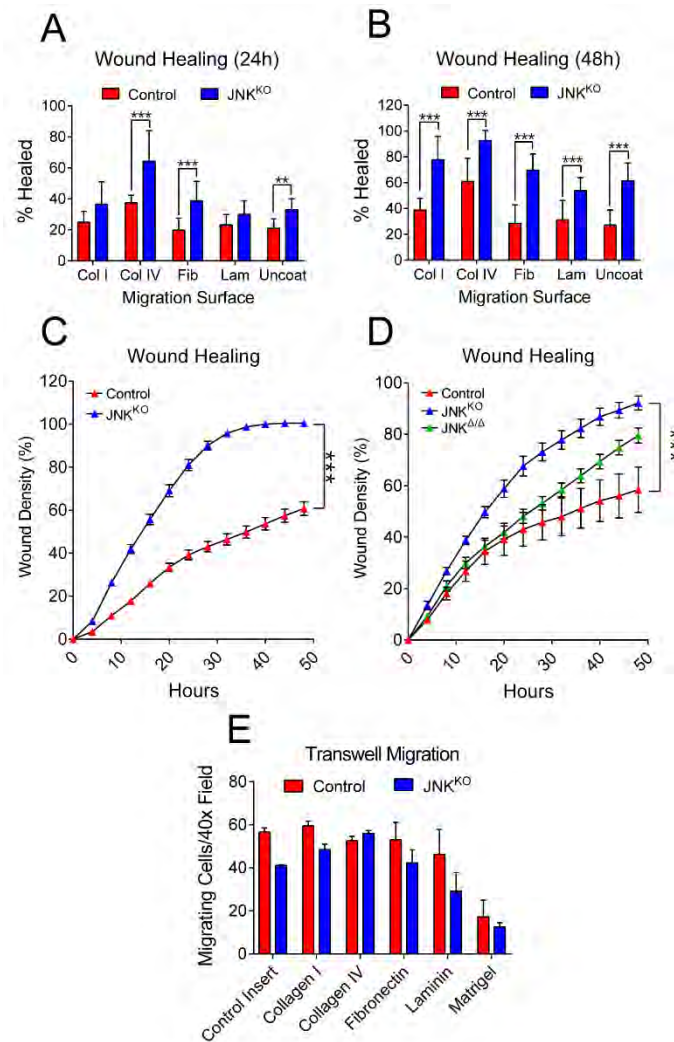


Figure A.3. Compound JNK-deficiency does not inhibit migration of kidney epithelial cells.

A, B) Confluent monolayers of Control and JNK^{KO} kidney epithelial cells were wounded and given low serum media. After 24 (A) or 48 (B) h the wound area was quantified and the percent healed was calculated based on the wound width at 0 h (mean ± SEM; **p<0.01, ***p<0.001, n=9-14). Similar data were obtained from 2 additional experiments.

C, D) Migration of confluent monolayers of Control and JNK^{KO} kidney epithelial cells (n=24) (C), or Control, JNK^{KO}, and JNK^{Δ/Δ} (*Mapk8^{ff} Mapk9^{ff} Rosa-Cre^{ERT}*) cells (n=7-8) (D) was monitored continuously every 4 h for 48 h using an IncuCyte ZOOM. The wound density was quantified (mean ± SEM; ***p<0.001). Similar data were obtained from 2 (C) or 1 (D) additional experiment.

E) Control and JNK^{KO} kidney epithelial cells were plated in transwells coated with the indicated matrix proteins. Migration was induced with a serum gradient (0 to 10%). After 20 h, migrating cells were quantified (mean \pm SEM of migrating cells/40x field). Similar data were obtained in 2 additional experiments. No significant differences were observed ($p > 0.05$, $n = 3$).

Throughout their life, the JNK^{KO} cells never expressed JNK2. Thus, the observed migration phenotype could be the result of compensation that occurred as a result of the absence of JNK2. To eliminate this possibility and confirm that JNK ablation promotes wound closure, I assayed the migration of *Rosa-Cre^{ERT}/+* *Mapk8^{LoxP/LoxP} Mapk9^{LoxP/LoxP}* (JNK^{Δ/Δ}) kidney epithelial cells. In contrast to the JNK^{KO} cells, these cells expressed both JNK proteins throughout development and had only experienced JNK loss after 4-hydroxy tamoxifen administration. Like the JNK^{KO} cells, the JNK^{Δ/Δ} cells migrate comparably to Control cells. However, the JNK^{Δ/Δ} cells do not exhibit the significantly increased rate of wound closure observed in the JNK^{KO} cells (Figure A.3D).

To examine individual cell migration instead of epithelial sheet migration, I performed Boyden chamber assays with collagen I, collagen IV, fibronectin, laminin, matrigel, or uncoated transwells. Regardless of transwell coating, there were no significant differences ($p > 0.05$) between Control and JNK^{KO} cell migration (Figure A.3E). Taken together, these data show that JNK is not essential for kidney epithelial cell migration.

JNK inhibitors produce different migration phenotypes

The evidence for JNK pathway promotion of migration comes largely from JNK inhibitor-based approaches (Huang et al. 2003; Huang et al. 2004). To test how drugs targeting the JNK pathway would impact kidney epithelial cell migration,

wound healing assays were performed in the presence of the commonly used JNK inhibitor SP600125. Surprisingly, SP600125 significantly increased Control and JNK^{KO} cell migration relative to their respective vehicle treated controls (Figure A.4A). This finding suggests that the previously observed changes in cell migration during JNK pathway inhibition may be the result of off-target effects of SP600125 (Bain et al. 2007).

A more specific JNK inhibitor (JNK-IN-8) has been developed (Zhang et al. 2012). Treatment of Control and JNK^{KO} cells with JNK-IN-8 had no effect on wound closure (Figure A.4B). Unlike treatment with SP600125 (Figure A.4A), JNK-IN-8 treatment did not enhance cell migration in either genotype (Figure A.4B). In the context of the JNK-deficient cells, this observation supports the conclusion that JNK-IN-8 is a highly specific JNK inhibitor. The inability of JNK-IN-8 treatment of Control cells to phenocopy genetic ablation of JNK may be evidence of off-target effects of the inhibitor or compensation in the JNK-deleted cells. Nevertheless, JNK-IN-8 treatment of Control cells also did not inhibit cell migration (Figure A.4B).

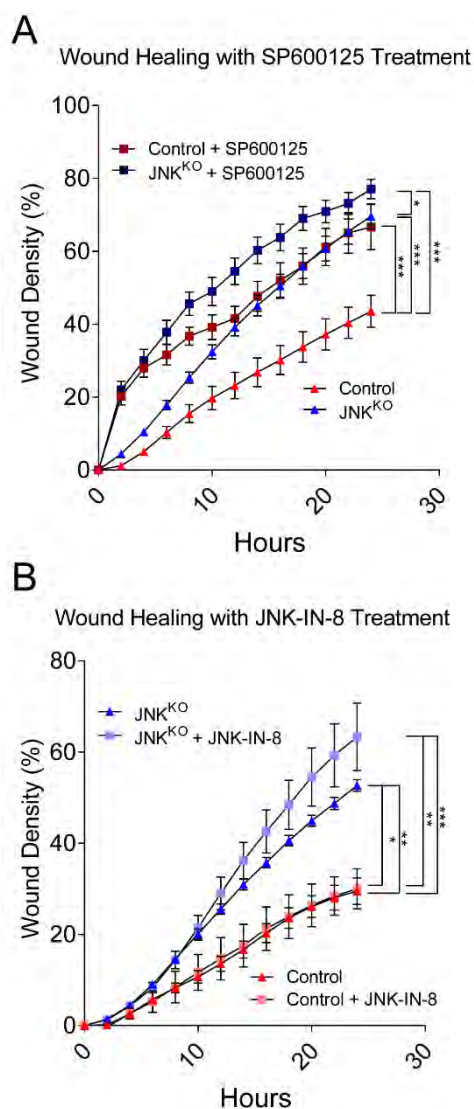


Figure A.4. Motility of Control cells is not repressed by JNK inhibitor treatment.

A, B) Confluent monolayers of Control and JNK^{KO} kidney epithelial cells were wounded and given low serum media with or without different JNK inhibitors (40 μ M SP600125 in A (n=6-18) or 5 μ M JNK-IN-8 in B (n=3-10)). Wound density was quantified every 4 h for 48 h using an IncuCyte ZOOM (mean \pm SEM; *p<0.05, ***p<0.01). Similar data were obtained in an additional experiment.

The enhanced migration in cells with genetic JNK inactivation may be the result of time course effects of JNK loss. Thus, acute loss of JNK activity through inhibitor treatment would produce a different migratory phenotype than JNK loss through gene deletion. As an alternative means to examine acute JNK pathway inhibition, I tested the effects of the drug 1-naphthylmethyl-4-amino-1-*tert*-butyl-3-[*p*-methylphenyl]pyrazolo(3,4-*d*)pyrimidine (NMPP1) on cells isolated from *Mapk8*^{-/-} *Mapk9*^{MG/MG} mice (Jaeschke et al. 2006). These mice express a JNK2 protein with an enlarged ATP binding pocket (Ventura et al. 2006) that allows targeted protein inhibition by treatment with NMPP1. Treatment of *Mapk8*^{-/-} *Mapk9*^{MG/MG} with NMPP1 cells did not affect transwell migration in response to a serum gradient (Figure A.5A). In wound healing assays, NMPP1 treatment of *Mapk8*^{-/-} *Mapk9*^{MG/MG} cells resulted in significantly delayed wound closure relative to vehicle-treated *Mapk8*^{-/-} *Mapk9*^{MG/MG} cells (Figure A.5B). However, WT cells treated with NMPP1 also healed wounds significantly slower than the vehicle-treated cells (Figure A.5B). This decreased cell motility is likely the result of inhibition of additional kinases by NMPP1 (Bain et al. 2007). Previous studies in MEFs had not observed NMPP1-mediated inhibition of cell migration in Control cells (Jaeschke et al. 2006). The use of different cell types in these studies likely accounts for this discrepancy. Thus, studies of the JNK pathway using drug-based approaches must be executed with caution.

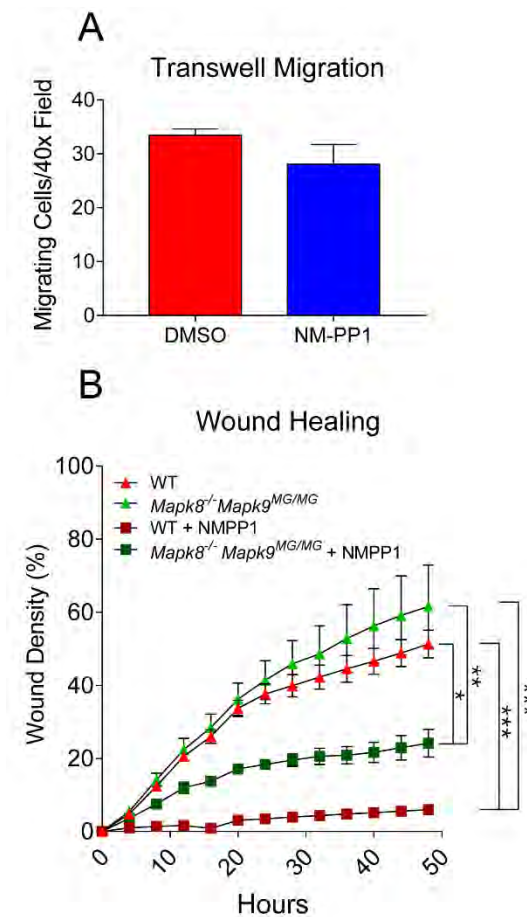


Figure A.5. Treatment of kidney epithelial cells with NMPP1 decreases wound healing regardless of genotype.

A) *Mapk8*^{-/-} *Mapk9*^{MG/MG} cells were plated in transwells and treated with vehicle (DMSO) or NMPP1. Cell migration was induced with a serum gradient (0 to 10%). Migrating cells were quantified (mean ± SEM of migrating cells/40x field; n=3). Similar data were obtained from 2 additional experiments.

B) Confluent monolayers of WT and *Mapk8*^{-/-} *Mapk9*^{MG/MG} cells were wounded and given low serum media with DMSO or NMPP1. Wound density was monitored every 4 h for 48 h using an IncuCyte ZOOM (mean ± SEM; n=2-5; ***p<0.01). Similar data were obtained in an additional experiment.

Relative contribution of JNK1 and JNK2 to migration

JNK1 and JNK2 serve partially redundant functions (Davis 2000; Tournier et al. 2000). However, there are distinct roles for JNK1 and JNK2 as evidenced by the eyes-open-at-birth phenotype observed in *Mapk8^{-/-} Mapk9^{+/-}* mice in contrast to the healthy *Mapk8^{+/-} Mapk9^{-/-}* mice (Weston et al. 2004). To assess the relative contributions of JNK1 and JNK2 to kidney epithelial cell migration, wound healing assays were performed with *Mapk8^{-/-}*, *Mapk9^{-/-}*, and WT cells. Neither *Mapk8^{-/-}* nor *Mapk9^{-/-}* cells exhibited reduced cell migration (Figure A.6). Indeed, *Mapk8^{-/-}* cells closed wounds faster than *Mapk9^{-/-}* or control cells, indicating that JNK1 may be the major isoform inhibiting cell migration in kidney epithelial cells (Figure A.6).

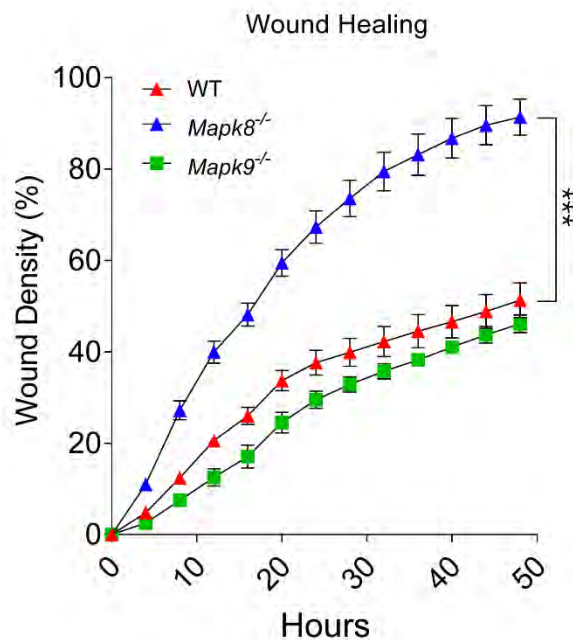


Figure A.6. Loss of JNK1 promotes wound healing.

Migration of confluent monolayers of C57Bl6/J (WT), *Mapk8*^{-/-}, and *Mapk9*^{-/-} kidney epithelial cells was monitored every 4 h for 48 h using an IncuCyte ZOOM and wound density was quantitated. Data (mean \pm SEM) from 1 of 2 representative experiments is presented (***p* < 0.001, *n* = 4-5).

Secreted factors from JNK-deficient cells do not enhance Control cell migration

The increased motility of JNK-deleted cells may be the result of a secreted factor that enhances migration. Indeed, JNK deficiency in MEFs causes increased TGF β expression, resulting in more motile cells (Ventura et al. 2004b). Gene expression analysis demonstrated that JNK^{KO} kidney epithelial cells expressed significantly increased TGF β message compared to control cells (Figure A.7A).

If JNK deficiency results in the production of migration-promoting secreted factors, then conditioned media from JNK^{KO} cells should enhance Control cell migration. To test this hypothesis, I applied conditioned media from migrating Control and JNK^{KO} cells on Control cells as well as JNK^{KO} cells. Regardless of which conditioned media the cells received, monolayers of JNK^{KO} cells healed wounds faster than Control monolayers (Figure A.7B,C). Furthermore, wound closure by Control cells was unaffected by the media they received (Figure A.7B,C). Thus, I found no evidence that the increased motility of JNK^{KO} cells is the result of a secreted factor stimulating migration.

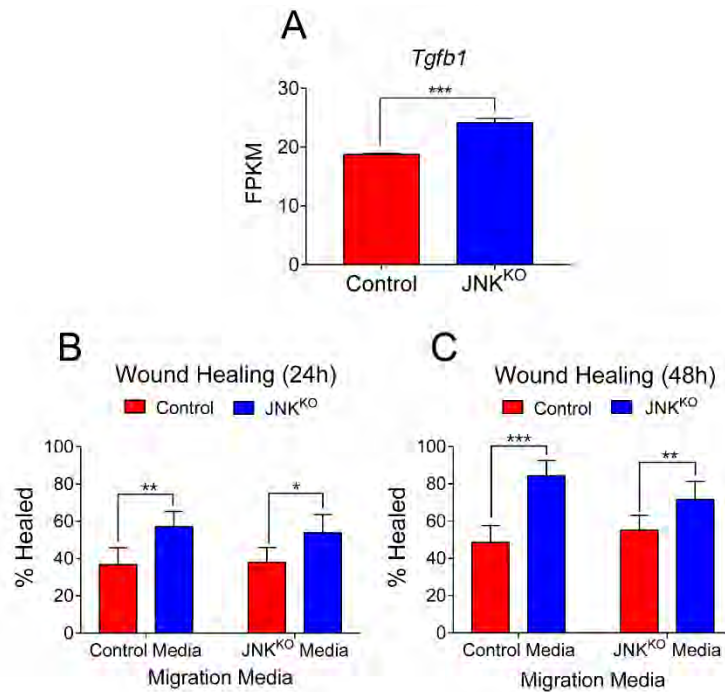


Figure A.7. Cell migration in response to conditioned media.

A) RNA sequencing was performed on Control and JNK^{KO} kidney epithelial cells. The expression of *Tgfb1* is presented as the mean fragments per kilobase of exon model per million mapped fragments (FPKM) \pm SEM (n=3; ***p<0.01).

B, C) Wound healing of confluent monolayers of Control and JNK^{KO} kidney epithelial cells was monitored (48 h). During the assay, cells were treated with media from plates of migrating Control or JNK^{KO} cells. Wound area was measured at 0, 24 and 48 h. The percentage healed was calculated and expressed as mean \pm SEM at 24 h (B) and 48 h (C). Data from 1 of 3 experiments are presented (n=6; ***p<0.001, **p<0.01, *p<0.05).

Discussion

It is widely accepted that JNK is a key promoter of cell migration (Huang et al. 2004). While observations based on experiments using JNK inhibitors may produce misleading results, observations from developmental studies of JNK-deficient animals support this conclusion (Riesgo-Escovar et al. 1996; Sluss et al. 1996; Riesgo-Escovar and Hafen 1997; Kuan et al. 1999; Sabapathy et al. 1999; Weston et al. 2003; Weston et al. 2004).

However, JNK-deficient adult colonic and intestinal epithelial cells show no defects in migration, and mammary epithelial cells devoid of JNK are also capable of migrating efficiently through the fat pad to elaborate ductal trees (Cellurale et al. 2012). Furthermore, observations made *in vitro* using mammary epithelial cells (Cellurale et al. 2012) in conjunction with my findings (Figure A.3) demonstrate that JNK in several epithelial cell types is dispensable for migration. These conflicting results indicate that the role of JNK in cell migration is more complicated than was previously thought.

How JNK regulates motility is not clear and may depend on cell type. Through AP1 transcription factors such as cJUN, JNK can regulate the expression of secreted factors that promote migration. Examples of such secreted proteins include TGF β in MEFs (Ventura et al. 2004b) or EGF in epidermal cells (Weston et al. 2004). However, I found no evidence that the expression of secreted factors promotes JNK^{KO} kidney epithelial cell migration

(Figure A.7B,C). Whereas JNK loss may not result in the production of secreted factors that promote migration, it may alter the cell surface receptor repertoire of JNK^{KO} cells. The differences in receptor expression could result in different sensitivities to these factors. Thus, examining candidate receptor expression and activation as well as downstream signaling in these two genotypes may reveal differences that would account for the increased motility of JNK^{KO} cells.

Another method for JNK to regulate migration could be through phosphorylation of proteins involved in migration, such as paxillin (Huang et al. 2003). The presence of phosphorylated paxillin in JNK-deficient cells (Figure A.2) indicates that another kinase (or kinases) compensates for JNK, allowing the kidney epithelial cells to migrate. Alternatively, JNK phosphorylation of paxillin may not be required for kidney epithelial cell migration. In neurons, JNK phosphorylation of MARCKSL1 results in actin stabilization and increased filopodia, leading to reduced migration (Bjorkblom et al. 2012). This function of MARCKSL1 is dominant to paxillin: MARCKSL1 expression in MEFs reverses the SP600125-mediated inhibition of migration in these cells, restoring cell motility to normal levels (Bjorkblom et al. 2012). The relevance of the JNK/MARCKSL1 pathway in kidney epithelial cell migration remains to be studied.

In conclusion, my study demonstrates that the role of JNK signaling in cell migration is more nuanced than previously appreciated (Xia and Karin 2004). Based on the data presented, it is clear that kidney epithelial cells do not require

JNK for their motility. Future mechanistic studies will not only clarify how JNK regulates kidney epithelial cell migration, but may also elucidate the reasons for the different migratory phenotypes observed across various cell types.

Materials and Methods

Mice

RosaCre^{ERT/+} Mapk8^{LoxP/LoxP} Mapk9^{-/-} mice (Das et al. 2007), *Mapk8^{-/-} Mapk9^{MG/MG}* mice (Jaeschke et al. 2006), *Mapk8^{-/-}* (Dong et al. 1998), *Mapk9^{-/-}* (Yang et al. 1998) mice, and *Mapk8^{LoxP/LoxP} Mapk9^{LoxP/LoxP}* mice (Han et al. 2013) have been previously described. C57BL/6J mice (Stock # 000664; RRID:IMSR_JAX:000664) and B6;129-Gt(*ROSA*)26Sor^{tm1(cre/ERT)Nat/J} mice (Stock # 004847; RRID:IMSR_JAX:004847) (Badea et al. 2003) were purchased from Jackson Laboratories. The mice were housed in a specific pathogen-free facility accredited by the American Association of Laboratory Animal Care. Both male and female mice (age 8 wks) were used to establish kidney epithelial cells. All animal studies were approved by the Institutional Animal Care and Use Committee at the University of Massachusetts Medical School.

Cell culture

Murine kidney epithelial cells were prepared (Follit et al. 2008) from kidneys of 8-week-old mice by digestion (37°C, <2 h, shaking) with 0.1% collagenase, 0.1% trypsin, and 150 mM NaCl in Dulbecco's modified Eagle's medium (DMEM) (Life Technologies). These cells were maintained in DMEM/F12 media containing 10% fetal bovine serum (FBS) and supplemented with 150 mM urea plus 150 mM NaCl. Kidney epithelial cells expressing conditional alleles as well as their controls were treated for 24 h with 1 μ M 4-hydroxytamoxifen (Millipore Sigma) to

induce CRE^{ERT}-mediated LoxP site recombination. C57Bl/6J and *Map2k4*^{-/-} *Map2k7*^{-/-} MEFs (Tournier et al. 2001) were immortalized using the 3T3 protocol. These cells were maintained in DMEM media containing 10% FBS.

Proliferation Assays

Cells were plated in 24-well plates, grown in 10% or 0.1% media, and fixed (100% methanol, -20°C) at different time points. Crystal violet dissolved in 20% methanol / 80% PBS at 0.1% was used to stain the cells. Proliferation was quantitated by extracting the crystal violet dye with 10% acetic acid and measuring the absorbance at 590 nm (Tecan Instruments). To observe proliferation during wound healing, confluent monolayers of cells grown on glass coverslips were scratched with a pipet tip and incubated with 1mM bromodeoxyuridine (BrdU) in 0.1% serum media for 4 hrs to label proliferating cells. Cells were stained according to the manufacturer's instructions (BD), counterstained with 2-(4-amidinophenyl)-1H-indole-6-carboxamide (DAPI), and examined using a Leica SP2 confocal microscope.

Wound healing

Confluent monolayers of cells were scratched with a pipet tip, washed, and given DMEM/F12 media containing 0.1% FBS. Images were taken at 0, 24, and 48 h using a Zeiss Axiovert 200M microscope. The bottom of the plates was marked in order to image the same area at each time point. Wound area was quantified

using ImageJ (Schneider et al. 2012). The 24 and 48 h time points were compared to the 0 h time point to calculate the percentage healed. Where indicated, tissue culture dishes were coated with fibronectin ($10\mu\text{g}/\text{cm}^2$), laminin ($5\mu\text{g}/\text{cm}^2$), collagen I ($15\mu\text{g}/\text{cm}^2$), and collagen IV ($2.5\mu\text{g}/\text{cm}^2$) for 16h (37°C), washed, and blocked with bovine serum albumin. To test the involvement of secreted factors, media was collected from migrating monolayers, centrifuged to remove debris, and applied to migrating cells. This procedure was performed at the start and 24 h into the wound healing assay.

For wound healing assays using the IncuCyte ZOOM (Essen Bioscience), cells were plated in 96-well ImageLock plates (Essen Bioscience) to achieve confluent monolayers. These were wounded using the WoundMaker (Essen Bioscience), washed, and given media containing 0.1% FBS. Images were acquired every 4 h for 48 h and the relative wound density (cell density within the wound area relative to cell density outside of the wound area) was calculated.

Transwell assays

Kidney epithelial cells ($6 \times 10^4/\text{well}$) in serum-free media were plated in the upper chamber of 8 μm transwells (Corning) and allowed to adhere overnight. A serum gradient was applied by adding media containing 10% FBS to the lower chamber and allowing cells to migrate (20 h). Following migration, cells remaining in the upper chambers were removed with a cotton swab. The migrating cells were

fixed (100% methanol, -20°C) and stained with DAPI. A Zeiss Axiovert 200M microscope was used to image 6 40x-fields per membrane for quantitation of cell migration. Where indicated, both sides of transwell inserts were coated with fibronectin (10 µg/cm²), laminin (5 µg/cm²), collagen I (15 µg/cm²), and collagen IV (2.5 µg/cm²) for 16 h (37°C), washed, and blocked with bovine serum albumin.

Immunoblot analysis

Cell lysates were prepared using Triton lysis buffer (20 mM Tris [pH 7.4], 1% Triton X-100, 10% glycerol, 137 mM NaCl, 2 mM EDTA, 25 mM β-glycerophosphate, 1 mM sodium orthovanadate, 1 mM phenylmethylsulfonyl fluoride, and 10 µg/mL of aprotinin plus leupeptin). Extracts (30 µg) were subjected to immunoblot analysis with antibodies to αTubulin (Sigma-Aldrich Cat# T5168; RRID:AB_477579), phospho-Paxillin (serine 178) (Bethyl Laboratories Cat# A300-100A), and Paxillin (Millipore Cat# 05-417, Clone 5H11). Immune complexes were detected with IRDye 680LT conjugated-donkey anti-mouse IgG antibody (LI-COR Biosciences Cat# 926-68022 RRID:AB_10715072) and IRDye 800CW conjugated-goat anti-rabbit IgG (LI-COR Biosciences Cat# 926-32211 RRID:AB_621843), and quantitated using the Odyssey infrared imaging system (LI-COR Biosciences).

RNA Sequencing

RNA was isolated using the RNeasy kit (Qiagen). RNA quality (RIN > 9) was verified using a Bioanalyzer 2100 System (Agilent Technologies). Total RNA was used to prepare each RNA-seq library by following the manufacturer's instructions (Illumina). Three independent libraries per genotype were examined. The cDNA libraries were sequenced by Illumina Hi-Seq with a paired-end 40-bp format. These RNA-seq data have been deposited in the Gene Expression Omnibus (GEO) database with accession number GSE88856. Reads from each sample were aligned to the mouse genome (UCSC genome browser mm10 build) using TopHat2 (Kim et al. 2013). The average number of aligned reads per library was > 30,000,000. Gene expression was quantitated as fragments per kilobase of exon model per million mapped fragments (FPKM) using Cufflinks (Trapnell et al. 2010). Differentially expressed genes were identified using the Cufflinks tools Cuffmerge and Cuffdiff.

Statistical Analysis

Data are presented as the mean and standard error. Statistical analysis was performed using GraphPad Prism version 6 (GraphPad Software). Pair-wise comparisons of data were performed using a t-test to determine significance ($p < 0.05$). When more than two populations were compared, ANOVA with Bonferroni's test was used to determine significance with an assumed confidence interval of 95%. Similarly, time courses were compared using repeated

measures two-way ANOVA with Bonferroni's multiple comparisons test and an assumed confidence interval of 95%.

APPENDIX B

BREAST CANCER CELL SENSITIVITY TO GENOTOXIC DRUGS IN THE CONTEXT OF JNK INACTIVATION

Abstract

Triple negative breast cancer cells lack specific targets for therapy. As a result, they are treated with DNA damaging agents, which are less specific than drugs that target particular pathways and thus produce more side effects. Sensitizing tumor cells to these agents could allow clinicians to administer lower doses with less toxicity. Inhibition of the cJUN NH₂-terminal kinase (JNK), a protein activated by several genotoxic agents, may provide a means for this sensitization. Here, I tested if JNK inhibition in a breast cancer cell line could enhance the toxicity of various chemotherapeutic agents. I also compared the genotoxic drug sensitivity of JNK-proficient and JNK-deficient mouse tumor cell lines. In these studies, I established a lack of cooperation between several chemotherapeutic agents and JNK inhibition. Furthermore, the data presented demonstrate that drugs that interact with JNK inhibitors may not produce the same effect in JNK-deficient tumor cells. These results have important implications in the development of new therapeutic approaches.

Introduction

Breast tumors that express the estrogen receptor (ER) or have amplified *ERBB2* (encoding HER2) respond to therapies that inactivate these two important pathways (Bange et al. 2001). This intrinsic tumor cell weakness can be exploited to combat the disease. In contrast, tumors that have not amplified *ERBB2* and that lack ER –called triple negative breast cancers (TNBC) – are not sensitive to ER antagonists or anti-HER2 monoclonal antibodies. Thus patients with these tumors receive chemotherapy or radiation therapy (Perou 2011). Frequently used genotoxic drugs in breast cancer include cisplatin, doxorubicin, and etoposide (Wahba and El-Hadaad 2015; Castrellon et al. 2017). Because these tumors are characterized by high rates of proliferation, they are sensitive to DNA damaging agents and respond to treatment (Perou 2011). However, chemotherapy causes toxicity in healthy cells, leading to side effects. Improved treatment, either through entirely new approaches or through sensitization to chemotherapeutic drugs, is needed for this group of patients.

Among the TNBC group are tumors bearing *BRCA1* mutations (Perou 2011). Cells that have lost *BRCA1* function are unable to perform homologous recombination, making them sensitive to inhibition of an alternative DNA repair pathway through poly(ADP-ribose), or PARP (Sonnenblick et al. 2015). This synergistic effect of inhibiting two DNA repair pathways to induce cancer cell

death is termed synthetic lethality, and discovering more such combinations for treatment is a major research goal (Helleday et al. 2008). Accomplishing this will require understanding the pathways that sense and repair DNA damage.

A potential pathway for this type of research is the stress-activated cJUN NH₂-terminal kinase (JNK) pathway (Davis 2000). JNK phosphorylates SIRT6 in the presence of oxidative stress to promote double strand break (DSB) repair (Van Meter et al. 2016). JNK also phosphorylates DGCR8 to initiate transcriptionally-coupled nucleotide exchange repair (Calses et al. 2017). In mouse embryonic fibroblasts (MEFs) JNK deficiency results in a rapid progression to aneuploidy (N. Kennedy, unpublished data). Also, JNK2-deficient tumors exhibit evidence of replicative stress and increased genomic instability compared to control tumors (Chen et al. 2010). These data indicate that JNK may be involved in genome maintenance. Indeed, the DNA damaging agents cisplatin, doxorubicin, and etoposide all activate JNK (Sanchez-Perez et al. 1998; Brantley-Finley et al. 2003; Helbig et al. 2011). Cisplatin-induced DNA adducts are sufficient for JNK activation (Helbig et al. 2011), and sustained activation during cisplatin treatment leads to increased cell death (Sanchez-Perez et al. 1998). Treatment with cisplatin also induces expression of several DNA repair proteins through JNK and its targets cJUN and ATF2 (Hayakawa et al. 2004). Finally, inhibition of JNK or loss of its activator *Map2k7* results in dampened DNA damage repair signaling and TP53 phosphorylation, respectively, during doxorubicin treatment (Schramek et al. 2011; Boege et al. 2017). Thus, not only

is JNK activated by DNA damage, its activation may impact how the cell responds to that damage.

Considering the treatment options for TNBC patients and the JNK pathway's relationship with DNA damage, I sought to identify a drug that would synergize with JNK inhibition to more efficiently kill tumor cells. I found that JNK inhibition with a small molecule did not sensitize MDA-MB-231 cells to cisplatin, doxorubicin, etoposide, or methyl methanesulfonate. Also, tumor cells responded similarly to these drugs, regardless of JNK pathway status. These studies eliminate these agents as candidates for combined therapies with JNK inhibitors or in treating JNK-deficient tumors. They also provide insight for designing therapeutic approaches in the context of JNK inhibition or JNK pathway loss.

Results and Discussion

JNK Inhibition in MDA-MB-231 Cells

JNK-IN-8 is a highly specific covalent inhibitor of JNK that binds in the activation loop of the kinase (Zhang et al. 2012). To test JNK pathway signaling and JNK-IN-8 potency in the TNBC cell line MDA-MB-231, I exposed the cells to ultraviolet light (UV) in the presence or absence of the inhibitor. Both JNK and cJUN were phosphorylated after UV exposure, indicating that the JNK pathway is functional in these cells (Figure B.1). Inhibition of JNK with JNK-IN-8 (2 μ M) following UV-stimulation resulted in decreased cJUN phosphorylation relative to DMSO treated controls (Figure B.1). In contrast, a 4 hour pretreatment with the drug nearly abolished cJUN phosphorylation (Figure B.1). Thus, all subsequent experiments were performed with a 4 hour pretreatment of JNK-IN-8.

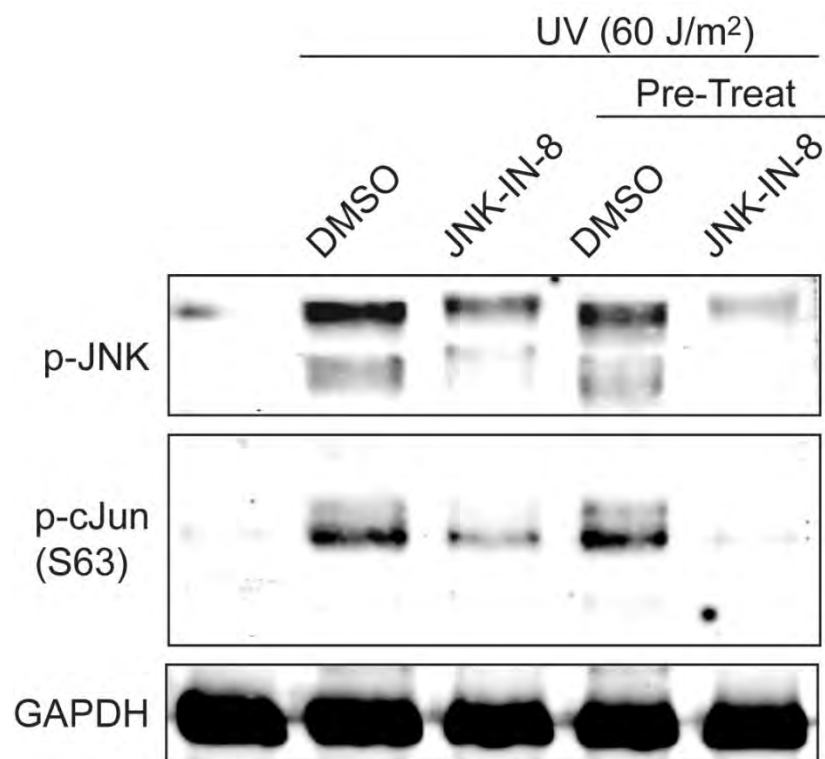


Figure B.1. JNK pathway inhibition in MDA-MB-231 by JNK-IN-8.

MDA-MB-231 cells were left unirradiated or were exposed to 60 J/m² ultraviolet (UV) light. Following UV exposure, cells received 2 μ M JNK-IN-8 or vehicle (DMSO). For the pre-treated condition, cells were incubated with JNK-IN-8 or DMSO for 4 h prior to UV exposure and treatment was continued until cells were harvested. Immunoblot analysis of p-JNK and p-cJUN (S63) was performed on the lysates. GAPDH served as a loading control.

Because cisplatin, doxorubicin, and etoposide are among the chemotherapeutic drugs used to treat TNBC, I chose to test if concomitant JNK inhibition would impact cell survival (Wahba and El-Hadaad 2015; Castrellon et al. 2017). Treatment of MDA-MB-231 cells with JNK-IN-8 alone had no effect on cell growth (Figure B.2). This finding suggests that any changes in sensitivity observed in JNK-inhibited cells would not be the result of changes in proliferation. It also demonstrates that JNK inhibition by itself does not negatively impact tumor cells. In contrast, MDA-MB-231 cell growth was significantly reduced by all three of the tested drugs (Figure B.2A-C). The addition of JNK-IN-8 to cisplatin or doxorubicin treated cells had no significant effect on cell proliferation (Figure B.2A & B), regardless of the drug concentration (Figure B.3). However, co-treatment of etoposide and JNK-IN-8 increased cell proliferation relative to etoposide-only treated cells (Figure B.2C), indicating that JNK is necessary for inhibiting tumor cell growth following etoposide treatment.

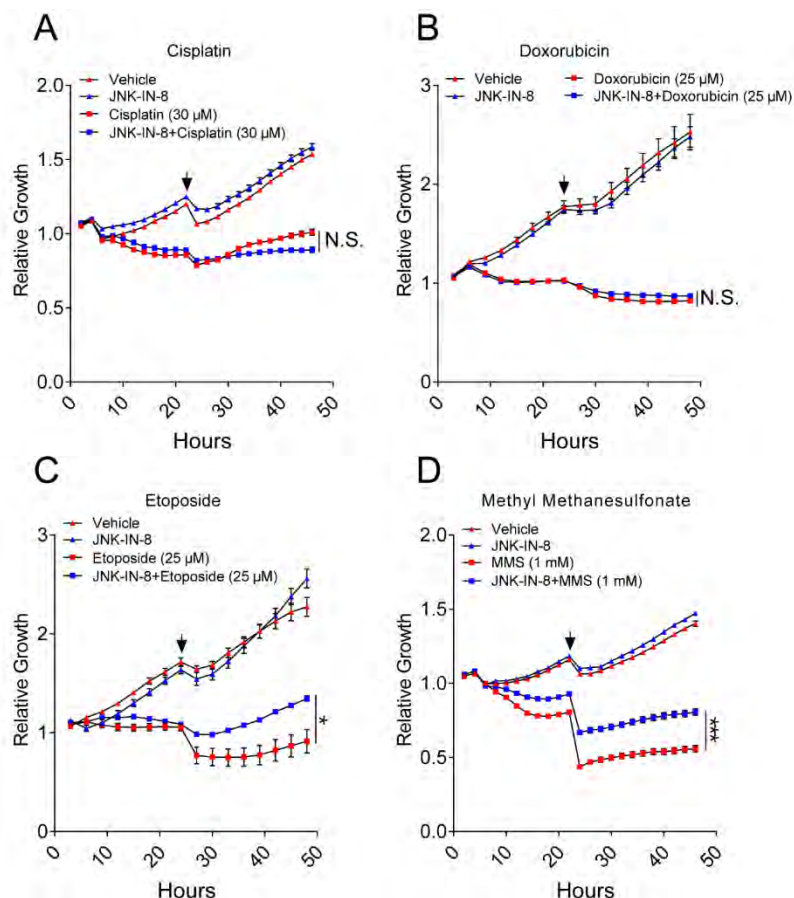


Figure B.2. JNK-IN-8 treatment does not sensitize MDA-MB-231 cells to cisplatin, doxorubicin, etoposide, or methyl methanesulfonate.

A-D) MDA-MB-231 cells were cultured with DMSO or JNK-IN-8 (2 μ M) for 4 h (starting at time 0 h) before addition of (A) cisplatin (n=24), (B) doxorubicin (n=8), (C) etoposide (n=8), or (D) methyl methanesulfonate (MMS; n=24). Cell confluence was monitored regularly for 48 h and plotted as relative growth, with each well normalized to its time 0 confluence. After 20 h of drug treatment, cells were washed and received fresh media containing the appropriate treatment (arrow). Graphs show mean \pm SEM of 1 of 2 (doxorubicin, etoposide), 3 (MMS), or 4 (cisplatin) experiments (* p <0.05, *** p <0.001, N. S. p >0.05).

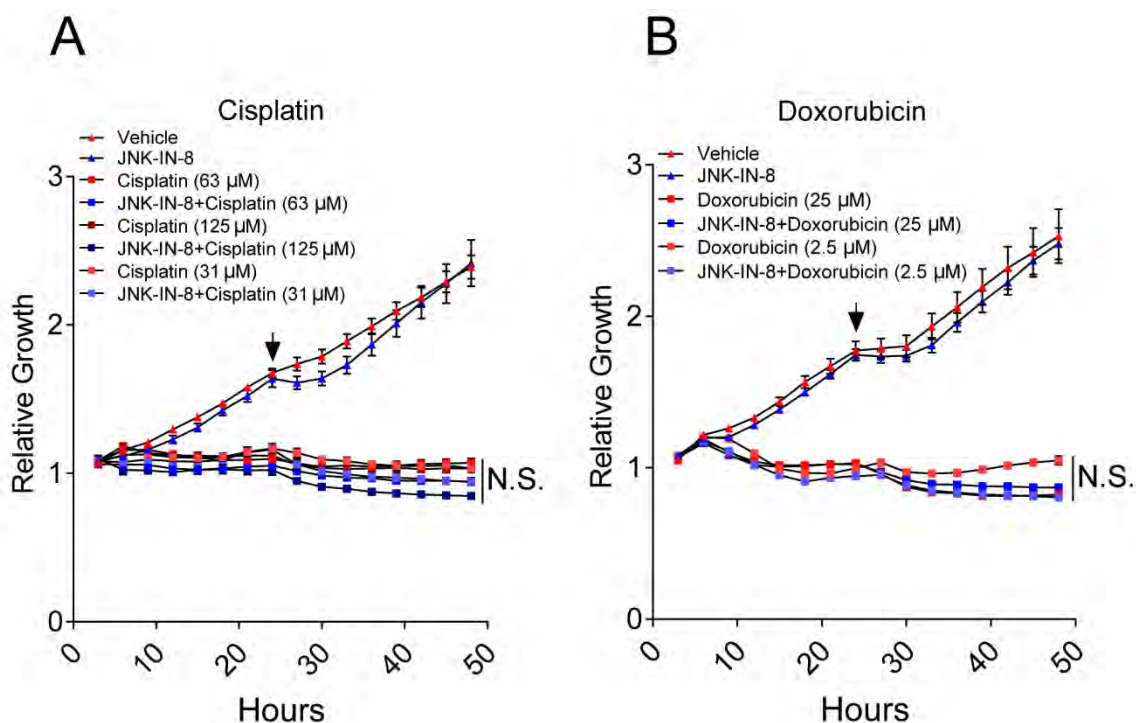


Figure B.3. Titration of cisplatin and doxorubicin concentrations results in similar growth of MDA-MB-231 cells, regardless of JNK-IN-8 treatment.

A, B) MDA-MB-231 cells were cultured with DMSO or JNK-IN-8 (2 μ M) for 4 h before addition of varying concentrations of (A) cisplatin or (B) doxorubicin. Cell confluence was monitored every 3 h for 48 h and plotted as relative growth, with each well normalized to its time 0 confluence. After 20 h of drug treatment, cells were washed and received fresh media containing the appropriate treatment (arrow). Graphs show mean \pm SEM ($n=8$; N. S. $p>0.05$)

The finding that JNK inhibition does not sensitize cells to cisplatin was surprising. Presumably, the ability of JNK to promote the expression of proteins that repair cisplatin-induced DNA adducts would promote cell survival (Hayakawa et al. 2004). Furthermore, higher concentrations of cisplatin in the context of JNK inhibition should result in more unrepaired lesions, causing additional cell death. However, increasing cisplatin doses had no significant effect on cell survival (Figure B.3A). Thus, alternative mechanisms must exist that compensate for JNK-mediated expression of repair proteins in cisplatin-treated cells.

Both etoposide and doxorubicin induce DNA damage by inhibiting topoisomerase; however doxorubicin can also cause the formation of reactive oxygen species (ROS) in treated cells (Thorn et al. 2011; Montecucco et al. 2015). The exact stimulus that activates JNK in response to doxorubicin is therefore unclear and may account for the different response of cells treated with these two agents. Metabolites of doxorubicin can also disrupt mitochondria and cause the release of cytochrome c (Thorn et al. 2011). Thus, JNK may be necessary for executing apoptosis during etoposide treatment, but dispensable for apoptosis induced by doxorubicin.

As a positive control for JNK inhibition affecting cellular response to a genotoxic drug, I treated cells with methyl methanesulfonate (MMS). MMS is known to activate JNK (Wilhelm et al. 1997), and JNK-deficient MEFs are protected from its cytotoxic effects (Tournier et al. 2000). Thus, treatment of MDA-MB-231 cells with MMS and JNK-IN-8 should result in increased tumor cell

survival. Indeed, JNK inhibition rendered cells more resistant to MMS than MMS treatment alone (Figure B.2D).

Collectively, these data show that JNK inhibition does not sensitize MDA-MB-231 cells to any of the tested drugs (Figure B.2 & B.3). In fact, JNK activity is required for the deleterious effects of etoposide and MMS treatment (Figure B.2C & D). These findings should be validated in additional TNBC cell lines. Studies determining which DNA lesions activate JNK and the consequences of JNK activation in response to these different types of DNA damage could inform which cytotoxic agents may synergize with JNK inhibitors.

While my studies did not reveal synergy between JNK-IN-8 and the tested agents, others have determined that JNK-IN-8 sensitizes MDA-MB-231 cells to the EGFR inhibitor lapatinib by increasing ROS production and subsequent tumor cell death (Ebelt et al. 2017). In BRAF^{V600E}-mutant melanoma, JNK inhibition prevents cells from becoming quiescent during RAF inhibitor treatment, thereby maximizing cell killing and reducing adaptation (Fallahi-Sichani et al. 2015). These results indicate that further studies of combinatorial therapies including JNK-IN8 are warranted.

Variable Sensitivity of JNK-Deficient Tumor Cells to Select Genotoxic Agents

I have previously described mouse tumor cell lines isolated from *Wap-Cre*^{-/+} *Trp53*^{LoxP/LoxP} (JNK^{WT}) and *Wap-Cre*^{-/+} *Trp53*^{LoxP/LoxP} *Mapk8*^{LoxP/LoxP} *Mapk9*^{LoxP/LoxP} (JNK^{KO}) tumors (Chapter IV). Overall, JNK^{WT} and JNK^{KO} cells proliferate similarly (Figure B.4).

To determine if JNK status in tumor cells affects sensitivity to different genotoxic drugs, I treated these cell lines with cisplatin, doxorubicin, etoposide and MMS. The presence of JNK in tumor cells did not predict their response to any of the tested drugs (Figure B.5). Instead, proliferation rate correlated with sensitivity to cisplatin and doxorubicin, as the two most proliferative cell lines exhibited significantly decreased growth relative to more moderately proliferating cells (Figures B.4, B.5A, & B). JNK^{WT} cells treated with etoposide also showed a pattern of increased proliferation leading to increased sensitivity (Figure B.5C). In contrast, the moderately proliferating JNK^{KO} lines had widely varying responses to etoposide (Figure B.5C). Interestingly, the slowest-growing JNK^{WT} cell line was the most resistant to cisplatin and etoposide, and this resistance was significantly greater than that observed in JNK^{KO} cells (Figure B.5A & C). This observation may indicate a tendency for JNK-deficient tumor cells to be more sensitive to these two agents. However this sensitivity is not strictly associated with JNK-deficiency since the JNK^{KO} lines respond similarly to the sensitive JNK^{WT} line.

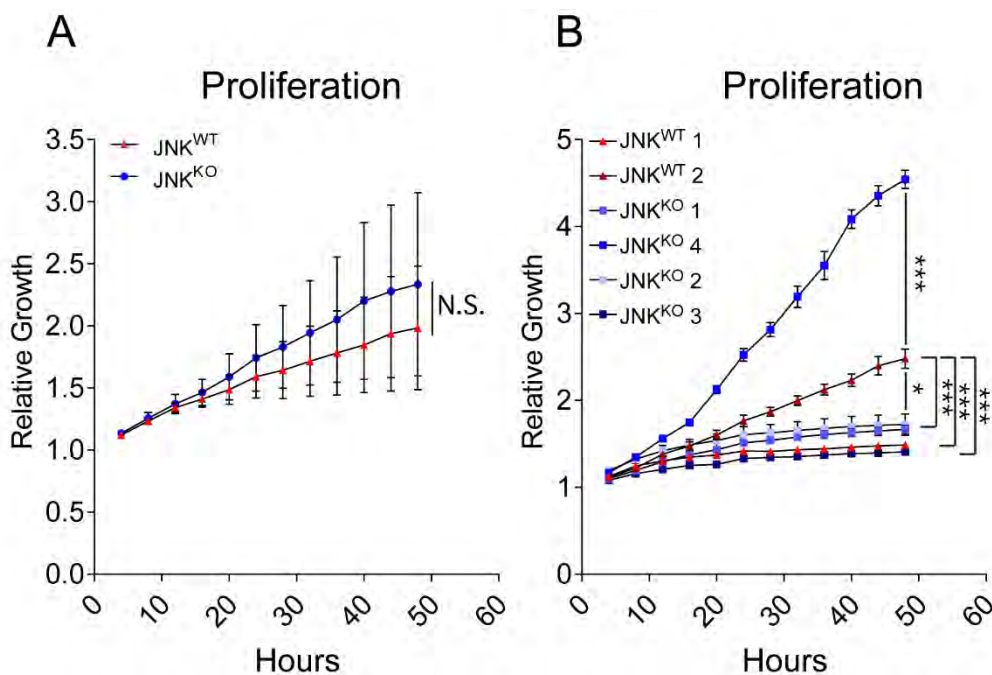


Figure B.4. Proliferation of tumor cells is similar regardless of JNK status.

A, B) Confluence of cell lines isolated from mouse tumors was monitored every 4 h for 48 h. The relative growth was calculated by normalizing each well to its confluence at time 0. The composite of JNK^{WT} (2 independent cell lines, n=2) and JNK^{KO} (4 independent cell lines, n=4) was plotted (A). Individual cell growth curves (B) are also presented (n=16). Graphs show mean \pm SEM of 1 of 3 experiments (* $p < 0.05$, *** $p < 0.001$, N. S. $p > 0.05$).

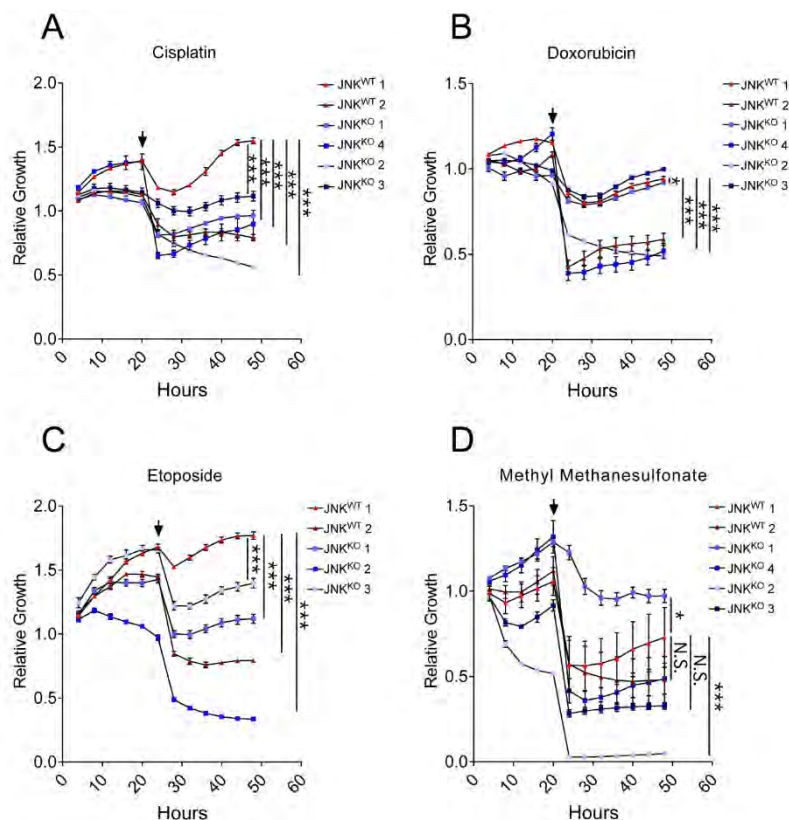


Figure B.5. Murine tumor-derived cells respond variably to drug treatments.

A-D) JNK^{WT} and JNK^{KO} cells were treated with (A) 31 μ M cisplatin, (B) 25 μ M doxorubicin, (C) 100 μ M etoposide, and (D) 1 mM MMS beginning at time 0. Cell confluence was monitored every 4 h for 48 h and plotted as relative growth, with each well normalized to its time 0 confluence. After 24 h, cells were washed and given fresh media with the appropriate treatment (arrow), then monitored for an additional 24 h. Graphs show mean \pm SEM (n=16; *p<0.05, ***p<0.001, N. S. p>0.05).

Neither proliferation nor genotype predicted the response to MMS treatment (Figure B.5D). There was no statistically significant difference between the growth rates of the JNK^{WT} cells (Figure B.5D). Furthermore, the most sensitive and the most resistant cell lines to MMS were both JNK-deficient cells with moderate rates of proliferation (Figure B.5D). This finding contrasts with observations made studying JNK-deficient MEFs (Tournier et al. 2000) and JNK-IN-8 treated MDA-MB-231 cells (Figure B.2D). This analysis highlights how different cell types (MEFs vs. tumor) and different time courses of JNK loss (acute inhibition with a small molecule vs. long-term deletion) can result in variable responses from the JNK pathway. Thus, treatments that synergize with JNK inhibitors cannot be assumed to benefit tumors with JNK mutations.

Conclusions

These data show that JNK pathway inhibition in TNBC cells does not render them selectively sensitive to cisplatin, doxorubicin, etoposide, or MMS. Furthermore, tumors with genetic inactivation of the JNK pathway are not sensitive to these agents. However, studies testing additional chemotherapeutic and cytotoxic agents in the presence of either chemical or genetic JNK inactivation may reveal synthetic lethalties that could be exploited in the clinic.

Human tumor sequencing studies (Teng et al. 1997; Parsons et al. 2005; Greenman et al. 2007) and *in vivo* models (Cellurale et al. 2011; Das et al. 2011; Davies et al. 2014; Gozdecka et al. 2014) have demonstrated that the JNK pathway contributes to other malignancies. Thus, performing these types of studies using cell lines from different tumor types may uncover JNK-dependent tumor cell sensitivities. Continuing studies like the ones described here will provide a better appreciation of the role of JNK in DNA damage signaling and could inform new therapeutic approaches.

Materials and Methods

Cell Culture

MDA-MB-231 cells were acquired from American Type Culture Collection (ATCC). The murine tumor cell lines have been previously described (Chapter IV, submitted). All cells were maintained in DMEM/F12 (Thermo Fisher Scientific) containing 10% fetal bovine serum (FBS) and 1% penicillin/streptomycin (Thermo Fisher Scientific).

JNK-IN-8 Inhibition

JNK inhibition by JNK-IN-8 was assayed by monitoring cJUN phosphorylation at serine 63 following pathway activation. Cells were left untreated or pre-treated with 2 μ M JNK-IN-8 (Millipore Sigma) for 4 hours prior to stimulation (60J/m² ultraviolet (UV) light). They were cultured for an additional 30 mins with or without the inhibitor before protein isolation.

Immunoblot Analysis

Protein lysates were prepared using Triton lysis buffer (20 mM Tris [pH 7.4], 1% Triton X-100, 10% glycerol, 137 mM NaCl, 2 mM EDTA, 25 mM β -glycerophosphate, 1 mM sodium orthovanadate, 1 mM phenylmethylsulfonyl fluoride, and 10 μ g/mL of aprotinin plus leupeptin). Extracts (50 μ g) were subjected to immunoblot analysis with antibodies to phospho-JNK (Cell Signaling

Technology Cat# 9255 RRID:AB_2307321), phospho-cJUN (S63) (Cell Signaling Technology Cat# 9261L RRID:AB_2130159), and GAPDH (Santa Cruz Biotechnology Cat# sc-25778; RRID:AB_10167668; dilution 1:1000). Immune complexes were detected using IRDye 680LT conjugated-donkey anti-mouse IgG antibody (LI-COR Biosciences Cat# 926-68022 RRID:AB_10715072) and IRDye 800CW conjugated-goat anti-rabbit IgG (LI-COR Biosciences Cat# 926-32211 RRID:AB_621843). Quantitation was performed using the Odyssey infrared imaging system (LI-COR Biosciences).

Drug Treatment

Cells were plated in 96-well plates at 30,000 cells/well. Before drug administration, MDA-MB-231 cells were pretreated with DMSO or 2 μ M of JNK-IN-8 for 4 h (time 0 h). After pretreatment, cells were given etoposide (Millipore Sigma), methyl methanesulfonate (MMS; Millipore Sigma), doxorubicin (Millipore Sigma), or cisplatin (Millipore Sigma) in addition to JNK-IN-8 or DMSO (time 4 h). Dead cells were washed from the well and fresh media with the appropriate compounds was given to the remaining cells 20 h after drug administration. Cell confluence was monitored at regular intervals for 48 h using an IncuCyte Zoom (Essen BioScience).

Statistical Analysis

Data are presented as the mean and standard error. Statistical analysis was performed using GraphPad Prism version 7 (GraphPad Software). Repeated measures two-way ANOVA using Bonferroni's multiple comparisons test with an assumed confidence interval of 95% was performed to compare cell confluence over time.

REFERENCES

- Adachi-Yamada T, Fujimura-Kamada K, Nishida Y, Matsumoto K. 1999. Distortion of proximodistal information causes JNK-dependent apoptosis in *Drosophila* wing. *Nature* **400**: 166-169.
- Adachi-Yamada T, O'Connor MB. 2002. Morphogenetic apoptosis: a mechanism for correcting discontinuities in morphogen gradients. *Dev Biol* **251**: 74-90.
- Adler V, Polotskaya A, Wagner F, Kraft AS. 1992. Affinity-purified c-Jun amino-terminal protein kinase requires serine/threonine phosphorylation for activity. *J Biol Chem* **267**: 17001-17005.
- Afghahi A, Kurian AW. 2017. The Changing Landscape of Genetic Testing for Inherited Breast Cancer Predisposition. *Curr Treat Options Oncol* **18**: 27.
- Agnes F, Suzanne M, Noselli S. 1999. The *Drosophila* JNK pathway controls the morphogenesis of imaginal discs during metamorphosis. *Development* **126**: 5453-5462.
- Alexander CM, Selvarajan S, Mudgett J, Werb Z. 2001. Stromelysin-1 regulates adipogenesis during mammary gland involution. *J Cell Biol* **152**: 693-703.
- American Cancer Society. 2013. Breast Cancer Facts & Figures 2013-2014. American Cancer Society, Atlanta.
- Andrews S. 2010. FastQC: a quality control tool for high throughput sequence data. .
- Avivar-Valderas A, Wen HC, Aguirre-Ghiso JA. 2014. Stress signaling and the shaping of the mammary tissue in development and cancer. *Oncogene* **33**: 5483-5490.
- Babaei S, Hulsman M, Reinders M, de Ridder J. 2013. Detecting recurrent gene mutation in interaction network context using multi-scale graph diffusion. *BMC Bioinformatics* **14**: 29.
- Badea TC, Wang Y, Nathans J. 2003. A noninvasive genetic/pharmacologic strategy for visualizing cell morphology and clonal relationships in the mouse. *J Neurosci* **23**: 2314-2322.
- Bain J, McLauchlan H, Elliott M, Cohen P. 2003. The specificities of protein kinase inhibitors: an update. *Biochem J* **371**: 199-204.
- Bain J, Plater L, Elliott M, Shpiro N, Hastie CJ, McLauchlan H, Klevernic I, Arthur JS, Alessi DR, Cohen P. 2007. The selectivity of protein kinase inhibitors: a further update. *Biochem J* **408**: 297-315.
- Banerji S, Cibulskis K, Rangel-Escareno C, Brown KK, Carter SL, Frederick AM, Lawrence MS, Sivachenko AY, Sougnez C, Zou L et al. 2012. Sequence analysis of mutations and translocations across breast cancer subtypes. *Nature* **486**: 405-409.
- Bange J, Zwick E, Ullrich A. 2001. Molecular targets for breast cancer therapy and prevention. *Nat Med* **7**: 548-552.

- Barutcu SA, Girnius N, Vernia S, Davis RJ. In press. Role of the cJun NH2-terminal kinase (JNK) signaling pathway in starvation-induced autophagy. *Autophagy*.
- Behrens A, Jochum W, Sibilila M, Wagner EF. 2000. Oncogenic transformation by ras and fos is mediated by c-Jun N-terminal phosphorylation. *Oncogene* **19**: 2657-2663.
- Behrens A, Sibilila M, David JP, Mohle-Steinlein U, Tronche F, Schutz G, Wagner EF. 2002. Impaired postnatal hepatocyte proliferation and liver regeneration in mice lacking c-jun in the liver. *EMBO J* **21**: 1782-1790.
- Behrens A, Sibilila M, Wagner EF. 1999. Amino-terminal phosphorylation of c-Jun regulates stress-induced apoptosis and cellular proliferation. *Nat Genet* **21**: 326-329.
- Berger AH, Brooks AN, Wu X, Shrestha Y, Chouinard C, Piccioni F, Bagul M, Kamburov A, Imielinski M, Hogstrom L et al. 2016. High-throughput Phenotyping of Lung Cancer Somatic Mutations. *Cancer Cell* **30**: 214-228.
- Biswas SC, Shi Y, Sproul A, Greene LA. 2007. Pro-apoptotic Bim induction in response to nerve growth factor deprivation requires simultaneous activation of three different death signaling pathways. *J Biol Chem* **282**: 29368-29374.
- Biteau B, Hochmuth CE, Jasper H. 2008. JNK activity in somatic stem cells causes loss of tissue homeostasis in the aging Drosophila gut. *Cell Stem Cell* **3**: 442-455.
- Bjorkblom B, Padzik A, Mohammad H, Westerlund N, Komulainen E, Hollos P, Parviainen L, Papageorgiou AC, Iljin K, Kallioniemi O et al. 2012. c-Jun N-terminal kinase phosphorylation of MARCKSL1 determines actin stability and migration in neurons and in cancer cells. *Mol Cell Biol* **32**: 3513-3526.
- Boege Y, Malehmir M, Healy ME, Bettermann K, Lorentzen A, Vucur M, Ahuja AK, Bohm F, Mertens JC, Shimizu Y et al. 2017. A Dual Role of Caspase-8 in Triggering and Sensing Proliferation-Associated DNA Damage, a Key Determinant of Liver Cancer Development. *Cancer Cell* **32**: 342-359 e310.
- Bolger AM, Lohse M, Usadel B. 2014. Trimmomatic: a flexible trimmer for Illumina sequence data. *Bioinformatics* **30**: 2114-2120.
- Bombonati A, Sgroi DC. 2011. The molecular pathology of breast cancer progression. *J Pathol* **223**: 307-317.
- Boudreau N, Simpson CJ, Werb Z, Bissell MJ. 1995. Suppression of ICE and apoptosis in mammary epithelial cells by extracellular matrix. *Science* **267**: 891-893.
- Bouillet P, Metcalf D, Huang DC, Tarlinton DM, Kay TW, Kontgen F, Adams JM, Strasser A. 1999. Proapoptotic Bcl-2 relative Bim required for certain apoptotic responses, leukocyte homeostasis, and to preclude autoimmunity. *Science* **286**: 1735-1738.
- Brantley-Finley C, Lyle CS, Du L, Goodwin ME, Hall T, Szwedo D, Kaushal GP, Chambers TC. 2003. The JNK, ERK and p53 pathways play distinct roles

- in apoptosis mediated by the antitumor agents vinblastine, doxorubicin, and etoposide. *Biochem Pharmacol* **66**: 459-469.
- Brumby AM, Richardson HE. 2003. scribble mutants cooperate with oncogenic Ras or Notch to cause neoplastic overgrowth in *Drosophila*. *EMBO J* **22**: 5769-5779.
- Calses PC, Dhillon KK, Tucker N, Chi Y, Huang JW, Kawasumi M, Nghiem P, Wang Y, Clurman BE, Jacquemont C et al. 2017. DGCR8 Mediates Repair of UV-Induced DNA Damage Independently of RNA Processing. *Cell Rep* **19**: 162-174.
- Cancer Genome Atlas N. 2012. Comprehensive molecular portraits of human breast tumours. *Nature* **490**: 61-70.
- Cantrell MA, Ebelt ND, Pfefferle AD, Perou CM, Van Den Berg CL. 2015. c-Jun N-terminal kinase 2 prevents luminal cell commitment in normal mammary glands and tumors by inhibiting p53/Notch1 and breast cancer gene 1 expression. *Oncotarget* **6**: 11863-11881.
- Cardiff RD, Anver MR, Gusterson BA, Hennighausen L, Jensen RA, Merino MJ, Rehm S, Russo J, Tavassoli FA, Wakefield LM et al. 2000. The mammary pathology of genetically engineered mice: the consensus report and recommendations from the Annapolis meeting. *Oncogene* **19**: 968-988.
- Cardone MH, Salvesen GS, Widmann C, Johnson G, Frisch SM. 1997. The regulation of anoikis: MEKK-1 activation requires cleavage by caspases. *Cell* **90**: 315-323.
- Carter H, Chen S, Isik L, Tyekucheva S, Velculescu VE, Kinzler KW, Vogelstein B, Karchin R. 2009. Cancer-specific high-throughput annotation of somatic mutations: computational prediction of driver missense mutations. *Cancer Res* **69**: 6660-6667.
- Castrellon AB, Pihdorecky I, Valero V, Raez LE. 2017. The Role of Carboplatin in the Neoadjuvant Chemotherapy Treatment of Triple Negative Breast Cancer. *Oncol Rev* **11**: 324.
- Cellurale C, Girnius N, Jiang F, Cavanagh-Kyros J, Lu S, Garlick DS, Mercurio AM, Davis RJ. 2012. Role of JNK in mammary gland development and breast cancer. *Cancer Res* **72**: 472-481.
- Cellurale C, Sabio G, Kennedy NJ, Das M, Barlow M, Sandy P, Jacks T, Davis RJ. 2011. Requirement of c-Jun NH(2)-terminal kinase for Ras-initiated tumor formation. *Mol Cell Biol* **31**: 1565-1576.
- Cellurale C, Weston CR, Reilly J, Garlick DS, Jerry DJ, Sluss HK, Davis RJ. 2010. Role of JNK in a Trp53-dependent mouse model of breast cancer. *PLoS One* **5**: e12469.
- Cerami E, Demir E, Schultz N, Taylor BS, Sander C. 2010. Automated network analysis identifies core pathways in glioblastoma. *PLoS One* **5**: e8918.
- Chakraborti S, Mandal M, Das S, Mandal A, Chakraborti T. 2003. Regulation of matrix metalloproteinases: an overview. *Mol Cell Biochem* **253**: 269-285.
- Chapman RS, Lourenco PC, Tonner E, Flint DJ, Selbert S, Takeda K, Akira S, Clarke AR, Watson CJ. 1999. Suppression of epithelial apoptosis and

- delayed mammary gland involution in mice with a conditional knockout of Stat3. *Genes Dev* **13**: 2604-2616.
- Chen P, O'Neal JF, Ebel ND, Cantrell MA, Mitra S, Nasrazadani A, Vandenbroek TL, Heasley LE, Van Den Berg CL. 2010. Jnk2 effects on tumor development, genetic instability and replicative stress in an oncogene-driven mouse mammary tumor model. *PLoS One* **5**: e10443.
- Chen YR, Wang X, Templeton D, Davis RJ, Tan TH. 1996. The role of c-Jun N-terminal kinase (JNK) in apoptosis induced by ultraviolet C and gamma radiation. Duration of JNK activation may determine cell death and proliferation. *J Biol Chem* **271**: 31929-31936.
- Chung J, Uchida E, Grammer TC, Blenis J. 1997. STAT3 serine phosphorylation by ERK-dependent and -independent pathways negatively modulates its tyrosine phosphorylation. *Mol Cell Biol* **17**: 6508-6516.
- Cibulskis K, Lawrence MS, Carter SL, Sivachenko A, Jaffe D, Sougnez C, Gabriel S, Meyerson M, Lander ES, Getz G. 2013. Sensitive detection of somatic point mutations in impure and heterogeneous cancer samples. *Nat Biotechnol* **31**: 213-219.
- Ciccio A, Elledge SJ. 2010. The DNA damage response: making it safe to play with knives. *Mol Cell* **40**: 179-204.
- Ciriello G, Gatza ML, Beck AH, Wilkerson MD, Rhie SK, Pastore A, Zhang H, McLellan M, Yau C, Kandoth C et al. 2015. Comprehensive Molecular Portraits of Invasive Lobular Breast Cancer. *Cell* **163**: 506-519.
- Conze D, Krah T, Kennedy N, Weiss L, Lumsden J, Hess P, Flavell RA, Le Gros G, Davis RJ, Rincon M. 2002. c-Jun NH(2)-terminal kinase (JNK)1 and JNK2 have distinct roles in CD8(+) T cell activation. *J Exp Med* **195**: 811-823.
- Cuadrado A, Nebreda AR. 2010. Mechanisms and functions of p38 MAPK signalling. *Biochem J* **429**: 403-417.
- Cui Y, Riedlinger G, Miyoshi K, Tang W, Li C, Deng CX, Robinson GW, Hennighausen L. 2004. Inactivation of Stat5 in mouse mammary epithelium during pregnancy reveals distinct functions in cell proliferation, survival, and differentiation. *Mol Cell Biol* **24**: 8037-8047.
- Czabotar PE, Lessene G, Strasser A, Adams JM. 2014. Control of apoptosis by the BCL-2 protein family: implications for physiology and therapy. *Nat Rev Mol Cell Biol* **15**: 49-63.
- Das M, Garlick DS, Greiner DL, Davis RJ. 2011. The role of JNK in the development of hepatocellular carcinoma. *Genes Dev* **25**: 634-645.
- Das M, Jiang F, Sluss HK, Zhang C, Shokat KM, Flavell RA, Davis RJ. 2007. Suppression of p53-dependent senescence by the JNK signal transduction pathway. *Proc Natl Acad Sci U S A* **104**: 15759-15764.
- Das M, Sabio G, Jiang F, Rincon M, Flavell RA, Davis RJ. 2009. Induction of hepatitis by JNK-mediated expression of TNF-alpha. *Cell* **136**: 249-260.
- Davies CC, Harvey E, McMahon RF, Finegan KG, Connor F, Davis RJ, Tuveson DA, Tournier C. 2014. Impaired JNK signaling cooperates with KrasG12D

- expression to accelerate pancreatic ductal adenocarcinoma. *Cancer Res* **74**: 3344-3356.
- Davis RJ. 2000. Signal transduction by the JNK group of MAP kinases. *Cell* **103**: 239-252.
- Del Barco Barrantes I, Stephan-Otto Attolini C, Slobodnyuk K, Igea A, Gregorio S, Gawrzak S, Gomis RR, Nebreda AR. 2017. Regulation of Mammary Luminal Cell Fate and Tumorigenesis by p38alpha. *Stem Cell Reports*.
- . 2018. Regulation of Mammary Luminal Cell Fate and Tumorigenesis by p38alpha. *Stem Cell Reports* **10**: 257-271.
- Derijard B, Hibi M, Wu IH, Barrett T, Su B, Deng T, Karin M, Davis RJ. 1994. JNK1: a protein kinase stimulated by UV light and Ha-Ras that binds and phosphorylates the c-Jun activation domain. *Cell* **76**: 1025-1037.
- Derksen PW, Liu X, Saridin F, van der Gulden H, Zevenhoven J, Evers B, van Beijnum JR, Griffioen AW, Vink J, Krimpenfort P et al. 2006. Somatic inactivation of E-cadherin and p53 in mice leads to metastatic lobular mammary carcinoma through induction of anoikis resistance and angiogenesis. *Cancer Cell* **10**: 437-449.
- Deugnier MA, Teuliere J, Faraldo MM, Thiery JP, Glukhova MA. 2002. The importance of being a myoepithelial cell. *Breast Cancer Res* **4**: 224-230.
- Dong C, Yang DD, Wisk M, Whitmarsh AJ, Davis RJ, Flavell RA. 1998. Defective T cell differentiation in the absence of Jnk1. *Science* **282**: 2092-2095.
- Donovan N, Becker EB, Konishi Y, Bonni A. 2002. JNK phosphorylation and activation of BAD couples the stress-activated signaling pathway to the cell death machinery. *J Biol Chem* **277**: 40944-40949.
- Douma S, Van Laar T, Zevenhoven J, Meuwissen R, Van Garderen E, Peeper DS. 2004. Suppression of anoikis and induction of metastasis by the neurotrophic receptor TrkB. *Nature* **430**: 1034-1039.
- Downward J. 2003. Targeting RAS signalling pathways in cancer therapy. *Nat Rev Cancer* **3**: 11-22.
- Ebelt ND, Kaoud TS, Edupuganti R, Van Ravenstein S, Dalby KN, Van Den Berg CL. 2017. A c-Jun N-terminal kinase inhibitor, JNK-IN-8, sensitizes triple negative breast cancer cells to lapatinib. *Oncotarget* **8**: 104894-104912.
- Ellis MJ, Ding L, Shen D, Luo J, Suman VJ, Wallis JW, Van Tine BA, Hoog J, Goiffon RJ, Goldstein TC et al. 2012. Whole-genome analysis informs breast cancer response to aromatase inhibition. *Nature* **486**: 353-360.
- Ewald AJ, Brenot A, Duong M, Chan BS, Werb Z. 2008. Collective epithelial migration and cell rearrangements drive mammary branching morphogenesis. *Dev Cell* **14**: 570-581.
- Fallahi-Sichani M, Moerke NJ, Niepel M, Zhang T, Gray NS, Sorger PK. 2015. Systematic analysis of BRAF(V600E) melanomas reveals a role for JNK/c-Jun pathway in adaptive resistance to drug-induced apoptosis. *Mol Syst Biol* **11**: 797.

- Farooq A, Zhou MM. 2004. Structure and regulation of MAPK phosphatases. *Cell Signal* **16**: 769-779.
- Fata JE, Chaudhary V, Khokha R. 2001. Cellular turnover in the mammary gland is correlated with systemic levels of progesterone and not 17beta-estradiol during the estrous cycle. *Biol Reprod* **65**: 680-688.
- Faure E, Heisterkamp N, Groffen J, Kaartinen V. 2000. Differential expression of TGF-beta isoforms during postlactational mammary gland involution. *Cell Tissue Res* **300**: 89-95.
- Feng Y, Manka D, Wagner KU, Khan SA. 2007. Estrogen receptor-alpha expression in the mammary epithelium is required for ductal and alveolar morphogenesis in mice. *Proc Natl Acad Sci U S A* **104**: 14718-14723.
- Follit JA, San Agustin JT, Xu F, Jonassen JA, Samtani R, Lo CW, Pazour GJ. 2008. The Golgin GMAP210/TRIP11 anchors IFT20 to the Golgi complex. *PLoS Genet* **4**: e1000315.
- Frisch SM, Francis H. 1994. Disruption of epithelial cell-matrix interactions induces apoptosis. *J Cell Biol* **124**: 619-626.
- Frisch SM, Screaton RA. 2001. Anoikis mechanisms. *Curr Opin Cell Biol* **13**: 555-562.
- Frisch SM, Vuori K, Kelaita D, Sicks S. 1996. A role for Jun-N-terminal kinase in anoikis; suppression by bcl-2 and crmA. *J Cell Biol* **135**: 1377-1382.
- Fuchs Y, Steller H. 2011. Programmed cell death in animal development and disease. *Cell* **147**: 742-758.
- Fung C, Lock R, Gao S, Salas E, Debnath J. 2008. Induction of autophagy during extracellular matrix detachment promotes cell survival. *Mol Biol Cell* **19**: 797-806.
- Gallo KA, Johnson GL. 2002. Mixed-lineage kinase control of JNK and p38 MAPK pathways. *Nat Rev Mol Cell Biol* **3**: 663-672.
- Garraway LA, Lander ES. 2013. Lessons from the cancer genome. *Cell* **153**: 17-37.
- Gawrzak S, Rinaldi L, Gregorio S, Arenas EJ, Salvador F, Urosevic J, Figueras-Puig C, Rojo F, Del Barco Barrantes I, Cejalvo JM et al. 2018. MSK1 regulates luminal cell differentiation and metastatic dormancy in ER(+) breast cancer. *Nat Cell Biol*.
- Gibson MC, Perrimon N. 2005. Extrusion and death of DPP/BMP-compromised epithelial cells in the developing Drosophila wing. *Science* **307**: 1785-1789.
- Girnius N, Davis RJ. 2017a. JNK Promotes Epithelial Cell Anoikis by Transcriptional and Post-translational Regulation of BH3-Only Proteins. *Cell Rep* **21**: 1910-1921.
- . 2017b. JNK promotes epithelial cell anoikis by transcriptional and post-translational regulation of BH3-only proteins. *Cell Reports* **21**: 1910-1921.
- Gozdecka M, Lyons S, Kondo S, Taylor J, Li Y, Walczynski J, Thiel G, Breitwieser W, Jones N. 2014. JNK suppresses tumor formation via a gene-expression program mediated by ATF2. *Cell Rep* **9**: 1361-1374.

- Greenman C, Stephens P, Smith R, Dalgliesh GL, Hunter C, Bignell G, Davies H, Teague J, Butler A, Stevens C et al. 2007. Patterns of somatic mutation in human cancer genomes. *Nature* **446**: 153-158.
- Grivennikov SI, Greten FR, Karin M. 2010. Immunity, inflammation, and cancer. *Cell* **140**: 883-899.
- Gu Z, Eils R, Schlesner M. 2016. Complex heatmaps reveal patterns and correlations in multidimensional genomic data. *Bioinformatics* **32**: 2847-2849.
- Guo W, Pylayeva Y, Pepe A, Yoshioka T, Muller WJ, Inghirami G, Giancotti FG. 2006. Beta 4 integrin amplifies ErbB2 signaling to promote mammary tumorigenesis. *Cell* **126**: 489-502.
- Gupta S, Barrett T, Whitmarsh AJ, Cavanagh J, Sluss HK, Derijard B, Davis RJ. 1996. Selective interaction of JNK protein kinase isoforms with transcription factors. *EMBO J* **15**: 2760-2770.
- Halaoui R, Rejon C, Chatterjee SJ, Szymborski J, Meterissian S, Muller WJ, Omeroglu A, McCaffrey L. 2017. Progressive polarity loss and luminal collapse disrupt tissue organization in carcinoma. *Genes Dev* **31**: 1573-1587.
- Halazonetis TD, Gorgoulis VG, Bartek J. 2008. An oncogene-induced DNA damage model for cancer development. *Science* **319**: 1352-1355.
- Han MS, Barrett T, Brehm MA, Davis RJ. 2016. Inflammation Mediated by JNK in Myeloid Cells Promotes the Development of Hepatitis and Hepatocellular Carcinoma. *Cell Rep* **15**: 19-26.
- Han MS, Jung DY, Morel C, Lakhani SA, Kim JK, Flavell RA, Davis RJ. 2013. JNK expression by macrophages promotes obesity-induced insulin resistance and inflammation. *Science* **339**: 218-222.
- Hanahan D, Weinberg RA. 2011. Hallmarks of cancer: the next generation. *Cell* **144**: 646-674.
- Harper KL, Sosa MS, Entenberg D, Hosseini H, Cheung JF, Nobre R, Avivar-Valderas A, Nagi C, Girnius N, Davis RJ et al. 2016. Mechanism of early dissemination and metastasis in Her2(+) mammary cancer. *Nature* **540**: 588-592.
- Hayakawa J, Mittal S, Wang Y, Korkmaz KS, Adamson E, English C, Ohmichi M, McClelland M, Mercola D. 2004. Identification of promoters bound by c-Jun/ATF2 during rapid large-scale gene activation following genotoxic stress. *Mol Cell* **16**: 521-535.
- Heberle H, Meirelles GV, da Silva FR, Telles GP, Minghim R. 2015. InteractiVenn: a web-based tool for the analysis of sets through Venn diagrams. *BMC Bioinformatics* **16**: 169.
- Helbig L, Damrot J, Hulskenbeck J, Koberle B, Brozovic A, Osmak M, Fiket Z, Kaina B, Fritz G. 2011. Late activation of stress-activated protein kinases/c-Jun N-terminal kinases triggered by cisplatin-induced DNA damage in repair-defective cells. *J Biol Chem* **286**: 12991-13001.

- Helleday T, Petermann E, Lundin C, Hodgson B, Sharma RA. 2008. DNA repair pathways as targets for cancer therapy. *Nat Rev Cancer* **8**: 193-204.
- Hess P, Pihan G, Sawyers CL, Flavell RA, Davis RJ. 2002. Survival signaling mediated by c-Jun NH(2)-terminal kinase in transformed B lymphoblasts. *Nat Genet* **32**: 201-205.
- Hoang VT, Yan TJ, Cavanaugh JE, Flaherty PT, Beckman BS, Burow ME. 2017. Oncogenic signaling of MEK5-ERK5. *Cancer Lett* **392**: 51-59.
- Hojilla CV, Jackson HW, Khokha R. 2011. TIMP3 regulates mammary epithelial apoptosis with immune cell recruitment through differential TNF dependence. *PLoS One* **6**: e26718.
- Horseman ND, Zhao W, Montecino-Rodriguez E, Tanaka M, Nakashima K, Engle SJ, Smith F, Markoff E, Dorshkind K. 1997. Defective mammopoiesis, but normal hematopoiesis, in mice with a targeted disruption of the prolactin gene. *EMBO J* **16**: 6926-6935.
- Huang C, Jacobson K, Schaller MD. 2004. MAP kinases and cell migration. *J Cell Sci* **117**: 4619-4628.
- Huang C, Rajfur Z, Borchers C, Schaller MD, Jacobson K. 2003. JNK phosphorylates paxillin and regulates cell migration. *Nature* **424**: 219-223.
- Huang CY, Tan TH. 2012. DUSPs, to MAP kinases and beyond. *Cell Biosci* **2**: 24.
- Huang DC, Strasser A. 2000. BH3-Only proteins-essential initiators of apoptotic cell death. *Cell* **103**: 839-842.
- Huang W, Loganantharaj R, Schroeder B, Fargo D, Li L. 2013. PAVIS: a tool for Peak Annotation and Visualization. *Bioinformatics* **29**: 3097-3099.
- Hubner A, Barrett T, Flavell RA, Davis RJ. 2008. Multisite phosphorylation regulates Bim stability and apoptotic activity. *Mol Cell* **30**: 415-425.
- Hubner A, Cavanagh-Kyros J, Rincon M, Flavell RA, Davis RJ. 2010. Functional cooperation of the proapoptotic Bcl2 family proteins Bmf and Bim in vivo. *Mol Cell Biol* **30**: 98-105.
- Hubner A, Mulholland DJ, Standen CL, Karasarides M, Cavanagh-Kyros J, Barrett T, Chi H, Greiner DL, Tournier C, Sawyers CL et al. 2012. JNK and PTEN cooperatively control the development of invasive adenocarcinoma of the prostate. *Proc Natl Acad Sci U S A* **109**: 12046-12051.
- Hui L, Bakiri L, Mairhorfer A, Schweifer N, Haslinger C, Kenner L, Komnenovic V, Scheuch H, Beug H, Wagner EF. 2007. p38alpha suppresses normal and cancer cell proliferation by antagonizing the JNK-c-Jun pathway. *Nat Genet* **39**: 741-749.
- Hui L, Zatloukal K, Scheuch H, Stepniak E, Wagner EF. 2008. Proliferation of human HCC cells and chemically induced mouse liver cancers requires JNK1-dependent p21 downregulation. *J Clin Invest* **118**: 3943-3953.
- Humphreys RC, Bieri B, Zhao L, Raz R, Levy D, Hennighausen L. 2002. Deletion of Stat3 blocks mammary gland involution and extends functional competence of the secretory epithelium in the absence of lactogenic stimuli. *Endocrinology* **143**: 3641-3650.

- Humphreys RC, Krajewska M, Krnacik S, Jaeger R, Weiher H, Krajewski S, Reed JC, Rosen JM. 1996. Apoptosis in the terminal endbud of the murine mammary gland: a mechanism of ductal morphogenesis. *Development* **122**: 4013-4022.
- Humphreys RC, Lydon J, O'Malley BW, Rosen JM. 1997. Mammary gland development is mediated by both stromal and epithelial progesterone receptors. *Mol Endocrinol* **11**: 801-811.
- Igaki T. 2009. Correcting developmental errors by apoptosis: lessons from Drosophila JNK signaling. *Apoptosis* **14**: 1021-1028.
- Igaki T, Pagliarini RA, Xu T. 2006. Loss of cell polarity drives tumor growth and invasion through JNK activation in Drosophila. *Curr Biol* **16**: 1139-1146.
- Igaki T, Pastor-Pareja JC, Aonuma H, Miura M, Xu T. 2009. Intrinsic tumor suppression and epithelial maintenance by endocytic activation of Eiger/TNF signaling in Drosophila. *Dev Cell* **16**: 458-465.
- Inman JL, Robertson C, Mott JD, Bissell MJ. 2015. Mammary gland development: cell fate specification, stem cells and the microenvironment. *Development* **142**: 1028-1042.
- Jaeschke A, Davis RJ. 2007. Metabolic stress signaling mediated by mixed-lineage kinases. *Mol Cell* **27**: 498-508.
- Jaeschke A, Karasarides M, Ventura JJ, Ehrhardt A, Zhang C, Flavell RA, Shokat KM, Davis RJ. 2006. JNK2 is a positive regulator of the cJun transcription factor. *Mol Cell* **23**: 899-911.
- Jaggi R, Marti A, Guo K, Feng Z, Friis RR. 1996. Regulation of a physiological apoptosis: mouse mammary involution. *J Dairy Sci* **79**: 1074-1084.
- Jindal S, Gao D, Bell P, Albrechtsen G, Edgerton SM, Ambrosone CB, Thor AD, Borges VF, Schedin P. 2014. Postpartum breast involution reveals regression of secretory lobules mediated by tissue-remodeling. *Breast Cancer Res* **16**: R31.
- Jurgensmeier JM, Xie Z, Deveraux Q, Ellerby L, Bredesen D, Reed JC. 1998. Bax directly induces release of cytochrome c from isolated mitochondria. *Proc Natl Acad Sci U S A* **95**: 4997-5002.
- Kaji T, Yoshida S, Kawai K, Fuchigami Y, Watanabe W, Kubodera H, Kishimoto T. 2010. ASK3, a novel member of the apoptosis signal-regulating kinase family, is essential for stress-induced cell death in HeLa cells. *Biochem Biophys Res Commun* **395**: 213-218.
- Kaminker JS, Zhang Y, Watanabe C, Zhang Z. 2007. CanPredict: a computational tool for predicting cancer-associated missense mutations. *Nucleic Acids Res* **35**: W595-598.
- Kan Z, Jaiswal BS, Stinson J, Janakiraman V, Bhatt D, Stern HM, Yue P, Haverty PM, Bourgon R, Zheng J et al. 2010. Diverse somatic mutation patterns and pathway alterations in human cancers. *Nature* **466**: 869-873.
- Kant S, Standen CL, Morel C, Jung DY, Kim JK, Swat W, Flavell RA, Davis RJ. 2017. A Protein Scaffold Coordinates SRC-Mediated JNK Activation in Response to Metabolic Stress. *Cell Rep* **20**: 2775-2783.

- Kant S, Swat W, Zhang S, Zhang ZY, Neel BG, Flavell RA, Davis RJ. 2011. TNF-stimulated MAP kinase activation mediated by a Rho family GTPase signaling pathway. *Genes Dev* **25**: 2069-2078.
- Karreth F, Hoebertz A, Scheuch H, Eferl R, Wagner EF. 2004. The AP1 transcription factor Fra2 is required for efficient cartilage development. *Development* **131**: 5717-5725.
- Kesavan K, Lobel-Rice K, Sun W, Lapadat R, Webb S, Johnson GL, Garrington TP. 2004. MEKK2 regulates the coordinate activation of ERK5 and JNK in response to FGF-2 in fibroblasts. *J Cell Physiol* **199**: 140-148.
- Khwaja A, Downward J. 1997. Lack of correlation between activation of Jun-NH2-terminal kinase and induction of apoptosis after detachment of epithelial cells. *J Cell Biol* **139**: 1017-1023.
- Kim D, Pertea G, Trapnell C, Pimentel H, Kelley R, Salzberg SL. 2013. TopHat2: accurate alignment of transcriptomes in the presence of insertions, deletions and gene fusions. *Genome Biol* **14**: R36.
- Kittrell FS, Oborn CJ, Medina D. 1992. Development of mammary preneoplasias in vivo from mouse mammary epithelial cell lines in vitro. *Cancer Res* **52**: 1924-1932.
- Kreuzaler PA, Staniszewska AD, Li W, Omidvar N, Kedjouar B, Turkson J, Poli V, Flavell RA, Clarkson RW, Watson CJ. 2011. Stat3 controls lysosomal-mediated cell death in vivo. *Nat Cell Biol* **13**: 303-309.
- Kritikou EA, Sharkey A, Abell K, Came PJ, Anderson E, Clarkson RW, Watson CJ. 2003. A dual, non-redundant, role for LIF as a regulator of development and STAT3-mediated cell death in mammary gland. *Development* **130**: 3459-3468.
- Kryston TB, Georgiev AB, Pissis P, Georgakilas AG. 2011. Role of oxidative stress and DNA damage in human carcinogenesis. *Mutat Res* **711**: 193-201.
- Krzywinski M, Schein J, Birol I, Connors J, Gascoyne R, Horsman D, Jones SJ, Marra MA. 2009. Circos: an information aesthetic for comparative genomics. *Genome Res* **19**: 1639-1645.
- Kuan CY, Yang DD, Samanta Roy DR, Davis RJ, Rakic P, Flavell RA. 1999. The Jnk1 and Jnk2 protein kinases are required for regional specific apoptosis during early brain development. *Neuron* **22**: 667-676.
- Labi V, Woess C, Tuzlak S, Erlacher M, Bouillet P, Strasser A, Tzankov A, Villunger A. 2014. Deregulated cell death and lymphocyte homeostasis cause premature lethality in mice lacking the BH3-only proteins Bim and Bmf. *Blood* **123**: 2652-2662.
- Lamb JA, Ventura JJ, Hess P, Flavell RA, Davis RJ. 2003. JunD mediates survival signaling by the JNK signal transduction pathway. *Mol Cell* **11**: 1479-1489.
- Langmead B, Salzberg SL. 2012. Fast gapped-read alignment with Bowtie 2. *Nat Methods* **9**: 357-359.

- Lei K, Davis RJ. 2003. JNK phosphorylation of Bim-related members of the Bcl2 family induces Bax-dependent apoptosis. *Proc Natl Acad Sci U S A* **100**: 2432-2437.
- Lei K, Nimnual A, Zong WX, Kennedy NJ, Flavell RA, Thompson CB, Bar-Sagi D, Davis RJ. 2002. The Bax subfamily of Bcl2-related proteins is essential for apoptotic signal transduction by c-Jun NH(2)-terminal kinase. *Mol Cell Biol* **22**: 4929-4942.
- Leung CT, Brugge JS. 2012. Outgrowth of single oncogene-expressing cells from suppressive epithelial environments. *Nature* **482**: 410-413.
- Ley R, Balmanno K, Hadfield K, Weston C, Cook SJ. 2003. Activation of the ERK1/2 signaling pathway promotes phosphorylation and proteasome-dependent degradation of the BH3-only protein, Bim. *J Biol Chem* **278**: 18811-18816.
- Li H. 2017. seqtk - Toolkit for processing sequences in FASTA/Q formats. <https://github.com/lh3/seqtk>.
- Li H, Handsaker B, Wysoker A, Fennell T, Ruan J, Homer N, Marth G, Abecasis G, Durbin R, Genome Project Data Processing S. 2009. The Sequence Alignment/Map format and SAMtools. *Bioinformatics* **25**: 2078-2079.
- Li M, Liu X, Robinson G, Bar-Peled U, Wagner KU, Young WS, Hennighausen L, Furth PA. 1997. Mammary-derived signals activate programmed cell death during the first stage of mammary gland involution. *Proc Natl Acad Sci U S A* **94**: 3425-3430.
- Lin EY, Gouon-Evans V, Nguyen AV, Pollard JW. 2002. The macrophage growth factor CSF-1 in mammary gland development and tumor progression. *J Mammary Gland Biol Neoplasia* **7**: 147-162.
- Lin J, Gan CM, Zhang X, Jones S, Sjoblom T, Wood LD, Parsons DW, Papadopoulos N, Kinzler KW, Vogelstein B et al. 2007. A multidimensional analysis of genes mutated in breast and colorectal cancers. *Genome Res* **17**: 1304-1318.
- Lindsten T, Ross AJ, King A, Zong WX, Rathmell JC, Shiels HA, Ulrich E, Waymire KG, Mahar P, Frauwirth K et al. 2000. The combined functions of proapoptotic Bcl-2 family members bak and bax are essential for normal development of multiple tissues. *Mol Cell* **6**: 1389-1399.
- Liu X, Robinson GW, Wagner KU, Garrett L, Wynshaw-Boris A, Hennighausen L. 1997. Stat5a is mandatory for adult mammary gland development and lactogenesis. *Genes Dev* **11**: 179-186.
- Lu C, Zhu F, Cho YY, Tang F, Zykova T, Ma WY, Bode AM, Dong Z. 2006. Cell apoptosis: requirement of H2AX in DNA ladder formation, but not for the activation of caspase-3. *Mol Cell* **23**: 121-132.
- Lund LR, Bjorn SF, Sternlicht MD, Nielsen BS, Solberg H, Usher PA, Osterby R, Christensen IJ, Stephens RW, Bugge TH et al. 2000. Lactational competence and involution of the mouse mammary gland require plasminogen. *Development* **127**: 4481-4492.

- Lund LR, Romer J, Thomasset N, Solberg H, Pyke C, Bissell MJ, Dano K, Werb Z. 1996. Two distinct phases of apoptosis in mammary gland involution: proteinase-independent and -dependent pathways. *Development* **122**: 181-193.
- Lyons TR, O'Brien J, Borges VF, Conklin MW, Keely PJ, Eliceiri KW, Marusyk A, Tan AC, Schedin P. 2011. Postpartum mammary gland involution drives progression of ductal carcinoma in situ through collagen and COX-2. *Nat Med* **17**: 1109-1115.
- Ma C, Ying C, Yuan Z, Song B, Li D, Liu Y, Lai B, Li W, Chen R, Ching YP et al. 2007. dp5/HRK is a c-Jun target gene and required for apoptosis induced by potassium deprivation in cerebellar granule neurons. *J Biol Chem* **282**: 30901-30909.
- Mailleux AA, Overholtzer M, Brugge JS. 2008. Lumen formation during mammary epithelial morphogenesis: insights from in vitro and in vivo models. *Cell Cycle* **7**: 57-62.
- Mailleux AA, Overholtzer M, Schmelzle T, Bouillet P, Strasser A, Brugge JS. 2007. BIM regulates apoptosis during mammary ductal morphogenesis, and its absence reveals alternative cell death mechanisms. *Dev Cell* **12**: 221-234.
- Mallepell S, Krust A, Chambon P, Briskin C. 2006. Paracrine signaling through the epithelial estrogen receptor alpha is required for proliferation and morphogenesis in the mammary gland. *Proc Natl Acad Sci U S A* **103**: 2196-2201.
- Manning AM, Davis RJ. 2003. Targeting JNK for therapeutic benefit: from junk to gold? *Nat Rev Drug Discov* **2**: 554-565.
- Marcotte R, Sayad A, Brown KR, Sanchez-Garcia F, Reimand J, Haider M, Virtanen C, Bradner JE, Bader GD, Mills GB et al. 2016. Functional Genomic Landscape of Human Breast Cancer Drivers, Vulnerabilities, and Resistance. *Cell* **164**: 293-309.
- Marino S, Vooijs M, van Der Gulden H, Jonkers J, Berns A. 2000. Induction of medulloblastomas in p53-null mutant mice by somatic inactivation of Rb in the external granular layer cells of the cerebellum. *Genes Dev* **14**: 994-1004.
- Marti A, Lazar H, Ritter P, Jaggi R. 1999. Transcription factor activities and gene expression during mouse mammary gland involution. *J Mammary Gland Biol Neoplasia* **4**: 145-152.
- Martinson HA, Jindal S, Durand-Rougely C, Borges VF, Schedin P. 2015. Wound healing-like immune program facilitates postpartum mammary gland involution and tumor progression. *Int J Cancer* **136**: 1803-1813.
- Maurer U, Charvet C, Wagman AS, Dejardin E, Green DR. 2006. Glycogen synthase kinase-3 regulates mitochondrial outer membrane permeabilization and apoptosis by destabilization of MCL-1. *Mol Cell* **21**: 749-760.

- McNally S, McArdle E, Gilligan E, Napoletano S, Gajewska M, Bergin O, McCarthy S, Whyte J, Bianchi A, Stack J et al. 2011. c-Jun N-terminal kinase activity supports multiple phases of 3D-mammary epithelial acinus formation. *Int J Dev Biol* **55**: 731-744.
- Melief CJ, Finn OJ. 2011. Cancer immunology. *Curr Opin Immunol* **23**: 234-236.
- Montecucco A, Zanetta F, Biamonti G. 2015. Molecular mechanisms of etoposide. *EXCLI J* **14**: 95-108.
- Morel C, Carlson SM, White FM, Davis RJ. 2009. Mcl-1 integrates the opposing actions of signaling pathways that mediate survival and apoptosis. *Mol Cell Biol* **29**: 3845-3852.
- Moreno E, Basler K. 2004. dMyc transforms cells into super-competitors. *Cell* **117**: 117-129.
- Moreno E, Basler K, Morata G. 2002. Cells compete for decapentaplegic survival factor to prevent apoptosis in Drosophila wing development. *Nature* **416**: 755-759.
- Morriss-Kay GM. 1981. Growth and development of pattern in the cranial neural epithelium of rat embryos during neurulation. *J Embryol Exp Morphol* **65 Suppl**: 225-241.
- Mouse EC, Stamatoyannopoulos JA, Snyder M, Hardison R, Ren B, Gingeras T, Gilbert DM, Groudine M, Bender M, Kaul R et al. 2012. An encyclopedia of mouse DNA elements (Mouse ENCODE). *Genome Biol* **13**: 418.
- Murtagh J, McArdle E, Gilligan E, Thornton L, Furlong F, Martin F. 2004. Organization of mammary epithelial cells into 3D acinar structures requires glucocorticoid and JNK signaling. *J Cell Biol* **166**: 133-143.
- Muzumdar MD, Tasic B, Miyamichi K, Li L, Luo L. 2007. A global double-fluorescent Cre reporter mouse. *Genesis* **45**: 593-605.
- Naldini L, Blomer U, Gallay P, Ory D, Mulligan R, Gage FH, Verma IM, Trono D. 1996. In vivo gene delivery and stable transduction of nondividing cells by a lentiviral vector. *Science* **272**: 263-267.
- Narita M, Shimizu S, Ito T, Chittenden T, Lutz RJ, Matsuda H, Tsujimoto Y. 1998. Bax interacts with the permeability transition pore to induce permeability transition and cytochrome c release in isolated mitochondria. *Proc Natl Acad Sci U S A* **95**: 14681-14686.
- Narzisi G, O'Rawe JA, Iossifov I, Fang H, Lee YH, Wang Z, Wu Y, Lyon GJ, Wigler M, Schatz MC. 2014. Accurate de novo and transmitted indel detection in exome-capture data using microassembly. *Nat Methods* **11**: 1033-1036.
- Nguyen AV, Pollard JW. 2000. Transforming growth factor beta3 induces cell death during the first stage of mammary gland involution. *Development* **127**: 3107-3118.
- Nik-Zainal S, Davies H, Staaf J, Ramakrishna M, Glodzik D, Zou X, Martincorena I, Alexandrov LB, Martin S, Wedge DC et al. 2016a. Landscape of somatic mutations in 560 breast cancer whole-genome sequences. *Nature* **534**: 47-54.

- Nik-Zainal S, Davies H, Staaf J, Ramakrishna M, Glodzik D, Zou X, Martincorena I, Alexandrov LB, Martin S, Wedge DC et al. 2016b. Landscape of somatic mutations in 560 breast cancer whole-genome sequences. *Nature* **534**: 47-54.
- Nishimoto S, Nishida E. 2006. MAPK signalling: ERK5 versus ERK1/2. *EMBO Rep* **7**: 782-786.
- Novaro V, Roskelley CD, Bissell MJ. 2003. Collagen-IV and laminin-1 regulate estrogen receptor alpha expression and function in mouse mammary epithelial cells. *J Cell Sci* **116**: 2975-2986.
- O'Brien J, Lyons T, Monks J, Lucia MS, Wilson RS, Hines L, Man YG, Borges V, Schedin P. 2010. Alternatively activated macrophages and collagen remodeling characterize the postpartum involuting mammary gland across species. *Am J Pathol* **176**: 1241-1255.
- O'Brien J, Martinson H, Durand-Rougely C, Schedin P. 2012. Macrophages are crucial for epithelial cell death and adipocyte repopulation during mammary gland involution. *Development* **139**: 269-275.
- O'Neill KL, Huang K, Zhang J, Chen Y, Luo X. 2016. Inactivation of prosurvival Bcl-2 proteins activates Bax/Bak through the outer mitochondrial membrane. *Genes Dev* **30**: 973-988.
- Ohsawa S, Sugimura K, Takino K, Xu T, Miyawaki A, Igaki T. 2011. Elimination of oncogenic neighbors by JNK-mediated engulfment in *Drosophila*. *Dev Cell* **20**: 315-328.
- Ormandy CJ, Camus A, Barra J, Damotte D, Lucas B, Buteau H, Edery M, Brousse N, Babinet C, Binart N et al. 1997. Null mutation of the prolactin receptor gene produces multiple reproductive defects in the mouse. *Genes Dev* **11**: 167-178.
- Page-McCaw A, Ewald AJ, Werb Z. 2007. Matrix metalloproteinases and the regulation of tissue remodelling. *Nat Rev Mol Cell Biol* **8**: 221-233.
- Park HS, Kim MS, Huh SH, Park J, Chung J, Kang SS, Choi EJ. 2002. Akt (protein kinase B) negatively regulates SEK1 by means of protein phosphorylation. *J Biol Chem* **277**: 2573-2578.
- Parmigiani G, Boca S, Lin J, Kinzler KW, Velculescu V, Vogelstein B. 2009. Design and analysis issues in genome-wide somatic mutation studies of cancer. *Genomics* **93**: 17-21.
- Parsons DW, Wang TL, Samuels Y, Bardelli A, Cummins JM, DeLong L, Silliman N, Ptak J, Szabo S, Willson JK et al. 2005. Colorectal cancer: mutations in a signalling pathway. *Nature* **436**: 792.
- Perou CM. 2011. Molecular stratification of triple-negative breast cancers. *Oncologist* **16 Suppl 1**: 61-70.
- Philp JA, Burdon TG, Watson CJ. 1996. Differential activation of STATs 3 and 5 during mammary gland development. *FEBS Lett* **396**: 77-80.
- Pinon JD, Labi V, Egle A, Villunger A. 2008. Bim and Bmf in tissue homeostasis and malignant disease. *Oncogene* **27 Suppl 1**: S41-52.

- Pradeep CR, Kostler WJ, Lauriola M, Granit RZ, Zhang F, Jacob-Hirsch J, Rechavi G, Nair HB, Hennessy BT, Gonzalez-Angulo AM et al. 2012. Modeling ductal carcinoma in situ: a HER2-Notch3 collaboration enables luminal filling. *Oncogene* **31**: 907-917.
- Pulverer BJ, Kyriakis JM, Avruch J, Nikolakaki E, Woodgett JR. 1991. Phosphorylation of c-jun mediated by MAP kinases. *Nature* **353**: 670-674.
- Puthalakath H, Strasser A. 2002. Keeping killers on a tight leash: transcriptional and post-translational control of the pro-apoptotic activity of BH3-only proteins. *Cell Death Differ* **9**: 505-512.
- Qian BZ, Pollard JW. 2010. Macrophage diversity enhances tumor progression and metastasis. *Cell* **141**: 39-51.
- Quinlan AR, Hall IM. 2010. BEDTools: a flexible suite of utilities for comparing genomic features. *Bioinformatics* **26**: 841-842.
- Ramo K, Sugamura K, Craige S, Keaney JF, Davis RJ. 2016. Suppression of ischemia in arterial occlusive disease by JNK-promoted native collateral artery development. *Elife* **5**.
- Reginato MJ, Mills KR, Paulus JK, Lynch DK, Sgroi DC, Debnath J, Muthuswamy SK, Brugge JS. 2003. Integrins and EGFR coordinately regulate the pro-apoptotic protein Bim to prevent anoikis. *Nat Cell Biol* **5**: 733-740.
- Riesgo-Escovar JR, Hafen E. 1997. Drosophila Jun kinase regulates expression of decapentaplegic via the ETS-domain protein Aop and the AP-1 transcription factor DJun during dorsal closure. *Genes Dev* **11**: 1717-1727.
- Riesgo-Escovar JR, Jenni M, Fritz A, Hafen E. 1996. The Drosophila Jun-N-terminal kinase is required for cell morphogenesis but not for DJun-dependent cell fate specification in the eye. *Genes Dev* **10**: 2759-2768.
- Ring JM, Martinez Arias A. 1993. puckered, a gene involved in position-specific cell differentiation in the dorsal epidermis of the Drosophila larva. *Dev Suppl*: 251-259.
- Roh HC, Tsai LT, Lyubetskaya A, Tenen D, Kumari M, Rosen ED. 2017. Simultaneous Transcriptional and Epigenomic Profiling from Specific Cell Types within Heterogeneous Tissues In Vivo. *Cell Rep* **18**: 1048-1061.
- Ryoo HD, Gorenc T, Steller H. 2004. Apoptotic cells can induce compensatory cell proliferation through the JNK and the Wingless signaling pathways. *Dev Cell* **7**: 491-501.
- Sabapathy K, Jochum W, Hochedlinger K, Chang L, Karin M, Wagner EF. 1999. Defective neural tube morphogenesis and altered apoptosis in the absence of both JNK1 and JNK2. *Mech Dev* **89**: 115-124.
- Sabio G, Das M, Mora A, Zhang Z, Jun JY, Ko HJ, Barrett T, Kim JK, Davis RJ. 2008. A stress signaling pathway in adipose tissue regulates hepatic insulin resistance. *Science* **322**: 1539-1543.
- Sakamoto K, Wehde BL, Yoo KH, Kim T, Rajbhandari N, Shin HY, Triplett AA, Radler PD, Schuler F, Villunger A et al. 2016. Janus Kinase 1 Is Essential for Inflammatory Cytokine Signaling and Mammary Gland Remodeling. *Mol Cell Biol* **36**: 1673-1690.

- Sakurai T, Maeda S, Chang L, Karin M. 2006. Loss of hepatic NF-kappa B activity enhances chemical hepatocarcinogenesis through sustained c-Jun N-terminal kinase 1 activation. *Proc Natl Acad Sci U S A* **103**: 10544-10551.
- Saldanha AJ. 2004. Java Treeview--extensible visualization of microarray data. *Bioinformatics* **20**: 3246-3248.
- Sanchez-Garcia F, Villagrasa P, Matsui J, Kotliar D, Castro V, Akavia UD, Chen BJ, Saucedo-Cuevas L, Rodriguez Barrueco R, Llobet-Navas D et al. 2014. Integration of genomic data enables selective discovery of breast cancer drivers. *Cell* **159**: 1461-1475.
- Sanchez-Perez I, Murguia JR, Perona R. 1998. Cisplatin induces a persistent activation of JNK that is related to cell death. *Oncogene* **16**: 533-540.
- Sargeant TJ, Lloyd-Lewis B, Resemann HK, Ramos-Montoya A, Skepper J, Watson CJ. 2014. Stat3 controls cell death during mammary gland involution by regulating uptake of milk fat globules and lysosomal membrane permeabilization. *Nat Cell Biol* **16**: 1057-1068.
- Sathirapongsasuti JF, Lee H, Horst BA, Brunner G, Cochran AJ, Binder S, Quackenbush J, Nelson SF. 2011. Exome sequencing-based copy-number variation and loss of heterozygosity detection: ExomeCNV. *Bioinformatics* **27**: 2648-2654.
- Saunders CT, Wong WS, Swamy S, Becq J, Murray LJ, Cheetham RK. 2012. Strelka: accurate somatic small-variant calling from sequenced tumor-normal sample pairs. *Bioinformatics* **28**: 1811-1817.
- Schaller MD. 2001. Paxillin: a focal adhesion-associated adaptor protein. *Oncogene* **20**: 6459-6472.
- Schedin P. 2006. Pregnancy-associated breast cancer and metastasis. *Nat Rev Cancer* **6**: 281-291.
- Scheele CL, Hannezo E, Muraro MJ, Zomer A, Langedijk NS, van Oudenaarden A, Simons BD, van Rheenen J. 2017. Identity and dynamics of mammary stem cells during branching morphogenesis. *Nature* **542**: 313-317.
- Schindelin J, Arganda-Carreras I, Frise E, Kaynig V, Longair M, Pietzsch T, Preibisch S, Rueden C, Saalfeld S, Schmid B et al. 2012. Fiji: an open-source platform for biological-image analysis. *Nat Methods* **9**: 676-682.
- Schmelzle T, Mailleux AA, Overholtzer M, Carroll JS, Solimini NL, Lightcap ES, Veiby OP, Brugge JS. 2007. Functional role and oncogene-regulated expression of the BH3-only factor Bmf in mammary epithelial anoikis and morphogenesis. *Proc Natl Acad Sci U S A* **104**: 3787-3792.
- Schneider CA, Rasband WS, Eliceiri KW. 2012. NIH Image to ImageJ: 25 years of image analysis. *Nat Methods* **9**: 671-675.
- Schramek D, Kotsinas A, Meixner A, Wada T, Elling U, Pospisilik JA, Neely GG, Zwick RH, Sigl V, Forni G et al. 2011. The stress kinase MKK7 couples oncogenic stress to p53 stability and tumor suppression. *Nat Genet* **43**: 212-219.

- Schreiber M, Kolbus A, Piu F, Szabowski A, Mohle-Steinlein U, Tian J, Karin M, Angel P, Wagner EF. 1999. Control of cell cycle progression by c-Jun is p53 dependent. *Genes Dev* **13**: 607-619.
- Schreiber RD, Old LJ, Smyth MJ. 2011. Cancer immunoediting: integrating immunity's roles in cancer suppression and promotion. *Science* **331**: 1565-1570.
- Schuler F, Baumgartner F, Klepsch V, Chamson M, Muller-Holzner E, Watson CJ, Oh S, Hennighausen L, Tymoszek P, Doppler W et al. 2016. The BH3-only protein BIM contributes to late-stage involution in the mouse mammary gland. *Cell Death Differ* **23**: 41-51.
- Selvarajan S, Lund LR, Takeuchi T, Craik CS, Werb Z. 2001. A plasma kallikrein-dependent plasminogen cascade required for adipocyte differentiation. *Nat Cell Biol* **3**: 267-275.
- Shah SP, Roth A, Goya R, Oloumi A, Ha G, Zhao Y, Turashvili G, Ding J, Tse K, Haffari G et al. 2012. The clonal and mutational evolution spectrum of primary triple-negative breast cancers. *Nature* **486**: 395-399.
- Shen J, Dahmann C. 2005. Extrusion of cells with inappropriate Dpp signaling from Drosophila wing disc epithelia. *Science* **307**: 1789-1790.
- Shim JH, Xiao C, Paschal AE, Bailey ST, Rao P, Hayden MS, Lee KY, Bussey C, Steckel M, Tanaka N et al. 2005. TAK1, but not TAB1 or TAB2, plays an essential role in multiple signaling pathways in vivo. *Genes Dev* **19**: 2668-2681.
- Shin KJ, Wall EA, Zavzavadjian JR, Santat LA, Liu J, Hwang JI, Rebres R, Roach T, Seaman W, Simon MI et al. 2006. A single lentiviral vector platform for microRNA-based conditional RNA interference and coordinated transgene expression. *Proc Natl Acad Sci U S A* **103**: 13759-13764.
- Siegel RL, Miller KD, Jemal A. 2015. Cancer statistics, 2015. *CA Cancer J Clin* **65**: 5-29.
- Sluss HK, Davis RJ. 1997. Embryonic morphogenesis signaling pathway mediated by JNK targets the transcription factor JUN and the TGF-beta homologue decapentaplegic. *J Cell Biochem* **67**: 1-12.
- Sluss HK, Han Z, Barrett T, Goberdhan DC, Wilson C, Davis RJ, Ip YT. 1996. A JNK signal transduction pathway that mediates morphogenesis and an immune response in Drosophila. *Genes Dev* **10**: 2745-2758.
- Smeal T, Binetruy B, Mercola DA, Birrer M, Karin M. 1991. Oncogenic and transcriptional cooperation with Ha-Ras requires phosphorylation of c-Jun on serines 63 and 73. *Nature* **354**: 494-496.
- Sonnenblick A, de Azambuja E, Azim HA, Jr., Piccart M. 2015. An update on PARP inhibitors--moving to the adjuvant setting. *Nat Rev Clin Oncol* **12**: 27-41.
- Sorlie T, Tibshirani R, Parker J, Hastie T, Marron JS, Nobel A, Deng S, Johnsen H, Pesich R, Geisler S et al. 2003. Repeated observation of breast tumor

- subtypes in independent gene expression data sets. *Proc Natl Acad Sci U S A* **100**: 8418-8423.
- Stein T, Morris JS, Davies CR, Weber-Hall SJ, Duffy MA, Heath VJ, Bell AK, Ferrier RK, Sandilands GP, Gusterson BA. 2004. Involution of the mouse mammary gland is associated with an immune cascade and an acute-phase response, involving LBP, CD14 and STAT3. *Breast Cancer Res* **6**: R75-91.
- Stein T, Salomonis N, Gusterson BA. 2007. Mammary gland involution as a multi-step process. *J Mammary Gland Biol Neoplasia* **12**: 25-35.
- Stephens PJ, Tarpey PS, Davies H, Van Loo P, Greenman C, Wedge DC, Nik-Zainal S, Martin S, Varela I, Bignell GR et al. 2012. The landscape of cancer genes and mutational processes in breast cancer. *Nature* **486**: 400-404.
- Sternlicht MD, Kouros-Mehr H, Lu P, Werb Z. 2006. Hormonal and local control of mammary branching morphogenesis. *Differentiation* **74**: 365-381.
- Taketani K, Kawauchi J, Tanaka-Okamoto M, Ishizaki H, Tanaka Y, Sakai T, Miyoshi J, Maehara Y, Kitajima S. 2012. Key role of ATF3 in p53-dependent DR5 induction upon DNA damage of human colon cancer cells. *Oncogene* **31**: 2210-2221.
- Talhouk RS, Chin JR, Unemori EN, Werb Z, Bissell MJ. 1991. Proteinases of the mammary gland: developmental regulation in vivo and vectorial secretion in culture. *Development* **112**: 439-449.
- Taraseviciute A, Vincent BT, Schedin P, Jones PL. 2010. Quantitative analysis of three-dimensional human mammary epithelial tissue architecture reveals a role for tenascin-C in regulating c-met function. *Am J Pathol* **176**: 827-838.
- Teng DH, Perry WL, 3rd, Hogan JK, Baumgard M, Bell R, Berry S, Davis T, Frank D, Frye C, Hattier T et al. 1997. Human mitogen-activated protein kinase kinase 4 as a candidate tumor suppressor. *Cancer Res* **57**: 4177-4182.
- Thorn CF, Oshiro C, Marsh S, Hernandez-Boussard T, McLeod H, Klein TE, Altman RB. 2011. Doxorubicin pathways: pharmacodynamics and adverse effects. *Pharmacogenet Genomics* **21**: 440-446.
- Thorvaldsdottir H, Robinson JT, Mesirov JP. 2013. Integrative Genomics Viewer (IGV): high-performance genomics data visualization and exploration. *Brief Bioinform* **14**: 178-192.
- Tiffen PG, Omidvar N, Marquez-Almuina N, Croston D, Watson CJ, Clarkson RW. 2008. A dual role for oncostatin M signaling in the differentiation and death of mammary epithelial cells in vivo. *Mol Endocrinol* **22**: 2677-2688.
- Tobiume K, Matsuzawa A, Takahashi T, Nishitoh H, Morita K, Takeda K, Minowa O, Miyazono K, Noda T, Ichijo H. 2001. ASK1 is required for sustained activations of JNK/p38 MAP kinases and apoptosis. *EMBO Rep* **2**: 222-228.

- Tournier C, Dong C, Turner TK, Jones SN, Flavell RA, Davis RJ. 2001. MKK7 is an essential component of the JNK signal transduction pathway activated by proinflammatory cytokines. *Genes Dev* **15**: 1419-1426.
- Tournier C, Hess P, Yang DD, Xu J, Turner TK, Nimnual A, Bar-Sagi D, Jones SN, Flavell RA, Davis RJ. 2000. Requirement of JNK for stress-induced activation of the cytochrome c-mediated death pathway. *Science* **288**: 870-874.
- Trapnell C, Roberts A, Goff L, Pertea G, Kim D, Kelley DR, Pimentel H, Salzberg SL, Rinn JL, Pachter L. 2012. Differential gene and transcript expression analysis of RNA-seq experiments with TopHat and Cufflinks. *Nat Protoc* **7**: 562-578.
- Trapnell C, Williams BA, Pertea G, Mortazavi A, Kwan G, van Baren MJ, Salzberg SL, Wold BJ, Pachter L. 2010. Transcript assembly and quantification by RNA-Seq reveals unannotated transcripts and isoform switching during cell differentiation. *Nat Biotechnol* **28**: 511-515.
- Uhlirova M, Bohmann D. 2006. JNK- and Fos-regulated Mmp1 expression cooperates with Ras to induce invasive tumors in Drosophila. *EMBO J* **25**: 5294-5304.
- Uhlirova M, Jasper H, Bohmann D. 2005. Non-cell-autonomous induction of tissue overgrowth by JNK/Ras cooperation in a Drosophila tumor model. *Proc Natl Acad Sci U S A* **102**: 13123-13128.
- Ursini-Siegel J, Hardy WR, Zuo D, Lam SH, Sanguin-Gendreau V, Cardiff RD, Pawson T, Muller WJ. 2008. ShcA signalling is essential for tumour progression in mouse models of human breast cancer. *EMBO J* **27**: 910-920.
- van 't Veer LJ, Dai H, van de Vijver MJ, He YD, Hart AA, Mao M, Peterse HL, van der Kooy K, Marton MJ, Witteveen AT et al. 2002. Gene expression profiling predicts clinical outcome of breast cancer. *Nature* **415**: 530-536.
- Van Meter M, Simon M, Tomblin G, May A, Morello TD, Hubbard BP, Bredbenner K, Park R, Sinclair DA, Bohr VA et al. 2016. JNK Phosphorylates SIRT6 to Stimulate DNA Double-Strand Break Repair in Response to Oxidative Stress by Recruiting PARP1 to DNA Breaks. *Cell Rep* **16**: 2641-2650.
- Ventura JJ, Cogswell P, Flavell RA, Baldwin AS, Jr., Davis RJ. 2004a. JNK potentiates TNF-stimulated necrosis by increasing the production of cytotoxic reactive oxygen species. *Genes Dev* **18**: 2905-2915.
- Ventura JJ, Hubner A, Zhang C, Flavell RA, Shokat KM, Davis RJ. 2006. Chemical genetic analysis of the time course of signal transduction by JNK. *Mol Cell* **21**: 701-710.
- Ventura JJ, Kennedy NJ, Flavell RA, Davis RJ. 2004b. JNK regulates autocrine expression of TGF-beta1. *Mol Cell* **15**: 269-278.
- Ventura JJ, Kennedy NJ, Lamb JA, Flavell RA, Davis RJ. 2003. c-Jun NH(2)-terminal kinase is essential for the regulation of AP-1 by tumor necrosis factor. *Mol Cell Biol* **23**: 2871-2882.

- Vousden KH, Prives C. 2009. Blinded by the Light: The Growing Complexity of p53. *Cell* **137**: 413-431.
- Wagner EF, Nebreda AR. 2009. Signal integration by JNK and p38 MAPK pathways in cancer development. *Nat Rev Cancer* **9**: 537-549.
- Wagner KU, Wall RJ, St-Onge L, Gruss P, Wynshaw-Boris A, Garrett L, Li M, Furth PA, Hennighausen L. 1997. Cre-mediated gene deletion in the mammary gland. *Nucleic Acids Res* **25**: 4323-4330.
- Wahba HA, El-Hadaad HA. 2015. Current approaches in treatment of triple-negative breast cancer. *Cancer Biol Med* **12**: 106-116.
- Wang J, Duncan D, Shi Z, Zhang B. 2013. WEB-based GEne SeT AnaLysis Toolkit (WebGestalt): update 2013. *Nucleic Acids Res* **41**: W77-83.
- Wang Y, Waters J, Leung ML, Unruh A, Roh W, Shi X, Chen K, Scheet P, Vattathil S, Liang H et al. 2014. Clonal evolution in breast cancer revealed by single nucleus genome sequencing. *Nature* **512**: 155-160.
- Watson CJ, Khaled WT. 2008. Mammary development in the embryo and adult: a journey of morphogenesis and commitment. *Development* **135**: 995-1003.
- Webb DJ, Parsons JT, Horwitz AF. 2002. Adhesion assembly, disassembly and turnover in migrating cells -- over and over and over again. *Nat Cell Biol* **4**: E97-100.
- Wei MC, Zong WX, Cheng EH, Lindsten T, Panoutsakopoulou V, Ross AJ, Roth KA, MacGregor GR, Thompson CB, Korsmeyer SJ. 2001. Proapoptotic BAX and BAK: a requisite gateway to mitochondrial dysfunction and death. *Science* **292**: 727-730.
- Wei Y, Pattingre S, Sinha S, Bassik M, Levine B. 2008. JNK1-mediated phosphorylation of Bcl-2 regulates starvation-induced autophagy. *Mol Cell* **30**: 678-688.
- Wen HC, Avivar-Valderas A, Sosa MS, Girnius N, Farias EF, Davis RJ, Aguirre-Ghiso JA. 2011. p38alpha Signaling Induces Anoikis and Lumen Formation During Mammary Morphogenesis. *Sci Signal* **4**: ra34.
- Wendl MC, Wallis JW, Lin L, Kandoth C, Mardis ER, Wilson RK, Ding L. 2011. PathScan: a tool for discerning mutational significance in groups of putative cancer genes. *Bioinformatics* **27**: 1595-1602.
- Weston CR, Wong A, Hall JP, Goad ME, Flavell RA, Davis RJ. 2003. JNK initiates a cytokine cascade that causes Pax2 expression and closure of the optic fissure. *Genes Dev* **17**: 1271-1280.
- . 2004. The c-Jun NH2-terminal kinase is essential for epidermal growth factor expression during epidermal morphogenesis. *Proc Natl Acad Sci U S A* **101**: 14114-14119.
- Whitfield J, Neame SJ, Paquet L, Bernard O, Ham J. 2001. Dominant-negative c-Jun promotes neuronal survival by reducing BIM expression and inhibiting mitochondrial cytochrome c release. *Neuron* **29**: 629-643.
- Whitmarsh AJ, Davis RJ. 2007. Role of mitogen-activated protein kinase kinase 4 in cancer. *Oncogene* **26**: 3172-3184.

- Wilhelm D, Bender K, Knebel A, Angel P. 1997. The level of intracellular glutathione is a key regulator for the induction of stress-activated signal transduction pathways including Jun N-terminal protein kinases and p38 kinase by alkylating agents. *Mol Cell Biol* **17**: 4792-4800.
- Williams JM, Daniel CW. 1983. Mammary ductal elongation: differentiation of myoepithelium and basal lamina during branching morphogenesis. *Dev Biol* **97**: 274-290.
- Wilm A, Aw PP, Bertrand D, Yeo GH, Ong SH, Wong CH, Khor CC, Petric R, Hibberd ML, Nagarajan N. 2012. LoFreq: a sequence-quality aware, ultra-sensitive variant caller for uncovering cell-population heterogeneity from high-throughput sequencing datasets. *Nucleic Acids Res* **40**: 11189-11201.
- Xia Y, Karin M. 2004. The control of cell motility and epithelial morphogenesis by Jun kinases. *Trends Cell Biol* **14**: 94-101.
- Xia Z, Dickens M, Raingeaud J, Davis RJ, Greenberg ME. 1995. Opposing effects of ERK and JNK-p38 MAP kinases on apoptosis. *Science* **270**: 1326-1331.
- Xie X, Kaoud TS, Edupuganti R, Zhang T, Kogawa T, Zhao Y, Chauhan GB, Giannoukos DN, Qi Y, Tripathy D et al. 2017. c-Jun N-terminal kinase promotes stem cell phenotype in triple-negative breast cancer through upregulation of Notch1 via activation of c-Jun. *Oncogene* **36**: 2599-2608.
- Xu P, Das M, Reilly J, Davis RJ. 2011. JNK regulates FoxO-dependent autophagy in neurons. *Genes Dev* **25**: 310-322.
- Xu P, Davis RJ. 2010. c-Jun NH2-terminal kinase is required for lineage-specific differentiation but not stem cell self-renewal. *Mol Cell Biol* **30**: 1329-1340.
- Yan C, Boyd DD. 2007. Regulation of matrix metalloproteinase gene expression. *J Cell Physiol* **211**: 19-26.
- Yang D, Tournier C, Wysk M, Lu HT, Xu J, Davis RJ, Flavell RA. 1997a. Targeted disruption of the MKK4 gene causes embryonic death, inhibition of c-Jun NH2-terminal kinase activation, and defects in AP-1 transcriptional activity. *Proc Natl Acad Sci U S A* **94**: 3004-3009.
- Yang DD, Conze D, Whitmarsh AJ, Barrett T, Davis RJ, Rincon M, Flavell RA. 1998. Differentiation of CD4+ T cells to Th1 cells requires MAP kinase JNK2. *Immunity* **9**: 575-585.
- Yang DD, Kuan CY, Whitmarsh AJ, Rincon M, Zheng TS, Davis RJ, Rakic P, Flavell RA. 1997b. Absence of excitotoxicity-induced apoptosis in the hippocampus of mice lacking the Jnk3 gene. *Nature* **389**: 865-870.
- Yang YA, Tang B, Robinson G, Hennighausen L, Brodie SG, Deng CX, Wakefield LM. 2002. Smad3 in the mammary epithelium has a nonredundant role in the induction of apoptosis, but not in the regulation of proliferation or differentiation by transforming growth factor-beta. *Cell Growth Differ* **13**: 123-130.

- Ye K, Schulz MH, Long Q, Apweiler R, Ning Z. 2009. Pindel: a pattern growth approach to detect break points of large deletions and medium sized insertions from paired-end short reads. *Bioinformatics* **25**: 2865-2871.
- Youn A, Simon R. 2011. Identifying cancer driver genes in tumor genome sequencing studies. *Bioinformatics* **27**: 175-181.
- Yuan TL, Cantley LC. 2008. PI3K pathway alterations in cancer: variations on a theme. *Oncogene* **27**: 5497-5510.
- Yujiri T, Sather S, Fanger GR, Johnson GL. 1998. Role of MEKK1 in cell survival and activation of JNK and ERK pathways defined by targeted gene disruption. *Science* **282**: 1911-1914.
- Yujiri T, Ware M, Widmann C, Oyer R, Russell D, Chan E, Zaitzu Y, Clarke P, Tyler K, Oka Y et al. 2000. MEK kinase 1 gene disruption alters cell migration and c-Jun NH2-terminal kinase regulation but does not cause a measurable defect in NF-kappa B activation. *Proc Natl Acad Sci U S A* **97**: 7272-7277.
- Zeitlinger J, Bohmann D. 1999. Thorax closure in *Drosophila*: involvement of Fos and the JNK pathway. *Development* **126**: 3947-3956.
- Zenz R, Scheuch H, Martin P, Frank C, Eferl R, Kenner L, Sibilio M, Wagner EF. 2003. c-Jun regulates eyelid closure and skin tumor development through EGFR signaling. *Dev Cell* **4**: 879-889.
- Zhan L, Rosenberg A, Bergami KC, Yu M, Xuan Z, Jaffe AB, Allred C, Muthuswamy SK. 2008. Deregulation of scribble promotes mammary tumorigenesis and reveals a role for cell polarity in carcinoma. *Cell* **135**: 865-878.
- Zhang JY, Green CL, Tao S, Khavari PA. 2004. NF-kappaB RelA opposes epidermal proliferation driven by TNFR1 and JNK. *Genes Dev* **18**: 17-22.
- Zhang L, Wang W, Hayashi Y, Jester JV, Birk DE, Gao M, Liu CY, Kao WW, Karin M, Xia Y. 2003. A role for MEK kinase 1 in TGF-beta/activin-induced epithelium movement and embryonic eyelid closure. *EMBO J* **22**: 4443-4454.
- Zhang T, Inesta-Vaquera F, Niepel M, Zhang J, Ficarro SB, Machleidt T, Xie T, Marto JA, Kim N, Sim T et al. 2012. Discovery of potent and selective covalent inhibitors of JNK. *Chem Biol* **19**: 140-154.
- Zhao L, Melenhorst JJ, Hennighausen L. 2002. Loss of interleukin 6 results in delayed mammary gland involution: a possible role for mitogen-activated protein kinase and not signal transducer and activator of transcription 3. *Mol Endocrinol* **16**: 2902-2912.
- Zong WX, Lindsten T, Ross AJ, MacGregor GR, Thompson CB. 2001. BH3-only proteins that bind pro-survival Bcl-2 family members fail to induce apoptosis in the absence of Bax and Bak. *Genes Dev* **15**: 1481-1486.